



# **Towards a Brain-inspired Information Processing System: Modelling and Analysis of Synaptic Dynamics**

Von der Fakultät für Mathematik und Informatik  
der Universität Leipzig  
angenommene

**D I S S E R T A T I O N**

zur Erlangung des akademischen Grades

**DOCTOR RERUM NATURALIUM**

(Dr. rer. nat.)

im Fachgebiet

**Informatik**

vorgelegt

von **MSc. Karim El-Laithy**

geboren am 23.03.1981 in Monofiya/Ägypten

Die Annahme der Dissertation wurde empfohlen von:

1. Prof. Dr. Martin Bogdan (Leipzig)
2. Prof. Dr. Julius Georgiou (Zypern)

Die Verleihung des akademischen Grades erfolgt mit Bestehen der  
Verteidigung am **19.12.2011** mit dem Gesamtprädikat ***summa cum laude.***



*"When hearing something unusual, do not primitively reject it, for that would be folly. Indeed, horrible things may be true, and familiar and praised things may prove to be lies. Truth is truth unto itself, not because [many] people say it is."*

**From Sharh' Ma'na Al Qanun (Explaining the Laws of Nature)- Ibn an-Nafis (1213 - 1288)**

*"Science is a wonderful thing if one does not have to earn one's living at it."*

**Albert Einstein**

# *Abstract*

## **Towards a Brain-inspired Information Processing System: Modelling and Analysis of Synaptic Dynamics**

Biological neural systems (BNS) in general and the central nervous system (CNS) specifically exhibit a strikingly efficient computational power along with an extreme flexible and adaptive basis for acquiring and integrating new knowledge. Acquiring more insights into the actual mechanisms of information processing within the BNS and their computational capabilities is a core objective of modern computer science, computational sciences and neuroscience. Among the main reasons of this tendency to understand the brain is to help in improving the quality of life of people suffer from loss (either partial or complete) of brain or spinal cord functions. Brain-computer-interfaces (BCI), neural prostheses and other similar approaches are potential solutions either to help these patients through therapy or to push the progress in rehabilitation. There is however a significant lack of knowledge regarding the basic information processing within the CNS. Without a better understanding of the fundamental operations or sequences leading to cognitive abilities, applications like BCI or neural prostheses will keep struggling to find a proper and systematic way to help patients in this regard. In order to have more insights into these basic information processing methods, this thesis presents an approach that makes a formal distinction between the essence of being intelligent (as for the brain) and the classical class of artificial intelligence, e.g. with expert systems. This approach investigates the underlying mechanisms allowing the CNS to be capable of performing a massive amount of computational tasks with a sustainable efficiency and flexibility. This is the essence of being intelligent, i.e. being able to learn, adapt and to invent. The approach used in the thesis at hands is based on the hypothesis that the brain or specifically a biological neural circuitry in the CNS is a dynamic system (network) that features emergent capabilities. These capabilities can be imported into spiking neural networks (SNN) by emulating the dynamic neural system. Emulating the dynamic system requires simulating both the inner workings of the system and the framework of performing the information processing tasks. Thus, this work comprises two main parts. The first part is concerned with introducing a proper and a novel dynamic synaptic model as a vital constitute of the inner workings of the dynamic neural system. This model represents a balanced integration between the needed biophysical details and being computationally inexpensive. Being a biophysical model is important to allow for the abilities of the target dynamic system to be inherited, and being simple is needed to allow for further implementation in large scale simulations and for hardware implementation in the future. Besides, the energy related aspects of synaptic dynamics are studied and linked to the behaviour of the networks seeking for stable states of activities. The second part of the thesis is consequently concerned with importing the processing framework of the dynamic system into the environment of SNN. This part of the study investigates the well established concept of binding by synchrony to solve the



information binding problem and to propose the concept of synchrony states within SNN. The concepts of computing with states are extended to investigate a computational model that is based on the finite-state machines and reservoir computing. Biological plausible validations of the introduced model and frameworks are performed. Results and discussions of these validations indicate that this study presents a significant advance on the way of empowering the knowledge about the mechanisms underpinning the computational power of CNS. Furthermore it shows a roadmap on how to adopt the biological computational capabilities in computation science in general and in biologically-inspired spiking neural networks in specific. Large scale simulations and the development of neuromorphic hardware are work-in-progress and future work. Among the applications of the introduced work are neural prostheses and bionic automation systems.

# *Acknowledgements*

First of all, "Praise be to GOD" who is beside me in every step of my life.

Foremost I offer my sincerest gratitude to my supervisor, Prof. Dr. Martin Bogdan, who has supported me throughout my work with his patience and knowledge whilst allowing me the room to work in my own way. I attribute the level of my work to his encouragement and effort and without him this thesis, too, would not have been completed or written. He has often had to bear the brunt of my frustration and rages against the world and non-working simulations with friendship. One simply could not wish for a better or friendlier supervisor.

Amira, you are my mentor, you are a dear lover, sincere friend and a perfect wife. Beside dedicating this work all to you and my mother, I would like to express my gratitude for all your patience and equanimity during all my moments of depression and frustration.

Words can not express my deepest gratefulness and appreciation to my parents, my sister and my brother for their valuable support, care and encouragement. And I am also so grateful to the Eberhardt family, their sincere support and encouragement are always a great help.

I am also indebted to the many countless contributors from my colleges Frank, Jörn, Wolfgang, Thomas and Riyadh. Finally, the department of computer engineering has provided the support and equipment I have needed to produce and complete my thesis. Special thanks are to Dr. Jens Glaser, without his help the mathematical derivations and analysis would never be available.

This work has been carried out as a part of a full PhD scholarship from the Deutsche Akademische Austausch Dienst (DAAD) with reference number: A/06/90455.

Leipzig, den 19.12.2011

Karim El-Laithy

# Contents

<b>Abstract</b>	<b>iv</b>
<b>Acknowledgements</b>	<b>vi</b>
<b>List of Figures</b>	<b>xi</b>
<b>List of Tables</b>	<b>xiii</b>
<b>1 Introduction and Overview</b>	<b>1</b>
1.1 Neuroscience in History . . . . .	1
1.2 Why to Study the Brain? . . . . .	1
1.3 What is it about Computational Neuroscience? . . . . .	3
1.4 Levels of Organization & Abstraction . . . . .	4
1.5 Computer Analogy & Emergence . . . . .	6
1.6 Simulating or Emulating the Brain . . . . .	7
1.7 Motivation of Current Work . . . . .	10
1.8 Aim and Organization of Thesis . . . . .	12
<b>2 Biological Foundations</b>	<b>15</b>
2.1 Introduction . . . . .	15
2.2 Central Nervous System . . . . .	15
2.3 The Neuron . . . . .	20
2.4 The Synapse . . . . .	22
<b>Part I EFFICIENT &amp; OPTIMIZED MODELING OF SYNAPTIC DYNAMICS</b>	<b>29</b>
<b>3 State of the Art: Modeling Neural Networks</b>	<b>31</b>
3.1 Introduction . . . . .	31
3.2 The Neural Code . . . . .	31
3.3 Artificial Neural Networks . . . . .	33
3.4 Neuronal Models . . . . .	34
3.5 Modelling of Synaptic Action . . . . .	38
3.6 Models of Short-Term Synaptic Plasticity . . . . .	41
3.7 Summary . . . . .	49

<b>4</b>	<b>The Modified Stochastic Synaptic Model</b>	<b>51</b>
4.1	Introduction: Why Another Model?	51
4.2	The Building Brick: Maass-Zador's Stochastic Synapse	52
4.3	Developing the Novel Model: Reformulating Maass-Zador's Model	55
4.4	The Modified Stochastic Synaptic Model (MSSM)	57
4.5	Basic Simulations	62
4.6	Steady-state Expressions	67
4.7	Synaptic Strength & Learning	68
4.8	Probability of Release & Synaptic Noise	71
4.9	Comparison with Existing Models	73
4.10	Limitations	75
4.11	Remarks for Implementation	76
<b>5</b>	<b>Validation: Prediction of Spike-Timing</b>	<b>77</b>
5.1	Introduction	77
5.2	Prediction of Spike-Timing	78
5.3	The Model & The Second Fold of STDP	79
5.4	Simulation Data and Training	82
5.5	Coincidence Measure	84
5.6	Results and Discussion	85
<b>6</b>	<b>Synaptic Energy</b>	<b>91</b>
6.1	Introduction	91
6.2	Operating Points of Dynamical Systems	92
6.3	Synaptic Energy and Synchrony	93
6.4	The Ansatz	94
6.5	Basic Analysis of Synaptic Energy Function	96
6.6	Stable Spiking Patterns Emerge from Stable Synaptic Energy?	100
6.7	Discussion about Energy/Synaptic States	103
<b>7</b>	<b>Discussion Part I</b>	<b>105</b>
7.1	Overview of the Used Approach	105
7.2	Modelling Synaptic Dynamics	106
<b>Part II SIMULATION OF BASIC INFORMATION PROCESSING IN CNS USING MSSM</b>		<b>109</b>
<b>8</b>	<b>Learning with Dynamic Synapses</b>	<b>111</b>
8.1	Introduction	111
8.2	Reinforcement Learning for Dynamic Synaptic Models	112
8.3	Reinforcement Learning Framework	115
8.4	Simulation and Results	120
8.5	Discussion	125
8.6	summary	127
<b>9</b>	<b>Synchrony States: Binding by Synchrony</b>	<b>129</b>
9.1	Introduction	129
9.2	The Binding Problem	130

9.3	Synchrony States . . . . .	137
9.4	Simulations . . . . .	139
9.5	Learning Framework . . . . .	141
9.6	Results . . . . .	142
9.7	Discussion . . . . .	147
9.8	Summary . . . . .	153
<b>10</b>	<b>Temporal Finite-State Machines</b>	<b>155</b>
10.1	Introduction . . . . .	155
10.2	Liquid State Machines . . . . .	156
10.3	Dynamic Networks . . . . .	159
10.4	Binding by Synchrony within Dynamic Networks . . . . .	160
10.5	Simulations . . . . .	164
10.6	Temporal Finite-State Machines vs. Liquid-State Machines . . . . .	169
10.7	Temporal Finite-State Machines vs. Cortical columns . . . . .	171
<b>11</b>	<b>Discussion &amp; Conclusions</b>	<b>173</b>
11.1	Discussion . . . . .	173
11.2	Conclusions . . . . .	178
<b>12</b>	<b>Outlook</b>	<b>181</b>
<b>A</b>	<b>Synaptic Models</b>	<b>183</b>
A.1	$\alpha$ -Function Postsynaptic Potential (PSP) . . . . .	183
A.2	Dittmann Facilitation and Depression Model . . . . .	183
A.3	Liaw-Berger Dynamic Synapse . . . . .	185
A.4	Destexhe-Mainen-Sejnowski Synaptic Model . . . . .	187
<b>B</b>	<b>Derivations for Modified Stochastic Synaptic Model</b>	<b>189</b>
B.1	Derivation of Discrete Version of Maass-Zador's Stochastic Model . . . . .	189
B.2	Derivation of Steady-state Expression . . . . .	190
B.3	Dynamic Threshold & Spike-Rate Adaptation . . . . .	194
B.4	Synaptic Energy . . . . .	196
<b>C</b>	<b>Mathematical Definitions for Dynamic Networks</b>	<b>199</b>
	<b>Abbreviations</b>	<b>201</b>
	<b>Bibliography</b>	<b>203</b>
	<b>Scientific Career</b>	<b>215</b>
	<b>Published Papers</b>	<b>217</b>
	<b>Bibliographic Details</b>	<b>219</b>
	<b>Declaration of Authorship</b>	<b>220</b>



# List of Figures

1.1	Papyrus about neuroscience . . . . .	2
1.2	The brain vs. the supercomputer. . . . .	3
1.3	The pig picture of Neuroscience. . . . .	4
1.4	Levels of abstraction in neuroscience . . . . .	5
1.5	Simulating vs. emulating . . . . .	8
1.6	Current status of neural implants . . . . .	12
2.1	Anatomy of Brain . . . . .	17
2.2	Cortical layers . . . . .	18
2.3	Biological neurons in the CNS . . . . .	20
2.4	The neuron . . . . .	21
2.5	The Action potential . . . . .	21
2.6	The chemical synapse . . . . .	23
2.7	The excitatory (inhibitory) postsynaptic potential . . . . .	26
3.1	Temporal coding with inter-spike intervals . . . . .	33
3.2	Schematic of classical artificial neural networks . . . . .	34
3.3	The Integrate-and-Fire neuronal model . . . . .	36
3.4	Kernels of the Spike-response neuronal model . . . . .	38
3.5	Facilitation and Depression . . . . .	40
3.6	Simulation of the Markram-Tsodyks synaptic model . . . . .	43
3.7	Simulation of the Lee-Anton-Poon synaptic model . . . . .	47
4.1	Overview of synaptic models . . . . .	52
4.2	Dynamics of the Maass-Zador stochastic synapse . . . . .	54
4.3	MSSM: Estimation of $N_t(t)$ . . . . .	59
4.4	Overview of the MSSM with equations . . . . .	62
4.5	Basic Simulation of the MSSM . . . . .	64
4.6	Simulation of the MSSM, influence of model parameters on the model dynamics . . . . .	65
4.7	Basic simulation of the MSSM with a postsynaptic neuron . . . . .	66
4.8	Simulation of the MSSM, influence of model parameters on the output variation. . . . .	67
4.9	MSSM: Effect of model parameters on the dynamic synaptic strength . . . . .	70
4.10	MSSM: Simulation with a true stochastic probability function . . . . .	72
4.11	Relative position of the MSSM to other synaptic models . . . . .	74
5.1	Prediction task: Schematic illustration of the experiment and simulation . . . . .	79

5.2	Prediction task: Evaluation of inter-spike intervals . . . . .	80
5.3	Example of the introduced dynamics through the second fold of MSSM . . . . .	81
5.4	Schematic illustration of the applied Hebbian learning scheme . . . . .	83
5.5	Training of model parameters to fit experimental data . . . . .	84
5.6	Performance in predicting spike timing . . . . .	86
5.7	Traces of the MSSM state parameters in predicting spiking activity . . . . .	86
5.8	Effect of fixed firing thresholds on the performance of predicting spiking activity . . . . .	88
6.1	Time evolutions of synaptic energy . . . . .	97
6.2	Behaviour of synaptic energy with different input frequencies . . . . .	98
6.3	Behaviour of synaptic energy in relation to synaptic strength . . . . .	99
6.4	Influence of synaptic energy on a network . . . . .	102
8.1	Schematic of a standard RL problem and the network simulation setup . . . . .	116
8.2	Spike timing-dependent Hebbian update . . . . .	119
8.3	Input and output spike trains for learning algorithm . . . . .	121
8.4	Learning simulation results . . . . .	122
8.5	Learning effect on tuned parameters . . . . .	123
8.6	Changes in synaptic model parameters from excitatory vs. inhibitory ones . . . . .	123
8.7	Dynamic synaptic strength and self-organizing behaviour . . . . .	124
8.8	Effect of bin window size on learning performance . . . . .	124
9.1	The Binding problem: Rosenblatt's example . . . . .	131
9.2	Simulation setup for synchrony . . . . .	140
9.3	Three neurons network behaviour during the search for synchrony states . . . . .	144
9.4	Internal network dynamics (three neurons) along the search for synchrony states . . . . .	145
9.5	Eight neurons network behaviour and internal dynamics during the search for synchrony states . . . . .	146
9.6	The influence of different noise levels on the eight neurons network behaviour . . . . .	147
9.7	The influence of successive different noise levels on the eight neurons network behaviour . . . . .	148
10.1	Overview of the LSM concept . . . . .	157
10.2	The Dynamic networks concept and the Liquid-state machines . . . . .	161
10.3	The novel computational power concept of dynamic networks . . . . .	163
10.4	LSM simulation setup and separation property of basic LSM . . . . .	165
10.5	The average distances between the inputs used for the simulation with the tFSM . . . . .	167
10.6	The tFSM simulation results . . . . .	168
10.7	The tFSM simulation results at higher density of the interconnectivity . . . . .	169
11.1	Levels of abstraction in neuroscience: Multi-scale perspective . . . . .	174
B.1	Check on steady-state calculations . . . . .	195



# List of Tables

2.1	The main synaptic neurotransmitters and related receptors. . . . .	25
4.1	Nomenclature of the MSSM model parameters . . . . .	61
5.1	Values of the MSSM's model parameters for predicting the spike-timing of a thalamic postsynaptic neuron . . . . .	82
5.2	Performance in predicting spiking activity . . . . .	88
6.1	Model parameters for synaptic energy states . . . . .	98
B.1	Values for MSSM to check steady-state formulas . . . . .	194



*Dedicated To ...*

*Nashwa, she brought me to life ...*

*She taught me how to live.*

*&*

*To Amira, she brings the life to me ...*

*She is my love.*



# Introduction and Overview

*"The last frontier of the biological sciences - their ultimate challenge - is to understand the biological basis of consciousness and the mental processes by which we perceive, act, learn, and remember."*

**Eric Kandel** (Kandel et al., 1995)

## 1.1 Neuroscience in History

The interest in understanding the brain functions is not new. It had started even before the word "brain" was known. Fig. 1.1 shows an Egyptian papyrus written in the 17th century B.C. (more than 3,700 years ago). It contains the earliest references to the brain problems anywhere in human records. In Fig. 1.1(a) the term is found in multiple occurrences and the Egyptian hieroglyphs for the term "brain" is given clearly in Fig. 1.1(b). According to J. Breasted, who translated and published the document in 1930, the word brain occurs only eight times in the available ancient Egyptian records, six of them are in this page, which describes the symptoms, diagnosis and prognosis of two patients, with compound fractures of the skull<sup>1</sup> (Kandel et al., 1995).

## 1.2 Why to Study the Brain?

The answer to the question, why to study the brain, is simple: Because the brain is strikingly an efficient computational system. In order to answer in a more elaborate way, one may compare the brain with a computer (see Fig. 1.2). In simple numbers, the human brain comprises  $\sim 10^{11}$  neurons. Each neuron has in average  $\sim 10^3$ – $10^4$  synaptic connections. The average working frequency of spiking in the brain<sup>2</sup> is  $\sim 100$  Hz. The overall size of the cranial capacity is

<sup>1</sup>The entire treatise is now in the Rare Book Room of the New York Academy of Medicine. From J. Breasted, 1930. The Edwin Smith Surgical Papyrus, 2 volumes, Chicago: The University of Chicago Press

<sup>2</sup>Some regions in the brain use frequencies up to 1 kHz, while in some other regions and during sleeping the frequency may drop to be less than 5 Hz.

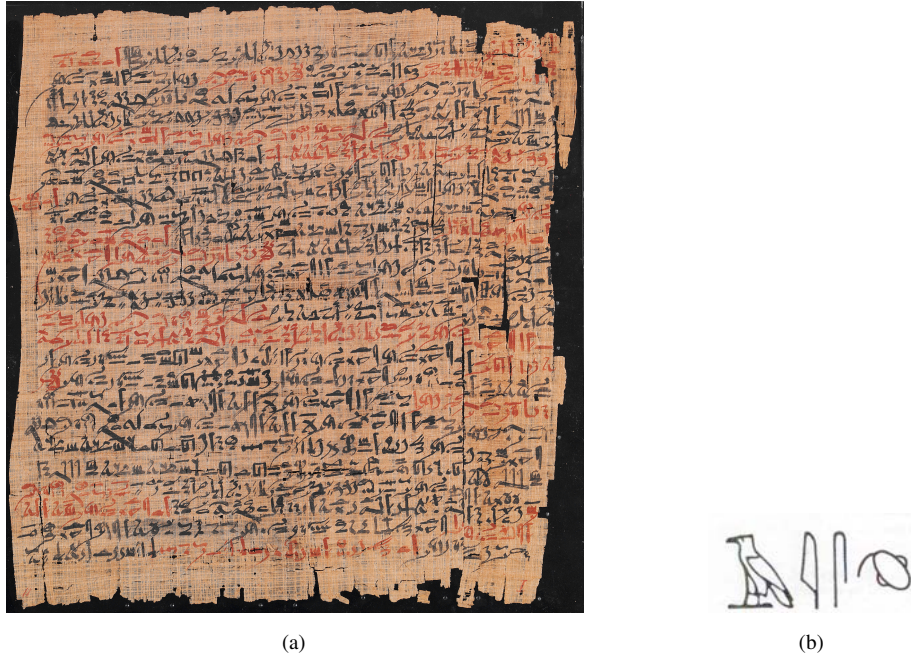


**FIGURE 1.1:** First known mention of the brain in human history (Courtesy of the New York Academy of Medicine Library). (a) Recto Column 2, contains multiple instances of the hieroglyph for brain in case 6, which begins on line 2, 17 and continues through the end of the first line on the following leaf (b) The hieroglyphic word of "brain".

$\sim 1400\text{--}1500\text{ cm}^3$  (Umar et al., 2006). With some analysis, it could be shown that the processing power of the visual cortex<sup>3</sup> alone in the brain is about  $\sim 10^{15}$  computer instructions per second (IPS).

As for a computer, the IBM Roadrunner was considered as the fastest supercomputer<sup>4</sup> on the planet till 2008<sup>5</sup>. It contains 6912 AMD-Opteron (8 True-Hyber-Threading processors) which turns to be  $\sim 55296$  processing unit. The supercomputer takes a hall with a surface area of  $510.96\text{ m}^2$  and consumes 2334.5 kW. This supercomputer has a computational power of  $\sim 1.33 \times 10^{15}$  IPS. Such a computing monster is only  $\sim 1.33$  times more powerful than the human visual cortex. It should be pointed out that this does not mean that the human brain is faster. On the contrary the brain is much slower when it comes to the working frequency, not to mention whether the comparison is fair or not. However, the complexity of the accomplished tasks by the brain along with its adaptivity and correctness are still far beyond the capabilities of any supercomputer (Koch and Tononi, 2008).

The brain is truly one of the most complex systems (if not the most complex one) to be studied. To say that all thoughts or actions are the result of simple electric signals in the brain is a total understatement. The difficulty in understanding the brain has some times a philosophical explanation (Crick and Koch, 2003; Koch and Tononi, 2008): It is difficult to imagine that the brain (of the

<sup>3</sup>The retina seems to process about ten one-million-point images per second

<sup>4</sup>Not to be compared with IBM's Watson; as it is an artificial intelligence computer (expert system).

<sup>5</sup>Since October 2010, the Tianhe-1A supercomputer has been the fastest in the world; it is located in China (wikipedia.org)

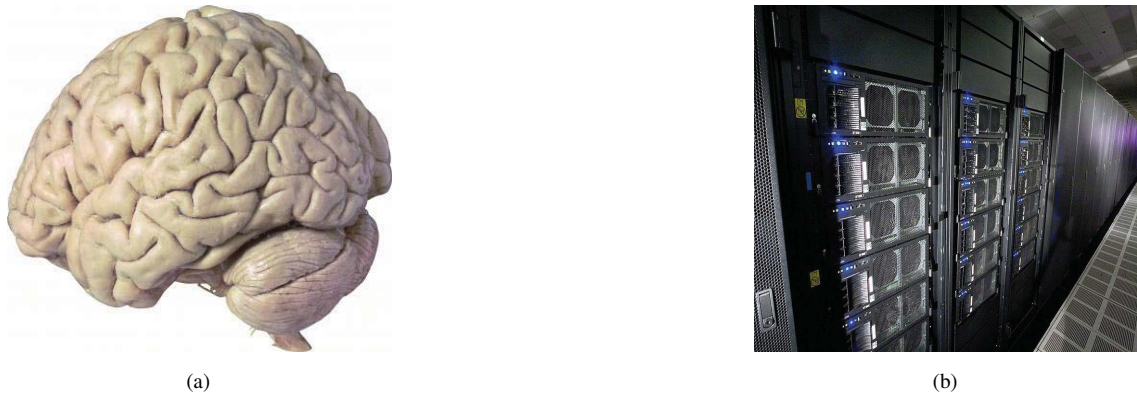


**FIGURE 1.2:** (a) The human brain. Photo courtesy of Premier Exhibitions. (b) Image of Road-runner, world's first petaFLOP computer (2008), wikipedia.org.

researcher) shall comprehend how itself is working; e.g. imagine waiting for a robot to understand and re-engineer itself. This issue was considered the reason why the early trials to understand the brain functions and what is beyond, i.e. studying cognition and conscious, led actually to the invention of the computer believing that a computer as a Turing machine shall be (one day) the artificial brain (Sejnowski et al., 1988).

### 1.3 What is it about Computational Neuroscience?

The current goal of neuroscience is to advance and to extend the understanding of the nervous system in general. Particularly, it aims to develop a better understanding of the organization, development and the information processing principles in the brain. The research in neuroscience is multidisciplinary and covers indeed a wide range of fields. As shown in Fig. 1.3 the main research fields are: 1) Subcellular and molecular neuroscience, 2) Computational neuroscience and 3) Cognitive neuroscience. This thesis belongs to the second class, i.e. Computational neuroscience.

The term computational neuroscience is scientifically used to indicate "*The theoretical study of the brain to uncover the principles and mechanism that guide the development, organization, information processing and mental abilities of the nervous system*" (Trappenberg, 2002). Note that at the end of this definition, the term nervous system is used instead of the brain. This distinction is crucial at this point; since the term nervous system here implies that the cognitive and higher *brain* functions do not represent the focus of the research. The main focus of the research in computational neuroscience is concentrated on the neural systems throughout the different regions in the central nervous system (CNS). In order to understand the distinction imposed here, the following example considers two general functions, e.g. memory and learning. The study of the working memory (short-term memory) and the basic learning abilities, e.g. the ability of a neural system to yield a certain output from a certain input, are typical research topics in computational neuroscience. While language learning and memorizing a poet after studying it are matters for cognitive neuroscience (Sejnowski et al., 1988; Trappenberg, 2002).

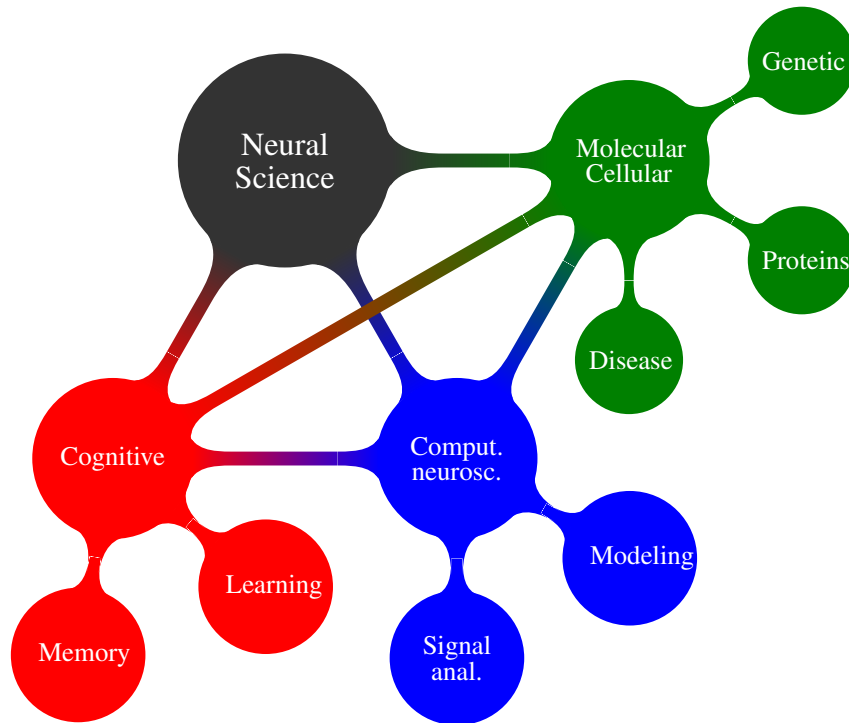


**FIGURE 1.3:** Basic fields of research in Neuroscience. The interconnections are made only between the main ones; the connections between the sublevels of research are omitted for clarity. In fact, this diagram is a strongly simplified illustration of the existing fields belong to neuroscience. Other fields may include: Neural engineering and neurolinguistics

The illustrated fields from Fig. 1.3 are the popular classifications of research in neuroscience. The neural system itself can be described in terms of levels of organization. It is also referred to as levels of abstraction, since this classification is based on the understanding or the abstraction by which the nervous system is regarded. The levels of organization and abstraction are discussed in the following section.

## 1.4 Levels of Organization & Abstraction

The nervous system has many spatial levels of organization, they range from the molecular level of a few angstroms to that of the whole nervous system on the scale of meters, the surface area of the human cerebral cortex is about  $2500 \text{ cm}^2$  (see Fig. 1.4). Neurobiological mechanisms on all these levels are important for the functions of the brain.

Fig 1.4 illustrates an example of the possible different levels of organization in the nervous system. An easily recognizable structure in the nervous system is the neuron, which is a cell specialized in signal processing. More formally, it is the structural and functional building unit of the nervous system. Depending on extra- and intracellular conditions it is able to generate time bounded electric potentials, known as action potentials (APs), that are used to transmit information to other cells to which it is connected. Mechanisms on a subcellular level are certainly important



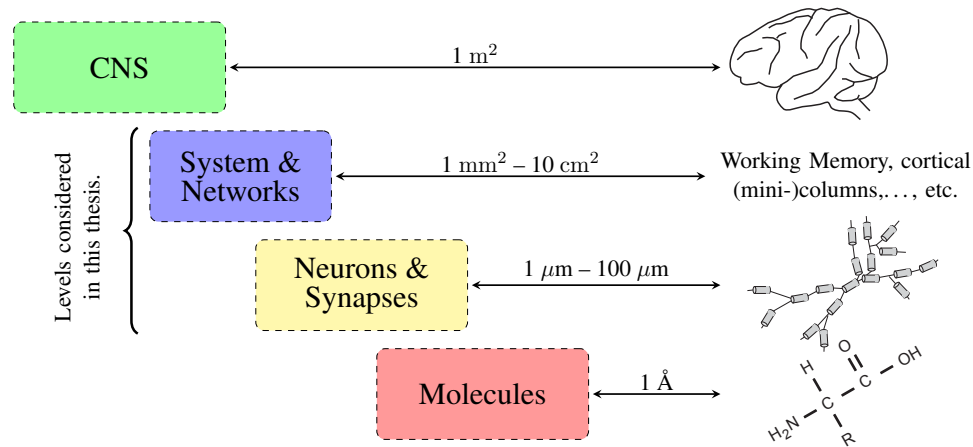


**FIGURE 1.4:** Illustration of some levels of organization in the central nervous system (CNS) on different scales. The illustrations include, from top to bottom, an outline of the brain symbolizing CNS, working memory, a model of a neuron with synapse, and an amino acid molecule. As indicated the work at hands is concerned with the levels of cellular/synaptic dynamics and the related higher functions at the level of networks, see Sec. 1.7 and 1.8 for details.

for such information transmission and to the subsequent processing capabilities. Processes in the neuron utilize cascades of biochemical reactions that must be understood on a molecular level. These include, for example, the transcription of genetic information that influences the neuronal firing mechanisms. Other structures within the neural circuitry are identified with specific functions such as synapses, which are particularly important for the understanding of signal processing within the nervous system. The complexity of a single neuron, and even that of isolated subcellular mechanisms, often makes biophysical and computational studies essential for the development and verification of hypotheses about biological information processing.

Single neurons are certainly not the entire story. Neurons contact each other and thereby build networks. A small number of interconnected neurons can exhibit complex behaviour and information-processing capabilities which are not achievable with a single neuron. Understanding the dynamics of such networks is a major domain in neuroscience, perhaps because there is so little understanding about such nonlinear interacting systems. Networks have additional information-processing capabilities beyond that of single neurons, such as representing information in a distributed way. Networks with a specific architecture and specialized information-processing capabilities are incorporated into larger structures that are able to perform even more complex information-processing tasks (cognitive). Studies of the brain on this level are certainly essential to understand higher-order brain functions, and it is at this level where probably the least understanding is available (Churchland and Sejnowski, 1988; Trappenberg, 2002).

One might ask: is it required to rebuild the brain in its entirety, e.g. in a computer, in order to comprehend the brain functions? Some arguments suggest that one can never achieve this. However, even if it were possible to simulate a whole brain on a computer with all the details from

its biochemistry to its large-scale organization, this would not necessarily imply that an adequate explanation of brain functions is comprehended (Trappenberg, 2002).

Which level is most appropriate for the investigation and abstraction depends on the scientific question asked. For example, the reason behind Parkinson disease is probably the death of dopaminergic neurons in the substantia nigra. There are signs that the death of dopaminergic neurons can be due to a genetic predisposition acting together with biochemical processes in single neurons (Kandel et al., 1995; Trappenberg, 2002). A detailed investigation on a neuronal level with detailed neuron models is thus obvious. However, it is also known about the important role of dopamine in the initiation of motor actions, and a more global system level study is necessary as well to understand the full scale of damage. Besides, it helps to develop better methods of coping with the conditions that might have facilitated this impairment. Therefore, the conditions must be studied at various levels and connections must be made among the different levels in order to elucidate how small-scale factors, such as genetic mechanisms or biochemical processes in single neurons, can influence the characteristics of large-scale systems, such as the behaviour of an organism (Sejnowski, 1989; Trappenberg, 2002).

### 1.5 Computer Analogy & Emergence

Standard computers nowadays, such as PCs and workstations, have a number of central processors. Each processor is rather complex with specialized hardware and microprograms implementing a variety of functions, e.g. loading data into registers, adding, multiplying, and comparing data, as well as communicating with external devices. These basic functions can be executed by instructions that are binary data loaded into a special interpreter module.

By contrast, information processing in the brain is very different in many (if not all) respects. It utilizes very simpler processing elements, but extremely lots of them. The use of many parallel working processors has led to the term parallel distributed processing being used in this area. However, with this term one is tempted to think that the processes are independent because only processes that are independent can be processed on different processors in parallel. In contrast to this, a major ingredient of the information processing in the brain is certainly the *interaction* of processing elements (nodes), and the interaction of nodes is accomplished by assembling them into large networks (neural circuits and their subcircuits).

In the study of neural systems, neuroscience is interested in understanding both the building process of networks from nodes and the consequences of interacting nodes. It is the interaction that enables processing abilities not available in single ones. Such interaction is also known as the complexity of the system. Such capabilities are good examples of *emergent* properties in rule based systems. Emergence is the single most defining property of neural computation, distinguishing it from parallel computing in classical computer science. Interacting systems can have unique properties beyond the multiplication of single processor capabilities. These system properties are

labelled as "emergent" to stress that they are not encoded (programmed) directly into the system. In other words, these emergent properties can not be tracked back to (derived from) a set of basic rules defining the system. That is, one should distinguish between the description of a system on two levels; the level of basic rules defining the system and the level describes the consequences of such rules.

Therefore the most debated and unresolved issue in computational and theoretical neuroscience questions about defining and implementing the rules governing the information processing in the CNS. Because these rules are emergent features based on the biophysical setup of the neural circuitries, another preceding basic question is involved: how can the emergent capabilities be copied in general from the biological counterparts into implementable frameworks? The general and simple answer for this question is that a system with emergent features can be either simulated or emulated. The differences between the two approaches of simulation and emulation, why and how to combine both of them are discussed in the following section.

## 1.6 Simulating or Emulating the Brain

Whether to simulate or to emulate the brain is an issue that examines specifically the optimum level of abstraction in viewing the brain rather than the proper technique in implementing an artificial brain. From the definition in computer science, the term "emulation" implies mimicking the function of a program or computer hardware *by having all its low-level functions and properties simulated* by another program. In other words, a simulator tries to duplicate the behaviour of a system only to get the same output from the given input regardless of how. Whereas an emulator tries to duplicate the inner workings of the system (at some suitable level of abstraction) to duplicate the overall behaviour. The emulation is regarded as successful if the emulated system produces the same output behaviour and results as the original (within accepted tolerance).

Mathematically, and following the definition in (Sandberg and Bostrom, 2008) a Turing-based definition of simulation could be that: Consider a system  $S$  consists of a state  $x(t)$  evolving by a particular dynamics  $h$ , triggered by inputs  $I(t)$  and delivers outputs  $O(t)$ ; it reads

$$O(t) : x(t+1) = h(I, x(t)), O(t) = g(x(t))$$

Another system  $T$  simulates  $S$  if it produces the same output (within a tolerance) for the same input time series starting with a given state (within a tolerance) if it satisfies:

$$O(t) : X(t+1) = H(I, X(t)), O(t) = G(X(t)),$$

where  $|x(t) - X(t)| < \epsilon$  and  $X(0) = x(0) + \epsilon$ . The simulation is an emulation if<sup>6</sup>  $H = h$ .

<sup>6</sup>up to a one-to-one transformation of  $X(t)$ , that is, the internal dynamics is identical and similar outputs are not due to the form of  $G(X(t))$

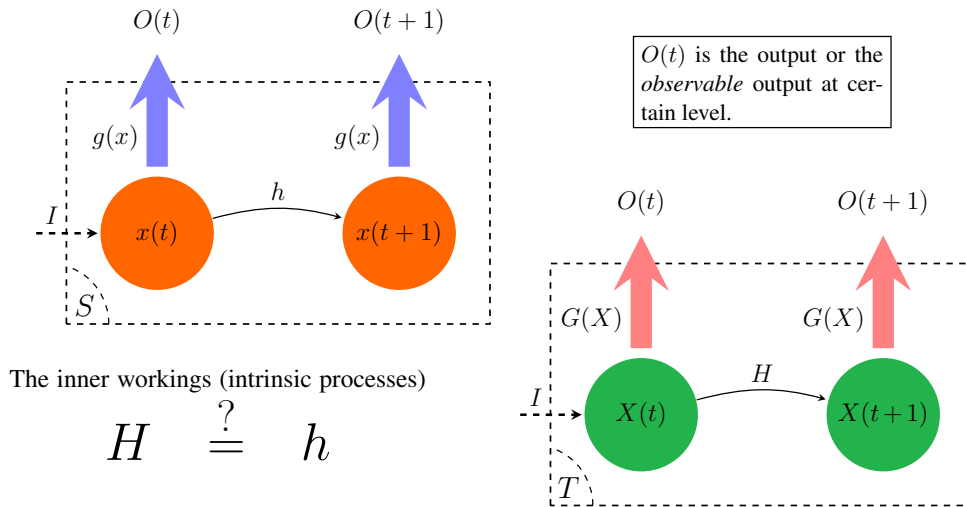


**FIGURE 1.5:** In case of simulating and emulating, the input and the output of the simulating/emulating system  $T$  are expected to be identical with tolerance (or similar) to the simulated/emulated system  $S$ . While, emulating requires the capture of the inner dynamics responsible for transition from one state to another. The output  $O(t)$  can be the general output of the system or the observable output at certain level and represents the input to the next outer level of organization (in case of nested structure).

To put it short,  $T$  simulates  $S$  if it generates  $O(t)$  from  $I(t)$ . And  $T$  emulates  $S$  if it generates  $O(t)$  from  $I(t)$  and  $h = H$ . Following this definition, chaotic systems can be emulated rather than being simulated (Sandberg and Bostrom, 2008). Without a proper adoption of the inner workings (achieving  $H = h$ ), chaotic systems will diverge after enough time if the initial conditions differ. Already a three neurons system can become chaotic (Herzog et al., 2007; Li et al., 2001) and it is very tenable that the brain contains chaotic dynamics and it is not strictly simulable. According to the Turing theory, a Turing machine (here it is the computer) can emulate any other Turing machine (the target system, the brain): It claims that every physically computable function can be computed by a Turing machine. For an example from software engineering, a computer simulator may simulate the processor, memory, input/output and so on of the target computer, but does not simulate the actual electronic workings of the components, only their qualitative function on the stored information (and its interaction with the outside world). When the electronic workings are simulated, this computer emulates the target one. The basis for brain emulation is: if, and only of, the brain activity is regarded as a function that is physically computed by the brain, then it should be possible to compute it on a Turing machine. Hence, a brain can be emulated by integrating the simulable relevant inner workings and low level processes.

Although brain emulation in general may seem attractive and feasible (Sandberg and Bostrom, 2008), defining what the relevant properties and functions is a crucial issue. The relevant functions and the involved properties are the target inner workings for the emulator to *simulate*. In other words, taking the brain as the target "computer", which level of organization should be simulated to build these inner workings of the brain? i.e. how deep should it be copied from the biological neural systems to capture the relevant functionalities? Some approaches have already decided

that starting from the molecular level is the required abstraction, see e.g. the Blue Brain project (Markram, 2006); this implied that the required modelling comprises (but not restrict to) details from the proteins formation and ion channels up to the synaptic and neuronal modelling. The incorporation of such low level details leads to inefficient results or irrelevant functionalities that are not in the heart of the research interests. And this may be the reason behind missing the expected published results from this project till the moment of writing these lines<sup>7</sup>.

The success in- and the plausibility of emulating the brain functionalities depend on the involved different levels of details. It might be also useful to incorporate different levels of details from different parts of the system. It is believed that in order to emulate the brain it is not need to understand the whole system. Rather the necessary low-level information about the brain and knowledge of the local update rules that change brain states from moment to moment are the mostly required. *"A functional understanding (why is a particular piece of cortex organized in a certain way) is logically separate from detail knowledge (how is it organized, and how does this structure respond to signals). Functional understanding may be a possible result from detail knowledge and it may help gather only the relevant information for brain emulation, but it is entirely possible that we could acquire full knowledge of the component parts and interactions of the brain without gaining an insight into how these produce (say) consciousness or intelligence"*, from (Sandberg and Bostrom, 2008).

There are some well established approaches that bridge over the need of simulating the inner processes in order to understand the collective emergent capabilities of the neural circuitries. In other words, the basic concept in these approaches is to simulate the input/output dynamics of certain neural circuitries, see e.g. (Eliasmith and Anderson, 2002). As to avoid the divergence problem of chaotic systems stated above, stability and controllability of these models is a significant criteria.

A different trial to present a bionic machine perception system was proposed by (Velik, 2008, 2010). It was based on simulating the general concepts of both combination coding and feature association in order to build a human-like visual perception system. The limitations of such an approach rise from the already limited understanding of the dynamics considered for modelling. The input/output relations are indeed an abstraction of the emergent general process taking place within the neural circuitry and these relations alone are not adequate to copy the essence of the process. *"The lowest levels of information processing turned out to be already of crucial importance for the efficiency and manifoldness of perception"* (Velik, 2008).

Therefore, the idea that gains more attention over the recent decade is that the brain might be emulated when the inner workings and the relevant functions are simulated on a cellular level of abstraction. This abstraction level should provide enough dynamic flexibilities for the important emerging capabilities to be inherited. Consequently, the inner workings and relevant neural functions require models of the functional units (cells and synapses), functional dynamics and dynamic

---

<sup>7</sup>Project's publication page: <http://bluebrain.epfl.ch/page26906.html>

states of information processing. This statement is a core principle and a pivotal concept in the work presented here.

Modelling and simulations of these targeted relevant inner workings should be performed in the light of the higher cognitive and perceptual findings. The importance of matching the results from both levels (cellular and cognitive) can be seen from e.g. the small network argument (Herzog et al., 2007). These arguments explain that if the network with millions of neurons is able e.g. to exhibit consciousness, this requires that small networks are able to feature some basic abilities of consciousness; these abilities are then integrated in the brain. Thus if a simulated artificial neural network is able to show certain basic biological information processing mechanisms, much larger scale simulations are expected then to scale up these information processing mechanisms and integrate them into more complex cognitive-like capabilities. Investigating the ability of simulated artificial neural network to show the basic biological information processing mechanisms belongs to the focus of the work at hands as well.

### 1.7 Motivation of Current Work

There is an increasing demand on importing the computational power of the brain into the world of technical applications. These applications cover mainly two fields: the computational sciences and neural science. The field of computational sciences, in general, needs novel solutions for already existing and new computational problems related to biology and ecosystems. Although there are significant enhancements in the tools of processing, e.g. hardware and required processing resources, the algorithms and methodologies are still incapable of delivering the required solutions, see e.g. the applications of reservoir computing as classifiers in (Lukoševičius and Jaeger, 2009). Transferring the knowledge about the techniques utilized in biological neural systems (BNS) into the world of computational science will support and empower the available tools in principle.

Regarding neural science, some surveys report that 2% of the world population suffer from inoperable problems in the central nervous system<sup>8</sup>. These problems vary from post-accidental loss (either partial or complete) of functions in the brain or spinal cord to diseases like amyotrophic lateral sclerosis or stroke which can lead to a locked-in-syndrome. Brain-computer-interfaces (BCI), neural prostheses and other similar approaches are possible solutions either to help these patients through therapy or to push the progress in rehabilitation. Commonly, the stricken functions are poorly understood in terms of the underlying mechanisms of information processing.

Thus, there is still a significant lack of knowledge regarding basic information processing strategies within neural systems (De Schutter, 2008). Without a better understanding of the fundamental operations or sequences leading to cognitive processing, applications like closed-loop BCI or neural prostheses (e.g. to bridge damaged and impaired neural areas) will not be achievable in the near future. In order to get an impression about how limited the available knowledge

---

<sup>8</sup>See <http://www.neural-prosthesis.com/index.html>

about the processes in CNS is, Fig. 1.6 shows a number of facts about the development of neural prostheses. In this figure, the number of in-service cases of most known neural implants are summarized. There are mainly three classes: the number of cases in clinical use as either for therapy or rehabilitation<sup>9</sup>, and research cases. The figure reports the number of heart pacemakers<sup>10</sup> per year. On one hand, since the mechanism and features of the cardiac neural circuit are completely understood, there are 350 thousand clinical cases that use pacemakers annually. The grasp control, on the other hand, requires the complete understanding of the motor control in both the CNS and in the limbs. The motor control in the CNS calls for being acquainted with planning and action in the CNS which involves the processing of the visual and ambient feedbacks. Since this process is poorly understood, if ever, the number of registered cases using neural prosthesis for grasp control are 300 in the last 10 years (Stieglitz, 2010). It should be pointed out that grasp control in general still does not represent a complex cognitive task like "language learning" or "face memorizing/recognition". Therefore, the availability of either therapy or rehabilitations for any brain impaired function depends significantly (but not solely) on whether adequate knowledge about the impaired functions is available or not. This meaning is indicated in Fig. 1.6 with the down decaying arrow, the availability of the neural implant follow the complexity of the mechanism and the available knowledge about it.

Note that the number of cases drops significantly when the target functions are changed from pure involuntary to a mixed voluntary/involuntary functions. All the brain/spinal cord stimulations repair the firing profile of the stimulated regions, these methods runs completely and independently from the patient control. Similarly, the Vagal nerve stimulation does not encounter any feedback from the patient. In the cases of bladder control and grasp, the connection between the patient control and the target region is a must. This involves and requires a sufficient level of understanding of the process not only between the CNS and the target region (peripheral neural circuit) but within the specialized regions in the CNS as well.

Having an ultimate goal of constructing a neural prostheses that can fit, coexist and bidirectionally communicate within the CNS, a plausible theoretical and practical framework is required. For this purpose a deep understanding of the underlying mechanisms and intrinsic processes of the brain functions is necessary. In the work at hands, the author is concerned with investigating as well as developing the hypothetical and conceptual approaches which are plausible to implement some basic information processing functions from the CNS. These hypothetical and conceptual approaches are viewed as plausible since they are based on a rigorous combination of experimental and theoretical foundations from the literature as it will follow in the next chapters. According to the levels of abstraction mentioned in Sec. 1.4, this work belongs to an investigation level that

<sup>9</sup>There is a debate in terminology about whether therapy is more complex than rehabilitation or vice versa. Therapy implies the treatment and suppression of the pathological symptoms with or without regard to the lost function, e.g. pain or function disorders. The re-establishment of the lost (impaired) function is the core of rehabilitation. The latter can be performed with or without treating the sick region, e.g using an artificial limb instead of an amputated one.

<sup>10</sup>Biologically, the heart beats are regulated through a closed-loop neural circuit that involves self-initiating neural nodes (a collection of packed neural cells)

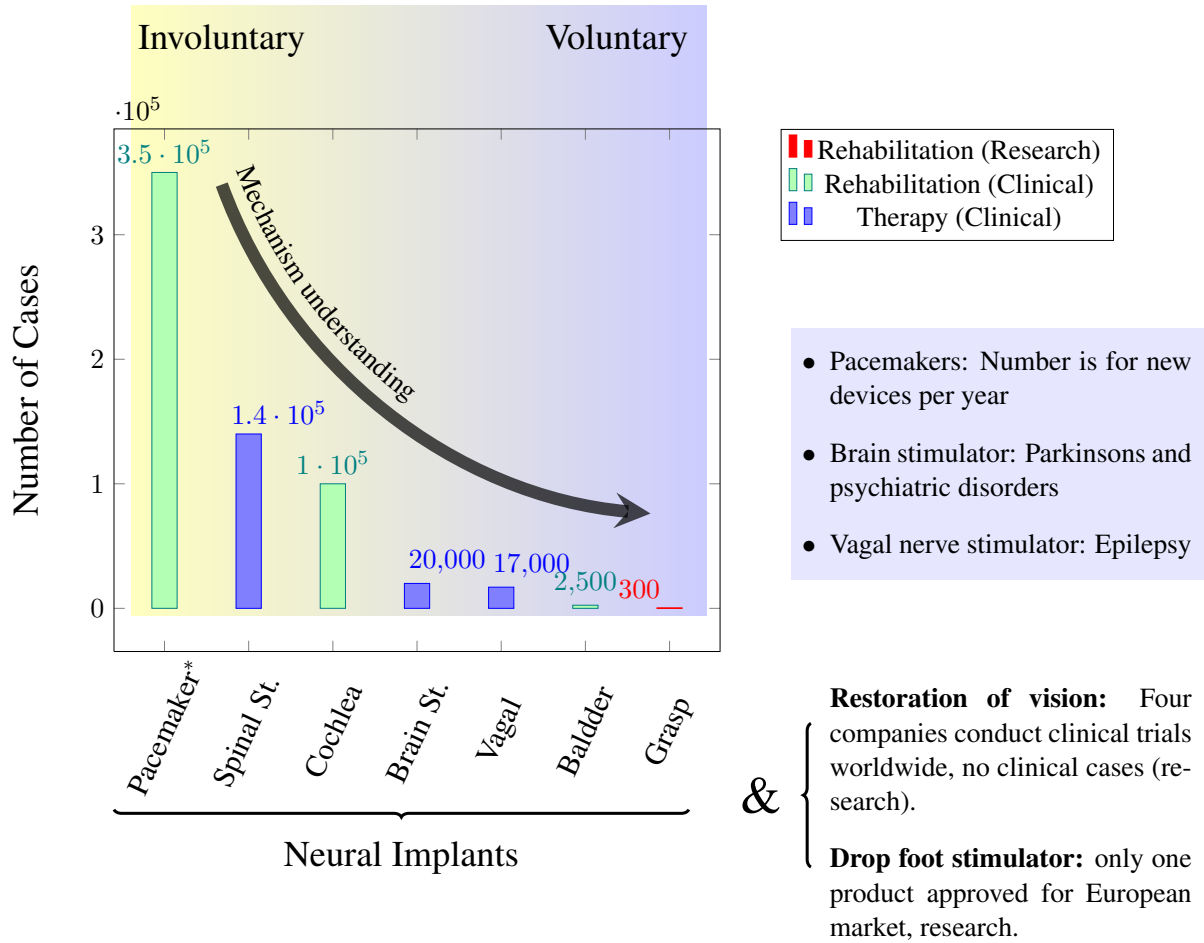


**FIGURE 1.6:** Current status of neural implants. Based on recent analysis about advances in developing biocompatible neural prosthesis (Stieglitz, 2010). The number of cases drops significantly when the target functions are changed from pure involuntary to a mixed voluntary/involuntary function. The down decaying arrow indicates that the availability of the neural implant follows the complexity of the mechanism and the available knowledge about it.

combines the second and the third level in Fig. 1.4. It addresses topics that start with studying functional units and up to network activities. Hence, the main pivots of this work are: First, it is concerned with synaptic dynamics; it involves the introduction of an optimum synaptic representation that allows for realizing the required computational power at relatively low complexity. Second, it is concerned with the mechanisms viewed as being used by the brain to handle cognitive tasks. It is namely the synthesis of neural states via temporal correlations. This permits the adoption of the standard concepts from finite-state machines to explain computations and information processing within neural systems.

## 1.8 Aim and Organization of Thesis

Having defined most of the basic conceptual paradigms discussing how the brain is organized and how theoretically emulating cognitive functions are seen feasible, the concrete aim of this thesis is



stated here. The first aim of this work is to introduce a biologically plausible as well as a practical model for synaptic dynamics. This model represents the needed balance between being biophysical and still tunable and implementable for large scale applications. The second aim is to show that this model fits within frameworks that emulate basic information processing functions in the CNS.

As a direct implication of proposing this model and relevant to it, the following topics are part of validating the adopted approaches in this thesis: a) an energy based analysis of the synaptic role in information processing, b) a reinforcement learning framework for dynamic synapses, c) a plausible binding-by-synchrony framework for artificial neural networks, and d) a theoretical framework for information processing based on the computational model of state-machines is introduced.

In the current chapter the major conceptual background topics are addressed. Afterwards, in Ch. 2 the relevant biological anatomy and functional details of the CNS are briefed, a detailed description about synapses is given. As this thesis is concerned with two levels of organization in the CNS, the manuscript after the second chapter consists of two main parts: Part I tackles the quest for a balanced synaptic modelling via introducing a novel synaptic model. It extends the analysis to explore the energy related synaptic dynamics. Part II illustrates how to import the new achieved capabilities from the novel synaptic model in order to emulate the basic biological information processing framework. This is accomplished by investigating certain basic and principle information processing aspects on the network level rather than on the cellular level. Throughout the thesis special care is taken to keep a logical flow of information. Explicit as well as implicit links between different topics are mentioned when appropriate.



# Chapter 2

## Biological Foundations

*"Erforsche die Welt, denn es gibt keinen anderen Weg, der Wahrheit auf die Spur zu kommen."*

Seneca

### 2.1 Introduction

The human nervous system is considered to be the most complex nervous system throughout mammals. The central nervous system (CNS) and peripheral nervous system (PNS) make up the human nervous system. As their names suggest, PNS is responsible for the sensor, communication with and control of the upper-, lower extremities, internal organs and glands. CNS is the master and maestro of the PNS and the entire body as a consequent. In this thesis only the CNS and particularly the brain is the focus of interest.

### 2.2 Central Nervous System

Here, the anatomical main regions in the CNS are briefly reviewed. The CNS is a bilateral and symmetrical structure. Seven main components build up the CNS: the spinal cord, medulla oblongata, pons, cerebellum, midbrain, diencephalon, and the cerebral hemispheres. Excluding the spinal cord, all make up the brain. The brain is also commonly divided into three parts: the hindbrain (the medulla, pons, and cerebellum), midbrain, and forebrain (diencephalon and cerebral hemispheres). The hindbrain (excluding the cerebellum) and midbrain comprise the brain stem. Fig. 2.1 shows the main anatomy of the brain. In the following only relevant regions to the further chapters are listed with brief comments.

### 2.2.1 The Neocortex

The neocortex is the largest structure in the human brain (90% of the cerebral cortex is neocortex) (Kandel et al., 1995). The neocortex is the main seen structure when the skull is removed as it is the outer layer of the cerebral hemispheres. The term "cortex" is a Greek word means bark and "neo" is for new. The cortex lies indeed like a bark over the rest of the brain, see Fig. 2.1(a) and 2.1(c). In essence, the neocortex is a two-dimensional structure a few millimetres thick. The human cortex is like a thick sheet of a huge number of fine structures that are perfectly packed to each other. The cortical area is about  $2500 \text{ cm}^2$  (equivalent to  $\approx 50 \text{ cm} \times 50 \text{ cm}$ ). To fit all this structure into the skull, the cortex is folded (convoluted) like a crumbled sheet of paper. In most other mammals (except dolphins) the convolution is less as there is less cortex to fit in. The cortex is made up of six layers labelled with I to VI; the labelling start from the outermost layer I. Due to its relative size in human brain, it is believed that it is important for the higher order processing and functions unique to humans. The involved functions are e.g. sensory perception, motor commands, spatial reasoning language and conscious<sup>1</sup>.

As illustrated in Fig. 2.1 the following parts are (roughly) functionally distinguishable (Kandel et al., 1995; Purves, 2008):

1. In the back there is the occipital area, this area is important for visual processing. Removing this part leads to blindness, or partial loss of function (such as color vision, or motion detection). A very large part (some 40%) of the human brain is devoted to visual processing, and humans have compared to other animals a very high visual resolution. Visual processing here refers to the visual memory as well despite the lack of clear separation between the different neural circuitries responsible for input processing and information retrieval.
2. The medial part (the side part) is involved in higher visual processing, auditory processing, and speech processing. Damage in these areas can lead to specific deficits in object recognition or language. More on top there are areas involved with somato-sensory input, motor planning, and motor output.
3. The frontal part is the "highest" area. The frontal area is important for short-term or working memory (lasting up to a few minutes). Planning and integration of thoughts takes place here. Removal of the frontal parts (frontal lobotomy) makes peoples into zombies without long-term goals or liveliness. Damage to the prefrontal has varied high-level effects.

In lower animals, the layout of the nervous system is more or less fixed. In insects the layout is always the same: if one studies a group of flies, one finds the same neuron with the same dendritic tree in exactly the same place. But in mammals the precise layout of functional regions in the cortex can vary strongly between individuals. Left or right-handedness and native language will also be reflected in the location of functional areas. After a stroke other brain parts can take over

---

<sup>1</sup>Some of these functions are observed as well among dolphins.

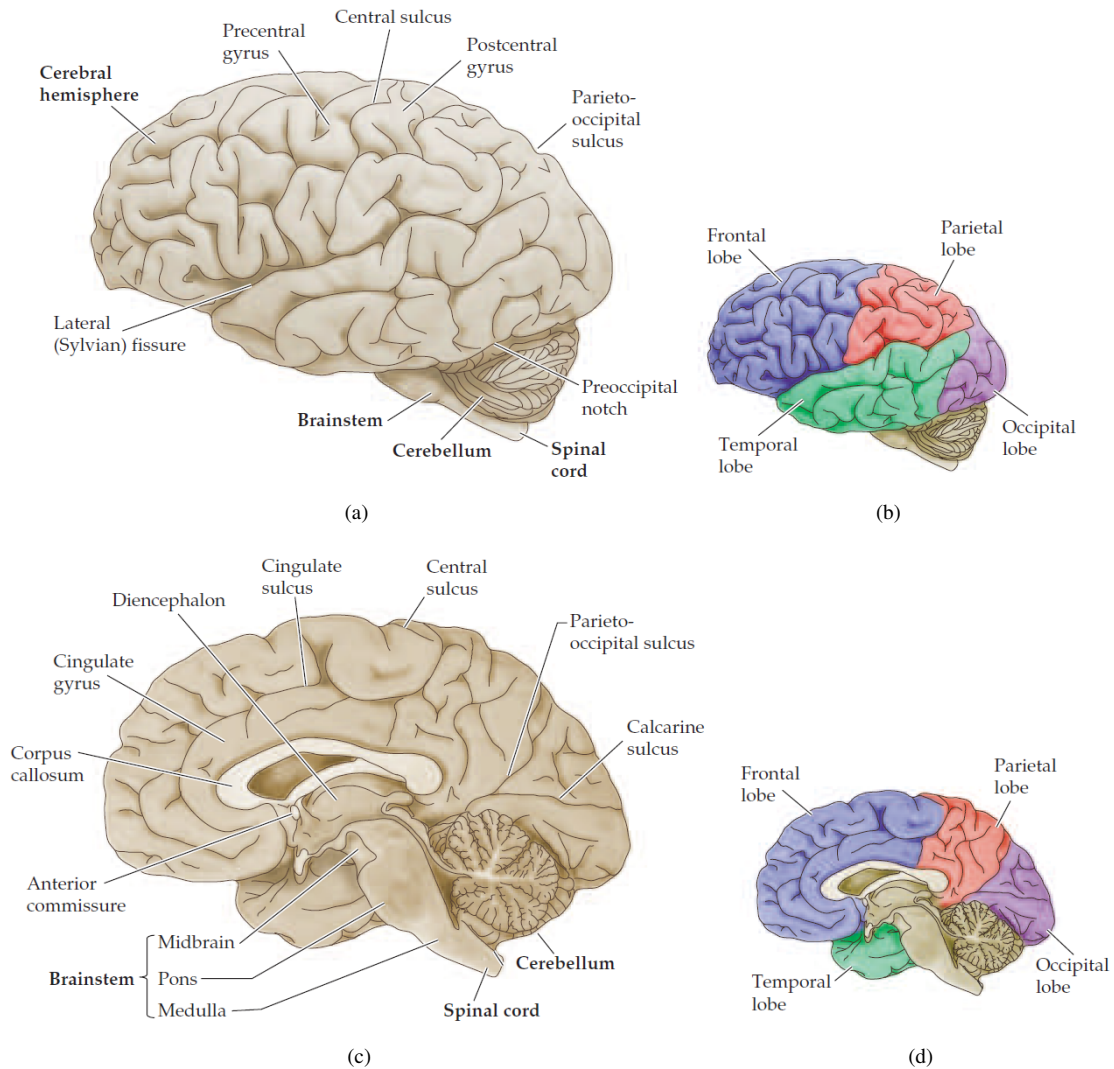


**FIGURE 2.1:** Main anatomy of the brain, images adapted from (Purves, 2008). (a) Cerebral hemisphere surface anatomy, showing the four lobes of the brain and the major sulci and gyri. The ventricular system and basal ganglia can also be seen in this phantom view. (b) and (d) illustrate the different lobes of each hemisphere from the outer and sagittal views respectively. (c) Midsagittal view showing the location of the hippocampus, amygdala, thalamus and hypothalamus.

the affected part's role. With young children in particular who have part(s) of their brains removed (might be up to half the brain), spared parts of the cortex can take over many functions, see e.g. (Immordino-Yang, 2007). Lesions of small parts of the cortex can produce very specific deficits, such as a loss of color vision, a loss of calculation ability, or a loss of reading a foreign language. This localization of functions in the cortex is supported with fMRI studies. This is important as it shows that computations are carried out in a distributed manner over the brain (unlike a conventional computer, where most computations take place in the CPU). Similarly, long-term memory seems distributed over the brain (Kandel et al., 1995).

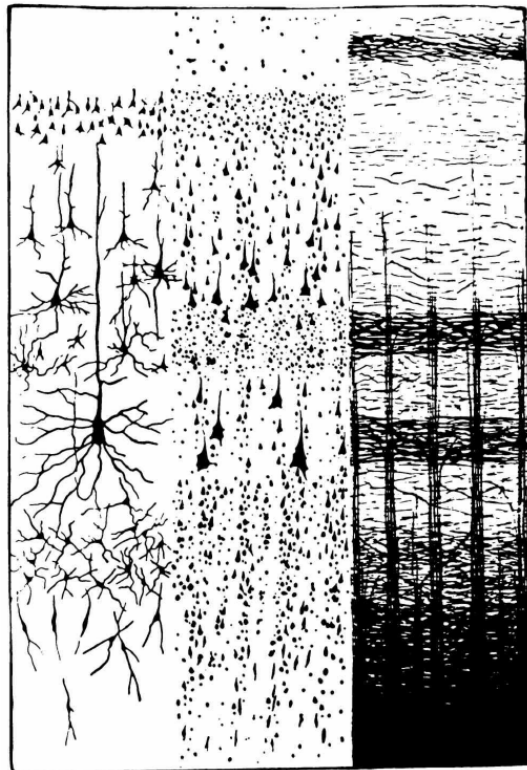


**FIGURE 2.2:** Layers in the cortex made visible with three different stains. The Golgi stain (left) labels the soma and the thicker dendrites (only a small fraction of the total number of cells is labelled). The Nissl stain shows the cell bodies. The Weigert stain labels axons. Note the vertical dimension is one or two millimeters. These drawings are originally from S. Cajal (1899) and adopted From (Abeles, 1991).

**Cortical layers** A sample of cortex tissue beneath  $1\text{mm}^2$  of surface area will contain about 100,000 cells. By staining, a regular lay-out of the cells can be seen as shown in Fig. 2.2. In this illustration, the input and output layers are arranged in a particular manner that holds for cortical areas with functions related to lower and higher vision, audition, planning, and motor actions. Although this particular layout of layers of cells is so common, the exact reasons behind it and what its exact computational function is, is not clear (Purves, 2008).

The connectivity within the cortex is huge (about 100,000 km of fibers). Instead of a hierarchical arrangement, as feed-forward networks, a particular area in the cortex receives not only feed-forward input from lower areas, but also many lateral and feedback connections. The feed-back connections are usually excitatory (Purves, 2008).

### 2.2.2 The Cerebellum

Despite the term "cerebellum" in Latin stands for little brain, it is a large structure (10% of the total volume of the brain) looks separate and attached to the bottom of the brain. The cerebellum is a highly convolved structure as well and it is a beautiful two-dimensional structure, i.e. it is actually a continuous thin layer of neural tissue (the cerebellar cortex), perfectly and tightly folded in similar fashion to the neocortex.

Functionally, it is involved in many cognitive functions. Its movement-related functions are the most clearly understood. The cerebellum does not initiate movement, but it contributes to coordination, precision, and accurate timing. Within this thin layer are several types of neurons with a highly regular arrangement. Notably are the Purkinje cells and granule cells. This complex neural network gives rise to a massive signal-processing capability as the cerebellum is involved in precise timing functions. It integrates inputs from sensory systems, other regions in the brain and spinal cord, the processed output signals are fed to fine tune motor activity (Fine et al., 2002). Based on this fine-tuning functions, malfunctioning or dissection of the cerebellum does not cause paralysis; instead it disrupts fine movement, equilibrium, posture, and motor learning (Fine et al., 2002; Kandel et al., 1995).

### 2.2.3 The Hippocampus

The hippocampus (Latin for sea-horse<sup>2</sup>) is a structure which lies deep in the cerebral hemispheres. As a whole, it has the shape of a curved tube and is composed of four regions CA1 through CA4. It plays a pivotal role in the consolidation of information from short-term memory to long-term memory and spatial navigation in mammals. Removal of the hippocampus leads to (anterograde) amnesia. That is, although events which occurred before removal are still remembered, new memories are not stored, see e.g. the H.M. case (Kandel et al., 1995, Ch. 35). Therefore, it is assumed that the hippocampus works as an association area which processes and associates information from different sources before storing it. It has been suggested that the hippocampus is a temporary archive for long-term memories; it may store long-term memories for long time intervals (up to weeks) and gradually transfer these memories to predefined certain regions of the cerebral cortex.

### 2.2.4 The Glial Cells

Beside neurons (explained in next sections) there is another important cell<sup>3</sup> type in the brain, the so-called glial cells. The term "glial" comes for the Greek word of glue, but they do not glue the neurons to each other. There are 10 to 50 times more glial cells than neurons in the CNS. These cells don't contribute any computation, rather they provide structural support to the neural tissue; they act as buffers maintaining the concentrations of ions in the extracellular fluids. Moreover, they suck up the spilt over neurotransmitters, and others provide myelin sheets around the axons of neurons.

---

<sup>2</sup>or *Cornu Ammonis* the Latin for ram's horn

<sup>3</sup>The word cell originates from the Latin *cellula*, that is a small room. This term for the smallest living biological structure was first coined by Robert Hooke in his book *Micrographia*, 1665. From wikipedia.org

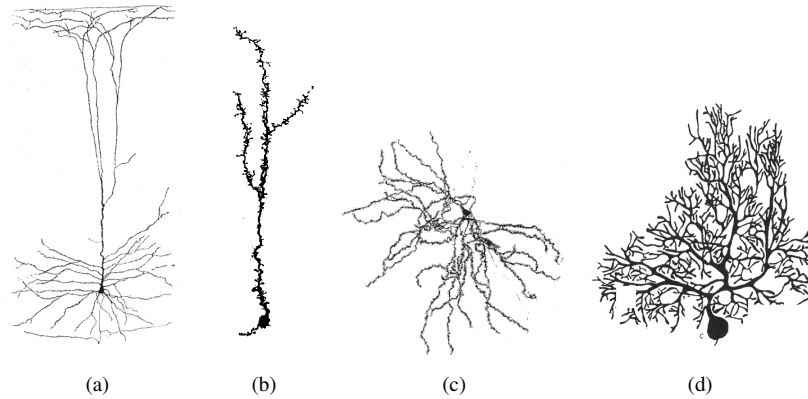


**FIGURE 2.3:** Examples of morphologies of different neurons. Images are adapted from (Trapenberg, 2002). (a) Pyramidal cell from the motor cortex: Layer V neocortical pyramidal cell in rat (1.03 mm) (Koch, 1993) (b) Granule neuron from olfactory bulb of mouse (0.26 mm). (c) Spiny neuron from the caudate nucleus. (d) Golgi-stained Purkinje cell from the cerebellum.

### 2.3 The Neuron

The term "neuron" was coined by the German scientist Heinrich Wilhelm Gottfried von Waldeyer-Hartz in 1891, actually he has invented this fortunate term. In the human brain, there are some  $10^{11}$  neurons of various types and shapes corresponding to their location and function, see e.g. Fig. 2.3. Every neuron has a cell body, or the soma, that contains the nucleus of the cell. The nucleus is essential for the cell, as it is the metabolic central factory where the protein synthesis takes place. The neuron receives its input through synapses on its dendrites (dendrite: Greek for branch). The dendritic trees can be very elaborate and often receive more than 10,000 synapses. The axon may extent up to one meter as in the case of the sciatic nerve feeding the muscles of lower limbs. Around the axons, lipid based sheets of cells are built in segments separated at different distances. These lipid segments are the myelin sheets, separated by the Ranvier nodes where the action potentials are regenerated. The myelin sheets are responsible of increasing the speed of signal propagation along axons. The basic anatomy of the neurons is shown in Fig. 2.4.

The axons (between  $0.2\text{--}20\text{ }\mu\text{m}$  in diameter) are the main conducting element of the neurons. The generation of a spike rises from the difference in the chemical composition between intra- and extracellular fluids (Hammond, 2001, Ch. 5); both liquids contain a variety of ions such as  $\text{K}^+$ ,  $\text{Na}^+$ ,  $\text{Ca}^{2+}$  and  $\text{Cl}^-$ . For example the  $\text{K}^+$  concentration outside the neuron is much lower than inside the neuron. The membrane embeds a variety of so called ion channels which are usually permeable for only one type of ions. The permeability of the membrane and the specific distribution of ions result in a potential difference across the membrane, it is the membrane resting potential. If there are no inputs impinging onto the neuron the membrane is at its resting potential. The value of the resting potential varies between  $-30\text{ mV}$  and  $-90\text{ mV}$  depending on the cell type. If the input to a cell drives the membrane potential at the axon hillock (a small bump at the start of the axon) above a certain threshold an action potential or a spike is initiated (depolarization phase). After a spike has been rendered the neuron enters a refractory period (phase of after hyperpolarization).



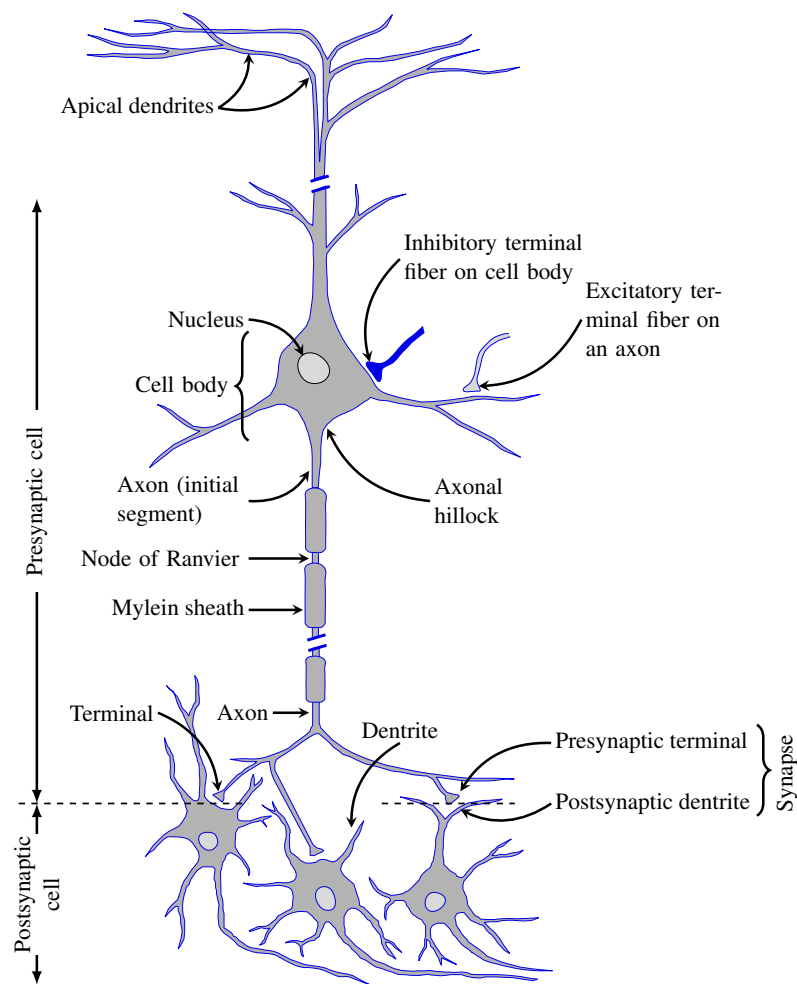


**FIGURE 2.4:** Sketch of the typical morphology of a pyramidal neuron (multipolar). The components outlined in the drawing are typical for most major neuron types (Kandel et al., 1995).

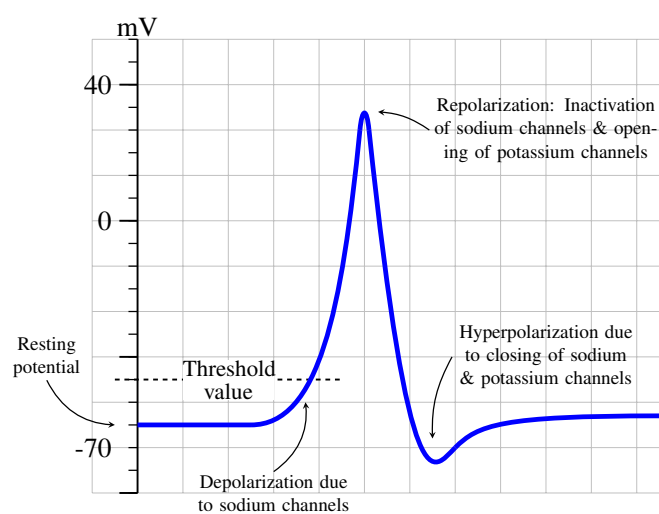


**FIGURE 2.5:** An example of a typical action potential in phasic spiking. The action potential is simulated using the Hodgkin-Huxley model (Hodgkin and Huxley, 1952) with Matlab (MathWorks). In phasic spiking, a neuron fires a single spike at the onset of the stimulus and remains quiet afterwards (Hammond, 2001, Ch. 20).

Immediately after a spike it is impossible to generate a spike, as the threshold for generating a spike is infinitely high. After this absolute refractory period (2–5 msec) the threshold approaches its nominal value. This period is called relative refractory period (2–20 msec). During this relative refractory period the membrane often goes well below the resting potential. The firing threshold value is not a static constant, i.e. it varies according to the history of cell's spiking activity, cell type and density of interconnectivity. A schematic of an action potential is illustrated in Fig. 2.5.

The electrical signals that propagate along the axons are the action potentials (APs or spikes). They follow the all-or-none law. Action potentials are rapid (up to 100 m/sec) and short impulses (about 1 msec) with an overall amplitude of 100 mV (usually from the resting potential of -70 mV and to the maximum point at 40 mV). The spike propagates along the axon and dendrites (i.e. both ways). Travelling spikes along axons are the main means of information transfer in the neural circuitry<sup>4</sup>.

The axons in cortical regions are connected to each other with axons forming what is called the white matter, because the layer of fat gives the neurons a white appearance. The axon ends in many axon terminals where the connections (synapses) to next neurons in the circuit are formed. The number of synaptic connections may vary from 10,000 (2000 contacts on the cell body while 8000 are on the dendrites) for a spinal motor cell up to 150,000 contacts in a Purkinje cells (Kandel et al., 1995, Ch. 2).

From a biological perspective, the spike trains that carry e.g visual information are similar (if not identical) to other signals that carry e.g. auditory information (in terms of form and amplitude). This reflects one of the main principles in cerebral action: The characterization of the information conveyed by spikes are determined by the pathway over which the signal travels rather than the form of the spikes (Kandel et al., 1995).

## 2.4 The Synapse

In the nervous system, a synapse is a junction that permits a neuron to pass an electrical or chemical signal to another cell. The word "synapse" comes from "synaptein", which Sir Charles Scott Sherrington and colleagues used from the Greek "syn-" ("together") and "haptein" ("to clasp").

### 2.4.1 Connecting Element: The Synapse

Synapses are essential to neural functions as they are the means to pass signals to individual target cells. At a synapse, the cellular membrane of the presynaptic neuron comes proximately to the membrane of the target (postsynaptic) cell. Both the presynaptic and postsynaptic sites contain extensive assembly of molecular machinery that carries out the signalling process.

There are fundamentally two different types of synapses:

---

<sup>4</sup>Although it is not yet well understood, proteins and hormones along with other chemical constituents of the CNS are believed to play an important role as well in information storing, processing and retrieval (Koch, 1993; Purves, 2008).

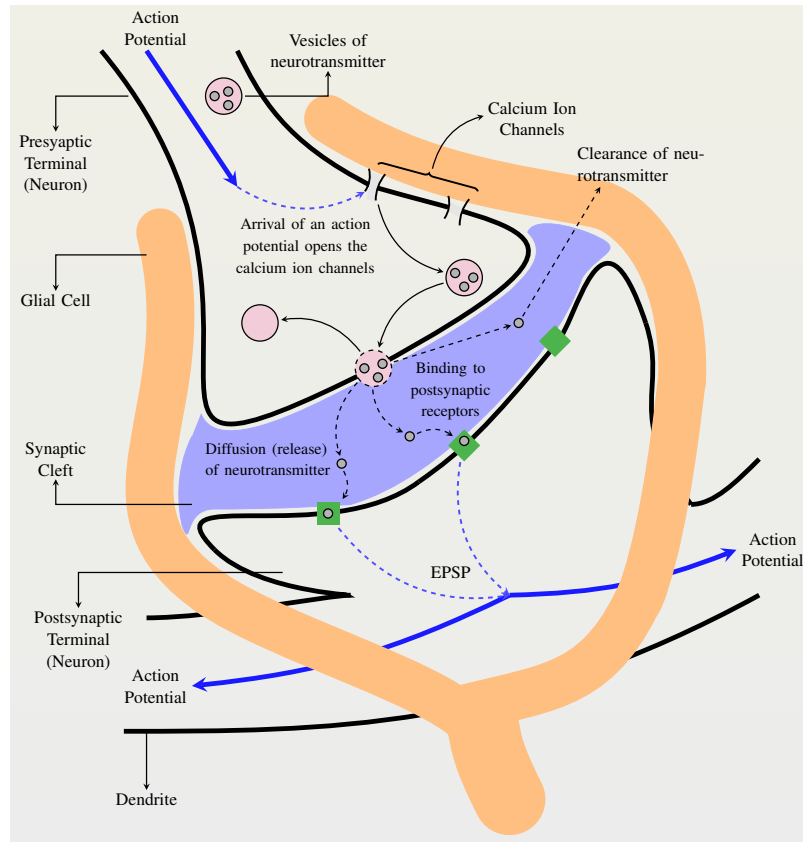


**FIGURE 2.6:** Schematic illustration of chemical synapses. The accumulation of excitatory post synaptic potentials (EPSP) is illustrated in relation to both the arriving and generated action potentials.

- Chemical synapse:** The presynaptic neuron releases a chemical called a neurotransmitter that binds to receptors on the postsynaptic cell membrane facing the presynaptic one. The binding process is the key to the transmission of the signal from the presynaptic cell to the postsynaptic one (Kandel et al., 1995).
- Electrical synapse:** Or gap-junction where both the presynaptic and postsynaptic cell membranes are connected by channels at the synaptic site, where currents can pass through. This lets voltage change in the presynaptic cell to stimulate voltage changes in the postsynaptic cell. This allows the action potential to cross from the membrane of one neuron to the next without the utilization of a neurotransmitter. Electrical synapses lack the directional specificity of chemical synapses and may transmit a signal in either direction<sup>5</sup>. During biological activity, electrical synapses do not have a wide spectrum of internal dynamics as in the case with chemical synapses (Kandel et al., 1995; Purves, 2008). Unless otherwise is stated, gap-junctions are not considered any further. In this thesis the used notation of a synapse refers only to a chemical synapse.

<sup>5</sup>Some experimental evidences describe the same effect for chemical synapses as well, see (Burt, 1993; Kandel et al., 1995, Ch. 15,16)

The overwhelming majority of synapses in the human brain are chemical synapses. Thus, the release and capture of neurotransmitter substances from one neuron to another forms the basis of neural communications. There are three primary components (regions) within a synapse, see Fig. 2.6: the presynaptic terminal, the synaptic cleft, and the postsynaptic site (Burt, 1993; Kandel et al., 1995):

- **Presynaptic Specializations:** Most synapses occur between the axon of a presynaptic neuron and the dendrite or cell body of a postsynaptic neuron. Excluding cell to cell synapses all other combinations are possible.

The axon terminal is a swelling in the axon which contains synaptic vesicles. Synaptic vesicles are small packages filled with molecules of the neurotransmitter. When the axon terminal is depolarized by an action potential, another kind of voltage-gated channel opens and allows calcium ( $\text{Ca}^{2+}$ ) ions to flow into the axon terminal. The  $\text{Ca}^{2+}$  ions cause the synaptic vesicles to migrate toward the cell membrane. They fuse with the membrane, and discharge their package of molecules into the synaptic cleft. This process is called exocytosis (The rush in of  $\text{Ca}^{2+}$  is vital for synaptic transmission, i.e. without  $\text{Ca}^{2+}$  there is no exocytosis).

The membranes of empty vesicles become part of the presynaptic membrane and new vesicles pinch off from an adjacent area of the membrane. These new vesicles are subsequently refilled with newly synthesized or "recycled" neurotransmitters. Fig. 2.6 illustrate a general schematic of the process.

- **Synaptic Cleft:** It is the narrow gap between the pre- and postsynaptic neuron. It is filled with the same fluid which all neurons are bathed in. It is approximately 10-20 nm across; the molecules of neurotransmitter merely drift (diffuse) across the fluid filled gap. The gap is so narrow, however, that on average it requires only 0.1 millisecond for this diffusion to occur. The total delay associated with synaptic communication, from the arrival of an action potential at the presynaptic membrane until the time a postsynaptic response is observed, is approximately 0.5 ms.

There are literally hundreds of neurotransmitters. Some are fairly simple compounds such as acetylcholine, serotonin, the catecholamines (dopamine, norepinephrine, and epinephrine) and a number of the amino acids. Many are more complex and belong to the vast array of neuropeptide transmitters. Once released into the synaptic cleft, neurotransmitters remain active until they are either altered chemically or taken back into the synaptic knob by special carrier systems and recycled.

- **Postsynaptic Specializations:** At the postsynaptic membrane, neurotransmitter molecules bind to membrane-bound receptor molecules with recognition sites specific for each neurotransmitter. Binding of the neurotransmitter to the receptor triggers a postsynaptic response particular for that receptor. The responses can be either excitatory or inhibitory, depending

**TABLE 2.1:** The main synaptic neurotransmitters and related receptors.

Neurotransmitters	Details	Function & Receptor
Glutamate	Amino acid	AMPA & NMDA receptors, Excitatory
GABA	$\gamma$ -aminobutyric acid	GABA <sub>a</sub> & GABA <sub>b</sub> * receptors, Inhibitory
Acetylcholine	Ester of acetic acid and choline	Neuromuscular and CNS
Noradrenaline	N-methyl-D-aspartic acid	Modulator

\* GABA<sub>b</sub> receptors are also known as the second messengers.

on the properties of the receptor. If receptor stimulation results in the postsynaptic membrane becoming more electrically positive (depolarized), it is an excitatory postsynaptic potential (EPSP). If more negative (hyperpolarized), it is an inhibitory postsynaptic potential (IPSP). Examples of both local responses are illustrated in Fig. 2.7. In this illustration,  $\alpha$ -function is used as a phenomenological model to parametrize the synaptic action rather than describing the actual biochemical mechanisms of ion channels. Either excitation or inhibition depends on the properties of the receptor and not on the neurotransmitter, see Tab. 2.1 for an overview. Receptors coupled to sodium or calcium channels are excitatory and produce a depolarization of the postsynaptic membrane (AMPA and NMDA receptors), whereas receptors coupled to chloride or potassium channels are inhibitory and produce a hyperpolarization of the postsynaptic membrane (GABA<sub>a</sub>). Such receptors coupled to ion channels are called ionotropic receptors (Hammond, 2001, Ch. 9). Excitatory AMPA<sup>6</sup> and NMDA<sup>7</sup> receptors are responsible for another kind of special feature which is known as the long-term potentiation (LTP). As its name may infer, LTP is characterized by a long-lasting enhancement in signal transmission between two neurons that induced by high frequency paired-firing between pre- and postsynaptic cells. LTP is believed to contribute to memory expression and storage.

Other receptors are coupled to "second-messenger" systems (GABA<sub>b</sub>) that initiate a series of biochemical reactions in the postsynaptic cell. These are metabotropic receptors. Metabotropic receptors can produce many different postsynaptic events. These range from the direct activation of adjacent ion channels, to alteration of receptor sensitivity, to transcription of specific messenger ribonucleic acids (RNAs), or even the activation of specific genes. See (Hammond, 2001, Ch. 7–15) for an extensive detailed explanations of the neurotransmitter-receptor dynamics and the biological underlying mechanisms.

In summary, chemical synapses build a very adaptable and flexible communication system. They are not static anatomical structures with fixed properties but are dynamic structures, able to change their molecular properties with changing circumstances (Burt, 1993).

<sup>6</sup>2-amino-3-(5-methyl-3-oxo-1,2-oxazol-4-yl) propanoic acid (Hammond, 2001; Kandel et al., 1995)

<sup>7</sup>N-Methyl-D-aspartic acid or N-Methyl-D-aspartate (Hammond, 2001; Kandel et al., 1995)

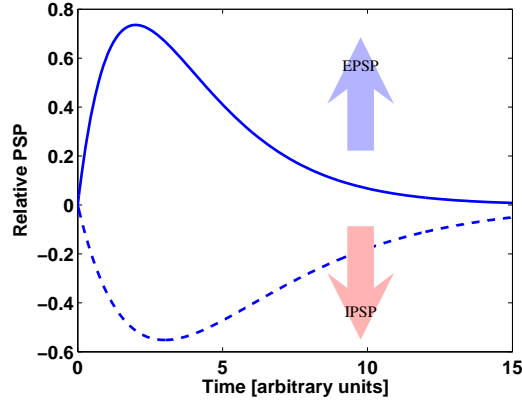


**FIGURE 2.7:** Examples of an EPSP (solid line) and IPSP (dashed line). Both are simulated as  $\alpha$ -functions for the local synaptic response after the synaptic delay. The  $y$ -axis shows the relative post synaptic potential (PSP). The used  $\alpha$ -functions are:  $t \cdot e^{-t/2}$  in case of EPSP and  $-0.5t \cdot e^{-t/3}$  for IPSP (Trappenberg, 2002). The time scale is variable and not meant to fit any experimental data.

## 2.4.2 The Stochastic Nature of Synaptic Transmission

As for chemical synapses, the above described process of synaptic release is an idealization of the real unreliable process. Synaptic release of neurotransmitters due to an invading action potential is a stochastic binary event with relatively low probability around 0.1 (Dobrunz and Stevens, 1997; Natschl ger, 1999). It has been shown that the release of the contents from each vesicle (quantum of neurotransmitter) is probabilistic and it is independent of previous releases. The quantal concept of release was first investigated and introduced in (Fatt and Katz, 1952), see (Augustine and Kasai, 2007) for a comprehensive review. At each synapse, there is a number  $n$  of release sites: where the vesicles can fuse in the membrane and release their contents. If each such site independently releases either no or only a single packet or quantum of transmitter with probability  $p$ , then the probability  $p(k; n)$  of  $k$  packets being released at the entire functional synapse (the synaptic site) is given by a binomial distribution:

$$p(k, n) = \frac{n!}{(n - k)!k!} p^k (1 - p)^{n - k}. \quad (2.1)$$

At the neuromuscular junction, where motor neurons contact muscle cells, the probability of release can be significantly low. This comes from the fact that there exist on the order of 100 to 1000 release sites, the overall synaptic transmission from the nerve onto the muscle is still very reliable. In contrast to the neuromuscular junctions, in the central synapses, e.g. in the hippocampus or the cortex, each synaptic terminal contains only one or a few active release sites, rather than the hundreds found at the neuromuscular junction (Dobrunz and Stevens, 1997; Markram et al., 1997). This means that, upon arrival of an action potential at an individual anatomical synapse, typically none or only one vesicle is released (the one-vesicle hypothesis) (Yusim et al., 2001).

For large  $n$  (many quanta that can be released) and for small probability of release (small  $p$ ) the Poisson distribution describes the release probability better than the binomial one, otherwise the

binomial model is reliable. The Poisson distribution, which is a special case of the binomial one, is a discrete probability distribution that expresses the probability of a number of events occurring in a fixed period of time if these events occur with a known average rate and independently of the time since the last event. In other words, in the case of a Poisson distribution, one defines the average rate of release  $r$  over a time period  $t$  after the arrival of an action potential. Let  $m = r \cdot t$ , then the probability of having  $k$  releases is

$$p(k) = \frac{m^k e^{-m}}{k!}, \quad (2.2)$$

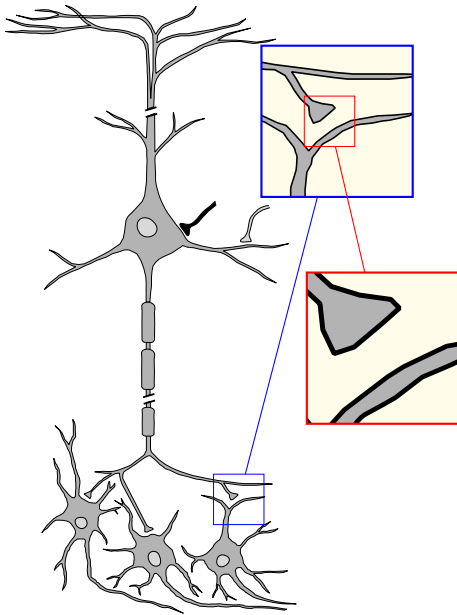
where  $k$  is the number of released quanta.  $m$  is the mean value of the Poisson distribution. The Poisson distribution better matches, thus, the case of neuromuscular junctions while the situation of central synapses, e.g. within the hippocampus, is well fitted to the binomial model (Branco et al., 2008).





# Part I

## EFFICIENT & OPTIMIZED MODELING OF SYNAPTIC DYNAMICS



Part I tackles the first level of abstraction out of the two levels investigated in this thesis. It is concerned with the detailed inspection and modelling of synaptic dynamics. The state-of-the-art models of neuronal as well as synaptic dynamics are listed in Ch. 3. In Ch. 4 our novel proposed synaptic model is given in details. In this chapter more light is shed over the relevance of the adopted level of abstraction in modeling the synaptic dynamics. Ch. 5 illustrates a case study in which the proposed synaptic model is used to predict the exact spike timing of a postsynaptic neuron in the visual cortex. This case study represents a validation to the modelled dynamics against its biological counterparts. Ch. 6 discusses the energy-related aspects of the proposed synaptic model. In this chapter a novel theoretical consideration of the synaptic energy is introduced.



# Chapter 3

## State of the Art: Modeling Neural Networks

*"As far as the laws of mathematics refer to reality, they are not certain; and as far as they are certain, they do not refer to reality."*

**Albert Einstein, "Geometry and Experience", 1921**

### 3.1 Introduction

In this chapter the basic methods of modelling the functional units of neural systems (neurons and synapses) are reviewed. In the following section, the representation of neural information (or the neural code) is discussed. Afterwards the state of the art models of neuronal and synaptic dynamics are listed. Special details about the models of synaptic dynamics are discussed.

### 3.2 The Neural Code

Finding the proper representation of neural information is an active research field. The most general types of representing neural information (actually spike trains) are: rate coding and temporal coding (Dayan and Abbott, 2005).

#### 3.2.1 Rate Coding

There are three different subclasses of rate coding in the literature (Gerstner, 1999). First, it is the rate coding as spike count defined with the simple temporal average of arriving spikes from a single neuron over a certain time period. Second, the rate as spike density that is defined as an average over several runs. Finally, the population activity which is the same as spike count but the

averaging involves a population of neurons rather than a single one. The latter is called space rate coding as well (Koch, 1993).

Rate coding is regarded as plausible in describing the relation between neural spiking and muscular contraction (Kandel et al., 1995). However, the evidences from both theoretical and experimental studies suggest that the concept of rate coding based on the temporal averaging is away too simple for describing CNS activities. A basic argument is that some reaction times in cognitive experiments are too short to permit slow temporal averaging. Moreover, the observed precise temporal correlations between different neural spiking activities and synchronization in populations of neurons refuse the naive simplification of rate coding. As computational units, it is questionable whether biological neurons can perform analogue computations with analogue variables represented as firing rates (Dayan and Abbott, 2005; Koch, 1993).

### 3.2.2 Temporal Coding

Temporal coding considers that the exact timing of spikes carries the neural information. There exist many forms of applying this concept. The most relevant are time-to-first-spike, correlation with synchrony and what is called the simple temporal coding (Dayan and Abbott, 2005). In time-to-first-spike, the information is coded as the elapsed time from each incoming spike to the first occurring one. It has been shown that this type of coding permits networks to perform very fast computations (Maass, 1997). In correlation with synchrony, spikes from different neurons are used as reference for certain internal code. Thus, synchrony between a pair of neurons or among populations could indicate the transfer of certain information that can not be contained in the averages of spikes (Singer, 2007). Moreover, spatio-temporal spike patterns are believed to be meaningful and informative (Iglesias and Villa, 2010). Synchrony in particular is investigated in much more details in Ch. 9 where synchrony is proposed as a basic mechanism of information preprocessing and information representation within neural networks.

The simple temporal coding scheme is the most used in simulations, see (Koch, 1993) for a review. With this type of coding a spike train is represented as a sequence of stereotyped events that mark the time instants at which a spike (action potential) occurs. A spike train  $F$  is represented as:

$$F = \sum_i \delta(t - t_i), \quad i = 0, 1, 2, \dots \quad (3.1)$$

where  $t_i$  is the timing of the  $i$ th spike.  $\delta(t)$  is the Dirac-delta function, with  $\delta(x) = 0$  for  $x \neq 0$  and  $\int_{-\infty}^{\infty} \delta(x) dx = 1$ . Spikes are reduced then to sharp segments located at the spiking times, see Fig. 3.1. The actual information is then stored in the inter-spike intervals (ISIs). As shown in Fig. 3.1, the time intervals between each couple of subsequent spiking times define  $\Delta_{isi}$ . Before the very first spike,  $\Delta_{isi}$  is taken to be a very large value or it vanishes. The choice depends on the required boundary conditions within the different models. The time series defined by the sequence of intervals between spikes carry the temporal information from the spike train. A Poisson

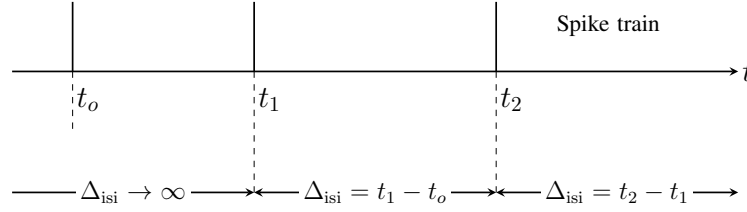


**FIGURE 3.1:** Simple temporal coding: spike representations and inter-spike intervals.

distributed spike train implies thus that the probability density function of this time series follows a Poisson distribution.

Neuronal models that implement temporal coding are referred to as spiking models. Synaptic models featuring temporal coding are called in general dynamic synapses (Dayan and Abbott, 2005). Based on the reported limitations of rate coding in Sec. 3.2.1 and as it is suggested from Ch. 1 regarding the main target of understanding and capturing basic capabilities in CNS, solely temporal coding and temporal coding based models are adopted and used for simulations in the presented work.

### 3.3 Artificial Neural Networks

The term neural network was traditionally used to refer to a network or circuit of biological neurons. The modern usage of the term often refers to artificial neural networks (ANN), which are composed of artificial neurons (or computation nodes). The biological paragon is the neural system. ANN are composed of interconnecting artificial neurons. They may either be used to gain an understanding of biological neural networks, or for solving artificial intelligence problems without necessarily creating a model of a real biological system. ANN are used as well in a wide diversified range of technical applications.

The real, biological nervous system is highly complex: artificial neural network approaches attempt to *abstract* this complexity and focus on what may hypothetically matter most from an information processing point of view as mentioned in Ch. 1. And this is the very core of this thesis. A general motivator for the abstraction imposed in developing the ANN is to reduce the amount of computation required to simulate ANN, so as to allow one to experiment with larger networks and train them on larger data sets. Good performance in terms of mimicking animal or human behaviour (actions), can then be used as one source of evidence towards supporting the hypothesis that the abstraction indeed captured something important regarding information processing in the brain.

A typical feedforward ANN is shown in Fig. 3.2. In this network there are mainly three groups of neurons: the input neurons in the input layer, the hidden neurons in the hidden layer(s) and the output neurons in the output layer. The neurons are illustrated as circles and the synapses are those

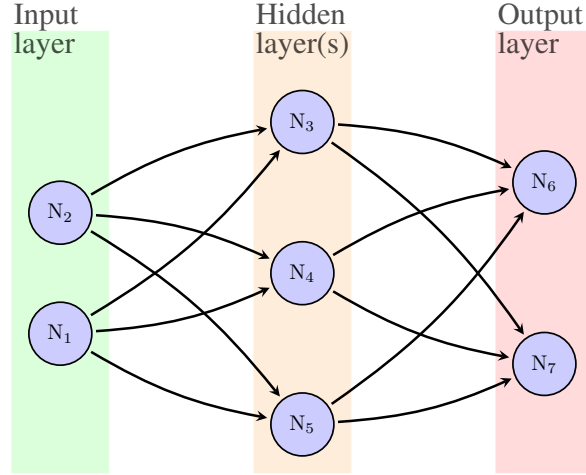


**FIGURE 3.2:** Schematic of artificial neural networks (feedforward configuration). Circles indicate computation nodes which are neurons implemented as neuronal models (either rate coded or spiking models). Arrows are the connections that represent the synapses and they are implemented as either synaptic weights (rate coding) or dynamic synaptic models (temporal coding). The neurons are usually arranged in three main layers: input layer, hidden layer(s) and output layer. The hidden layer can be layers, i.e. the hidden neurons might be arranged in multiple layers.

arrows connecting the neurons. Being a feedforward ANN implies that all the synapses carry information along the same direction from input layer into the output layer through the hidden layer(s). Recurrent networks are then those with synapses connecting all neurons to each other. Mixed settings between feedforward and recurrent networks are also used (Neelakanta and DeGroff, 1994), the task complexity and available computing resources usually decide the network configuration.

Different approaches are used in modelling the computational units of neurons and synapses. A classical type of ANN uses models of rate coding (Neelakanta and DeGroff, 1994). Synapses in classical ANN are represented with static weights (scaling factors) which belong to rate coding as well. When the neuronal models implement temporal coding (spiking neuronal models) the ANN are called spiking neural networks (SNN), see e.g (Gerstner, 1999) for a review. Considering dynamic synapses, a network that uses both spiking neuronal models and dynamic synapses is referred to as a dynamic network (*DN*) (Maass and Sontag, 2000).

As mentioned before in Sec. 3.2.1 rate coding is not regarded as the best approach of representing neural information in the CNS as it suppresses the relevant information feature of spike timing. Thus, in the context of the presented work, only the spiking neuronal models and dynamic synaptic models are explained and considered for the simulations in this thesis.

### 3.4 Neuronal Models

Models of neuronal dynamics range from the very basic McCulloch-Pitts neuron (the perceptrons and rate models) (McCulloch and Pitts, 1943) through the FitzHugh-Nagumo model (Fitzhugh, 1961) to the detailed biophysical model of Hodgkin-Huxley (Hodgkin and Huxley, 1952) and its

compartmental models<sup>1</sup>. For excellent reviews see (Gerstner, 1999; Gerstner and Naud, 2009). The models differ consequently in terms of the required computer power to simulate them (Izhikevich, 2004); this factor plays a vital role in the popularity of certain models.

The most common spiking models are addressed in the following section. Namely, the leaky integrate-and-fire and the spike-response models are explained. The first is regarded as simple in terms of the required computational power for implementation without loss of biological plausibility (Koch, 1993). The second model is more complex and is a mathematical generalization of the leaky integrate-and-fire model, i.e. the leaky integrate-and-fire is a special case of the second model (Gerstner, 1999). Unless otherwise stated, the simulations presented in this thesis use only the leaky integrate-and-fire model for the neuronal representation.

### 3.4.1 Leaky Integrate-and-Fire Model

The most common reduced model for spiking neurons is the leaky integrate-and-fire (LlIF) model. It was essentially introduced in 1907 by Lapique (Brunel and van Rossum, 2007). Because of its simplicity and efficient implementation, the LlIF neurons are used frequently in simulations. Each neuron is described with one internal state variable (one dimensional model), it is the neuron's membrane potential denoted by  $h(t)$ . The dynamic equation reads

$$C_h \cdot \frac{dh(t)}{dt} = -\frac{1}{R_h}(h(t) - h_{\text{rest}}) + \sum_i I_{\text{syn},i}(t), \quad (3.2)$$

where  $C_h$  and  $R_h$  are the capacitance and resistance of the membrane respectively.  $h_{\text{rest}}$  is the membrane resting potential. Without  $R_h$  the model is reduced to the standard IaF, i.e. not leaky anymore.  $I_{\text{syn}}$  is the synaptic current which can be either excitatory or inhibitory and the summation over  $i$  indicates the integration of all presynaptic inputs. Eq. 3.2 can be reduced to the more closed form:

$$\tau_h \frac{dh(t)}{dt} = h_{\text{rest}} - h(t) + \sum_i E_{\text{psp},i}, \quad (3.3)$$

where  $\tau_h$  is the membrane time constant, i.e.  $\tau_h = C_h \cdot R_h$ , the base line value  $h_{\text{rest}}$  is the membrane resting potential, and  $\sum_i E_{\text{psp},i}$  is the total accumulated and observed excitatory (or inhibitory) postsynaptic potential from all presynaptic terminals (inputs). The threshold mechanism is applied when  $h(t) \geq h_{\text{th}}$  where  $h_{\text{th}}$  is the firing threshold value: A spike is generated at time  $t$ , i.e. the membrane potential is set to the spiking potential ( $h(t) \leftarrow h_{\text{spike}}$ ) where  $h_{\text{spike}}$  is the maximum depolarization voltage (the spike voltage). At the moment after firing  $t^+$ , the membrane potential is dropped to the resting value  $h(t^+) \leftarrow h_{\text{rest}}$ . The refractory period is usually implemented by preventing the generation of a spike for certain duration  $\delta_{\text{abs}}$  after each spike,  $\delta_{\text{abs}}$  is the absolute refractory period. This is commonly performed by setting  $h_{\text{th}}$  to a very high value during  $\delta_{\text{abs}}$ .

<sup>1</sup>This order ascends in complexity rather in chronological order.

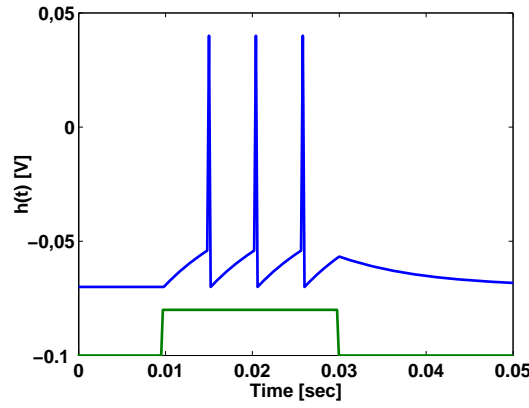


**FIGURE 3.3:** Simulation of the LIaF neuronal model. The input is a short synaptic current pulse 4 nA (green line) with a duration of 20 msec. The response of the model is shown with the blue line. In this simulation,  $\tau_h$  is set at 10 msec,  $h_{\text{rest}} = -70$  mV,  $h_{\text{spike}} = 40$  mV. The discretization step  $dt = 0.0002$  sec (implemented with the Euler-method on Matlab (MathWorks)).

LIaF is a spiking model. This implies that, the firing times defined with the time instants of threshold crossing are the output of this model. Thus, the set

$$F = \{t_1, t_2, \dots, t_i, \dots\}$$

defines the output of the model. By definition, this set is a sequence of increasing numbers, i.e.  $t_1 < t_2 < t_i$  and  $t_i \in \mathbb{R}^+ := \{z \in \mathbb{R} : z \geq 0\}$ . On contrary to the Hodgkin-Huxely model, LIaF model does not generate a real spike, rather the spike is a binary event either high or low. High might be a digital one or  $h_{\text{spike}}$ , and similarly low takes either zero or  $h_{\text{rest}}$ .

Following the analysis reported in (Izhikevich, 2004), the approximate number of floating point operations (FLOPS) required to simulate the LIaF model during a one msec time interval is around five FLOPS. In case of the Hodgkin-Huxely model, this number reaches 1200 FLOPS. Thus, LIaF model is considered to be the simplest available spiking neuronal model. Despite its simplicity<sup>2</sup>, it can be extended to count for many other dynamics as spike-rate adaptation (SRA), dynamic refractoriness and variable threshold value (this shall be used in Ch. 5). Formally, there are other popular and more complex relatives of the LIaF model, e.g. quadratic IaF and resonate-and-fire models (Izhikevich, 2004).

### 3.4.2 Spike Response Model

The spike response model (SRM) is more complex than LIaF, since it is almost a generalization of it. The central difference between the two models is that, the SRM models both the sub- and supra-threshold behaviour of the neuronal action. In other words, the form of the overshoot and its duration are calculated according to the input activity and the preceding spiking. Mathematically,

---

<sup>2</sup>LIaF model is not a linear model because of the threshold-spike-reset mechanism.



LlIF is usually represented as a differential equation, while SRM uses an integral equation to define the membrane potential.

Consider a postsynaptic neuron  $j$  that receives inputs from two presynaptic neurons  $i = 1$  and  $2$ . Neuron  $i = 1$  fires spikes at  $t_i^{(f)}$ :  $t_1^{(1)}, t_1^{(2)}, \dots$  and neuron  $i = 2$  send spikes at  $t_2^{(1)}, t_2^{(2)}, \dots$ . Each incoming spike evokes an EPSP (or IPSP) described by the functions  $\epsilon_{1j}$  and  $\epsilon_{2j}$ . The total change of the potential is approximately the sum of the individual PSPs, and the membrane potential is (Gerstner, 1999):

$$\begin{aligned} h_j(t) = & \eta(t - \hat{t}_j) + \sum_i w_{ij} \sum_f \epsilon_{ij}(t - \hat{t}_j, t - t_i^{(f)}) \\ & + \int_0^\infty \kappa(t - \hat{t}_j, s) I_{\text{syn}}(t - s) ds, \end{aligned} \quad (3.4)$$

where the functions  $\eta(\cdot)$  and  $\kappa(\cdot \cdot \cdot)$  are response kernels (filters) that describe the effect of spike emission and spike reception on the variable  $h_j$  respectively. With  $\hat{t}_j$  is the time instant of the last spike of neuron  $j$ , the kernel  $\eta(t - \hat{t}_j)$  for  $t > \hat{t}_j$  describes the form of the action potential (positive overshoot) and the (negative) spike post-potential that follows the spike, see Fig. 3.4(a). In Eq. 3.4,  $\kappa(t - \hat{t}_j, s)$  is the linear response of the membrane potential to an input current, and  $s$  is the time integral parameter. It models the impulse response of the membrane potential to a short current pulse; e.g. if an input current pulse is applied at a time  $t^*$  adequately after the firing at  $\hat{t}_j$ , it induces a standard response described by the function  $\kappa(\infty, t - t^*)$ , see Fig. 3.4(b). Therefore, the exact shape of the postsynaptic potential depends on the time  $t - \hat{t}_j$  that has passed since the last spike of the postsynaptic neuron  $j$ , see Fig. 3.4(c). The factor  $w_{ij}$  represents the strength of the connection (the synaptic weight) between neurons  $i$  and  $j$ , the synaptic modelling is explained more detailed in the following section. In the last term in Eq. 3.4,  $I_{\text{syn}}$  represents an external driving current. The two sums run over all presynaptic neurons  $i$  and all firing times  $t_i^{(f)} < t$  of each one of them. Similar to the LlIF model, when  $h_j(t)$  exceeds the firing threshold  $h_{\text{th}}$  at  $t_j^*$ , then  $\hat{t}_j \leftarrow t_j^*$  and the previous equation is calculated again. The absolute refractoriness is implemented by setting  $h_{\text{th}}$  to a very high value during  $\delta_{\text{abs}}$ .

The application of the kernels involves a convolution at each generated/incoming spike. Graphically, a contribution  $\eta$ ,  $\kappa$  or  $\epsilon$  is pasted in each time the membrane potential hits the threshold or a spike is received. This is the drawback of the model, as it requires relatively more computational power than LlIF model. Exact estimation of the FLOPS required for this model is not straight forward. The computation time required to calculate  $h_j(t)$  depends on the length of the kernels and the discretization step. The required number of FLOPS is believed to be around 100 FLOPS. More novel (and more complex) derivatives of the SRM were proposed aiming to account for the required high variability in neuronal actions (Jolivet et al., 2003, 2006; Kobayashi et al., 2009). The models were specially developed to predict the spike timing of cortical neurons (Jolivet et al., 2006). The main difference between these novel models and the basic SRM is the nonlinearity degree of the used kernels.

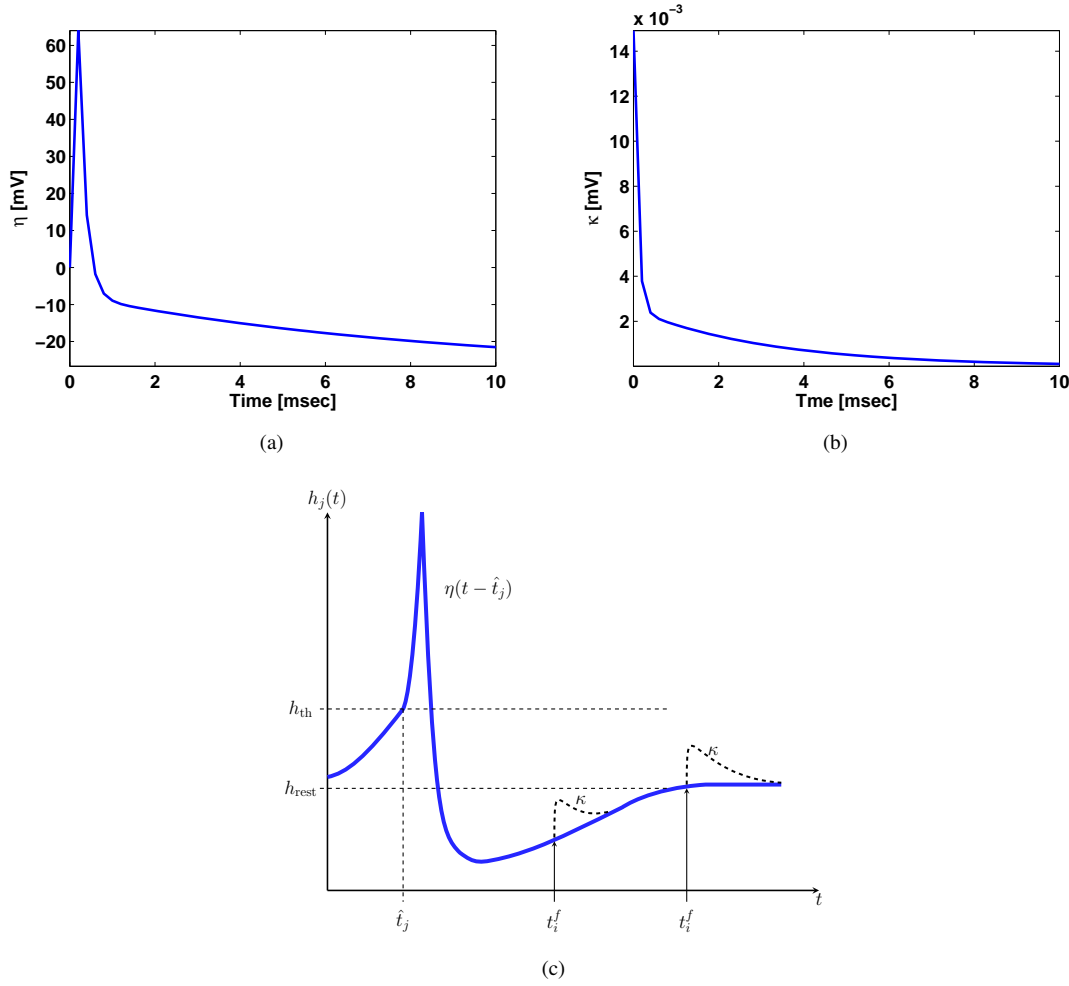


**FIGURE 3.4:** Examples of the internal kernels for SRM. (a) The  $\eta$  kernel forms the positive and negative portions of the spike. (b) The  $\kappa$  kernel represents the impulse response for an incoming presynaptic spike. (c) Schematic figure illustrates the shape of postsynaptic potentials (dashed lines) depends on the time  $t - \hat{t}_j$  that elapsed since the last spike of neuron  $j$ . The postsynaptic spike has been triggered at time  $\hat{t}_j$ . A presynaptic spike that arrives at time  $t_i^f$  shortly after the spike of the postsynaptic neuron induces a smaller PSP (here an EPSP) effect than a spike that arrives later.

### 3.5 Modelling of Synaptic Action

In this section only the class of the dynamic synaptic models are considered. Before listing the models, the main concepts of the basic synaptic features to be modelled are reviewed. This comprises the synaptic plasticity and the spike-timing dependent plasticity.

#### 3.5.1 Synaptic Weight

As it is described in Sec. 2.4, synapses are complex electro- and biochemical machinery systems. The question is: How properly can the synaptic action be modelled? The first and most popular answer for this was the *synaptic weight*. In a significant amount of studies, synapses were presented as weighting factors (scalar values), usually labelled as  $w_{ij}$ . The parameter  $w$  indicates the strength

of the synaptic connection between two neurons  $i$  as presynaptic and  $j$  as a postsynaptic neuron<sup>3</sup>. Based on the basic statistical analysis of the synaptic release in Sec. 2.4.2, it can be shown that  $w_{ij} = k \cdot n \cdot p$ , where  $k$  is the number of released quanta from  $n$  release sites, and  $p$  is the average probability of release.

The scalar representation of the synaptic strengths belongs to rate coding, because it does not take the timing of the input spikes into account. This representation considers the synapse as an amplifier for an input synaptic current. Example for this is the synaptic strength coupled directly to the summation of PSPs in Eq. 3.4.

As mentioned in Sec. 3.2, rate coding is not the best representation of neural information. This of course calls for the application of temporal coding. Implementing temporal coding in the synaptic models is a vital added value because this transfers key features from the synaptic actions into the models (Purves, 2008). Before discussing the dynamic synaptic models, the next section explains the dynamic behaviour of the synapses from a signal processing point of view.

### 3.5.2 Synaptic Plasticity

Synaptic plasticity in general is a basic and vital computational feature of the nervous system (Dobrunz and Stevens, 1997, 1999; Douglas et al., 1996; Sincich et al., 2007). The paradigm and the importance of synaptic changes has come first to live by the hypothesis of D. Hebb in 1949 (Hebb, 1949). Hebb postulated that learning actually is performed by synapses via storing (memorizing) the changes in response to certain activity. In other words, learning is dependent on the co-occurrence of activities in pre- and postsynaptic sites. Hence, synapses are localized sites for (unsupervised) learning via the ability to change their contribution in information transmission, this is latter known as Hebbian learning. This famous learning concept along with concepts of machine learning and what is related shall be discussed later in Ch. 8. As Hebb proposed, synaptic changes that are induced due to pairing of pre- and postsynaptic spiking is a sort of learning with a short time constant. After certain time interval the action is forgotten with decaying activity. However, longer lasting synaptic changes often cause plastic changes. These changes affect then the basic synaptic mechanism and properties. From a signal processing point of view, if the synaptic dynamics as function of time can be represented as a trajectory (or a set of trajectories), plasticity<sup>4</sup> means changing the working point (or jumping to a new trajectory). Thus, the synapse remains dynamic with new temporal features.

Synaptic plasticity is characterized in general with long-term and short-term potentiation (and depression) (LTP(D) and STP(D)). Potentiation over certain time scales requires that the synaptic

<sup>3</sup>In some articles this notation might be twisted, i.e.  $w_{ij}$  is the strength of the synapse between the postsynaptic neuron  $i$  and the presynaptic one  $j$ , see e.g. (Gerstner, 1999).

<sup>4</sup>It is important to notice that synaptic plasticity within the context of learning includes another equally important class of dynamic structural changes. This is referred to as structural plasticity or synaptogenesis, see e.g. (Whalley, 2009). This kind of plasticity is defined via the evoked (or spontaneous) process of adding new synapses and eliminating existing ones. This *rewiring* in the neural circuitry is evident and contributes to the rich repertoire of computational abilities attributed to synaptic dynamics, see e.g. (El-Laithy, 2011).

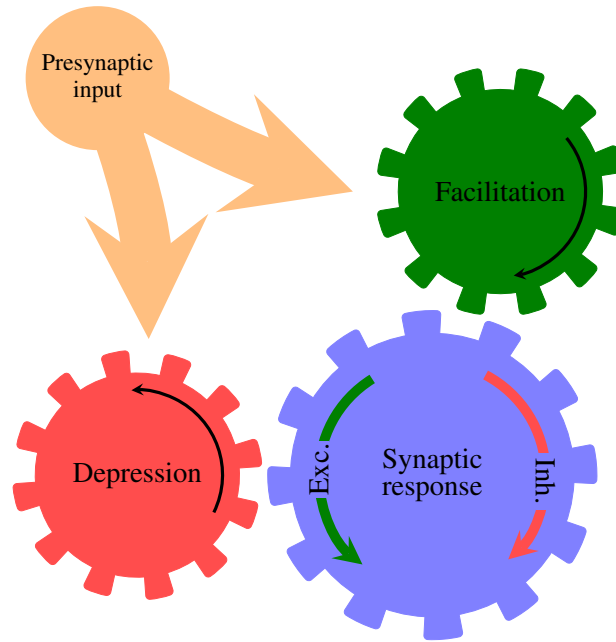


**FIGURE 3.5:** Cartoon illustration of the interaction between the processes of facilitation and depression. These actions are the core processes forming the synaptic plasticity. A model which integrates both in its state parameters, is an integrative model.

efficacy in transmitting the incoming spikes varies in accordance to varying the temporal density of these spikes. It is a use-dependent enhancement in the synaptic efficacy. Depression is then the deterioration of this efficacy upon certain coupling of activities, it is the unlearning mechanism that avoids saturation. The exact roles of the synaptic receptors in LTP and LTD are still debated (Abbott et al., 1997; Brager et al., 2002). It is believed that LTD is the reversal mechanism of LTP. The time scales involved with LTP(D) may vary from minutes to days and even longer. While STP(D) are those changes that stay effective for milliseconds and seconds (up to a couple of minutes).

STP(D) occurs in the synaptic action via two counteracting collective short-term mechanisms, they are facilitation and depression (Zucker and Regehr, 2002). Facilitation promotes the excitatory regime of synaptic action while depression reinforces the inhibitory one. Both mechanisms originate from the change in release probability from the presynaptic terminal, also described as the redistribution of the synaptic efficacy (Varela et al., 1997). This redistribution affects the temporal dynamics rather than the average gain of the synapse (synaptic strength). The redistribution of synaptic efficacy was reported and modelled clearly in the famous work of Markram and Tsodyks in 1996 as they succeeded to simulate the temporal pairing between pre- and postsynaptic spiking activity (Tsodyks and Markram, 1997). Based on this work they have developed their well established synaptic model (Markram et al., 1998), this model is discussed below in details. This class of models implement what is referred to as short-term spike-timing dependent plasticity (short-term STDP) to be distinguished from implementing the LTP(D).

In order to model the dynamic essence of the synaptic action as mentioned, models are required to count for the short-term synaptic plasticity by modelling both the facilitatory and depressive

mechanisms in the synaptic action. Fig. 3.5 abstracts the concept of the counteracting mechanisms in the synaptic action as two gears. Each of which rotates in a certain direction in response to the synaptic input. Assuming that the temporal information in the synaptic input affects the angular velocity of each gear, the overall synaptic action is defined through the resultant motion of the large gear. The angular velocity and the direction of rotation of this large gear are the properties of the synaptic response as either excitatory or inhibitory. The illustrated gear system reflects the existence of an internal feedback effect (closed loop or interdependency) since the resultant synaptic response affects the status of the internal processes from which it actually originates. In this example, the inertia of the blue gear prevents the simultaneous reversal of the rotation direction. Biologically, long lasting excitatory response decrease the sensitivity of the inhibitory receptors. Therefore it takes longer than normal to switch from an excitatory synapse to an inhibitory one<sup>5</sup>. Facilitation and depression can be either implicitly parametrized or explicitly over a number of state parameters. From a biological point of view, a fully featured state space of a synaptic action might involve more than one hundred independent parameter (Abul-Husn et al., 2009; Zhang et al., 2006). Since such a model is an extreme case, models reduce the model space into a couple of state variables. The reduction in state space results in capturing only some of the effects from the synaptic action or permits to count only for the main the mechanisms causing these effects. This reduction recalls the question mentioned in Sec. 1.4 regarding the required vs. the optimum level of abstraction in studying brain functions.

### 3.6 Models of Short-Term Synaptic Plasticity

The models of dynamic synapses in almost all cases parametrize only the short-term dynamics. Long-term features are often missing in the synaptic models, they can be modelled on a network level considering the relevant information to be stored for long-term usage. Models which account explicitly for both facilitation and depression processes are known as integrative models (Morrison et al., 2008). Models might be either phenomenological or biophysical. Within the class of phenomenological models, the state parameters describe the dynamics collectively without biophysical-based details. They refer implicitly to biophysical mechanisms. If the account for the biophysical details is implemented in a relative explicit manner, the model is said to be a biophysical one. At this point the model can be a detailed biophysical one or a simple biophysical alternative, it depends on the amount of the incorporated details.

Two examples of integrative models are presented in this chapter: the Markram-Tsodyks model (Markram et al., 1998) as an example of a phenomenological model and the Lee-Anton-Poon synaptic model (Lee et al., 2009) as an example of a biophysical one. Other models include Maass-Zador's stochastic synapse (Maass and Zador, 1999), Liaw-Berger dynamic synapse

<sup>5</sup>From a biological point of view, a single synapse is either excitatory or inhibitory. The switching behaviour described in the text is not attributed to single synaptic site. On a macroscopic scale for the overall synaptic connection between two neurons, thousands of synapses might be involved. The relative contribution between those excitatory and inhibitory ones decides for the observed overall synaptic behaviour.

(Liaw and Berger, 1996), Destexhe-Mainen-Sejnowski synaptic model (Destexhe et al., 1994), and Dittmann facilitation and depression model (Dittman et al., 2000). These models except the Maass-Zador model are briefly reviewed in App. A; these models are in general either too complex or not adequately defined to be incorporated in large scale network simulations. This leaves the Maass-Zador's stochastic synapse that is explained and discussed at the beginning of Ch. 4 because it introduces the novel proposed synaptic model.

### 3.6.1 Markram-Tsodyks Dynamic Synapse

The Markram-Tsodyks model is the well-established phenomenological model from Markram et al. (Markram et al., 1998; Tsodyks and Markram, 1997) for fast synaptic dynamics. In the following, it is referred to as the Markram-Tsodyks model. This model describes the effects of action potentials on the collective utilization of synaptic resources (the amount of neurotransmitter)  $u(t)$  and the subsequent process of their recovery  $r(t)$ . It is an integrative model that describes both synaptic actions of depression and facilitation:

$$\frac{dr(t)}{dt} = \frac{1 - r(t)}{\tau_{rec}} - u(t) \cdot r(t) \cdot \delta(t - t_i), \quad (3.5)$$

$$\frac{du(t)}{dt} = \frac{U - u(t)}{\tau_{fac}} + U \cdot (1 - u(t)) \cdot \delta(t - t_i). \quad (3.6)$$

where  $\tau_{rec}$  is the recovery time constant.  $\delta(t - t_i)$  is the Dirac delta function and represents an incoming spike at  $t_i$ .  $U$  is a constant value determining the step increase in  $u(t)$  and the baseline value of  $u(t)$ ; where  $U$  should be bounded to  $[0, 1]$ .  $\tau_{fac}$  is the relaxation time constant. Assuming a presynaptic action potential at time  $t_i$ , the depression process can be expressed by Eq. 3.5 in which  $r(t)$  represents the fraction of neurotransmitter pool available for transmission, and  $u(t)$  is the fraction of  $r(t)$  to be utilized due to each spike. The facilitation mechanism is caused by an increase in the synaptic utilization at each presynaptic spike and can be formulated by Eq. 3.6. Right after an incoming spike,  $u(t)$  is increased from its current value to  $u(t^+) = u(t) + U \cdot (1 - u(t))$  and drifts towards its baseline value  $U$  with a time constant  $\tau_{fac}$  between action potentials. The rule keeps  $u(t) < 1$  for any time instant  $t \geq 0$ . The synaptic response,  $E_{psp}$ , resulting from an action potential is obtained by

$$E_{psp}(t) = J \cdot u(t) \cdot r(t), \quad (3.7)$$

where  $J$  is the baseline level of synaptic output. Fig. 3.6 demonstrates the time evolutions of the state parameters  $u(t)$  and  $r(t)$  in response to a regular<sup>6</sup> input spike train with frequency of 100 Hz for an epoch of 200 msec. The details of the simulation values are given in the figure's caption.

---

<sup>6</sup>That is a spike train with a single fixed frequency

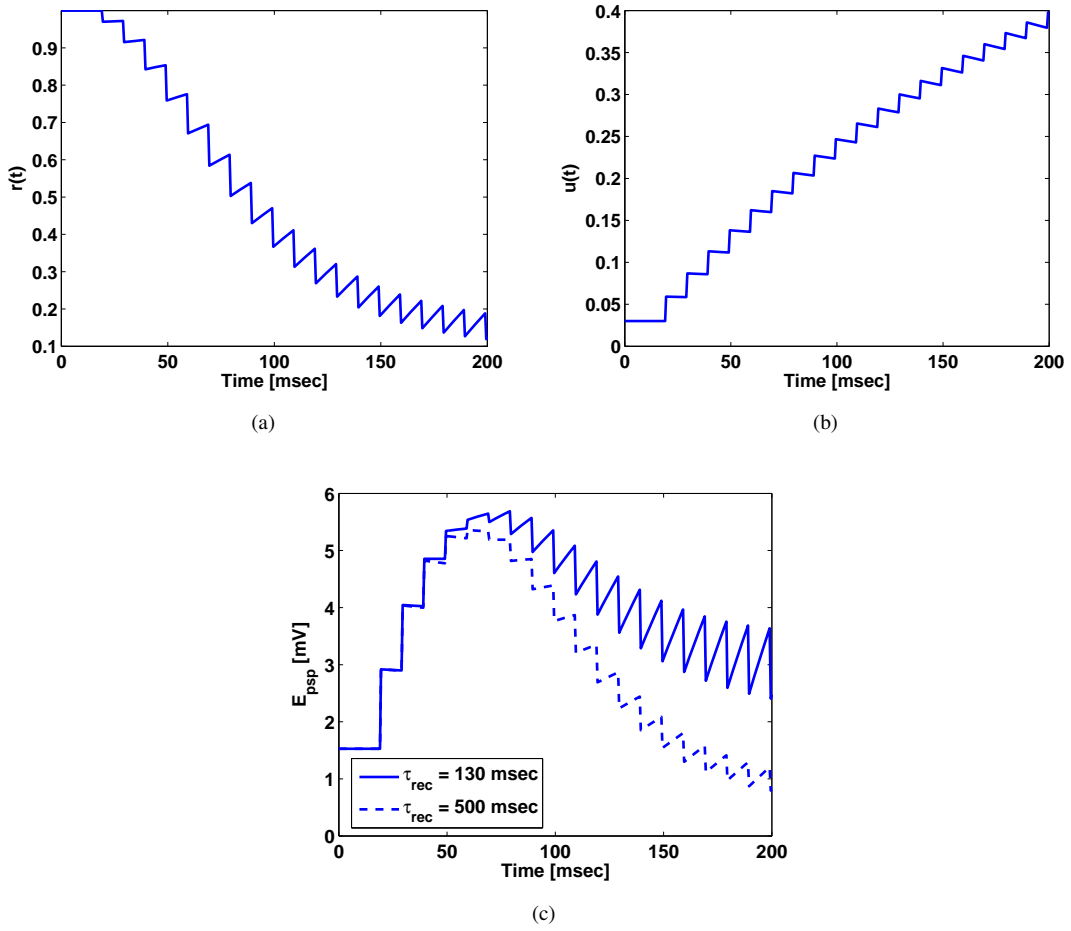


**FIGURE 3.6:** Simulating Markram-Tsodyks model. In this simulation  $dt$  is set at 0.5 msec,  $\tau_{rec} = 130$  msec,  $\tau_{fac} = dt/\tau_{rec}$  and  $j = 51.33$ . (a) and (b) illustrate the time courses of  $r(t)$  and  $u(t)$  in response to a regular spike train (stimulation frequency: 100 Hz) respectively. (c) The corresponding time evolution of  $E_{psp}$  at two values for  $\tau_{rec}$  130 and 500 msec.

**Expressions of Frequency Response** Because it is often difficult to fully comprehend the behaviour of a model in response to irregular<sup>7</sup> spike trains, it is helpful to understand the model's behaviour in response to a long lasting regular spike train with a constant spiking frequency. The simplicity of defining the frequency response expressions for the Markram-Tsodyks is one of the main reasons in its popularity.

The frequency response expressions are called sometimes the "steady-state" expressions, see e.g. (Lee et al., 2009; Levina et al., 2007). In fact, the system equations of almost all dynamic synaptic models including the Markram-Tsodyks model do not exhibit a real "steady-state" behaviour. There is always oscillations in the time evolutions of the state parameters in response to the input spike train, i.e. there is no constant non oscillating behaviour. The steady-state (non

<sup>7</sup>On contrary to a regular one, an irregular spike train features a varying firing frequency. Usually it refers to a randomly generated spike train. However, an overall firing frequency can be evaluated for the irregular case by dividing the number of spikes in the spike train over its epoch length.

oscillating) values might be observed only at very high input frequencies which are often not observed in biological neural systems. The frequency response expressions that are reported for the Markram-Tsodyks model and the following ones including the novel model proposed in next chapter represent actually the *time average* of the state parameters in response to a long lasting spike train with a constant frequency. Observing the distinction in the definitions of the two terms (steady-state or time average) decides about the correctness of the mathematical approach used to derive these expressions for any model. The notation of steady-state is used in this thesis to keep a common notation with the literatures. Both steady-state and time average notations are used interchangeably in the following and the implications of the mathematical approaches are given where applicable.

Defining the steady-state expressions for the Markram-Tsodyks model is not a straight forward task in general and it is more difficult with complex biophysical models. As for the Markram-Tsodyks model, from Fig. 3.1  $\Delta_{isi}$  denotes the interval between two successive spikes. For the time interval between the two spikes  $t_1$  and  $t_2$  only the relaxation dynamics dominate the state parameter  $u$ . Thus, it is assumed that the changes resulting from the decaying constants  $\tau_{fac}$  and  $\tau_{rec}$  are slow in comparison to the input and that the incremental step of increase in  $u(\cdot)$  and decrease are the same during  $\Delta_{isi}$ , i.e.  $\Delta_{isi} = 1/f$  and  $f$  is the incrementation time (this reduces an irregular spike train to a regular one with an overall frequency of  $f$ ). Then, from Eq. 3.6

$$u(t_2^-) = U + (1 - U) \cdot u(t_1^-) e^{-\Delta_{isi}/\tau_{fac}}, \quad (3.8)$$

where  $u(t_1^-)$  and  $u(t_2^-)$  are the available portions of  $u(t)$  before<sup>8</sup>  $t_1$  and  $t_2$  respectively. At stationariness, the input spikes feature an average inter-spike intervals of  $\langle \Delta_{isi} \rangle$  where  $\langle \cdot \rangle$  is the overall time average over the epoch. Similarly, it can be shown that  $\langle u(t_1^-) \rangle = \langle u(t_2^-) \rangle$ . Then, the overall time average of  $u(t)$  at stationariness (the steady-state level,  $u_{ss}$ ) in response to the input with frequency  $1/\langle \Delta_{isi} \rangle$  is (Levina et al., 2009)

$$u_{ss} \equiv \langle u(t) \rangle = \frac{U}{1 - (1 - U)e^{-\langle \Delta_{isi} \rangle / \tau_{fac}}} \quad (3.9)$$

In a similar fashion, it can be shown that the steady-state level of  $r(t)$ ,  $r_{ss}$  is (Levina et al., 2009)

$$r_{ss} \equiv \langle r(t) \rangle = \frac{1 - e^{-\langle \Delta_{isi} \rangle / \tau_{rec}}}{1 - (1 - U)e^{-\langle \Delta_{isi} \rangle / \tau_{rec}}} \quad (3.10)$$

The importance of such expression of steady state response is the ability to represent  $E_{psp}$  explicitly as a function of the input frequency  $f \approx 1/\langle \Delta_{isi} \rangle$ .

**Simplification** In the Markram-Tsodyks model, it has been basically accepted that the dynamic synaptic strength is  $S(t) = u(t) \cdot r(t)$  (Levina et al., 2009; Markram et al., 1998). It should be

---

<sup>8</sup>This is indicated by the minus in the exponent



noticed that  $\langle u(t) \cdot r(t) \rangle \neq \langle u(t) \rangle \cdot \langle r(t) \rangle$  in general, although the correlation between  $u(t)$  and  $r(t)$  is not significant as reported by (Levina et al., 2009).

The Markram-Tsodyks dynamic system can be simplified to a one dimensional depressive synaptic model (Morrison et al., 2008). The reduction is performed by assuming that  $\tau_{fac} \ll \tau_{rec}$ , i.e.  $\tau_{fac} \rightarrow 0$ . Facilitation is then not expected and  $u(t^+) \rightarrow U$  after each spike. The model is reduced to Eq. 3.5 with  $u(t) \leftarrow U$ . In this case, the synaptic response is  $E_{psp}(t) = J \cdot r(t)$  and the dynamic synaptic strength becomes  $S(t) = r(t)$ .

**Problems with Markram-Tsodyks Model** The Markram-Tsodyks model has been one of the most (if not the most one) used and implemented synaptic models in simulations. This arises from its mathematical simplicity relative to other models and because it was observed to give good fits with a range of experimental results (Markram et al., 1998; Tsodyks and Markram, 1997), see (Lehn-Schiøler and Olesen, 2002; Morrison et al., 2008) for a review.

However, some limitations in the Markram-Tsodyks model have called for a better synaptic modelling that manifests enhanced theoretical as well as biophysical basis:

- The values of the model parameters are seen as inhomogeneous (Lee et al., 2009; Morrison et al., 2008); there is no biophysical basis for the biological plausibility of the heterogeneity.
- There are some discrepancies in the original papers introducing the model, there are conflicts between portions of the graphs describing the steady state model behaviour and the text explaining them, see (Lehn-Schiøler and Olesen, 2002, p. 76) for a detailed description.
- It has been shown in (Morrison et al., 2008) that the dynamics describe  $u(t)$  and  $r(t)$  are trapped in the pair-based STDP that may give false predictions in certain experiments.
- The Markram-Tsodyks model is not able to account for certain required synaptic capabilities such as fast-varying frequencies and stable temporal-based operation.

These issues are investigated in more details in Chs. 4, 5, 9 and 10 in comparison to the proposed model.

### 3.6.2 Lee-Anton-Poon Synaptic Model

Till the moment of writing this thesis, this model is the recent biophysical model presented in late 2009 in parallel to- yet independently and separately from the one proposed in this thesis. It is an integrative biophysical model that unifies facilitation and depression dynamics in the synaptic action.

The model describes the synaptic action as two kinetics: a presynaptic process and a post-synaptic response. The presynaptic process involves a calcium buffering and calcium-dependent

vesicle trafficking. The important features reported in this model are the account for the Glutamate flux in the synaptic cleft (explicitly) and the role of the probability of release (explicitly and deterministically). The model reads (Lee et al., 2009)

$$\tau_C \frac{dC(t)}{dt} = (C_o - C(t)) + K_{Ca} \sum_{t_i} \delta(t - t_i) \quad (3.11)$$

$$\frac{dR_{rel}(t)}{dt} = k_{recov}(1 - R_{rel}(t)) - P_{rel}(t) \cdot R_{rel}(t) \cdot \sum_{t_i} \delta(t - t_i) \quad (3.12)$$

$$P_{rel}(t) = P_{rel,max} \frac{C(t)^4}{C(t)^4 + K_{rel,half}^4} \quad (3.13)$$

$$\text{Flux}_{Glu}(t) = n \cdot N_{total} \cdot R_{rel}(t) \cdot P_{rel}(t) \cdot \sum_{t_i} \delta(t - t_i) \quad (3.14)$$

$$\tau_{epsc} \frac{dE_{psc}(t)}{dt} = -E_{psc}(t) - K_{Glu} \cdot \text{Flux}_{Glu}(t) \quad (3.15)$$

Eqs. 3.11- 3.13 represent the presynaptic processes. In Eq. 3.11 the calcium concentration in the presynaptic terminal  $C(t)$  starts at  $C_o$  and increases incrementally by the arrival of each incoming spike represented by the Dirac delta function at  $t_i$ . The factor  $K_{Ca}$  is the calcium concentration gain per action potential<sup>9</sup>. The calcium concentration drifts back to the baseline with a time decay constant  $\tau_C$ . The releasable ratio of vesicles  $R_{rel}(t)$  is calculated using Eq. 3.12 as a function of the probability of release  $P_{rel}(t)$  from Eq. 3.13; where  $P_{rel,max}$  is the maximum allowed probability of release and  $K_{rel,half}$  is the calcium sensitivity regarding transmitter release. The factor  $k_{recover}$  is the recovery rate from an empty to a releasable pool. Eq. 3.14 models the flux of Glutamate neurotransmitter  $\text{Flux}_{Glu}(t)$  into the synaptic cleft where  $N_{total}$  is the total number of vesicles in a presynaptic terminal.  $n$  is the number of the involved release sites. Eq. 3.15 estimates the induced excitatory postsynaptic current  $E_{psc}(t)$  in response to the Glutamate influx with a time decay constant  $\tau_{epsc}$ . For more details about the biophysical basis of the models see (Lee et al., 2009).

Fig.3.7 shows sample time evolutions of the state parameters  $C(t)$  and  $R_{rel}$  in response to a regular input spike train. Note that the difference between  $E_{psc}$  from Eq. 3.15 and  $E_{psp}$  from Eq. 3.7 are only the notation and physical units of either current or potential. Both actually can be used interchangeably if the units are regarded correspondingly<sup>10</sup>.

**Expression of Steady-state Response** As shown for the Markram-Tsodyks model, and despite the complexity of this model the authors proposed a technique to simplify the model in order to define the steady-state postsynaptic response  $E_{psc,ss}$  as a function of stimulation frequency (Lee et al., 2009). The mathematical derivations is based on setting the differential parts (left hand sides

---

<sup>9</sup>See the limitations of this model on p. 47 for a comment about units discrepancy in this equation which is unclear in the original paper.

<sup>10</sup>In this work only the notation of potential ( $E_{psp}$ ) is used with the exception in this model and in the Dittman model (Sec. A.2) to keep the authors notations and definitions.

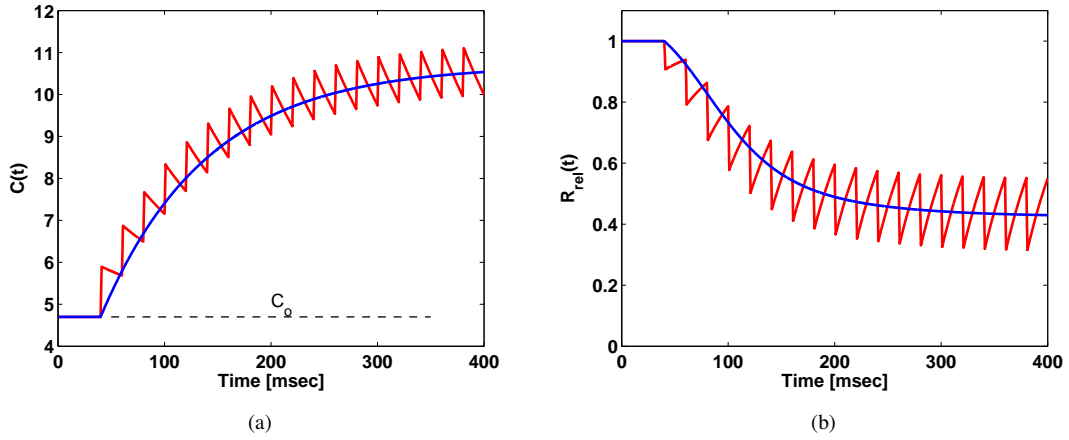


**FIGURE 3.7:** Simulating Lee-Anton-Poon model. (a) and (b) illustrate the time courses of  $C(t)$  and  $R_{\text{rel}}(t)$  in response to a regular spike train (stimulation frequency: 50 Hz) respectively. The zigzag lines are the instantaneous time courses of the state parameters, while the solid lines are average values. For the listing of the values required to get this response see (Lee et al., 2009); the figures are generated with the supplementary materials available from the authors.

in Eqs. 3.11–3.15) to zero. The dynamic system is solved then for  $E_{\text{psc}}$  resulting in its steady state formula as function of any stimulation input frequency  $f$  (Lee et al., 2009):

$$E_{\text{psc},ss}(f) = \left[ \frac{C_{ss}(f) + K_{\text{rel},\text{half}}^4}{P_{\text{rel},\text{max}} \cdot C_{ss}(f)} + \frac{f}{k_{\text{recov},ss}} \right]^{-1}, \quad (3.16)$$

where  $C_{ss}(f)$  is the steady-state calcium concentration in response to a stimulus with  $f$  input frequency and it equals  $f \cdot K_{\text{Ca}} + C_o$ . The factor  $k_{\text{recov},ss}$  is the steady state value of  $k_{\text{recov}}$ ; it is a function of  $C_{ss}(f)/(C_{ss}(f) + K_{\text{recov},\text{half}})$ . The scaling constant  $K_{\text{recov},\text{half}}$  is the calcium concentration giving one half of recovery rate. The synaptic strength of this model was not proposed by its authors. This approach in estimating the steady-state expressions is not correct from a pure mathematical point of view, details of such a problem is explained below as a part of discussing the model's limitations.

**Limitations** The authors of the model have shown that the model is capable of simulating pure facilitatory, depressive and mixed behaviours. The model, however, suffers from some drawbacks:

- Mathematically, some equations are incorrect. For example in Eq. 3.11 the units of the left hand side are of concentrations (M or Molar units); on the right hand side, the third term is  $K_{\text{Ca}} \cdot \sum_{t_i} \delta(t - t_i)$ . Recalling that  $K_{\text{Ca}}$  has units of concentration per time (M/sec) and the Dirac delta function has units of (1/sec), it implies that this term has units of M/sec<sup>2</sup>. The same remark is true for the last term of the right hand side in Eq. 3.12.

- Still from a mathematical point of view, the used approach in the derivation of the steady-state expressions is questionable. The authors have strictly estimated the steady-state expressions rather than the time average of the state parameters. By setting the differential term to zero, it implies that there is no oscillating behaviour observed in response to the expected range of input frequencies. This is true only when the input frequency is very high, i.e. when  $f \gg 100$  Hz. And of course this also depends on the settings of other timing parameters, i.e. the decay time constants. By reviewing the original study from (Lee et al., 2009), the maximum tested input frequency in the steady-state simulations has never exceeded 200 Hz. The difference between the approach implemented by the authors of this model and the one which is used with the novel proposed model in the next chapter can be explored with the following example. For Eq. 3.11, by setting the differential term to zero the estimated steady-state value of  $C_{ss}$  as a function of input frequency  $f$  follows (Lee et al., 2009):

$$C_{ss}(f)^{(1)} = C_o + K_{Ca} \cdot f$$

which suppresses the contribution of all the temporal parameters affecting the entire process. A proper approach, however, must calculate the time average of the function over a certain time interval  $[0, T)$  to account for the oscillating nature of the response as mentioned above with the Markram-Tsodyks model. For this example, the method with the time average results in:

$$C_{ss}(f)^{(2)} = C_o + K_{Ca} \cdot f \cdot \tau_C$$

The relative scaling between the input frequency and  $\tau_C$  affects the final values of  $C_{ss}$  significantly. Furthermore, the difference between the  $C_{ss}(f)^{(1)} - C_{ss}(f)^{(2)}$  is amplified through the succeeding calculations. This makes the entire results of the steady-state behaviour of this model questionable if not doubtable. Moreover, the physical units of the expressions of  $C_{ss}(f)^{(1,2)}$  are still not consistent because the base equation is not properly defined as mentioned in the previous remark.

- Although the model avoided the detailed calcium dynamics from (Dittman et al., 2000) and the extensive presynaptic mechanisms reported in (Liaw and Berger, 1996), it has modelled some relevant biophysical details in an unbalanced manner. For example, the balance in modelling the recovery of the pool of releasable vesicles and the cleaning action of neurotransmitter from the cleft is not regarded. The recovery process of the releasable pool of vesicles is detailed, the equations are not listed here for clarity. And although the model account for the flux of the neurotransmitter substance to the synaptic cleft, it does not consider its buffering in the cleft nor its removal action from the cleft. This buffering and removal actions are very crucial in synaptic transmission (Abbott et al., 1997; Durstewitz, 2003; Purves, 2008; Yeckel and Berger, 1998) but they are missing in this model.

From a biophysical point of view, the density of the neurotransmitter in the cleft is the reason for the induced EPSP. This density affects the sensitivity of the receptors of neurotransmitter and the long-term existence of the neurotransmitter in the cleft might cause a kind of saturation on the postsynaptic site. Thus, since the buffering of neurotransmitter in the cleft is missing in the model, there is a conceptual problem in considering that the  $E_{psp}(t)$  is a direct function of the Glutamate flux rather than its concentration in the cleft, Eq. 3.14.

- The model uses a calcium-dependent probability function, Eq. 3.13. This implies that the probability of release is independent of the size and dynamics of the releasable pool of vesicles. This is strikingly strange, because logically the probability of release process must be related (not to mention being function of) the dynamics of releasable vesicles ( $R_{rel}(t)$ ) which is missing according to Eq. 3.13. This issue makes the predictions reported with the model questionable in terms of plausibility and the reliable usage in further experiments.
- Despite the claim of introducing a simple biophysical model compared to Dittman's and Liaw-Berger's models, more than 30 parameters and scaling factors are involved in the dynamics and compiled into six state parameters. The drawback of such complexity is the inherited difficulty in attributing the effect of each parameter in the model to its influence on the synaptic response. Moreover, the required extensive sensitivity analysis and missing a definition for the synaptic strength together make it difficult to develop needed learning algorithms for this model. The difficulty in deriving proper learning algorithms are one of the limiting factors against increasing the interest in developing biophysical models for the synaptic dynamics (Morrison et al., 2008).
- A conceptual conflict arises from the choice of modelling the Glutamate neurotransmitter in particular. Regardless of the role of Glutamate as predecessor for the synthesis of the inhibitory GABA, Glutamate is known to be the most abundant excitatory neurotransmitter in the nervous tissues. Consequently, using the flux of Glutamate in modelling a pure depressive or an inhibitory synapse might be seen inappropriate.

### 3.7 Summary

Having explained the different available models of neuronal and synaptic dynamics, it is important to recall that the aim of developing those models is to represent computational units which are then relevant to be involved in building the SNN. These SNN tries to abstract and imitate the behaviour of biological neural systems (neural circuitries). Two macroscopic concerns determine the extend of the usability and applicability of any model in empowering the available tools within neuroscience: the biophysical relevance (or the biological plausibility) and the computational complexity. Taking synapses as the focus of the discussion, the available models for synaptic dynamics suffer from drawbacks and limitations either regarding both concerns or at least in one of them.

This motivates the need for a novel model that achieves a sort of the required balance with efficiency as being biophysical at low computational complexity. This balance contributes positively to support the usage of the model to transfer the biological computational capabilities into the networks level. Meanwhile, it advances the understanding of the relevant biophysical mechanisms for modelling and simulation in neuroscience.

# The Modified Stochastic Synaptic Model

*"Everything should be made as simple as possible, but not one bit simpler."*

**Albert Einstein, *attributed***

## 4.1 Introduction: Why Another Model?

As seen from the previous review of synaptic models, more work is required to overcome the problems encountered in these models. Fig. 4.1 illustrates an overview of the synaptic models and how they are seen as being biophysical vs. their complexity. In the lower right corner of this figure an ideal synaptic model is expected (the ideal case). By studying Fig. 4.1, there was a strong tendency to capture more details from the biology. This has led to a number of biophysical models that are able to model reliably many important aspects of the required variability in synaptic dynamics, as already discussed in the previous chapter(s) and in App. A. These model suffer from many conceptual inconsistencies which make modifying them either difficult or not worthy beside being computationally expensive. From the author's point of view, being simple is as important as being biophysical. It is worth mentioning that developing a biophysical model is usually not the difficult part. Adding equations, integrating dynamics and making the model more complex is not a challenging task. The real challenge lies in the trade-off (balanced compromise) between modelling enough biophysical processes and keeping the mathematical description comprehensible. Such a balanced model should be able to simulate the essence of variability and the required rich repertoire of dynamics attributed to the synapses in information processing within the CNS. Meanwhile, the model should be computationally inexpensive; this permits being implementable for hardware applications and usable in large scale network simulations.

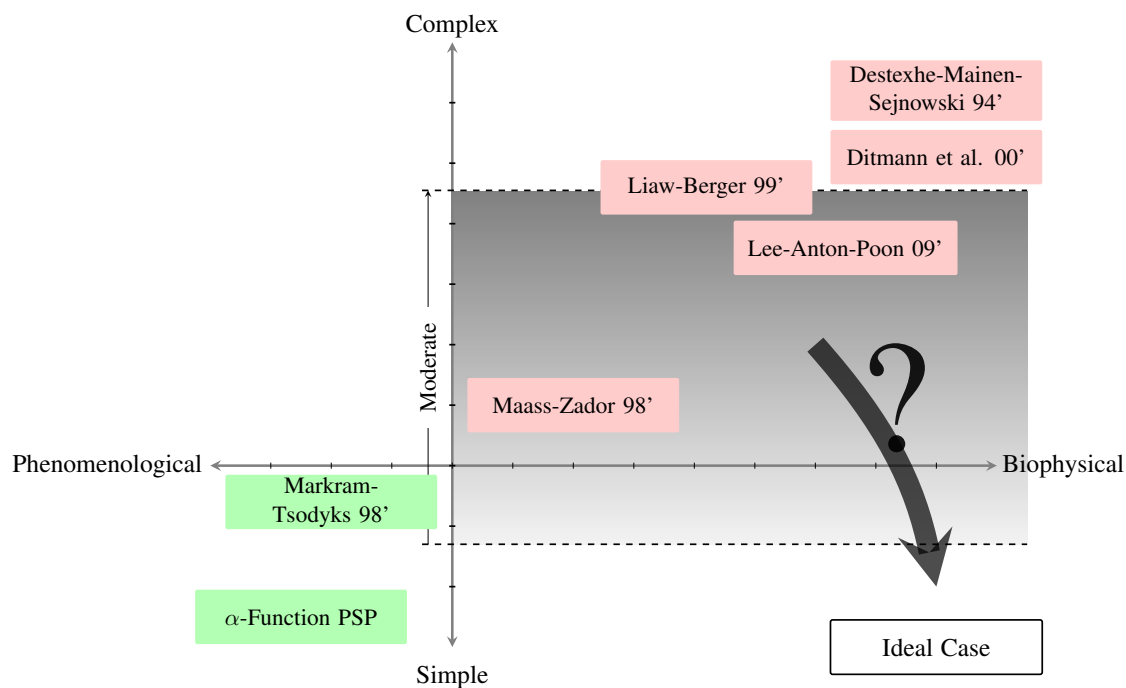


**FIGURE 4.1:** Schematic of relative positioning of synaptic models in terms of being biophysical vs. complexity (not an exact scale). The  $\alpha$ -function PSP is explained in App. A.1

In this chapter, a novel model is introduced: The modified stochastic synaptic model (MSSM). The MSSM represents the required balanced optimization in accounting for the underlying synaptic mechanisms and the simplicity in presenting these mechanisms in the model. With this realization, it is a tool that simplifies the incorporation of essential synaptic dynamics in simulations of large networks.

The model is built on the concepts and the basic work presented in the Maass-Zador's stochastic synapse (Maass and Zador, 1999). Thus, the following section lists this model as it is the building brick of the MSSM. The explanation highlights the reason behind building the MSSM based on it, as well as why the Maass-Zador's stochastic synapse is seen to be not enough as a synaptic model. Following sections explain the mathematical details of the model and its behaviour. Further analysis of the steady-state response is reported as well. Finally, the added values in using the MSSM and its limitations are discussed. Validating the claims of being enough as a biophysical model for modelling the required synaptic dynamics is given separately in Ch. 5.

## 4.2 The Building Brick: Maass-Zador's Stochastic Synapse

The Maass-Zador stochastic synaptic model was first introduced by Maass and Zador in (Maass and Zador, 1999). It is the base of the model proposed in this thesis. The very basic version of the Maass-Zador model extends the seminal work of (Dobrunz and Stevens, 1999; Varela et al., 1997; Zador and Dobrunz, 1997) and the related analysis to the stochastic nature of the synaptic release reported in (Markram et al., 1998). These studies have emphasized the importance of



realizing the stochastic synaptic release in modelling the synaptic dynamics and confirmed the role of the synaptic contribution to the processing of neural information. The model was first used in approximating nonlinear functions in combination with classical rate coded neuronal models (Natschl ger, 1999; Natschl ger et al., 2001).

The Maass-Zador synaptic parametrization models a stochastic synaptic connection (Maass and Zador, 1999). It maps an input spike train  $F$  to a subset sequence of time instants  $S(F) \in F$  on which release of neurotransmitter occurs (a release pattern).  $F$  and thus  $S$  are by definition a sequence of increasing positive values as explained in Sec. 3.2.2. Whether a release at  $t_i$  occurs or not is governed via a probability value  $P(t_i)$ . This probability value is a function of two state parameters  $C(t)$  and  $V(t)$ , they model the two counteracting internal synaptic processes: facilitation and depression respectively. The probability function reads

$$P(t_i) = 1 - e^{-C(t_i) \cdot V(t_i)}, \quad (4.1)$$

where  $C(t)$  models the buffering of the calcium ions in the presynaptic terminal and  $V(t)$  is the size of the ready to release pool of vesicles in the presynaptic terminal as well. For a release to occur,  $P(t_i) \geq P_{th}$ ; where  $P_{th}$  is a probability threshold. The state parameters  $C(t)$  and  $V(t)$  are then defined as

$$C(t) = C_o + \sum_{t_i \in F} c(t - t_i), \quad (4.2)$$

$$V(t) = \max\{0, V_o - \sum_{t_i \in S(F)} v(t - t_i)\} \quad (4.3)$$

where

$$c(t - t_i) = \begin{cases} \alpha \cdot e^{-(t-t_i)/\tau_C}, & \text{if } t_i < t \\ 0, & \text{otherwise} \end{cases} \quad (4.4)$$

and

$$v(t - t_i) = \begin{cases} e^{-(t-t_i)/\tau_V}, & \text{if } t_i < t \\ 0, & \text{otherwise} \end{cases} \quad (4.5)$$

Eq. 4.2 models the calcium buffering in the presynaptic terminal that represents the facilitation dynamics in the model.  $c(t - t_i)$  is the response of  $C(t)$  to an incoming spike at  $t_i$ . The baseline of calcium concentration is  $C_o$  and  $\alpha$  is the rush in amount of calcium upon an incoming spike. Between two successive spikes, the concentration drifts back to the baseline with a time constant  $\tau_C$ .

The depression is modelled as the dynamics of trafficking the vesicles in the presynaptic terminal, see Eq. 4.3.  $V(t)$  models the size of ready to release pool of vesicles in the presynaptic terminal. The summation is performed only over those time instants at which release occurs, i.e. when  $P(t_i) \geq P_{th}$ . Similar to  $c(t - t_i)$ ,  $v(t - t_i)$  is the response of  $V(t)$  to a preceding release at

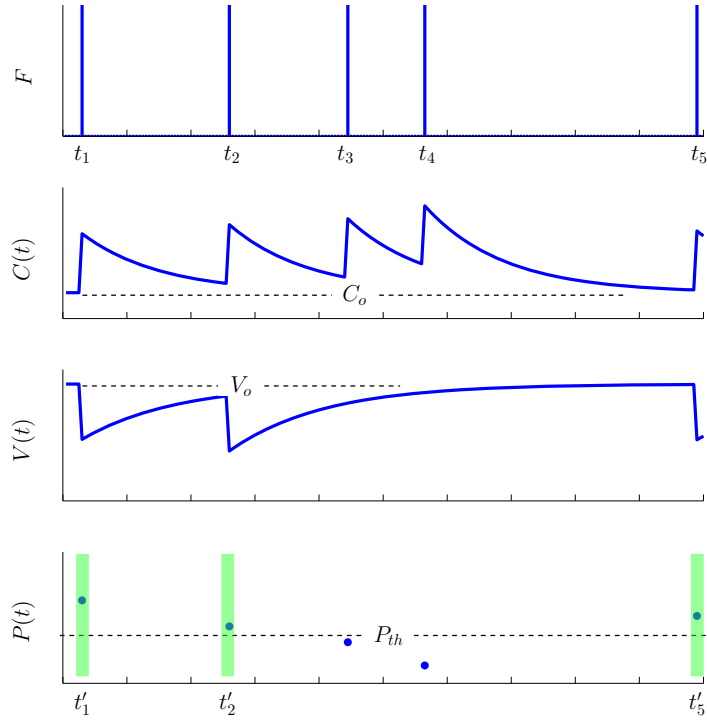


**FIGURE 4.2:** The dynamics of the Maass-Zador stochastic synapse. Schematic illustration of the time evolution of the state parameters from top  $C(t)$  (second panel),  $V(t)$  (third panel) and  $P(t)$  in the last panel. The time instants correspond to  $P(t) \geq P_{th}$  construct  $S(F)$ . Thus, the synaptic output (the release pattern) is  $S(F) = \{t'_1, t'_2, t'_5\}$ .

$t_i$  that relaxes to  $V_o$ . The parameter  $V_o$  is the maximum allowed size of the ready to release pool of vesicles. The operator  $\max\{\cdot\}$  ensures that  $V(t) \geq 0$ . Fig. 4.2 shows a schematic of time courses of state parameters and probability.

A little attention has been paid to the model even after its implementation in (Natschlager, 1999; Natschlager et al., 2001). The possible reasons for lack of interest in this model are summarized in the following (Kanter, 2007; Lehn-Schioler and Olesen, 2002):

- The model was introduced in a non-standard mathematical form. The continuous time equations are usually difficult to implement especially for dense interconnections and for long simulation epochs. In this representation, a summation over the entire time span is required at each spike. This makes the model not practical. The discrete difference versions of Eqs. 4.2 and 4.3 were introduced then by (Natschlager, 1999). The derivation of these difference equations from the continuous ones was not given; which is why the correctness of the equations were questionable and doubted. In App. B.1 a possible derivation is introduced and discussed.
- Although the model implements temporal coding, as the timing of input spikes modulate the time evolutions of the state parameters, the introduced usages of the model was only made

with rate neuronal models (sigmoidal (Neelakanta and DeGroff, 1994)). In this context,  $S(F)$  was assumed to be the effective synaptic output as a "release pattern". Moreover, the model describes the synaptic dynamics merely on the presynaptic site. The process of transferring the release pattern to a sequence of postsynaptic events is completely absent. This closed the door in front of further utilization of the model. Because a link between the synaptic dynamics and a spiking neuronal model, e.g. LIaF model, is then unaccounted for.

- The used mathematical notation made it very difficult to introduce an expression of steady-state response as discussed for previous models in Ch. 3. The analysis of the model and expressing the synaptic actions could not be extended for more than three subsequent spikes (Maass and Zador, 1999; Natschläger, 1999). This added to the aforementioned points have interrupted the further development and usage of the model.

However, the merit in this model lies in three main aspects:

1. In spite of its simplicity it accounts for the stochastic nature of release with being function of both the facilitatory and depressive kinetics.
2. The biophysical plausibility of the described dynamics exists.
3. Most important, the model is integrative; these aspects are main milestones for capturing the required synaptic dynamics.

Hence, and inspired from this model the above concepts and formulations are used as a building brick to introduce the novel model in this thesis. It is the modified stochastic synaptic model (MSSM).

### 4.3 Developing the Novel Model: Reformulating Maass-Zador's Model

Developing the modified stochastic synaptic model has required main three steps that overcome the problems with the Maass-Zador's parametrization:

- Reformulating the state equations from Maass-Zador's stochastic model into more appropriate mathematical form. Specifically the equations are better used in differential equations form.
- Attaching the dynamics of the neurotransmitter within the synaptic cleft. These dynamics are core functions of the synaptic transmission.
- Adding the postsynaptic dynamics. It represents the actual output of the synapse.

In this section, the first step is demonstrated, the latter two steps are explained in Sec. 4.4. The reformulation implies restating the state equations to be in the form of ordinary differential

equations (ODE). Deriving the ODEs from Eq. 4.2 and 4.3 is not a straightforward task because  $c(t - t_i)$  and  $v(t - t_i)$  are noncontinuous functions, i.e. they are not differentiable. The mathematical approach used to reduce the equations to the differential form is briefed below. Starting with Eq. 4.2, it can be rewritten as

$$C(t) = C_o + \sum_{t_i \in F} \alpha \cdot e^{-(t-t_i)/\tau_C}, \quad (4.6)$$

The second term of the right hand side in Eq. 4.6 is the result of a convolution operation between two functions:  $f(t)$  and  $g(t)$ ; where  $g(t) = e^{-t/\tau_C}$  and  $f(t) = \sum_{t_i \in F} \delta(t - t_i) \forall t_i < t$ . The equation can be rewritten,

$$C(t) = C_o + \int_0^t ds g(t-s) \cdot \alpha f(s), \quad (4.7)$$

which is continuous by definition due to the integration. By differentiating both sides, then

$$\frac{dC(t)}{dt} = 0 + \frac{d}{dt} \left[ \int_0^t ds g(t-s) \cdot \alpha f(s) \right] \quad (4.8)$$

from convolution rules

$$= \int_0^t ds g(t-s) \cdot \alpha f'(s)$$

integrating by parts and substituting with integration endings

$$\begin{aligned} &= 0 + \alpha \cdot f(t) \cdot (1) + \int_0^t ds g'(t-s) \cdot \alpha f(s) \\ &= \alpha \cdot f(t) + \left( \frac{-1}{\tau_C} \right) \underbrace{\left[ \int_0^t ds g(t-s) \cdot \alpha f(s) \right]}_{\text{from Eq. 4.7} = C(t) - C_o} \end{aligned}$$

by rearranging the terms, the dynamics of calcium buffering in the standard ODE form with balanced units of both sides are formulated (see remarks in Sec. 3.6.2); it is

$$\frac{dC(t)}{dt} = \frac{C_o - C(t)}{\tau_C} + \alpha \sum_{t_i \in F} \delta(t - t_i). \quad (4.9)$$

In similar fashion, Eq. 4.3 can be reformulated to a standard ODE form; however, the mapping  $F \rightarrow S(F)$  is to be resolved first. Assuming  $P(t)$  takes only a binary value either one or zero and using

$$v(t - t_i) \leftarrow P(t) \cdot v(t - t_i),$$

the usage of the threshold value  $P_{th}$  can be avoided. Then, Eq. 4.3 can be expressed as

$$\begin{aligned} V(t) &= \max\{0, V_o - P(t) \cdot \sum_{t_i \in F} v(t - t_i)\} \\ &= \max\{0, V_o - \sum_{t_i \in F} P(t_i) v(t - t_i)\} \end{aligned} \quad (4.10)$$

At any time instant  $t_i$ , the probability value  $P(t_i)$  is a scalar value that is not function of time. Thus, the approach applied in Eq. 4.6 can be repeated for Eq. 4.10. In the ODE form it reads

$$\frac{dV(t)}{dt} = \frac{V_o - V(t)}{\tau_V} - P(t) \cdot \sum_{t_i \in F} \delta(t - t_i) \quad (4.11)$$

The assumption of taking  $P(t_i)$  as a binary value is not restrictive. The assumption is made to introduce the derivation;  $P(t)$  can be any real positive value following the implicit exponential distribution from Eq. 4.1. The physical meaning of the parameter is then changed to be the estimated amount of release at that instant  $t_i$ . In other words,  $P(t_i)$  is an average amount of release defined at each time instant  $t_i \in F$ . The correctness of the differential formulations in Eqs. 4.9 and 4.11 can be checked by integrating them back relative to time between zero and any time instant  $t$ .

So far, two major changes are applied on the Maass-Zador stochastic synapse. First, the mathematical representations of the two state parameters are redefined in order to put them in an appropriate usable mathematical form for all scales of simulations (even for embedded systems implementation). Second, the physical meaning and units of the probability function are changed to represent the average released amount of vesicles. These reformulations enables the integration of missing dynamics into the Maass-Zador stochastic synapse. In the following section, the kinetics of neurotransmitter buffering in the cleft and the binding process on the postsynaptic terminal are presented. With these novel kinetics I introduce the modified stochastic synaptic model (MSSM).

## 4.4 The Modified Stochastic Synaptic Model (MSSM)

Before introducing the kinetics of neurotransmitter buffering in the synaptic cleft, the new formulations of the state parameters defined in the previous section are reviewed. Each synaptic connection models a stochastic synapse. In this synapse, the synaptic response raises from three subsequent dynamics: the presynaptic dynamics, buffering in the synaptic cleft and the postsynaptic response.

### 4.4.1 Presynaptic Dynamics

Upon the arrival of a spike at  $t_i$  from an input spike train  $\sum_i \delta(t - t_i)$ , the release probability induced by this action potential is estimated  $P(t_i)$ . This probability-of-release involved is governed by two counteracting mechanisms: facilitation and depression. Facilitation reflects the calcium concentration in the presynaptic neuron (calcium buffering),  $C(t)$ , while depression represents the

effect of the concentration of ready-to-release vesicles in the presynaptic neuron (vesicles trafficking),  $V(t)$ . They read (El-Laithy and Bogdan, 2009):

$$\frac{dC(t)}{dt} = \frac{C_o - C(t)}{\tau_C} + \alpha \cdot \sum_{t_i; t > t_i} \delta(t - t_i), \quad (4.12)$$

$$\frac{dV(t)}{dt} = \frac{V_o - V(t)}{\tau_V} - P(t) \cdot \sum_{t_i; t > t_i} \delta(t - t_i), \quad (4.13)$$

$$P(t) = 1 - e^{(-C(t) \cdot V(t))}, \quad (4.14)$$

In Eq. 4.12, the intracellular calcium concentration at the presynaptic terminal starts at  $C_o$  and is raised incrementally by each stimulus impulse,  $\delta(t - t_i)$ . The impact of each stimulus impulse to the intracellular calcium concentration is equal to the calcium gain (calcium current),  $\alpha$ , caused by a single action potential. Once the stimulus sequence ends,  $C(t)$  decays with time constant  $\tau_C$  towards  $C_o$ . In Eq. 4.13,  $V(t)$  is the expected number of vesicles of neurotransmitter in the ready-to-release pool at time instant  $t$ .  $V_o > 0$  is the maximum number of vesicles that can be stored in the pool. In a similar fashion to  $C(t)$ ,  $V(t)$  starts at  $V_o$ , each stimulus impulse decreases it by an amount equal to the expected average of released amount (of vesicles) at this time instant  $P(t)$ . The presented form of  $P(t)$  forces an exponential distribution on the values of release probability. This choice was made originally by Maass and Zador to fit the available experimental data (Maass and Zador, 1999). A possible reason for this is that among all continuous probability distributions within  $[0, \infty)$  (positive and continuous) and at any mean value, the exponential distribution has the largest entropy.

Note that the notation of  $t_i \in S(F)$  is no longer used with the summation in Eq. 4.13 as it is not relevant any more. In the MSSM, the synaptic response (explained below) is not defined as the release pattern.

#### 4.4.2 Synaptic Cleft: Buffering of Neurotransmitter

The concentration of the neurotransmitter  $N_t(t)$  in the synaptic cleft is estimated by tracing the amount of vesicles of neurotransmitter that remains in the presynaptic neuron,  $V(t)$ , over time. The decrease in the size of the ready-to-release pool of vesicles in the active zone reflects the incremental increase of the neurotransmitter in the cleft (El-Laithy and Bogdan, 2009, 2011c). Fig. 4.3 illustrates this using a hypothetical trace of  $V(t)$ . The decrease in  $V(t)$  is  $-\Delta V(t)$ ; where  $\Delta V(t) = V(t + \Delta t) - V(t)$ . The concentration of the released neurotransmitter in the synaptic cleft  $N_t(t)$  is determined as in Eq. 4.15. It is worth mentioning that there is a formal distinction between a release site and a synapse; i.e. each quantum of neurotransmitter is stored in one synaptic vesicle. Thus, the concentration of neurotransmitter  $N_t(t)$  in the synaptic cleft is meant to be the corresponding concentration of quanta of neurotransmitter (Kandel et al., 1995;

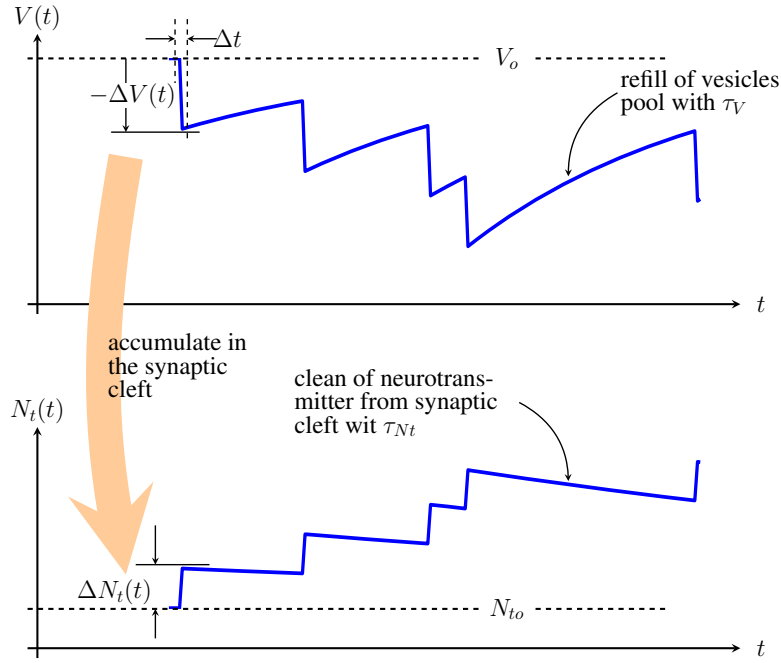


**FIGURE 4.3:** Estimation of the concentration of the neurotransmitter  $N_t(t)$  from the time evolution of the ready to release pool size of vesicles  $V(t)$ . The decrease in the pool size is the added amount to the cleft. The conversion factor between the concentration of vesicles and that of neurotransmitter is the scaling parameter  $K_{N_t,V}$ . The decay of  $N_t(t)$  to the base line reflects the cleaning action of the neurotransmitter from the synaptic cleft.

Morrison et al., 2008). It reads:

$$\frac{dN_t(t)}{dt} = \underbrace{k_{N_t,V} \cdot (\max\{0, -\frac{dV(t)}{dt}\})}_{\text{buffering of released amounts}} + \underbrace{\frac{N_{to} - k_{N_t} \cdot N_t(t)}{\tau_{N_t}}}_{\text{residual after removal}}, \quad (4.15)$$

Eq. 4.15 is a first-order nonlinear differential equation similar to Eqs. 4.12 and 4.13; the incremental raise in this case is then the decrease in the concentration of vesicles (first term), where the  $\max\{\cdot\}$  avoids changes of  $N_t(t)$  due to an increases of  $V(t)$ . The drift term (second term) allows the value of  $N_t(t)$  to decay to the minimum accepted concentration of neurotransmitter in the synaptic cleft,  $N_{to}$ , with a decay time constant  $\tau_{N_t}$ , see Fig. 4.3. This decay reflects the biological cleaning action (removal of the neurotransmitter from the cleft).  $k_{N_t,V}$  and  $k_{N_t}$  are scaling factors, their meanings and effects are explained below.

The decrease in the vesicles pool  $-dV(t)/dt$  is converted to the concentration of neurotransmitter with  $k_{N_t,V}$ ; where  $k_{N_t,V} > 0$ . By setting this factor below unity it implies that either only a portion of the vesicles are involved in the synaptic transmission or it models a slow diffusion of the neurotransmitter to the cleft. At  $k_{N_t,V} > 1$ , it represents an increased diffusion rate or multiple release sites in the active zone on the presynaptic terminal.

The scaling factor  $k_{N_t}$ ; where  $k_{N_t} > 0$  and usually  $k_{N_t} \geq 1$ , models implicitly two biological features related to the removal of the neurotransmitter from the cleft. First, it accounts

for the removal rate of neurotransmitter from the cleft. This rate is determined by the amount of injected enzymes into the cleft. These enzymes are responsible for the degradation of the neurotransmitter molecules in the cleft, this facilitates their re-uptake by the cellular cytoplasm for the re-manufacturing (synthesize) of new neurotransmitter molecules. The rate  $k_{N_t}$  involves the diffusion rate of some other small neurotransmitters which are able to travel back to the intracellular machinery (Hammond, 2001). Second, the sensitivity of the receptors to the concentration of neurotransmitters is not constant. It is subject to changes due to postsynaptic activity or other protein-dependent mechanisms. If this sensitivity is decreased for any of these reasons, it seems as if the rate of neurotransmitter removal action becomes higher.

As for  $N_{to}$  and from a biophysical perspective, the release of the neurotransmitter substances involves mainly two classes of substances (Kandel et al., 1995): a) The small molecules, e.g. Acetylcholine, biogenic amines and some amino acids, and b) The neuroactive peptides. Both classes can coexist in the presynaptic terminal, can be co-released, and both are subject to removal from the cleft. The time scale for a complete removal of neurotransmitter from the cleft differs significantly according to the substance being removed. This difference is related to the biochemical mechanisms involved in the removal process of the neurotransmitter from previous releases. The long-term steady state residual amount of neurotransmitter should be zero provided that no more spikes arrive at the presynaptic terminal, i.e.  $N_{to}(\infty) \rightarrow 0$ . This condition, however, is a rare condition especially in a simulation environment where the input is continuously fed to the synapse. According to Eq. 4.15 it is assumed that the dynamics describing the amount of the neurotransmitter in the cleft permits a minimum of  $N_{to} \geq 0$ . This assumption has two reasons: a) some neurotransmitter substances take much more time to be cleaned from the cleft (for some neuroactive peptides it could be in the order of seconds (Kandel et al., 1995, Ch. 16)), and b) The dynamics described here represent the overall concentration of neurotransmitters in the cleft. And for certain simulation cases,  $N_{to}$  might be required to be nonzero in order to allow for fast rising responses after a silent-input interval.

#### 4.4.3 Postsynaptic Response

The binding process of neurotransmitter to the receptors on postsynaptic membrane induces the excitatory post synaptic potential  $E_{psp}$  which is calculated as:

$$\tau_{\text{epsp}} \frac{dE_{\text{psp}}(t)}{dt} = E_o - E_{\text{psp}}(t) + k_{\text{epsp}} \cdot N_t(t), \quad (4.16)$$

where  $\tau_{\text{epsp}}$  is a decay time-constant and  $k_{\text{epsp}}$  is a scaling factor that models the localized gain (amplification) caused by the influx of neurotransmitter at the postsynaptic membrane. This equation is a modified version of the one used in Liaw-Berger dynamic synapse (Liaw and Berger, 1996).



**TABLE 4.1:** Nomenclature of the MSSM model parameters.

Parameter	Definition (see text for more details)	Units
$\tau_C$	Decay time constant for calcium buffering	Seconds
$\tau_V$	Recovery rate for vesicles' trafficking	Seconds
$\tau_{N_t}$	Decay time constant for neurotransmitter removal	Seconds
$\tau_{epsp}$	Decay time constant for postsynaptic potential	Seconds
$N_{to}$	Initial concentration of neurotransmitter	Molar Concentration (M)
$E_o$	Baseline of postsynaptic potential	Volts
$\alpha$	Calcium rush in gain after spike	M
$C_o$	Baseline of calcium concentration	M
$V_o$	Baseline of pool size of ready-to-release vesicles	M
$k_{epsp}$	Scaling factor from neurotrans. to postsynaptic potential	Volts/M
$k_{N_t}$	Removal (cleaning) rate of neurotrans. from synaptic cleft	-
$k_{N_t,V}$	Transfer factor from vesicles to neurotrans.	-

According to this definition, the time evolution of the  $E_{psp}(t)$  is the synaptic output corresponding to the input spike train. Added to the novel presented dynamics in the cleft, this is another main difference between MSSM and Maass-Zador's stochastic synapse, since in their model the output was the release pattern, i.e. the time instant at which the probability of release exceeds a certain threshold.

#### 4.4.4 MSSM System Overview

From the above analysis and derivations, for any input spike train  $F = \sum_{t_i} \delta(t - t_i)$  the MSSM system of equations are defined as follow:

$$\text{MSSM} \left\{ \begin{array}{l} \frac{dC(t)}{dt} = \frac{C_o - C(t)}{\tau_C} + \alpha \cdot \sum_{t_i; t > t_i} \delta(t - t_i) \\ \frac{dV(t)}{dt} = \frac{V_o - V(t)}{\tau_V} - P(t) \cdot \sum_{t_i; t > t_i} \delta(t - t_i), \\ \frac{dN_t(t)}{dt} = k_{N_t,V} \cdot (\max\{0, -\frac{dV(t)}{dt}\}) + \frac{N_{to} - k_{N_t} \cdot N_t(t)}{\tau_{N_t}} \\ \tau_{epsp} \frac{dE_{psp}(t)}{dt} = E_o - E_{psp}(t) + k_{epsp} \cdot N_t(t) \end{array} \right.$$

where  $P(t) = 1 - e^{-C(t) \cdot V(t)}$ . It should be noted that in this work there is a strict distinction between state parameters (or state variables) and model parameters. The state parameters are those listed in the equations set directly above, i.e.  $C(t)$ ,  $V(t)$ ,  $N(t)$  and  $E_{psp}(t)$  are state parameters that describe the state of the synaptic dynamics at any time instant. Whereas model parameters are any other parameter in the above listing that contribute to the dynamics of the state parameters. The nomenclature of the model parameters are summarized in Tab. 4.1.

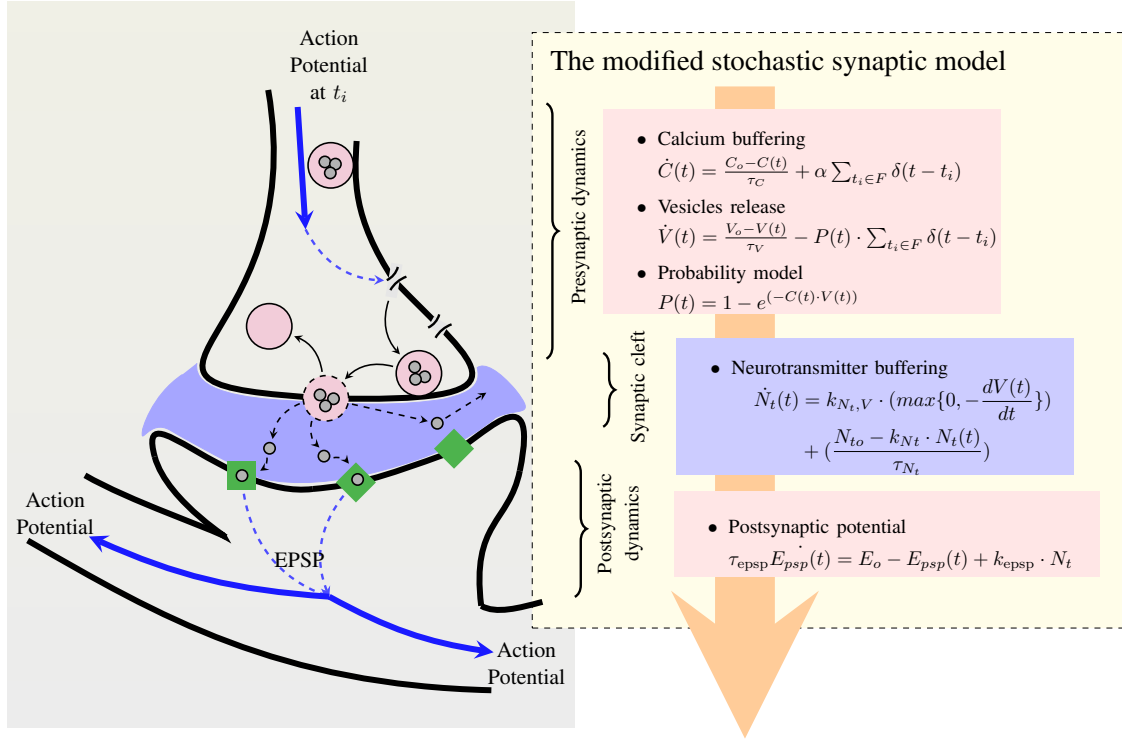


**FIGURE 4.4:** Overview of the MSSM with equations. The descriptions of the biological regions and components of the synapse are omitted for clarity. The full biological illustration is given before in Fig. 2.6. The MSSM captures and possesses the main synaptic properties and features by accounting for the three main regions of synaptic actions in sequence: the presynaptic role, the synaptic cleft, and the coupling at the postsynaptic terminal.

Hence, the MSSM is a biophysical model of short-term synaptic dynamics that is described with the above list of equations. The MSSM unifies facilitatory and depressive dynamics, it captures the main required biological features of the synaptic action; this is illustrated in Fig. 4.4. As shown in this figure, the MSSM unites the main synaptic properties and features by considering the three main biophysical regions of synaptic actions: the presynaptic terminal, the synaptic cleft, and the coupling at the postsynaptic terminal.

## 4.5 Basic Simulations

For the sake of having a quick impression about the behaviour of the MSSM, a pair of simple simulations are given in this section. A sample response of the MSSM and the time courses of the state parameters to an irregular spike train is given in Fig. 4.5. An input spike train with a total epoch of 200 msec stimulates the synapse that is described by the MSSM. Fig. 4.5(a) shows the assumed input spike train with five spikes distributed irregularly over time. Fig. 4.5(b) illustrates the time evolution of the calcium buffering according to Eq. 4.12 with  $C_o$  set to 0.5,  $\alpha = 0.2$  and  $\tau_C = 52$  msec. Similarly,  $V(t)$ ,  $N_t(t)$  and  $E_{\text{psp}}(t)$  are given in Figs. 4.5(c), 4.5(e) and 4.5(f) respectively. The values of the model parameters are summarized in the figure's caption.

This simulation is repeated with two different set of values for the model parameters. The first set is the same as the one used in Fig. 4.5. The values of the model parameters in the second case are selected to be a percentage of those values used in the first one. For example,  $C_o^{(2)} = 0.999 \times C_o^{(1)}$  and the value of  $C_o^{(1)}$  is given in the caption of Fig. 4.5, the same applies for all other involved parameters. For both cases, the input to the synapse is the same one shown in Fig. 4.5(a). Time evolutions corresponding to both sets of values are given for each state parameter in Fig. 4.6. The blue traces are the same shown in Fig. 4.5, while the green ones correspond to the new values of the model parameters. The used values are summarized in the caption of Fig. 4.6. Comparing both traces elucidates how slight changes in the model parameters are reflected on the time courses of the state parameters and especially on  $E_{psp}(t)$  in Fig. 4.6(e). Since  $E_{psp}$  is the synaptic output of the MSSM, both traces represent two different synaptic outputs that correspond to two settings of model parameters.

In order to view the manifested response via the postsynaptic potentials from the latter two synaptic outputs, a LIaF neuronal model is coupled to the synaptic model to represent a postsynaptic neuron, see Fig. 4.7(a). The output spiking activities corresponding to the postsynaptic potentials from the postsynaptic neuron are illustrated in Fig. 4.7(b); the input spike pattern is given as well for a better comparison.

As seen from the spread of the output spikes in Fig. 4.7(b), the different output spiking patterns reflect the essence of variability inherited by utilizing temporally-coded models. Although the input pattern is identical in both cases and the changes in the values of model parameters are relatively not large, the flow of- and the finally delivered information via output spikes are significantly affected by the change in the biophysical ambient represented here through the values of the model parameters. The clear differences between the output spike patterns reflects qualitatively the amount of information processing carried out through the synaptic dynamics. How much are these output spike pattern different from each other, is a general question in neuroscience. In the literature there is relatively a large number of methods to compare the degree of variability within one spike pattern and among different ones. For simplicity the standard coefficient of variation (Koch, 1993) is used for this simple simulation example. More informative measures are introduced and discussed in following chapters. The coefficient of variation measures the degree of variability in a given spike train as the ratio between the standard deviation to the mean of the inter-spike intervals' (ISI) histogram. For a spike pattern  $F$  with a sequence of ISIs, the histogram of these intervals is calculated  $\Delta_{isi}^{(F)}$ . For this histogram,

$$\text{Coeff. of Variation} \equiv \frac{\text{Std}\{\Delta_{isi}^{(F)}\}}{\hat{\Delta}_{isi}^{(F)}}, \quad (4.17)$$

where  $\text{Std}\{\cdot\}$  is the standard deviation of the histogram and  $\hat{\Delta}_{isi}^{(F)}$  is its mean.

In order to have relevant information about the degree of variability in the output spike trains using the coefficient of variation, the simulation settings used in Fig. 4.6 is extended for an epoch

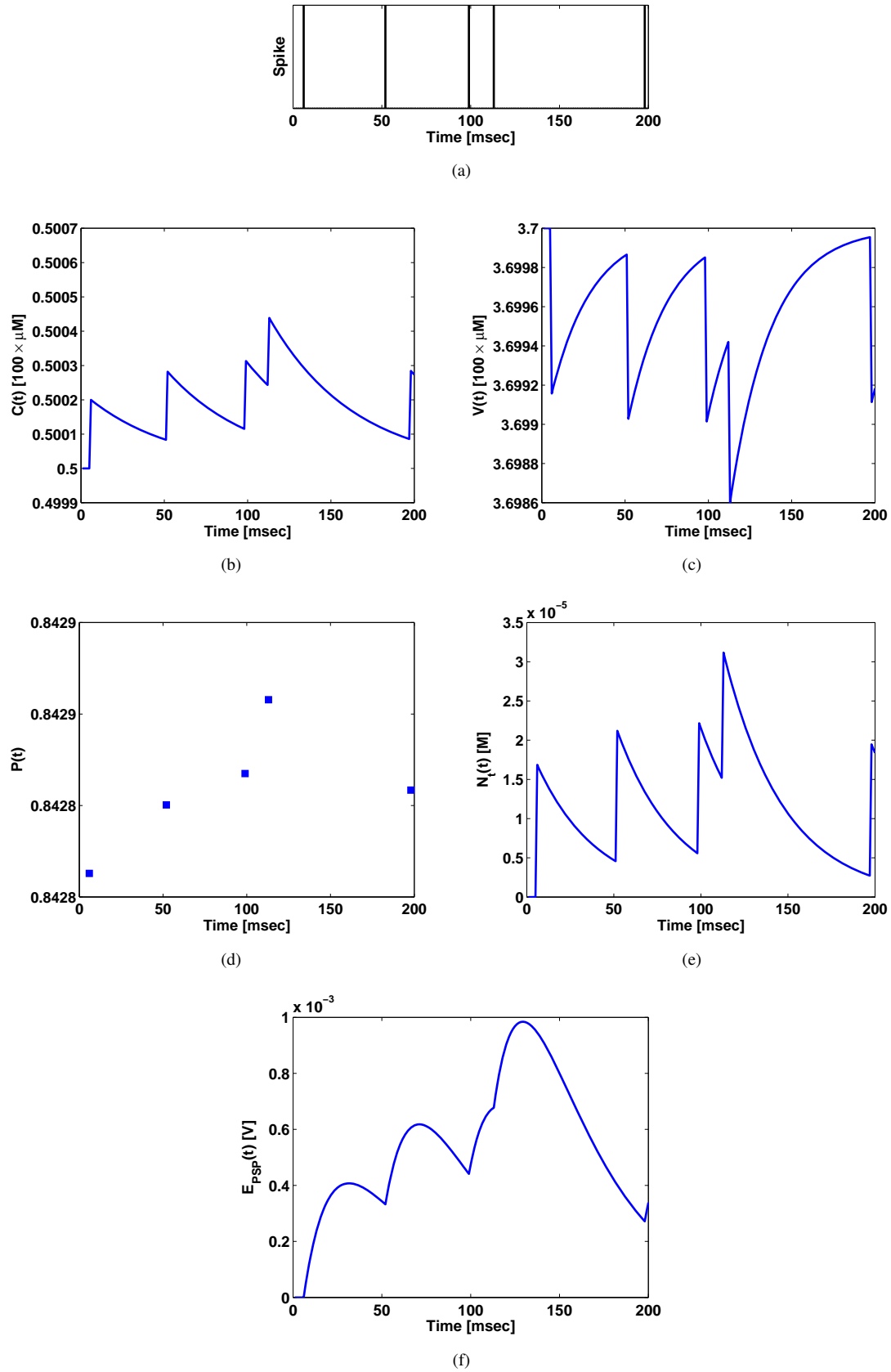


**FIGURE 4.5:** Simulation of the MSSM (Case 1). (a) Input spike pattern. (b) Time course of  $C(t)$ :  $\alpha = 0.2$ ,  $C_o = 0.5$ , and  $\tau_C = 52$  msec (c) Time course of  $V(t)$ :  $V_o = 3.7$  and  $\tau_V = 25$  msec. (d) The probability of release  $P(t)$ . (e) Time course of  $N(t)$ :  $N_o = 0$ ,  $k_{N_t} = 1$ , and  $\tau_{N_t} = 35$  msec. (f) Time course of  $E_{\text{psp}}(t)$ :  $k_{N_t, V} = 20$ ,  $E_o = 0$ ,  $k_{\text{epsp}} = 50$ , and  $\tau_{\text{epsp}} = 20$  msec.

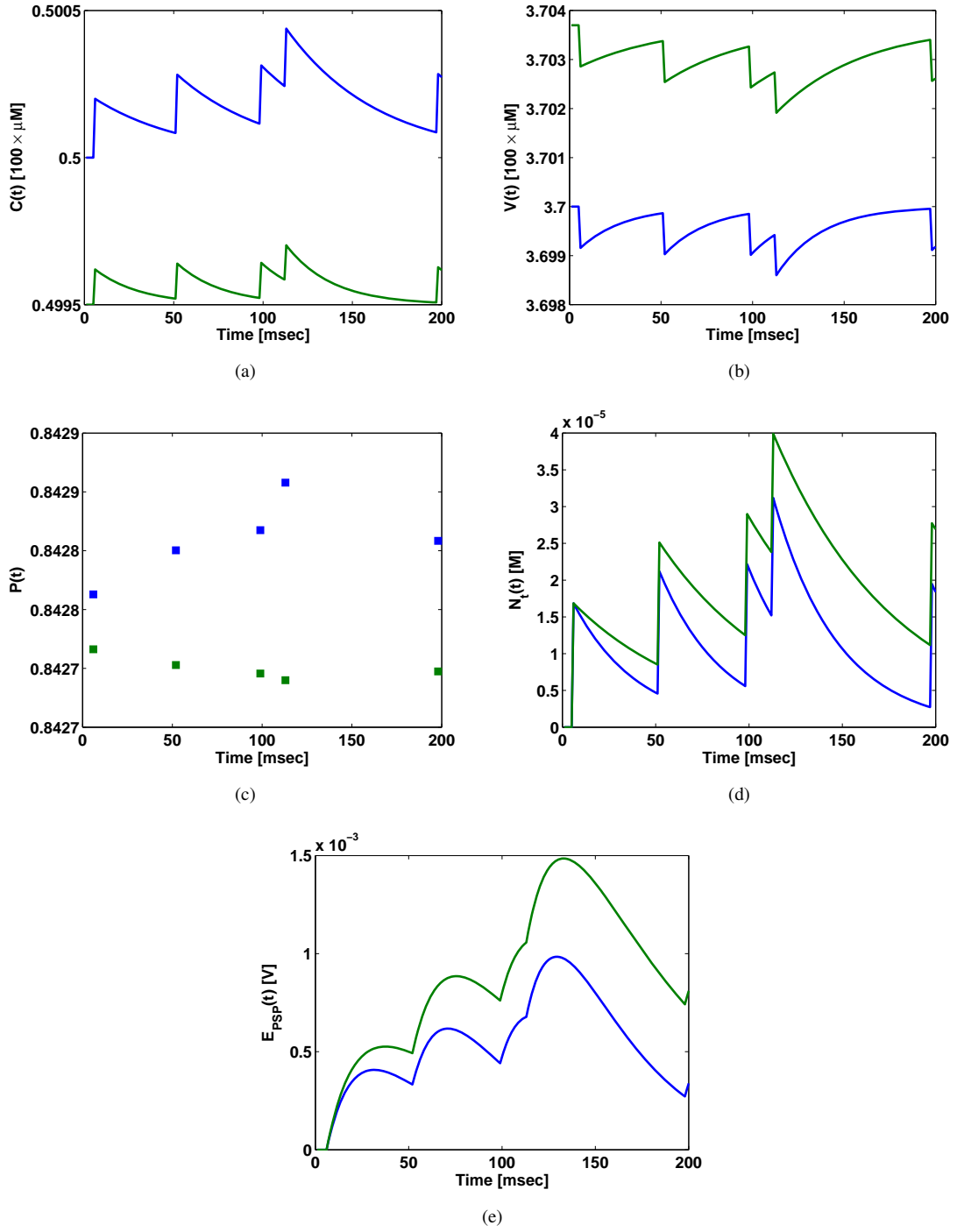


**FIGURE 4.6:** Simulation of the MSSM, influence of model parameters on the model dynamics (Case 1 vs. Case 2). For all subfigures, the superscript (1) indicates the blue trace of case 1 while (2) is for the green one of case 2. (a) Time course of  $C(t)$ :  $\alpha^{(2)} = 0.6 \times \alpha^{(1)}$ ,  $C_o^{(2)} = 0.999 \times C_o^{(1)}$ , and  $\tau_C^{(2)} = 0.5 \times \tau_C^{(1)}$ . (b) Time course of  $V(t)$ :  $V_o^{(2)} = 1.001 \times V_o^{(1)}$  and  $\tau_V^{(2)} = 1.9 \times \tau_V^{(1)}$ . (c) The probability of release  $P(t)$ . (d) Time course of  $N(t)$ :  $N_o = 0$ ,  $k_{N_t} = 1$ , and  $\tau_{N_t}^{(2)} = 1.9 \times \tau_{N_t}^{(1)}$ . (e) Time course of  $E_{psp}(t)$ :  $k_{N_t, V} = 20$ ,  $E_o = 0$ ,  $k_{epsp} = 50$ , and  $\tau_{epsp}^{(2)} = 0.9 \times \tau_{epsp}^{(1)}$ .

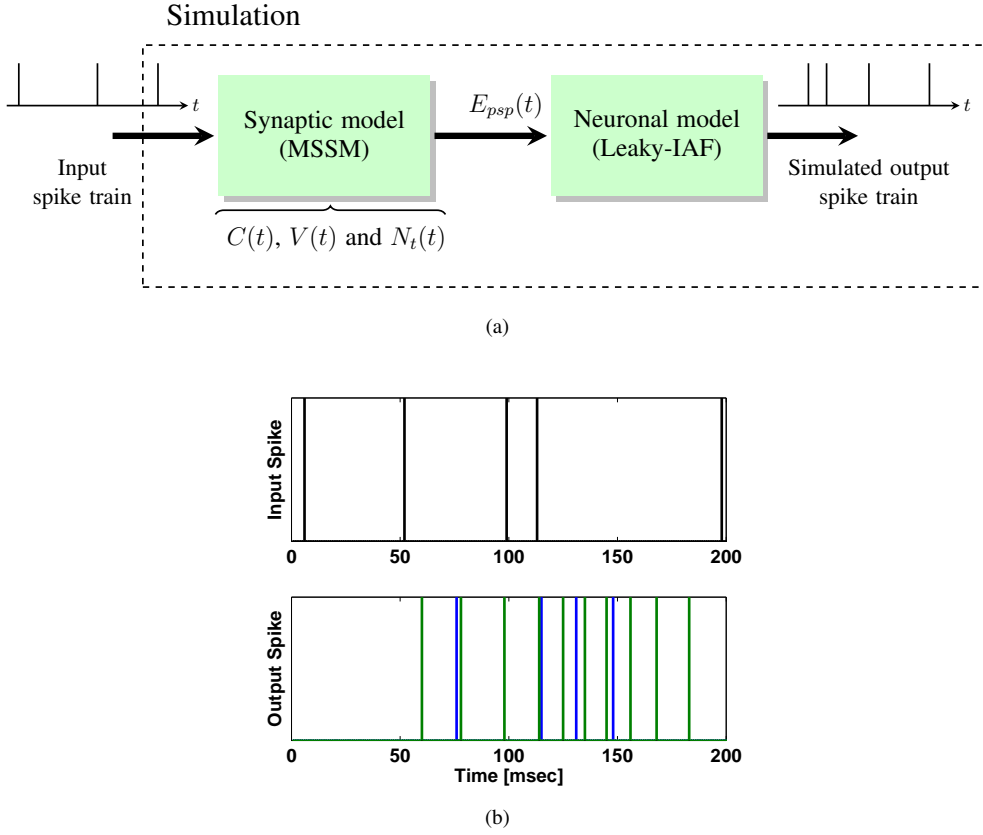


**FIGURE 4.7:** Basic simulation of the MSSM with a postsynaptic neuron. (a) The simple simulation setup. The neuron is represented as a LIAF model. (b) Influence of model parameters on output patterns. The input spike train is shown in the upper panel. The corresponding output for both cases is given in the lower panel. The LIAF model parameters are:  $\tau_h = 20$  msec and  $h_{th}^{(1)} = h_{th}^{(2)} = -69.5$  mV.

of two seconds with an input spike train of uniformly distributed inter-spike intervals. The output spike patterns corresponding to the two cases of model parameters (as in Fig. 4.6) are given in Fig. 4.8(a). In this figure, the upper panel shows the postsynaptic spike pattern with the set values of case (1), while the lower panel shows it for the case with set values (2). Coefficients of variation are 1.7376 for the first case and 2.7391 for the second one. This implies that the second spike pattern is as double irregular as the first one. The difference in variability is supported as well by the distribution of the  $P(t)$  from both cases given in Fig. 4.8(b). The difference in density distribution of estimated release probability indicates that the MSSM processes differently the information carried in the input spike train based on the model parameters. Although this may sound unsurprising, this role of re-representing the information carried in the inputs is a vital role of synaptic dynamics that has little attention in the literature. Furthermore, it emphasizes the importance of having a reliable model for these dynamics. This remark is further used and extended in Ch. 9 and 10 within the second part of this work as the concept of multitasking within a single neural ensemble is introduced. The density distributions of ISIs from both cases are shown in Fig. 4.8(c).

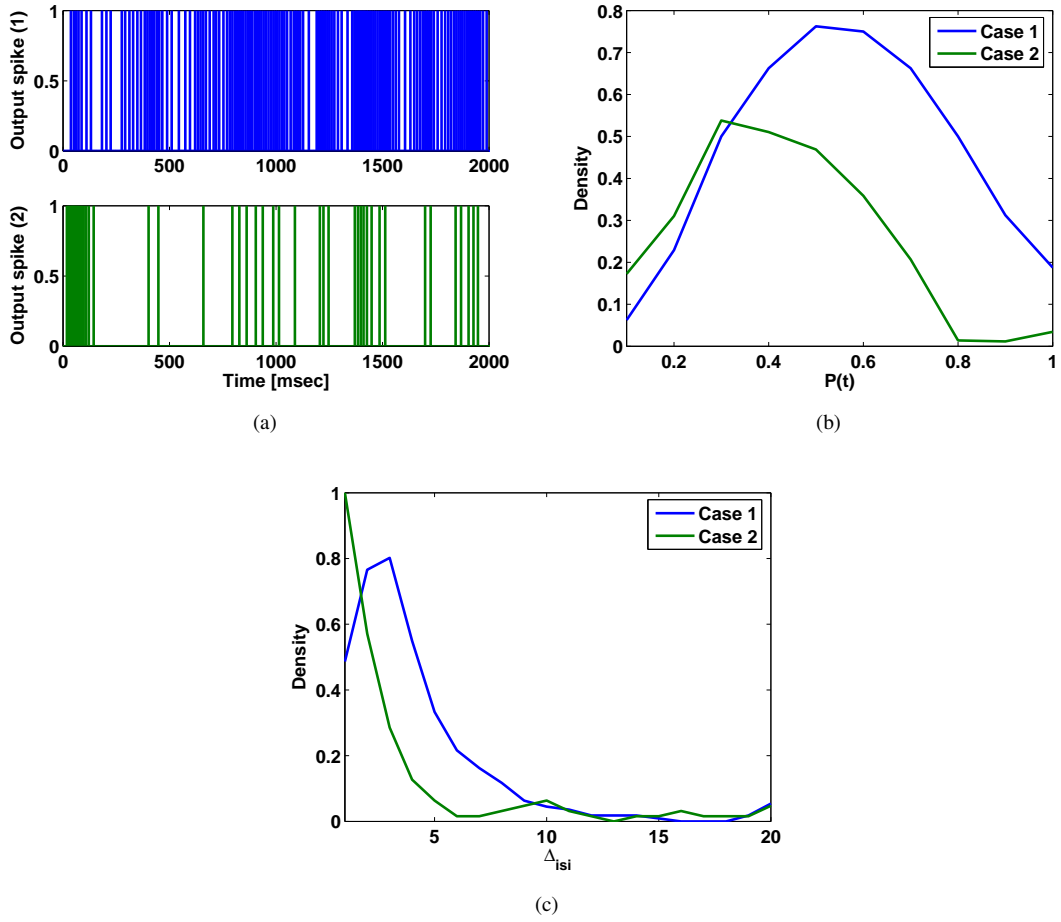


**FIGURE 4.8:** Simulation of MSSM, influence of model parameters on output variability. (a) The output spike pattern from case 1 (upper panel) and case 2 (lower panel) corresponding to an input spike pattern. For both cases the same input is used, it is a spike train with uniformly distributed inter-spike intervals, effective input frequency (number of spikes/simulation epoch) is 40 Hz.  $\tau_h = 20$  msec,  $h_{th}^{(1)} = h_{th}^{(2)} = -68.5$  mV. (b) Normalized density distribution (histogram) of  $P(t)$  for both cases (density is normalized to unity). (c) Normalized density distribution of the ISIs from the output spikes in (a), i.e. the inter-spike intervals histogram normalized to one.

## 4.6 Steady-state Expressions

Detailed derivation of the steady-state expressions is listed in App. B. Here the basic concepts and the closed forms of the steady-state equations for MSSM are given.

Starting with Eq. 4.12, for a regular spike train with a frequency  $f = 1/\Delta_{\text{isi}}$ , the time average of calcium buffering  $C_{ss}(f)$  is estimated by calculating the time average of the function  $C(t)$  from a starting time  $t = 0$  till any arbitrary time instant  $T \gg \tau_C$  and  $T \gg \Delta_{\text{isi}}$ . This is expressed as

$$\langle C(t) \rangle = \frac{1}{T} \int_0^T dt C(t)$$

where  $C(t)$  is substituted in the right hand side with Eq. 4.6 (which is fortunately the continuous time form). Following the derivation in App. B, the final closed form for the steady-state calcium

buffering is Eq. 4.18. Similar approach is applied for other state parameters, the corresponding closed forms are listed in Eqs. 4.18– 4.21.

$$C_{ss}(f = \frac{1}{\Delta_{isi}}) \equiv \langle C(t) \rangle = C_o + \alpha \times \frac{\tau_C}{\Delta_{isi}}, \quad (4.18)$$

$$V_{ss}(\frac{1}{\Delta_{isi}}) \equiv \langle V(t) \rangle = \frac{1}{C_{ss}} \left[ \mathcal{Lam}\{x \cdot C_{ss} \cdot e^{(-C_{ss} \cdot y)}\} + x \cdot y \right] \quad (4.19)$$

$$N_{ss}(\frac{1}{\Delta_{isi}}) \equiv \langle N(t) \rangle = N_o + 2 \frac{\tau_{N_t}}{\Delta_{isi}} \cdot \left( \frac{dV(t)}{dt} \right)_{ss} \quad (4.20)$$

$$E_{psp,ss}(\frac{1}{\Delta_{isi}}) \equiv \langle E_{epsp}(t) \rangle = E_o + k_{epsp} \cdot N_{ss} \quad (4.21)$$

In Eq. 4.19,  $\mathcal{Lam}\{\cdot\}$  is the "lambertw" function and the solution is performed using Matlab Symbolic Toolbox (MathWorks),  $x = \tau_V / \Delta_{isi}$  and  $y = V_o - x$ .

The valuableness of these analytical formulas is that though simple, they indicate the synaptic tendency of being depressive or facilitatory in response to certain input frequencies. Furthermore, this reveals the functional influence of different biophysical contributions through the model parameters on the synaptic action.

It should be noted that these equations are completely different from those presented by (Lee et al., 2009) as mentioned before on page 47. Moreover, the authors of the Lee-Anton-Poon model did not validate their steady-states formulations against the calculated averages of the actual oscillating time evolutions in response to any regular input spike trains. In this thesis, the equations derived for the steady-state expressions for the MSSM are checked and compared to the calculated averages of the actual oscillating time evolutions, see Sec. B.2.

## 4.7 Synaptic Strength & Learning

It should be noted that the internal processes of facilitation and depression can not be isolated from each other in the above listed dynamics. In other words, there are no strict lines indicating the role of each individual model parameter to the final synaptic response independent of the contribution of other parameters, the influence is relative rather than being absolute.

In order to understand this concept, the following example highlights the required meaning. The calcium buffering in general plays a facilitatory role. It enhances the transmission of the input spike by urging the release of neurotransmitter from the vesicles. However, this role is relative to the contribution of other model parameters rather than being absolute. For example if the size of the vesicles pool is relatively small ( $V_o$  is small) and the synapse features a long recovery time constant ( $\tau_V$  is large), a high calcium gain ( $\alpha$  is large) will stimulate a quick consumption of the available vesicles. After a short time, the synapse shall be depressed as one of the synaptic resources is depleted. The opposite logic is also correct, i.e. in case of small  $\tau_V$  and a large  $V_o$  with a small calcium gain  $\alpha$ , the facilitation effect is not enhanced. This kind of inter-dependence



among the model parameters is for an extreme benefit. It permits to model a wide range of synaptic actions. In view of this it supports the plausibility of the model proposed in this work.

In general, it is useful to have a better understanding of the independent effects and the collective influence of the model parameters on the final synaptic response. This understanding is important as well for the sake of developing the required learning algorithms for the MSSM, and for any other dynamic synaptic model. The availability of a learning algorithm is usually a crucial issue when any synaptic (or neuronal) model in a simulation is asked to perform a certain task that involves mapping of predefined inputs into output patterns. In order to investigate this aspects, the synaptic strength has to be defined. In exact words, the *dynamic* synaptic strength has to be defined in terms of the synaptic state parameters. A similar definition to the one proposed by (Levina et al., 2007) for the dynamic synaptic strength of the Markram-Tsodyks model is used. The following definition generalizes the one from (Levina et al., 2007), it was first proposed in (El-Laithy and Bogdan, 2011a):

**Definition 4.1.** A dynamic synaptic model is fully described by its time varying state parameters and its synaptic response  $E_{psp}(t)$ . These state parameters constitute the time varying state vector  $\mathbf{s}(t) = \{s_1(t), s_2(t), \dots\} \forall t \geq 0$ . The synaptic response is explicitly a function of these state parameters, and the value of the dynamic synaptic strength  $S(t)$  of this synaptic model is indicated by the product of the values of the synaptic state parameters. It reads

$$S(t) \equiv \prod_i s_i(t), \quad (4.22)$$

Hence, applying the rule from Eq. 4.22 on the MSSM, the dynamic synaptic strength  $S(t)$  at any time instant  $t$  is

$$S(t) \equiv C(t) \times V(t) \times N(t) \quad (4.23)$$

Note that the equivalence sign is used to ensure that the units are not imported to  $S(t)$ . The dynamic synaptic strength is a dimensionless quantity and its value is calculated as described in Eq. 4.23.

This dynamic synaptic strength carries implicitly and integrates all the information transferred from the input signals. Now, it is possible to study the effect of changing certain model parameter on the synaptic response through its influence on the synaptic strength. In order to illustrate this a simulation example is given. The simulation with the five input spikes from Fig. 4.6 is considered again with changing only the value of  $\tau_V$ . The first value of  $\tau_V$  is set to 25 msec and the simulation with this value is the reference trial. The simulation is repeated twice independently with  $\tau_V$  is set to  $15 \times 10^{-3}$  msec and  $21 \times 10^{-3}$  msec respectively. Fig. 4.9 summarizes these simulations. Using smaller time constants for the recovery of the ready to release pool of vesicles leads to a rapid refill of the pool. This effect amplifies the fluctuations in  $V(t)$  and increases the values of  $N(t)$  consequently. These changes can be seen from the traces of  $S(t)$  in Fig. 4.9(a) (the synaptic strength from the reference case is omitted for clarity). With  $\tau_V = 15 \times 10^{-3}$  msec

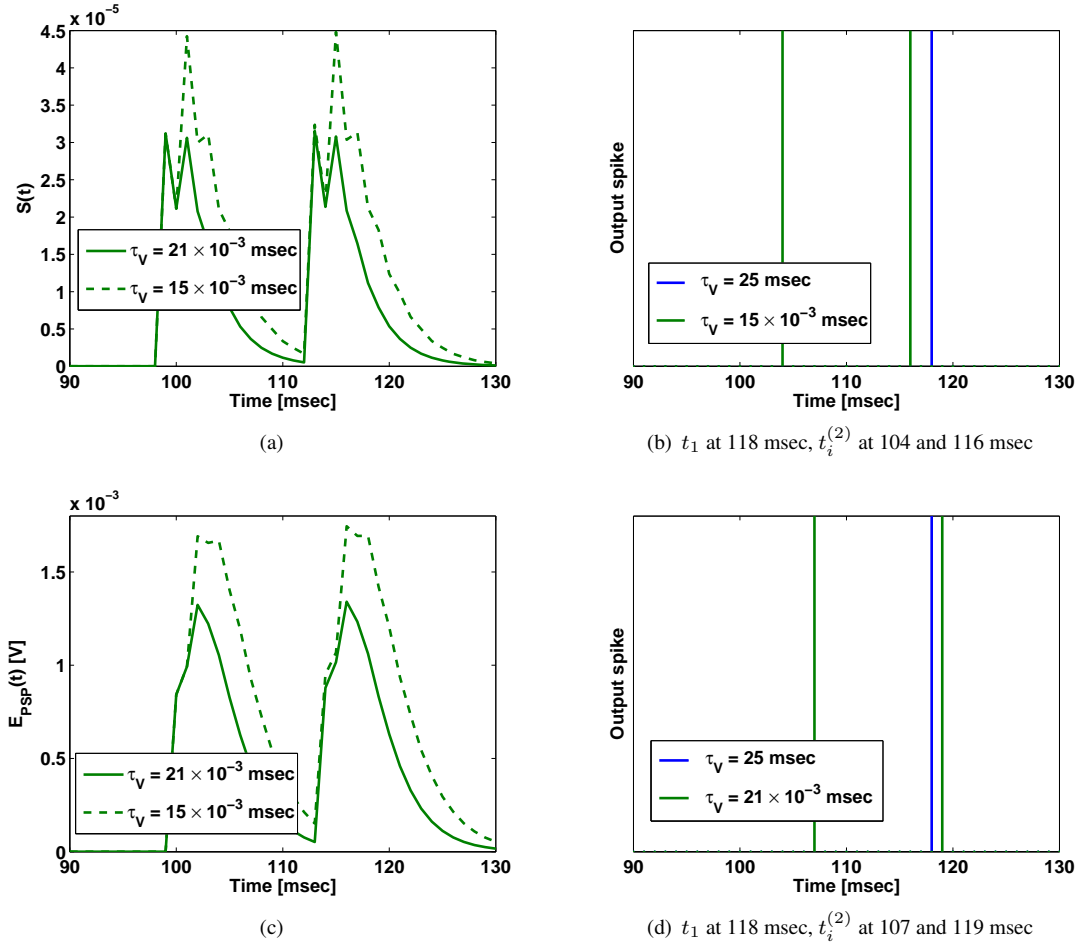


**FIGURE 4.9:** Effect of model parameters on the dynamic synaptic strength and corresponding postsynaptic effects. The input spike train is similar to the one used in Fig. 4.5. (a) The time evolutions of  $S(t)$  at different values of  $\tau_V = 15 \times 10^{-3}$  msec and  $21 \times 10^{-3}$  msec. (c) The corresponding time evolutions of  $E_{psp}(t)$ . (b) and (d) illustrate the output postsynaptic spikes for the two cases (green spikes) at  $\tau_V = 15 \times 10^{-3}$  msec ( $t_i^{(2)}$  in (b)) and  $21 \times 10^{-3}$  msec ( $t_i^{(2)}$  in (d)). The reference output at  $\tau_V = 25$  msec is the blue spike ( $t_1$ ). See text for more details.

there is a fast increase in the synaptic strength, whereas this increase occurs delayed and lasts longer in comparison to the case with  $21 \times 10^{-3}$  msec. This effect is also reflected in the final synaptic response  $E_{psp}(t)$ , Fig. 4.9(c) illustrates the two corresponding time courses. Figs. 4.9(b) and 4.9(d) show the output postsynaptic spikes for both latter cases (green spikes) and the reference output at  $\tau_V = 25$  msec (blue spike). From the spikes timing, it can be observed that relative to the reference blue spike, increasing the value of  $\tau_V$  from  $15 \times 10^{-3}$  msec to  $21 \times 10^{-3}$  msec has shifted the green spikes to the right along the time axis (+3 msec) and has shortened the inter-spike interval (-2 msec). It is much easier and more convenient to figure out the required changes and to observe them through  $S(t)$  rather than following these changes across all the involved synaptic state parameters.

This example demonstrates how changing the values of model parameters can lead to specific changes in the postsynaptic spiking activity. These effects are in direct relation to how a dynamic

synaptic model such as MSSM can be tuned to accomplish predefined certain tasks and represent a simulation based proof that learning can be directly applied to the synaptic model parameters. In fact, this point pursues a more general question, because all dynamic synaptic models are still trained via their scalar synaptic weights when possible, otherwise the models are not incorporated in such tasks that require tuning. All these aspects of learning are discussed in details in Ch. 8.

## 4.8 Probability of Release & Synaptic Noise

Recalling the listing of the equations describing the MSSM on p. 61, the equation that describes the release probability is not listed within. This is made consciously in order to indicate an important strength point and a unique feature in the MSSM. Different to all other models, the used probability function in MSSM forces an exponential probability density function, although being dependent on the instantaneous values of the state parameters  $C(t)$  and  $V(t)$ . This suggests that other probability functions might be used instead of the already used one. These functions shall evaluate the release probability in a similar fashion to the original one, i.e. as a function of the values of the state parameters. For example, it can be assumed that  $P(t)$  reads

$$P(t) \leftarrow \text{EXP} \sim (C(t) \cdot V(t)), \quad (4.24)$$

where  $\text{EXP} \sim (x)$  is a probability value drawn from an exponential distribution with a mean value  $x$ . The usage of this real *stochastic* function instead of the deterministic original probability function adds two important features to the MSSM: First, the typical and essential variability in synaptic response is guaranteed. Simply stated, different output responses (and consequently different postsynaptic spike patterns) are expected from the same input pattern and at the same values of model parameters. It emphasizes the third word in the model's name, stochastic. Second, this real stochastic input represents an implicit source of noise in the synaptic action. Such synaptic noise is also referred to as the background noise (Fellous et al., 2003). Usually, this effect is simulated by adding white Gaussian noise on the values of  $E_{psp}$  (Fellous et al., 2003). This is performed to simulate the required background synaptic activity. This background noise influences directly the synaptic activity, its effect is as important as the effect of the input spike train itself (Fellous et al., 2003). Hence, implementing the probability as described with a true random variable is sufficient and avoids adding external white Gaussian noise. More information about the role of background synaptic noise in information processing is given in Ch. 9.

Fig. 4.10 illustrates the possible variation of the synaptic response and the corresponding post-synaptic spiking when  $P(t)$  is implemented as described in Eq. 4.24. In this figure, MSSM is simulated in response to an input spike pattern with 10 spikes as shown in Fig. 4.10(a). This input is fed twice, once with  $P(t)$  implemented with the original release probability from Eq. 4.14 (case 1), and second with Eq. 4.24 (case 2). This all is repeated for the sake of illustrating the variability in case of using Eq. 4.24, compare the second case in Figs. 4.10(b) and 4.10(d).

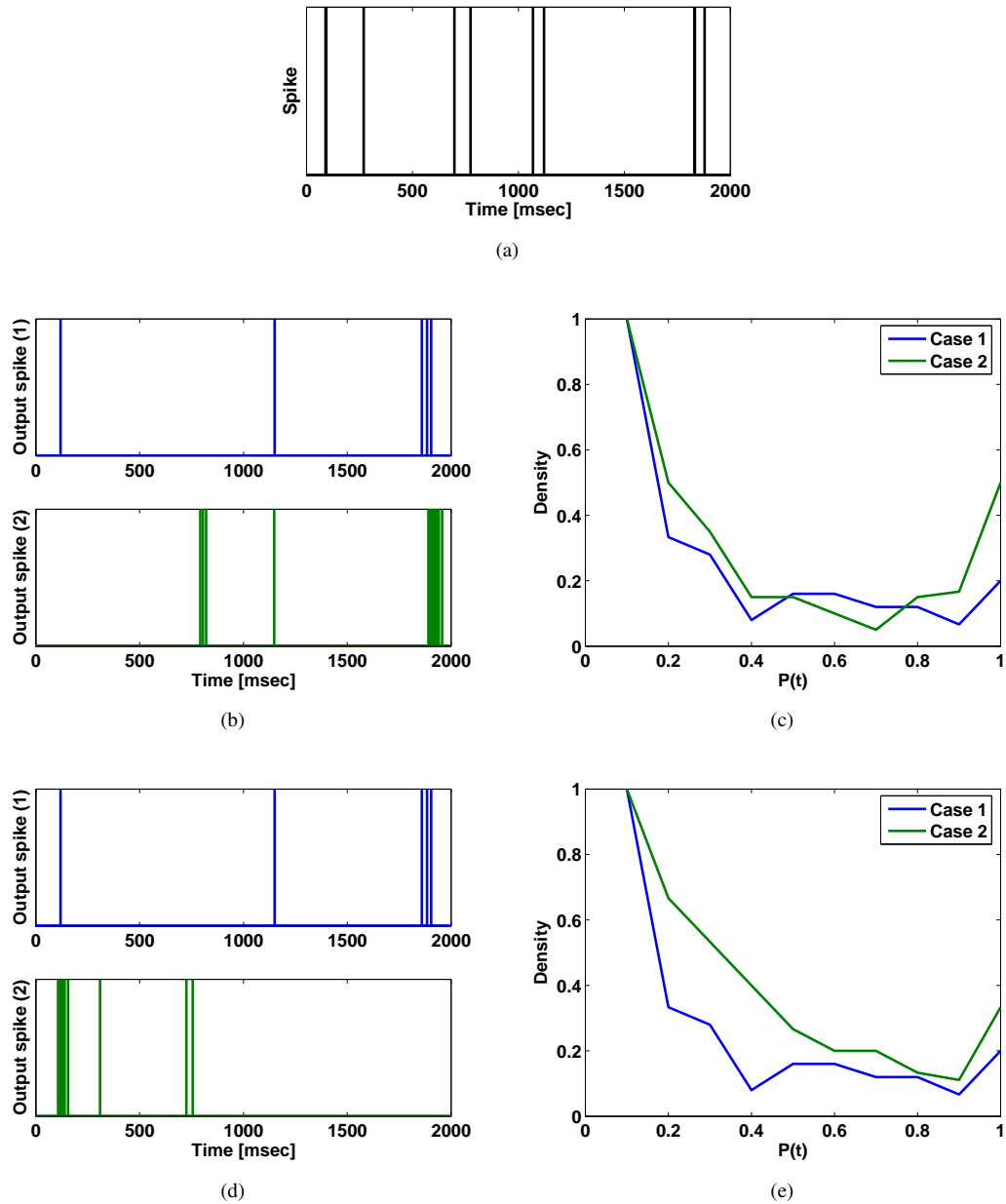


**FIGURE 4.10:** Using a stochastic probability function in MSSM instead of the deterministic evaluation leads to varying output patterns for the same input pattern. (a) Input spike pattern. (b) and (d) The postsynaptic spiking output pattern corresponding to the input pattern from (a). Upper panel is generated with  $P(t) = 1 - \exp(-C(t) \cdot V(t))$ , while lower one is generated with  $P(t) \leftarrow \text{EXP} \sim (C(t) \cdot V(t))$ . (c) and (d) Normalized density distributions (histograms) of  $P(t)$  for both cases (density is normalized to unity)

The example given in Eq. 4.24 can be any other probability function. This opens the way for a series of derivative models from the MSSM to be developed and studied. Although using this true stochastic source in the model seems attractive, it would make the analyses more cumbersome. Hence, in the following chapters, this alternative is not used and investigating the implications of this option is left for future studies.

## 4.9 Comparison with Existing Models

Fig. 4.11 illustrates the relative position of the MSSM in comparison to the previously discussed synaptic models. Intuitively, the MSSM is closer to the expected ideal synaptic model as being biophysically full featured and thus at less computational complexity. Compared to the previous models, the MSSM is based on the essential physiological reactions regimes with standard mathematical formulations. The model is more tractable than the previous complex ones. Furthermore, by being biophysical it is more informative than abstract phenomenological synaptic representations. The main advantages and strength points of the MSSM are clear from the basic simulations and topics discussed above. As for the two main models presented in the previous chapter, the specific differences and advantages of the MSSM in relation to Markram-Tsodyks and Lee-Anton-Poon models are explained below.

First, the comparison between the MSSM and the Markram-Tsodyks model highlights many advantages of the MSSM:

- The MSSM is a biophysical model, this implies a direct added value over the phenomenological model of Markram-Tsodyks. All kinetics and mathematical formulations are related and attributed to real electro-chemical processes in the synaptic action.
- Mathematically, the presynaptic mechanisms in the MSSM can be considered as a generalization of the entire Markram-Tsodyks model. A reduced version of the MSSM can be stated with  $C_o \ll \alpha$  and with the nonlinear relation between the release probability and  $C(t)$  is ignored. With such reduced formulation similar steady-state results to those from Markram-Tsodyks model can be estimated.
- The Markram-Tsodyks model is deficient in important dynamical issues such as missing the explicit modelling of synaptic resources: calcium and neurotransmitter (as vesicles and in the cleft).
- The MSSM accounts for the dynamic nature of the coupling at the postsynaptic membrane while in the Markram-Tsodyks model the linear coupling between the state parameters  $u(t)$  and  $r(t)$  with the synaptic response  $E_{psp}(t)$  is non-realistic. It is worth mentioning that the Dittman dynamic model suffers from the same draw back (see App. A).
- This all reflects the limited capabilities of the Markram-Tsodyks model compared to the MSSM. More quantitative as well as qualitative comparisons in terms of the performance in

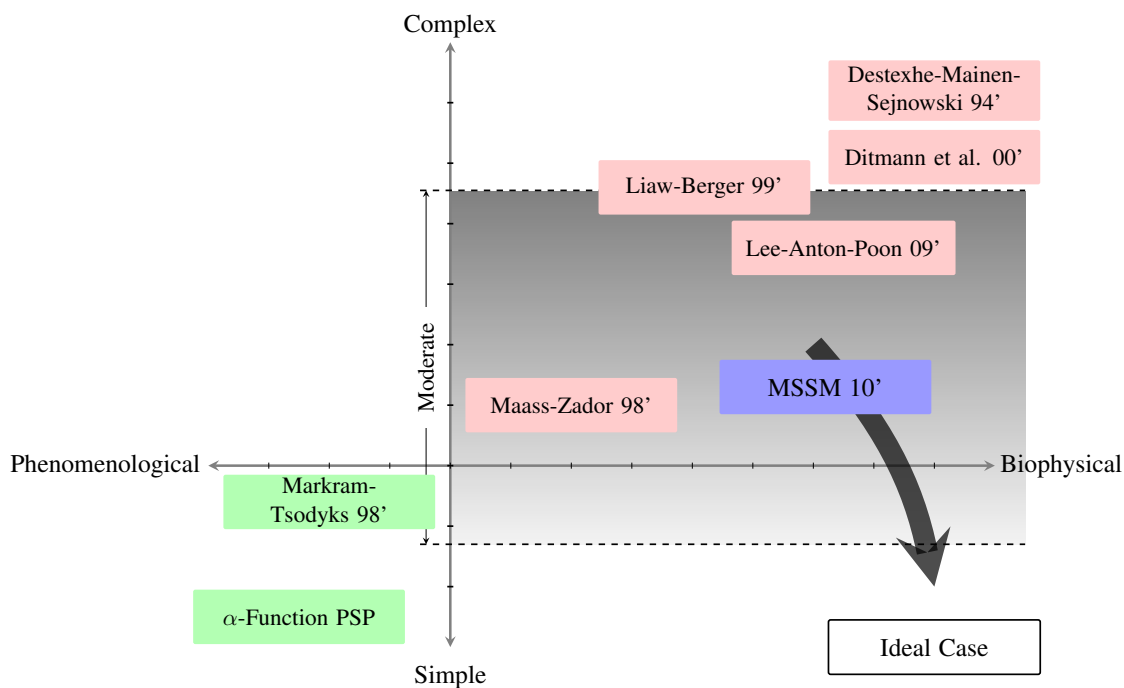


**FIGURE 4.11:** Schematic of relative position of the MSSM to other synaptic models (not an exact scale).

a variety of computational tasks between the MSSM and the Markram-Tsodyks model are given in the following chapters.

Second, comparing the MSSM to Lee-Anton-Poon reveals that MSSM overcomes indeed all the drawbacks encountered in that model:

- All the mathematical formulations of the MSSM are correctly stated and derived with special care to the consistency of units.
- As mentioned above, the MSSM uses the concentration of the neurotransmitter in the cleft to induces  $E_{psp}$  and it accounts for the buffering of neurotransmitter in the cleft which is missing in the Leen-Anton-Poon model. Missing this buffering effect is a conceptual problem in considering that the  $E_{psp}$  is a direct function of the Glutamate flux rather than its concentration in the cleft.
- The conceptual conflict in the dependency of the release probability only on the state parameter of calcium kinetics is resolved in the MSSM.  $P(t)$  is a function of two counteracting state parameters with its original version and its alternative ones, see Eqs. 4.14 and 4.24. As discussed in Sec. 4.8, the flexibility in inserting a true stochastic release probability equips the MSSM with a very important feature that is not available in any other model, the MSSM with this flexibility can be used as a true stochastic synaptic model instead of being deterministic by definition.

- The MSSM avoids the discrepancy introduced in the Lee-Anton-Poon model by modelling a certain neurotransmitter substance. MSSM models collectively the concentration of the neurotransmitter in the cleft. This modelling accounts for the cleaning action of the substance from the cleft as well.
- Being perfectly balanced in modelling the electro-chemical processes in the synaptic action is not (and will not be) an easy task. The MSSM is slightly better than the Lee-Anton-Poon in this regards. The reason for this is that, the MSSM is far simpler than the Lee-Anton-Poon model while it features the same amount of biophysical details as shown in Fig. 4.11; although both models capture more kinetics from the presynaptic sites.

## 4.10 Limitations

Like any other model, the MSSM is limited by some simplifying assumptions. In case of using the deterministic version of release probability, being deterministic may be seen as a limitation factor in capturing the complete essence of variability from synaptic actions. However, the deterministic nature relies on the assumption that MSSM does not model a single synapse, it models rather a the synaptic connections between two neurons in which a large amount of synapses exist. This assumption is true for almost all cases in the brain (Kandel et al., 1995).

The process of calcium buffering is assumed to be a homogeneous and not localized process (this applies to Lee-Anton-Poon model as well). The homogeneity in a biological synapse is altered through other mechanisms of storing and release of calcium ions, e.g. mitochondria and endoplasmic reticulum are able of influencing the concentration of the calcium concentration in the presynaptic terminal specifically and in the cell in general. Therefore, the calcium concentrations are localized. A number of concentration gradients may coexist in a single intracellular fluid region. The assumption of having one gradient (first-order differential equation) is true only near the release sites and maybe only for short intervals of stimulation. This means that only the effects of pumping and diffusion of ions are taken into account. Considering a wider range of possible gradients affects mainly the steady-state responses in terms of the resonance frequencies. Being not localized is true for the trafficking of vesicles as well. The size of the active zone on the presynaptic terminal determines the rate of the releasable vesicles (ready-to-release pool of vesicles) that may change due to many electro-chemical interactions within the cell.

The same limitation can be attributed to the buffering of neurotransmitter in the cleft. The accumulation of the neurotransmitter in the cleft is assumed to be linear and additive, this assumption is true in itself. But the effect of the accumulated amount in inducing  $E_{psp}$  maybe accomplished over a wide range of time scales depending on the type of the receptor. In the MSSM an average is assumed to integrate all the contributing receptors. Again this assumption is justified by considering a synapse instead of a synaptic site. In addition, the removal of the neurotransmitter from the

cleft is affected by the size of the synapse and the stimulation type. Many enzymes are regulating this effect. In the MSSM, a single rate of removal is implemented.

### 4.11 Remarks for Implementation

Throughout this work the Euler method is used to implement both the synaptic and neuronal representations. Unless otherwise is stated, the discretization step  $dt$  is set at 0.002. During the implementation of Eq. 4.14,  $P(t)$  is substituted with  $P(t - 1)$ ; i.e. at any time instant the available preceding probability value is used instead on the current. This substitution was first introduced in Fuchs (1998); Natschläger (1999) assuming stationariness and slow variation of input firing rate.



## Validation: Prediction of Spike-Timing

*"You can know the name of a bird in all the languages of the world, but when you're finished, you'll know absolutely nothing whatever about the bird... "*

**Richard Feynman**

### 5.1 Introduction

In order to check the plausibility of any model, it should be tested against the real system it models. In the case with the MSSM, the real system is the biological chemical synapse. Former studies that have introduced synaptic models, compare only the performance of their models in terms of the steady-state responses against the biological counterparts, see e.g. the work from (Markram et al., 1998) and (Lee et al., 2009). This approach of validating the model dynamics suppresses the very important meaning of modeling a dynamic synapse when only its steady-state responses to long lasting regular spike trains are checked for being biologically plausible. A more appropriate approach should test the ability of the model to deliver reliable predictions of the activity from real biological systems. This concept has motivated a series of studies to validate already existing models of neuronal actions and to call for contributions from the experimental studies to provide more reliable recordings about the neuronal spiking activities especially where the neural circuit is clear and known (Gerstner and Naud, 2009; Jolivet and Gerstner, 2004; Morrison et al., 2008).

This chapter validates the MSSM performance as a dynamic synaptic model by testing its contribution against a biological data set of recordings that incorporates a combination of neuronal and synaptic actions. The contribution of the synaptic dynamics is believed to be dominating which makes this data set a perfect challenging task for any synaptic model. The next section review the work of predicting the spike timing in general and introduce the prediction task considered for the MSSM to achieve.

## 5.2 Prediction of Spike-Timing

The work in the field of predicting exact neuronal spike-timing of certain neuronal sites comprises either the development of new models (Jolivet et al., 2006) or designing algorithms for automatic parameter fitting (Jolivet et al., 2008a) for the already available ones. It was shown that if no synaptic action was involved, some of the *neuronal* models are able to yield good and reliable predictions when compared to biological data, see e.g. (Jolivet et al., 2008a) for a short review.

Recently, studying the role of synaptic actions in corresponding neuronal activities gained more importance (Gerstner and Naud, 2009). Carandini et al. presented a notable study for predicting the exact spike-timing from a single postsynaptic neuron in the lateral geniculate nucleus (LGN) knowing the spike train on the presynaptic side, i.e. in a retinal ganglion cell. This challenging task is based on the work of Carandini et al. (Carandini et al., 2007). The experiment setup and acquisition of neuronal activity were extensively described in (Carandini et al., 2007; Sincich et al., 2007). In short, extracellular recordings were performed in-vivo in visual cortex of Rhesus monkeys. Retinal postsynaptic potentials and geniculate action potentials were extracted by off-line waveform templating. Postsynaptic activities from LGN neurons were taken as the response of the stimuli. A light source was used to stimulate the center of the optical receptive field. The light intensity varied continuously with a temporal frequency power spectrum between 0.2 and 80 Hz. This visual stimulus has a duration of 10 sec each and was repeated 76 times. Simplified illustration of the experiment is given in the upper panel in Fig. 5.1. For the purpose of predicting the recorded spike-timing of the postsynaptic neuron, a LIAF neuronal model along with a simple synaptic parametrization ( $\alpha$ -function for postsynaptic response) were used by (Carandini et al., 2007). The entire experimental setup is very complex and the experiment conditions are usually difficult to control. Considering these experimental issues along with the described reliability of the recordings, the results reported by (Carandini et al., 2007) were considered as the benchmark for this prediction.

In this chapter, the MSSM's contribution in the above described prediction task is presented. Specifically, the simulation and the analysis reported here show the performance of the MSSM in predicting the exact spike-timing from a single postsynaptic neuron in the LGN knowing the incoming spike train on the presynaptic side (the retinal ganglion cell). For this, the same data set as used by Carandini et al. (Carandini et al., 2007) is used in order to perform a real comparison on biological data. The data set were made publicly available in the International Neuroinformatics Coordinating Facility (INCF) 2009 competition, part D. An extension of the MSSM is used: This extension equips the MSSM with a second fold of spike-timing dependence; this allows the magnitudes of the synaptic responses to adapt accordingly to the embedded temporal information in the input spike train, i.e. to be influenced by the inter-spike intervals along the simulation epoch (explained below). The postsynaptic neuron (from the LGN) is implemented as a LIAF neuron. Fig. 5.1 shows a schematic of both the used setup (simulation) and the experiment from Carandini et al. (Carandini et al., 2007).

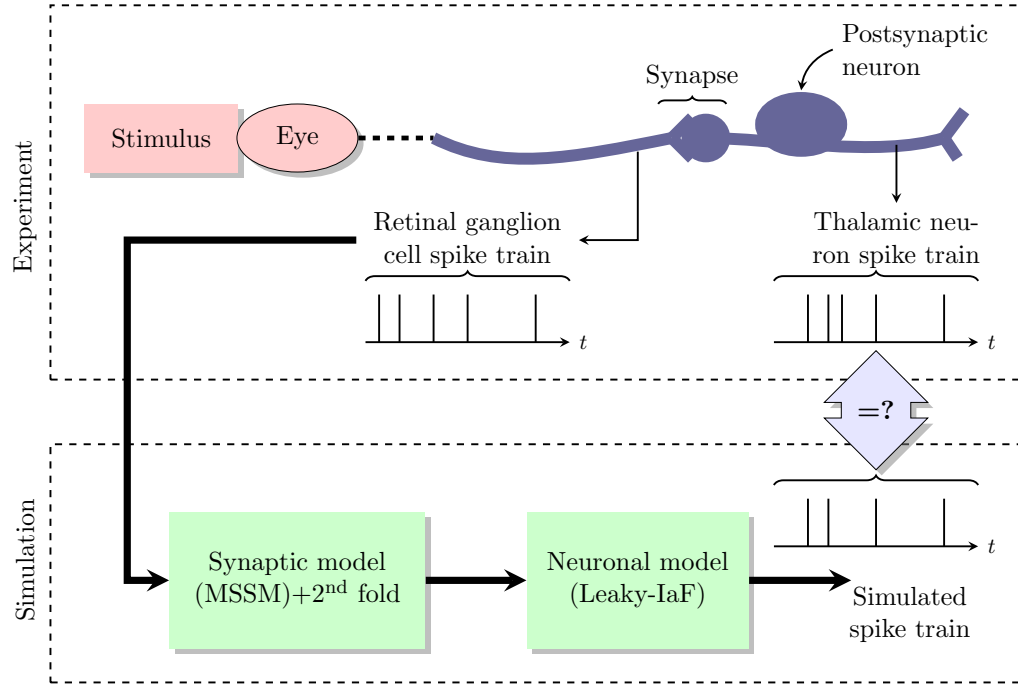


**FIGURE 5.1:** Schematic illustration of the experiment of Carandini et. al (Carandini et al., 2007) (Upper panel) and the proposed simulation setup is shown in the lower panel. The prediction task is to predict the spike timing of the LGN postsynaptic neuron when the presynaptic RGC spiking activity is known. In the simulation (lower panel), the MSSM with its second fold of dynamics simulate the synaptic connection in the experimental illustration (upper panel). The LIaF neuron models the LGN postsynaptic neuron. The double-headed arrow (to the right) compares between the spike trains from the thalamic neuron (upper) and the simulation one (lower). This comparison is performed using the coincidence measure that calculates the similarity between the two signals (explained in section 5.5).

### 5.3 The Model & The Second Fold of STDP

**Synaptic Model** Basically, the synaptic model is the MSSM as listed before on p. 61. The output from the synapse is then fed to an LIaF neuronal model. The neuronal model thus represents the postsynaptic LGN thalamic neuron. The lower panel in Fig. 5.1 shows a schematic of the used setup.

The synaptic action with the previously mentioned synaptic dynamics (basic MSSM) is a function of temporal information represented in the spike-timing of the input signal, i.e. it is a function of inter-spike intervals. This dependence affects how fast either the decay or the build-up of any of the above synaptic state variables occurs in accordance to the timing of input spikes (El-Laithy and Bogdan, 2009). The second fold of this activity dependence is introduced to allow the synaptic action to adapt more precisely to the required variability. This is done by adapting the magnitudes of the responses to the temporal informations as well. The timing dependence is implemented for the response constants themselves, e.g.  $\alpha$  and  $C_o$ . Consequently, the magnitudes of the responses themselves are tuned according to the inter-spike intervals  $\Delta_{isi}$  between successive spikes.

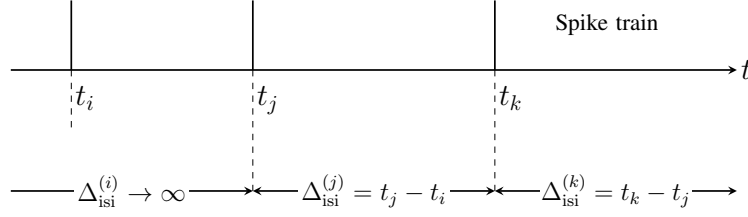


**FIGURE 5.2:** Evaluating inter-spike-intervals ( $\Delta_{\text{isi}}$ ). For a spike train that starts at  $t_i$ , during the time intervals before  $t_i$  and until  $t_j$ ,  $\Delta_{\text{isi}}^{(i)} \rightarrow \infty$  and the corresponding parameters from Eqs. 5.1–5.4 are kept at their minimum accepted values. This leads to a minute error in predictions only for the very first couple of spikes. After the arrival of the second spike,  $\Delta_{\text{isi}}^{(j)}$  is evaluated as indicated.

Thus, for a sequence of successive input spikes at  $t_i, t_j$  and  $t_k$  and  $\Delta_{\text{isi}}^{(j)} = t_j - t_i$  (see Fig. 5.2) and based on the MSSM, the following is defined for all  $t : t_j < t < t_k$  (El-Laithy and Bogdan, 2010b):

$$C_o(t) = \max\{C_{o,\min}, \begin{cases} C_{o,\text{st}} \cdot e^{-\Delta_{\text{isi}}^{(j)}/\tau_C} & , \text{at } t = t_j \\ 0.632 \times C_o(t) & , \text{for } t_j < t < t_k \end{cases} \} \quad (5.1)$$

$$\alpha(t) = \max\{\alpha_{\min}, \begin{cases} \alpha_{\text{st}} \cdot e^{-\Delta_{\text{isi}}^{(j)}/\tau_C} & , \text{at } t = t_j \\ 0.632 \times \alpha(t) & , \text{for } t_j < t < t_k \end{cases} \} \quad (5.2)$$

$$V_o(t) = \max\{V_{o,\min}, \begin{cases} V_{o,\text{st}} \cdot e^{-\Delta_{\text{isi}}^{(j)}/\tau_V} & , \text{at } t = t_j \\ 0.632 \times V_o(t) & , \text{for } t_j < t < t_k \end{cases} \} \quad (5.3)$$

$$k_{\text{epsp}}(t) = \max\{k_{\text{epsp},\min}, \begin{cases} k_{\text{epsp},\text{st}} \cdot e^{-\Delta_{\text{isi}}^{(j)}/\tau_{\text{epsp}}} & , \text{at } t = t_j \\ 0.264 \times k_{\text{epsp}}(t) & , \text{for } t_j < t < t_k \end{cases} \} \quad (5.4)$$

The parameters  $V_{o,\text{st}}, C_{o,\text{st}}, \alpha_{\text{st}}$  and  $k_{\text{epsp},\text{st}}$  are the starting values of the corresponding variables. In the simulation, these equations are implemented following the detection of the input spike at time  $t_j$ . During the time between input spikes  $C_o(t), V_o(t), \alpha(t)$  and  $k_{\text{epsp}}(t)$  undergo an exponential decay. The used implementation does not allow these parameters to drop below certain minimum plausible values:  $C_{o,\min}, \alpha_{\min}, V_{o,\min}$  and  $k_{\text{epsp},\min}$ . These minimum values are set to be less than 5% of the corresponding starting ones. According to Eqs. 5.1–5.4 the increase in the value of any of these parameters scales exponentially with  $\Delta_{\text{isi}}$ . As an example, Fig. 5.3 shows a part of simulating Eq. 5.2 for  $\alpha(t)$  with a sample input spike train where this effect can be clearly seen.

The second fold of spike-timing dependency extends the short-term synaptic plasticity represented in the magnitudes of the modelled synaptic processes:  $V_o, C_o, \alpha$  and  $k_{\text{epsp}}$ . By modulating the values of these parameters according to the temporal information embedded in the input signal, it provides extra means of adaptivity to capture the required variability in the experiment output.

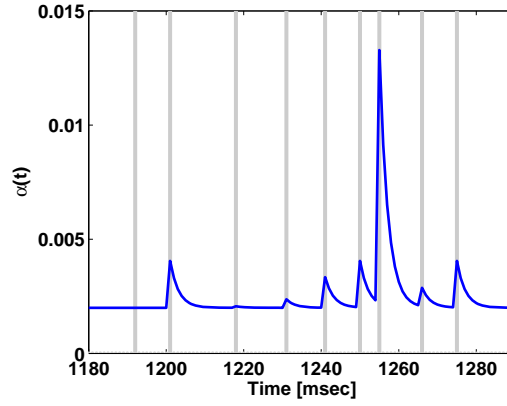


**FIGURE 5.3:** Example of the effect from the second fold of spike-timing dependency. The light gray vertical lines are the input spikes. The trace illustrates the effect of the inter-spike intervals  $\Delta_{isi}$  on the magnitude of the parameter  $\alpha(t)$ . In this example, the minimum accepted value  $\alpha_{\min} = 0.002$ .

Inserting the above dynamics (Eqs. 5.1–5.4) in the mathematical representation of the MSSM (the list on p. 61), the model in this case reads

$$\text{MSSM (+2}^{\text{nd}} \text{ fold)} \left\{ \begin{array}{l} \frac{dC(t)}{dt} = \frac{C_o(t) - C(t)}{\tau_C} + \alpha(t) \cdot \sum_{t_i; t > t_i} \delta(t - t_i), \\ \frac{dV(t)}{dt} = \frac{V_o(t) - V(t)}{\tau_V} - P(t) \cdot \sum_{t_i; t > t_i} \delta(t - t_i), \\ \frac{dN_t(t)}{dt} = k_{N_t, V} \cdot (\max\{0, -\frac{dV(t)}{dt}\}) + \frac{N_{to} - k_{N_t} \cdot N_t(t)}{\tau_{N_t}}, \\ \frac{dE_{psp}(t)}{dt} = \frac{1}{\tau_{epsp}} (E_o - E_{psp}(t) + k_{epsp}(t) \cdot N_t(t)) \end{array} \right. \quad (5.5)$$

Values of the model parameters are listed in Tab. 5.1. The proposed second fold of spike-timing dependency here may be viewed as an abstraction of the effects triggered by some synaptic proteins. From a neurobiological point of view and away from the aspects of long term memory, many experiment-based evidences postulated that synaptic proteins play an important role in short-term plasticity (Douglas et al., 1996; Rosahl et al., 1993). This is supported by other studies emphasizing that certain "brain-specific" proteins modulates short-term synaptic plasticity in excitatory synapses, e.g. (von Engelhardt et al., 2010). These proteins in general affect two main issues in the synaptic transmission: a) Both the formation and release of vesicles from the presynaptic terminal (Rosahl et al., 1993). b) The sensitivity of the AMPA receptors in synaptic spines (von Engelhardt et al., 2010). The proposed second fold of dynamics models partially these effects covering the two synaptic sites: the presynaptic terminal in terms of altering the values of  $C_o$ ,  $\alpha$  and  $V_o$ , and with modulating  $k_{epsp}$  on the postsynaptic site.

**Neuronal Model** Referring to Fig. 5.1, the postsynaptic neuron is modelled as a LIAF neuron, see Sec. 3.4.1. It is described by its voltage membrane potential  $h(t)$  following Eq. 3.3.  $\tau_h$  is the membrane time constant set arbitrarily at 20 msec,  $h_{\text{rest}} = -70$  mV and  $h_{\text{th}} = -60$  mV.

**TABLE 5.1:** Values of the MSSM's model parameters for predicting the spike-timing of a thalamic postsynaptic neuron.

Parameter	Definition	Units	Value
$\tau_C$	Decay time constant for calcium buffering	msec	2.34
$\tau_V$	Recovery rate for vesicles' trafficking	msec	9.18
$\tau_{N_t}$	Decay time constant for neurotransmitter removal	msec	8
$\tau_{epsp}$	Decay time constant for postsynaptic potential	msec	10
$N_{to}$	Initial concentration of neurotransmitter	$\mu\text{M}$	1
$E_o$	Baseline of postsynaptic potential	mV	
$\alpha \rightarrow \alpha_{st}$	Calcium rush in gain after spike	$\mu\text{M}$	0.095
$C_o \rightarrow C_{o,st}$	Baseline of calcium concentration	$\mu\text{M}$	0.05
$V_o \rightarrow V_{o,st}$	Baseline of pool size of ready-to-release vesicles	$\mu\text{M}$	3.7
$k_{epsp} \rightarrow k_{epsp,st}$	Scaling factor from neurotrans. to postsynaptic potential	mV/ $\mu\text{M}$	6
$k_{N_t}$	Removal rate of neurotrans. from synaptic cleft	-	1
$k_{N_t,V}$	Transfer factor from vesicles to neurotrans.	-	1400

## 5.4 Simulation Data and Training

The data set consists of 76 pairs of spike trains (for 76 repetitions of the visual stimuli). Each pair holds both the input spiking-times from the presynaptic neuron (retinal ganglion cell) and the output spiking-times from the LGN thalamic one (please refer to (Carandini et al., 2007) for the details of experimental setup and acquisition details). Each repetition represents 10 seconds of stimulus/response. The odd repetitions out of the 76 ones (36 repetitions) were used as the training set, while the even ones were the test set<sup>1</sup>.

In order to fit the model parameters, training is implemented by applying the Hebbian rules on by-pattern basis to the starting values of the response constants,  $V_{o,st}$ ,  $C_{o,st}$ ,  $\alpha_{st}$  and  $k_{epsp,st}$ . The training process involves 200 simulation episodes. In each episode, the input of a randomly selected repetition from the Carandini training set is fed to the model and the parameters are tuned accordingly using its output as the reference signal. To ensure the introduction of the available 38 repetitions, each repetition is not allowed to appear more than six times during the whole training process.

As for the Hebbian learning rule, denote by  $m$  each of the parameters subject to training:  $V_{o,st}$ ,  $C_{o,st}$ ,  $\alpha_{st}$  and  $k_{epsp,st}$ . According to the pre- and postsynaptic activity, the value of  $m$  is either increased or decreased following the Hebbian approach<sup>2</sup>. The update of the contributing values of a parameter,  $m$ , reads (El-Laithy and Bogdan, 2010b):

$$\Delta m = \eta \cdot m, \quad (5.6)$$

<sup>1</sup>The output spiking-times of the test repetitions are not available for download from INCF at present, however they were used by the INCF committee to calculate the challenge results.

<sup>2</sup>In Ch. 8 the theoretical basics of applying this learning rule directly to the synaptic model parameters are discussed.

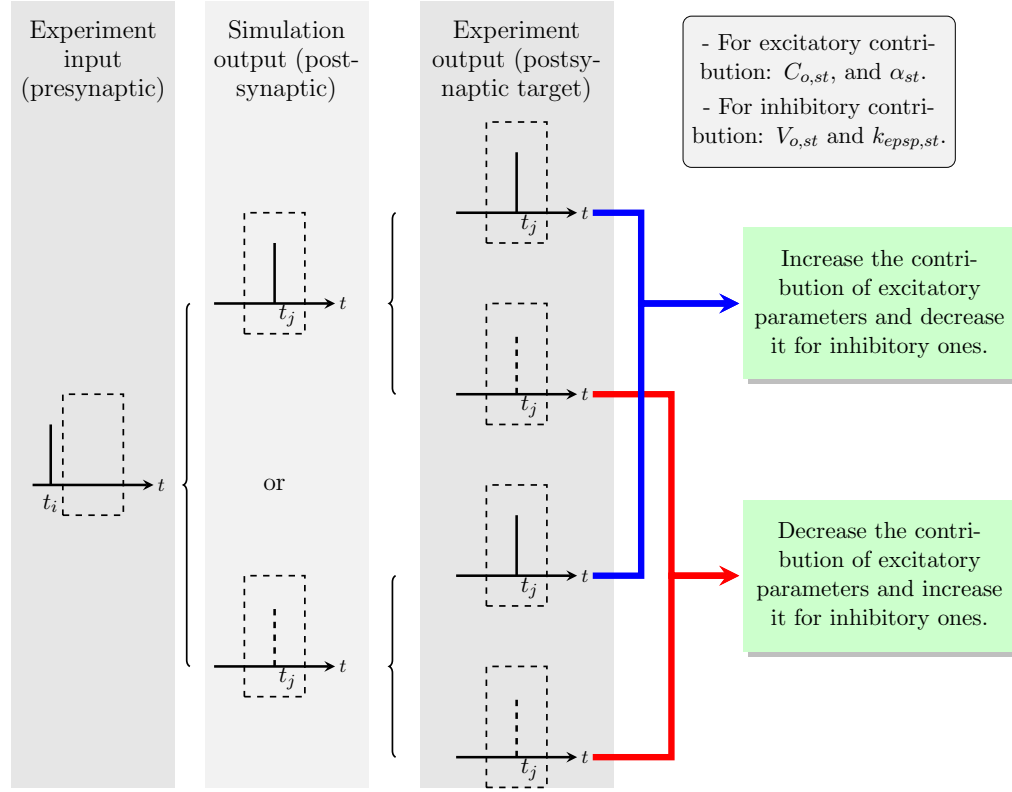


**FIGURE 5.4:** Schematic illustration of the applied Hebbian learning scheme in case of input spike arriving the presynaptic terminal at  $t_i$ . Dashed vertical segments indicate a missing spike at the shown time instant. Dashed boxes illustrate the span of coincidence time window over which correct spike timing is regarded. Having the same existing/missing spike between the second and the third column indicates a correct event. In case that there is no input spike at  $t_i$ , the same logic is applied.

where  $|\eta| < 1$  is the learning rate. It is set arbitrarily to 0.001 (El-Laithy and Bogdan, 2010b). The fitting according to the Hebbian scheme that is implemented in Eq. 5.6 can be summarized as follows: each constant  $m$  from  $(V_{o,st}, C_{o,st}, \alpha_{st}$  and  $k_{epsp,st})$  contributes to either a facilitatory (promoting postsynaptic spiking) or a depressive (demoting postsynaptic spiking) regime during the synaptic action. According to the pre- and postsynaptic activity, its value is either increased or decreased following the Hebbian rule; i.e. if a spike at the presynaptic neuron induces a correct timed spike at the postsynaptic neuron within a time window of 4 msec, the value of the facilitatory variables (that contribute to the facilitatory regime) are increased while it is decreased for the depressive ones, see Fig. 5.4 for an illustration. If the postsynaptic neuron fires and misses the correct timing, the value of the facilitatory variables are decreased while they are increased for the depressive ones. If a postsynaptic spike is generated and preceded with a spike at the presynaptic neuron the same logic applied. Following the challenge conditions, the accepted temporal window between experimental and simulated output spikes is  $\pm 2$  msec.

Applying the Hebbian algorithm for both cases (whether a presynaptic input spike exists or not) ensures that the tuning process can serve as a Hebbian/anti-Hebbian updating mechanism of the values (Farries and Fairhall, 2007). In other words, it compensates for the preliminary

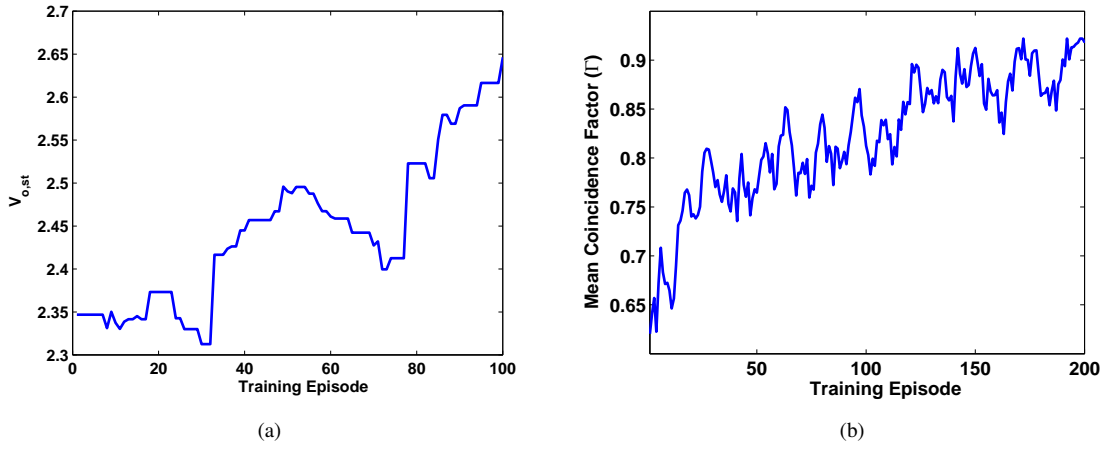


**FIGURE 5.5:** Training model parameters to fit experimental data. (a) Part of the tuning process of  $V_{o,st}$ . The final resting value is 3.7. (b) Performance vs. training given as the mean coincidence factor across the training Carandini data set.

classifications of the contribution of each parameter from being either excitatory or inhibitory. In the introduced dynamics,  $C_{o,st}$  and  $\alpha_{st}$  are considered to contribute to the excitatory action while  $V_{o,st}$  and  $k_{\text{epsp},st}$  are viewed to contribute to the inhibitory action (Fuchs, 1998; Natschlager, 1999). Other synaptic decay constants are held fixed within simulations.

Fig. 5.5(a) illustrates a part of the tuning process of  $V_{o,st}$ . The training process sets the values of  $V_{o,st}$ ,  $C_{o,st}$ ,  $\alpha_{st}$  and  $k_{\text{epsp},st}$  to 3.7, 0.05, 0.09 and 6 respectively. The initial values before the training are taken from (Fuchs, 1998), and they are: 2.35, 0.45, 1 and 2.5 respectively. All non-trained timing decay constants are set to biologically plausible values similar to those reported in (Fuchs, 1998). The finally trained and other fixed simulation parameters are summarized in Tab. 5.1. Fig. 5.5(b) shows the enhancement in the performance as training advances. The performance is shown using the mean of the coincidence factor that is used to indicate the reliability of prediction (to be explained in next section).

## 5.5 Coincidence Measure

The coincidence measure was originally introduced by R. Jolivet et al. (Jolivet and Gerstner, 2004). This test evaluates quantitatively the predictions between two spike trains as a coincidence factor  $\Gamma$ . To evaluate this quantity, the number of coincidences  $N_{\text{coinc}}$  is calculated; it is the coincidence between the spikes in the Carandini spike train from each repetition (as target) and the corresponding spike train from simulation (the model). This is done by counting the number of target spikes for which one can find at least one simulated spike within  $\pm 2$  msec apart from each target spike. Then  $\langle N_{\text{coinc}} \rangle$  is subtracted from it, which is the expected number of coincidences that a Poisson spike train with the same average frequency would give, and then divided by the



number of spikes in the two spike trains:

$$\Gamma = \frac{N_{coinc} - \langle N_{coinc} \rangle}{0.5(N_{Expr} + N_{Mdl})} \frac{1}{\nu} \quad (5.7)$$

where  $N_{Expr}$  and  $N_{Mdl}$  denote the number of spikes recorded from the experiment data and model spike trains respectively;  $\nu$  is a factor that normalizes the coincidence factor  $\Gamma$  to a maximum of 1.  $\Gamma = 0$  implies that the prediction is not better than chance level.  $\Gamma = 1$  implies that the prediction by the model is optimal. For more details please review (Jolivet and Gerstner, 2004; Jolivet et al., 2008a). Using this measure, the predictions from (Carandini et al., 2007) yield a coincidence factor of  $\Gamma = 79.1\% \pm 0.6$  for the benchmark data set. This coincidence factor represented the former benchmark of this prediction task.

## 5.6 Results and Discussion

According to Carandini et al. (Carandini et al., 2007), the used experiment setup can, to some extent, filter out the major contributions of the background noise to the LGN neuronal spiking output. For this reason, no additive noise is considered in the simulation reported here. In the following, the data sets of the recorded spike-timings are referred to as experimental data. Each experiment input spike train from each repetition is processed through the synaptic model and the neuronal model as described above. The timing of the simulated output spikes are then compared to the corresponding experiment output data for each repetition. The spike-timing coincidence factor  $\Gamma$  is calculated accordingly. Fig. 5.6(a) illustrates the value of this  $\Gamma$  factor for the available 38 experiment repetitions; the mean of the  $\Gamma$  factor is  $92.1\% \pm 1.9$ . The second experiment output data set used by the organizers of the competition to validate the proposed models during the competition is not available. However, the results have been calculated and announced by the organisers and the computed mean  $\Gamma$  factor for this set using the MSSM with its second fold is  $90.6\% \pm 0.3$ . Fig. 5.6(b) shows a sample of the model (simulated) and the target output (experiment) spikes. The results illustrate a high precision in predicting the spike-timing within a time window of 2 msec. These results with the above mentioned coincidence factor (90.6%) have been considered as the new benchmark for this prediction by INCF<sup>3</sup>.

In order to provide a better understanding of the internal processes within the simulation, Fig. 5.7 shows 200 msec of the simulation using the ninth repetition with the corresponding time evolution of the state variables  $N_t(t)$ ,  $h(t)$  and  $E_{psp}(t)$ . In Fig. 5.7(a) the experiment input for an arbitrarily selected interval is shown with the corresponding trace of  $N_t(t)$ . Fig. 5.7(b) illustrates the corresponding  $E_{psp}(t)$ , postsynaptic membrane potential and the required target output spike-timings. The synaptic dynamics are mainly responsible for the timing of the generated spikes. An example for this can be seen by investigating Fig. 5.7(b) within the time interval between 1400 and

<sup>3</sup>Model prediction files are available at <http://www.incf.org/community/competitions/spike-time-prediction/2009/challenge-d/submissions>

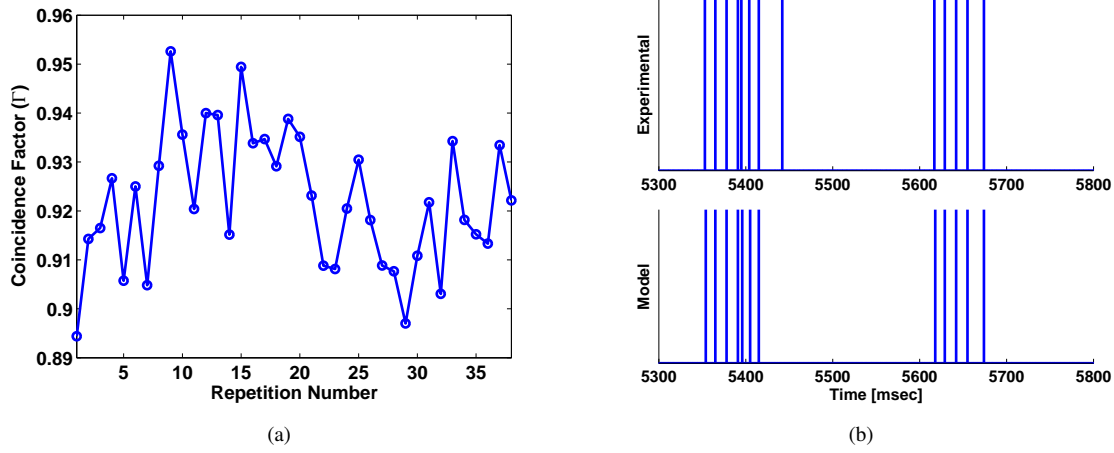


**FIGURE 5.6:** (a) After parameter optimization: The performance of the setup with 38 training repetitions; mean value at  $92.1\% \pm 1.9$ . (b) The spiking times of the simulation using the presented model (lower panel) and the recorded data from experiment (upper panel) of the 33th repetition from Carandini et al. (2007).

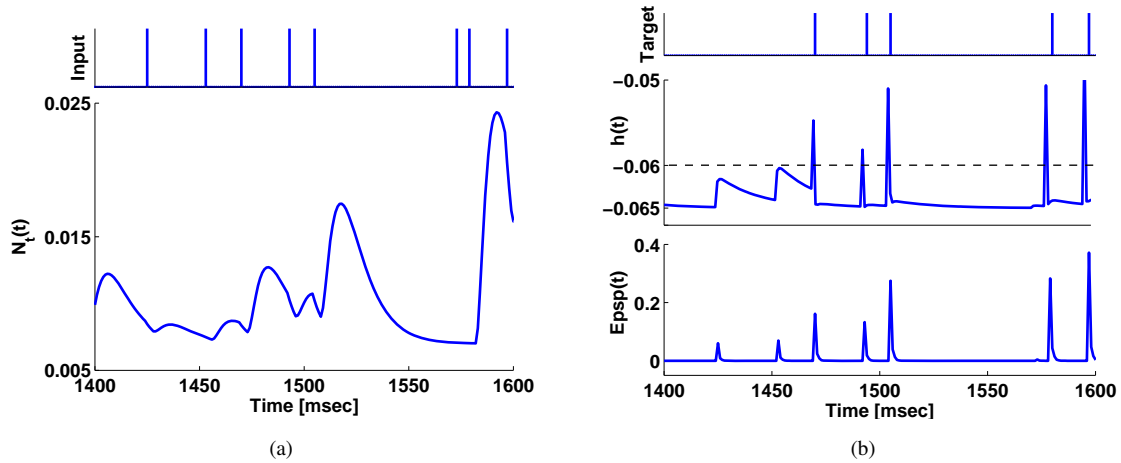


**FIGURE 5.7:** (a) Upper panel: Carandini input spikes over 200 msec from the ninth repetition. Lower panel: The corresponding concentration of neurotransmitter to this input. (b) Upper panel: The target Carandini output spikes. Middle panel: The subthreshold membrane potential  $u$ . Lower panel: The excitatory postsynaptic potential ( $E_{psp}$ ). The narrow short spikes along the trace  $E_{psp}(t)$  is due to the short timing constant  $\tau_{epsp}$ . The spike-like behaviour seen along the trace of  $h(t)$  after crossing the firing threshold value comes from the reset mechanism of the membrane potential to  $h_{rest}$ .

1450 msec, there is a steady depolarization over the rest potential (yet below the firing threshold value). This is induced by the raise in the local  $E_{psp}$  caused by the accumulated  $N_t$ . In Fig. 5.7(a) (lower panel), there is actually a small raise in the concentration of neurotransmitter in this time window. There is no spike generated by this raise since the synaptic dynamics does not deliver enough stimulation on the postsynaptic terminal.

Further analysis is made to learn more about the contribution of each intrinsic process. These processes are the role of the second fold of spike-timing dependency, firing threshold and refractoriness. As for the role of the added second spike-timing dependency to the basic MSSM, the simulation is repeated using the basic MSSM without the contribution of Eqs. 5.1–5.4. After parameter optimization the mean  $\Gamma$  factor across the available repetitions is found to be  $85.6\% \pm 2.3$ . Thus, the second fold has obviously a positive effect on the prediction result. Note that this performance with the basic MSSM is still better than the performance obtained by Carandini et al. (Carandini et al., 2007).

As mentioned in Ch. 3 the firing threshold and the refractory period of the biological neurons are varying due to many factors (Kandel et al., 1995). In order to investigate the effects from both the firing threshold and refractoriness, the simulation for both versions of the synaptic model (basic and twofold MSSM) is repeated with two modifications to the neuronal action: First, the dynamics of  $h_{th}$  is introduced that the firing threshold varies between -56 mV and -50 mV (see App. B.3 for mathematical details). Second, a dynamic refractoriness is introduced, i.e. instead of an absolute refractory period at 2 msec, a new term is introduced in Eq. 3.3 that accounts for a refractory potential that implements a spike-rate adaptation (SRA) (see App. B.3 for mathematical details).

With the basic MSSM and after proper parameter optimization, the introduction of both the dynamics of  $h_{th}$  and the dynamic refractoriness leads to a performance of  $86.4\% \pm 0.6$ . For the twofold MSSM, using the first modification the performance is  $92.1\% \pm 1.1$ . While with the second modification, i.e. using a constant firing threshold and a dynamic refractoriness, the performance is  $92.3\% \pm 1.7$ . All the achieved performances for the different variations of implementations are summarized in Tab. 5.2.

Furthermore, using the twofold MSSM different constant values of  $h_{th}$  are tested under both conditions of absolute and dynamic refractoriness. The performance in both cases are illustrated in Fig. 5.8. The maximum mean values are indicated in both cases.

By studying the performances reported in Tab. 5.2, it can be argued that, in the case under investigation the contribution of the second fold of spike-timing dependency is far more important than the dynamics of the threshold value and refractoriness. This is elucidated when the added value to the performance is regarded in respect to the added complexity from each involved dynamic process. The enhancement in performance is less than 1% in case of using the dynamic threshold and refractoriness while the second fold of synaptic dynamics improves the performance with  $\sim 5.6\%$ . It should be pointed out, that this does not underestimate the role that could be played by using dynamic threshold and refractoriness in general. However, it highlights the role of the synaptic action presented here through the MSSM and its second fold. This agrees with the discussions highlighting the role of synaptic dynamics as a key player in neural signal processing; and that *simple* neuronal models (without both adaptive firing threshold and dynamic refractoriness)

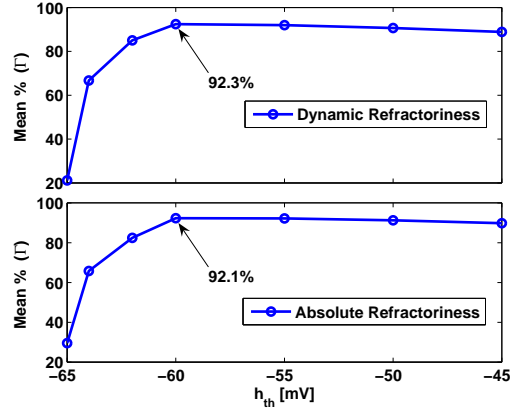


**FIGURE 5.8:** Effect of altering the neuronal contribution via dynamics of threshold and refractoriness. Upper panel: Performance measured as mean  $\Gamma$  factor across all repetitions in case of dynamic SRA and refractoriness at different static values of  $u_{th}$ . Lower panel: Performance measured as mean  $\Gamma$  factor across all repetitions in case of fixed absolute refractory period at different static values of  $u_{th}$ .

**TABLE 5.2:** List of maximal performances for different model variations

Model	$\hat{\Gamma}$ (%)	Comments
Carandini et al.	79.1*	$\alpha$ -function for postsynaptic action
Markram-Tsodyks	83.1	$h_{th} = -60$ mV + 2 msec refr.
MSSM (basic)	85.6	$h_{th} = -60$ mV + 2 msec refr.
MSSM (basic)	85.9	$h_{th} = -60$ mV + dynamic refr.
MSSM (basic)	86.1	dynamic threshold + 2 msec refr.
MSSM (basic)	86.4	dynamic threshold + dynamic refr.
MSSM (twofold)	92.1	$h_{th} = -60$ mV + 2 msec refr.
MSSM (twofold)	92.4	dynamic threshold. + dynamic refr.
MSSM (twofold)	92.1	dynamic threshold + 2 msec refr.
MSSM (twofold)	92.3	$h_{th} = -60$ mV + dynamic refr.
Lee-Anton-Poon	90.4	$h_{th} = -60$ mV + 2 msec refr.
Lee-Anton-Poon	90.8	dynamic threshold + dynamic refr.

- \* Results provided by INCF, see <http://www.incf.org/Events/competitions/spike-time-prediction/2009/challenge-d/submissions/carandini>.
- **dynamic threshold:** The firing threshold dynamics,  $u_{th}$ , are implemented. Otherwise stated.
- **dynamic refr.:** dynamic refractoriness, the SRA-refractory dynamics,  $E_{ref}$ , are implemented. Otherwise  $E_{ref} = 0$ .
- All results are from simulations made after proper parameter training.

are adequately able to simulate the contribution of *neuronal* action (Brette and Gerstner, 2005; Carandini et al., 2007; Jolivet et al., 2008a, 2006).

Guided with those trained parameters from the MSSM, the simulations are repeated with the synaptic models of Markram-Tsodyks and Lee-Anton-Poon independently after proper parameter optimization. The performance of these models are listed in Tab. 5.2. The relative performance of both models in comparison to the performance with the MSSM does not follow the logical expectations when the complexity of the models are considered. The performance of the Markram-Tsodyks model is significantly below the accepted performance threshold at 85% that indicates an actual contribution. This threshold originates from the fact that the mean value of Gamma coincidence factor between both the *recorded Carandini* input and output spikes is  $\sim 85\%$ . This means that, by coupling the pre- and postsynaptic neurons through a dummy linear synaptic weight of unity in the simulation, the goodness of the prediction shall be 85%. It implies that the minimum accepted performance for this prediction task using a synaptic model should have been set to the latter value instead of the old benchmark of 79.1%. The dynamics of Markram-Tsodyks model does not allow for fast switching between the facilitatory and depressive dynamic regimes. This results in a sort of delayed response to a frequent stimulation after an interval of input silence and vice versa. The Lee-Anton-Poon model does not suffer from this drawback. Its performance is better than the one with the basic MSSM while it is quite below the performance of the MSSM with the second fold. Although the model space of the Lee-Anton-Poon model features 33 model parameters (which are compiled into six state parameters) that describe the synaptic action, see Sec. 3.6.2, the enhancement in the performance is insignificant with a maximum enhancement of  $\sim 3.6\%$  over the best performance with the basic MSSM<sup>4</sup> especially when the added complexity of the model is taken into account. The MSSM with the second fold features a maximum set of 16 model parameters<sup>5</sup> with only four state parameters for the synaptic action. Not to mention that certain mathematical formulations within the Lee-Anton-Poon model are computationally very expensive. For example, the probability equation of Eq. 3.13 requires three calculations to power four and a division which makes only this equation computationally at least three times more expensive than its counterpart from the MSSM (Eq. 4.14).

It should be noted that the second fold of dynamics introduced to the MSSM does not add more complexity to the model because no new parameters are attached. The second fold of the STDP presented here does not alter either the model state space or the model's complexity (in terms of new parameters). The number of parameters involved in the dynamics remain unchanged unless the starting values from Eqs. 5.1–5.4 are considered. The main difference is the involvement of the temporal dimension with the response constants in order to be time variant.

<sup>4</sup>A submission with this performance to the INCF challenge would not have shared the first position with the MSSM. An absolute difference of 1% is required to be separately ranked as a winning submission.

<sup>5</sup>They are basic 12 model parameters and the second fold might be viewed to add four constants which are the starting values from Eqs. 5.1–5.4

The main advantages in the MSSM are: a) MSSM models the essence of the variable nature of the neurotransmitter release process through Eq. 4.13 and 4.14, b) It accounts *explicitly* for the activity of two synaptic resources, which are the calcium ions and the neurotransmitter as in Eq. 4.12 and 4.15, and c) The two advantages (a) and (b) are made at a balanced level of complexity which is one of the main advantages of the MSSM over all other approaches. Highlighting the role of explicit modelling of the concentration of the calcium ions agrees with many studies emphasizing that the dynamics of calcium ion channels and the involved accumulation of these ions are key players in the synaptic action (Abbott et al., 1997; Durstewitz, 2003; Jolivet et al., 2006; Yeckel and Berger, 1998). This argument in addition to the novelty of the approach consolidated in the MSSM along with its relative simplicity have motivated its usage for the above prediction task. It is difficult to determine exactly which part of the model is more important or has a more important role. The key challenging requirement in the considered prediction task is that a perfect model should be able of providing both fast and slow postsynaptic responses in response to a highly dynamic input frequencies. The model itself should be equipped with enough features to capture the required dynamics. This has been accomplished in the MSSM through an optimum modelling of the counter acting mechanisms of facilitation and depression: a) The general facilitation and depression via  $C(t)$  and  $V(t)$  at the presynaptic site, b) The facilitation and depression in the synaptic cleft by modelling both the accumulation and removal of neurotransmitter in  $N_t(t)$ , and c) The fast adaptive response performed via the second fold in Eqs. 5.1–5.4.

Within the context of the considered prediction task, the MSSM is not proposed as a superior to all other synaptic models in general, but it still represents the winning performance and the best achieved performance based on this specific data set. As all results obtained using only one data set in order to calculate its performance, results cannot simply be resumed for other data sets.

The results show that, using the introduced framework, the spike-timing can reliably be predicted. Both the model and results were *a winning submission of a recent international challenging competition* (Gerstner and Naud, 2009; Jolivet et al., 2008b; Kobayashi et al., 2009) for predicting spiking times from biological neurons<sup>6</sup>. These results are the new current benchmark for this task of prediction. These results represent a validation and a biological based check on the relevance of using the MSSM as a core computational unit within simulations aiming at incorporating more computational power and more biologically plausible behaviour on a network level.

---

<sup>6</sup><http://www.incf.org/community/competitions/spike-time-prediction/2009/challenge-d>

# Synaptic Energy

*"The release of atomic energy has not created a new problem. It has merely made more urgent the necessity of solving an existing one."*

**Albert Einstein, *attributed***

## 6.1 Introduction

Within the previous chapters the MSSM is introduced and analysed. The level of simulations so far does not exceed the cellular level with one synapse and one neuron. In these simulations it is shown so far that the MSSM represents an adequate synaptic parametrization that permits for reliable and efficient modelling of the required synaptic dynamics. As mentioned in the very beginning of this thesis, it is important to import this reliability and efficiency then to the next higher level of computations, it is the level of systems and networks. In order to understand the behaviour of a network that uses the MSSM for its synaptic connections, more insights about the dynamics and the behaviour of the MSSM are to be extracted first. Specifically, the behaviour of the network is related to the operating trajectories of the MSSM. The MSSM is a model that describes a physical dynamical system which is the chemical synapse. Each dynamical system features regimes of operation that involve certain operating points. These operating points may be characterized as being stable, critically stable, or chaotic.

The approach used to study the operation of the synaptic model in this chapter relies on an energy-based concept developed basically for the information processing in the brain (Friston and Stephan, 2007). In the next sections, the concept of energy-based analysis is reviewed and its relevance to study the synaptic dynamics is explained.

## 6.2 Operating Points of Dynamical Systems

The methods of analysing the physical dynamical systems are frequently used in the study of neurobiological systems. For example, based on the lattice Ising model Hopfield introduced his network as a recurrent neural network having a symmetric synaptic connection pattern (Hopfield, 1982). In this network there is an underlying monotonically decreasing energy function controlling the network dynamics. Started in any initial state, the state of the system evolves to a final state that is a (local) minimum of the energy function. Later on, in (Hopfield, 1999), he argued that a biological system in the general case can be modelled as a complex analogue computer as well. This analogue computer contains a flow-field with a set of energy minima. Thus, the computer activity is a simple motion in the flow-field from the initial point to the nearest stable point. Each energy minimum acts as a point attractor in the space field of the system.

Many behavioural aspects were analysed in a trial to relate these behavioural observations to known attractor dynamics, see e.g. (Eliasmith and Anderson, 2002; Stringer et al., 2005). It was illustrated that there is a class of features which can be described as dynamic attractors, they were referred to as attractor networks. Levina et al. tackled the self-organizing behaviour regarding critical-stability in a fashion similar to the analysis of Avalanche dynamics (Levina et al., 2009). It has been shown that a network interacting via timing-dependent synapses attains criticality in a certain region of the parameter space. That space is bounded by phase transitions that can be reached by tuning the synaptic strengths. Friston et al. have theoretically shown that for a biological system to hold its self-organizing behaviour, seeking for stable operating points, it should always exhibit a bounded interaction with *its environment* (Friston, 2009), under the condition that this bounded interaction can be defined in terms of the internal states of the system. It was therefore proposed that the *energy* of the system that is *delivered* to this environment can represent this bounding functionality, and that the system continuously tries to minimize this energy. This concepts was termed the Free-Energy principle. This bound (or exchange energy) is not mean to be the thermodynamic free energy of the system.

On the level of detailed networks, some studies have investigated the concept of energy minimization and its relation to synchronized activity of networks acting as dynamic systems, see e.g. (Sarasola et al., 2005). Torrealdea et al. studied extensively the energy and its related global balance in two bidirectionally coupled neurons (Torrealdea et al., 2006). It has been shown that in order to maintain the synchronized regime, there must be some kind of steady energy flow holding the coupling strength between the neurons. It has been shown that this flow of energy is also required for both the cooperative and collective behaviour in any neural ensemble. Furthermore, it was stated that this energy should be supplied (according to their analysis) through *the coupling mechanisms itself*, i.e. through the synaptic connections (Torrealdea et al., 2006). This conceives the synapses to have a more vital role in the information processing in general and in the manifestation of synchrony in spiking neural networks (SNN) specifically.



The relation between synaptic dynamics and synchronous firing is of special interest in this work. As it will be clear in Ch. 9, synchrony is a major constitute of a potential biological information processing mechanism which is binding by synchrony. Hence, based on an energy-based paradigm, the dynamics of the MSSM can be studied to explore whether the dynamic system described by the system equations of the MSSM features any stable (or chaotic) operating points. Consequently, the relation between these expected operating points and synchrony in a network as described in the work by (Sarasola et al., 2005; Torrealdea et al., 2006) is investigated.

### 6.3 Synaptic Energy and Synchrony

The ensuing remarks from the above are: a) The physical system underlying a biological neural system tries to find stable (or critically stable) operating points. These operating points act, in an abstract way, as dynamic attractors. b) The search for such stable operating points is performed in a self-organized manner. The idea of studying those operating points was, however, less studied from the energy point of view excluding those related to the Hopfield net. It was argued that, for a proper analysis of the activity of biological neural systems with regard to energy, the non-equilibrium free energy theorems are rather of particular importance in studying these neural ensembles (Friston et al., 2006; Friston and Stephan, 2007). Because the standard equilibrium rules are defined for time-irreversible behaviour and for macroscopic closed systems. However, the biological neural systems are open systems exchanging matter, entropy and energy with the surrounding environment.

Following these remarks, a synapse is a physical system that functions at certain operating points which are defined through its internal state parameters. Furthermore, these remarks suggest that a synapse is able to operate at a stable operating point for a certain interval. Intuitively, this implies that a synapse as a physical system can exist in a certain *state* of activity and it is able then to switch from this state to a new one. From a neurbiological point of view, one might ask whether a synapse can exist in more than one physical state. Experimental studies have shown that synapses change their strength by jumping between discrete mechanistic states, rather than by simply moving up and down in a continuum of dynamic strength, see e.g. (Montgomery and Madison, 2004). This agrees with studies that have provided a framework for understanding the potential mechanistic underpinnings of synaptic plastic states (Montgomery and Madison, 2002). Furthermore, a recent study has postulated that the LTP(D) dynamics of the synapse feature state transitions among six different biophysical states (Barrett et al., 2009). This was a model of synaptic plasticity at hippocampal synapses which reproduces several slice experiments. If the synapse is able to operate at a specific discretely defined state of activity as pointed in the above cited papers, these findings raise questions about the energy related aspects of such behaviour. Moreover, what kind of contribution might be attributed to the synapses in generating stable synchronous firing among cortical neural ensembles.

Therefore, here the energy-related intrinsic process that may be involved in the *synaptic action* of the MSSM is investigated. This analysis is based on the preliminary observations reported in (El-Laithy and Bogdan, 2011a,c). It represents the first theoretical basis to explain the synaptic behaviour of transitions among different biophysical states. Furthermore, it aims to determine the role of synaptic dynamics as whether it contribute to the coherent activity (synchrony states) and to what extent. The importance of revealing the mechanism underlying synchrony can be explained through discussing the role of synchrony itself in the information processing within the brain. The issue of synchrony and its role in information processing is discussed in much details in the second part of this study, see Ch. 9. As for a short summary at this point, synchrony implies that a group of neurons within a single population or across several ones fire synchronously for a certain time interval and feature specific firing patterns. Some studies call this the construction of cell assemblies (von der Malsburg, 1981, 1999). As for the information processing, *"the recombination of neurons, each of which encodes individual elementary features, makes it possible to represent an infinite number of objects - even those that [one has] never seen before"* (Singer, 2007). In other words, the binding between neuronal activities on temporal basis is a key (basic) operation for information processing within neural ensembles (El-Laithy and Bogdan, 2011c). Understanding the role of synaptic actions in the process of synchrony opens the way for capturing a vital characteristics from the biological neural systems and presenting a new and fundamental property of synapses within the CNS into SNN.

The main questions can be formulated as: is the MSSM as a model enough to accomplish the required dynamics to drive the synaptic response (from an energy-based perspective) into a set of definite states? Consequently, what is the role of synapses through the MSSM dynamics to achieve this kind of synchronous neuronal behaviour within SNN? The answers of these questions are tackled in the following sections.

### 6.4 The Ansatz

The basic approach used in this thesis adopts the energy-based principle for biological neural systems from Friston et al. (Friston, 2009) whereas the synapse is considered to be the separate dynamical system represented with the dynamic system of the MSSM. The presented approach aims at determining the intrinsic energy-based operation of the dynamical system of the MSSM. Furthermore, it aims at developing an analytical explanation of the role of the synaptic dynamic (here of the MSSM) itself in achieving synchrony. It is postulated that the available stable energy levels are responsible for the observed stable synchronous discharge.

Basically, this analysis assumes that each neuron is not able to raise its internal energy over the level at which its membrane potential,  $h(t)$ , reaches the firing threshold value,  $h_{th}$ . Thus, at any time instant, the overall sum of the energies of the *neurons* are either equal or less than a certain fixed maximum. This assumption is used as a fundamental concept relating statistical mechanics to

neural analysis (Neelakanta and DeGroff, 1994). Moreover, up to the author's knowledge there is no conceptual obstacle that stands against dealing with the synapses in terms of energy as separate systems from the pre- and postsynaptic neurons.

### 6.4.1 The Postulates

Here, it is stated that the aforementioned free-energy principle can be adopted describing the dynamics of the synaptic behaviour, specifically regarding the synchronous activity. Considering each synapse as a physical dynamical system described by the system equations of the MSSM,  $E_{psp}$  is the only output exchange quantity between the synapse and a postsynaptic neuron. The electrical energy held by (and transferred via)  $E_{psp}$ , consequently, represents, in an abstract way, what is termed here "the free synaptic energy" (FSE). The following definition of the FSE is introduced:

**Proposition 6.1.** *As an open thermodynamic system, a synapse has a total free energy that is a function of two parameters: The output state parameter corresponding to the sensory inputs to the synapse and the "recognition density that is encoded by its internal states" (Friston, 2010). When  $E_{psp}(t)$  is the postsynaptic potential (synaptic response),  $S(t)$  is the synaptic dynamic strength (recognition density), and  $\tau > 0$  is a presynaptic-dependent constant, the free synaptic energy (FSE) is defined as*

$$\text{FSE} \equiv E_{\text{syn}}(t) \approx S(t) \times E_{psp}(t) \times e^{\frac{-\Delta_{\text{isi}}}{\tau}}, \quad (6.1)$$

*Proof.* For the mathematical proof please refer to Sec. B.4 in App. B. □

In other words, the energy represented in  $E_{psp}$  is the bounded function that the biological system (here the synapse) tries to *minimize* and to *stabilize* by optimizing its internal states. These states (in the synapse) are the activity-dependent concentrations of the chemical constituents holding (and responsible for) the synaptic transmission.  $E_{\text{syn}}$  *does not* represent the thermodynamic free energy of the synapse. The notation "free" is adopted since the synapse as a biological system tries to minimize this exchange energy in a fashion similar to that known from the second law of thermodynamics. This is performed through the minimization of the free energy of a system parallel to the maximization of its entropy. Based on the considerations above, the following concepts are postulated consequently:

1. A synapse is in a continuous trial to bound (regulate) the interaction between itself and its postsynaptic neuron. Assuming that the synapse is an open biological system (from a thermodynamic point of view), the bounding is accomplished, through its inherited dynamics, by keeping its energy as low as possible. It is implicitly assumed that the synapse is able to change those state parameters affecting these dynamics (via e.g. learning or an update rule) in a self-organizing manner.

2. The synaptic transferred energy is a direct function of the internal synaptic electrochemical activities. As illustrated in Sec. 4.7 with Def. 4.1, the synaptic strength can be defined as the product of the state parameters of the synaptic model excluding the state parameters carrying the synaptic response ( $E_{psp}(t)$ ). As described for the MSSM<sup>1</sup> the dynamic synaptic strength is  $S(t) = C(t) \cdot V(t) \cdot N_t(t)$ , see Sec. 4.7.
3. At each minimum (either global or local, if any exists) in the state space, the synapse undergoes a stable level of energy transfer that represents a certain state of stable activity.
4. The stable level of energy transfer at the local minima (which results in a specific firing activity) does not strictly imply a constant firing rate. It can be a firing pattern, if the system does not operate continuously and exactly at the minimum but within the finite region around it as well. This is actually the case when the synaptic background noise is considered in the simulations.

## 6.5 Basic Analysis of Synaptic Energy Function

In order to analyse the MSSM as a dynamical system with regard to energy, the definitions of the synaptic strength (Eq. 4.1) and the synaptic energy (Eq. 6.1) are added to the listing of the MSSM equations, the mathematical details are summarized in see Sec. B.4.2 in App. B in order not to interrupt the reader with equations at this point. The synaptic dynamical system is solved to obtain the trajectories of solution describing the synaptic energy  $E_{syn}(t)$  and the dynamic synaptic strength  $S(t)$  in response to a hypothetical input spike train with overall firing frequency  $\Delta_{isi}^{-1}$ . It should be noted that there is no simulations involved in this analysis. The synaptic model is assumed to take an input with a constant frequency and the required quantities are the time evolutions of the  $E_{syn}(t)$  and  $S(t)$ . They are function of: a) The frequency of the input spike train  $\Delta_{isi}^{-1}$ , and b) The synaptic resources and decay timing constants which are the values of the model parameters. The system is solved using Matlab ode45-solver (MathWorks).

A family of curves are illustrated in Fig. 6.1 showing the time courses of the solutions in case of different starting initial conditions. Fig. 6.1(a) gives the time courses of the synaptic energy for three different initial conditions and model parameters (see Tab. 6.1), the input spike train features an input frequency  $\Delta_{isi}^{-1} = 200$  Hz. The synaptic energy raises at the beginning of applying the input, as time advances the energy level falls down to a set of stable steady state values  $\sigma = \{\sigma_1, \sigma_2, \sigma_3\}$ . These states (i.e. these energy levels) are function of the initial conditions and timing values listed in Tab. 6.1. The solution of the dynamical system of the MSSM shows three different states of energy for the same input spike train following three different settings in terms of initial conditions and timing constants. From Fig. 6.1(b), it turns out that each state of synaptic energy correspond to a different course of the operating synaptic strength. This implies that in case

---

<sup>1</sup>A reduced definition was used in (El-Laithy and Bogdan, 2011a). It reads,  $S(t) = C(t) \cdot V(t)$  considering that the third state variable  $N_t$  is dependent on the second state variable  $V$ . Here, the general definition as in Sec. 4.7 is used.

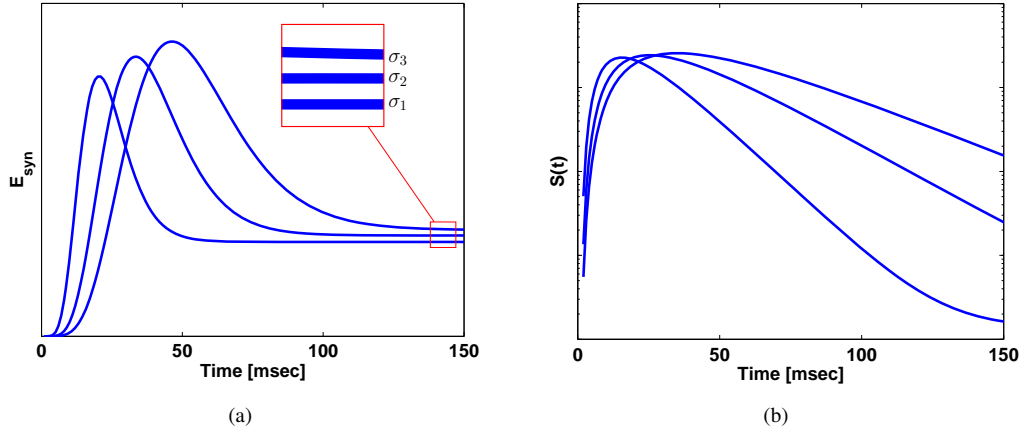


**FIGURE 6.1:** Solutions and time evolutions of synaptic energy and corresponding synaptic strength. (a) Time courses of  $E_{\text{syn}}$  with three different initial resources and timing constants, see Tab. 6.1. The final stable states of synaptic energies are the those labelled as  $\sigma_1$ ,  $\sigma_2$  and  $\sigma_3$  (b) Semilog scale for the  $y$ -axis to show the final synaptic strength values corresponding to the different energy states from (a).

this synaptic model is coupled to a postsynaptic neuron, the corresponding postsynaptic response (postsynaptic spiking activity) will be accordingly different with each energy state. Consequently, the postsynaptic firing pattern shall be unique to this energy state and it corresponds to the time course of the energy function and the related steady-state value of the synaptic strength.

The effect of changing the input frequency  $\Delta_{\text{isi}}^{-1}$  on the synaptic energy states is investigated. Fig. 6.2(a) gives the solution of the dynamic system in case of inputs with  $\Delta_{\text{isi}} = 200$  Hz (blue lines, the same as those in Fig 6.1) and with  $\Delta_{\text{isi}}^{-1} = 50$  Hz (green lines). As seen from this figure, changing the input frequency has a significant influence on the stable energy levels. One important observation to be pointed out here, the relative positioning and values of the synaptic energy levels are not relevant. The distinguishing factor is the ability to feature a wide as well as a flexible set of stable synaptic energies. The relation between the input frequency and the levels of energy states can not be read out as being inversely proportional. Because the levels of the energy states are numerically function of the values of the initial resources and the timing constants. The corresponding time courses of synaptic strengths are given in Fig. 6.2(b).

The effects of noisy inputs are investigated as well. Adding background noise to the model dynamics is not practical during solving the dynamical system within the Matlab solver. Instead, the input frequency is perturbed with  $\pm 10\%$  during the second half of the simulation time. This change in the input frequency represents the influence of a background synaptic noise on the input frequency. The results of this trial are illustrated in Fig. 6.3(a). When the change in input frequency is fed after a while, the final states are considered variations from the main one. The opposite of this process is tested as well, the  $\pm 10\%$  change in frequency value is used during the first half of the simulation time then followed by the standard input frequency. The response to the latter case is given in Fig. 6.3(b). On contrary to the previous case, using different input frequencies at the

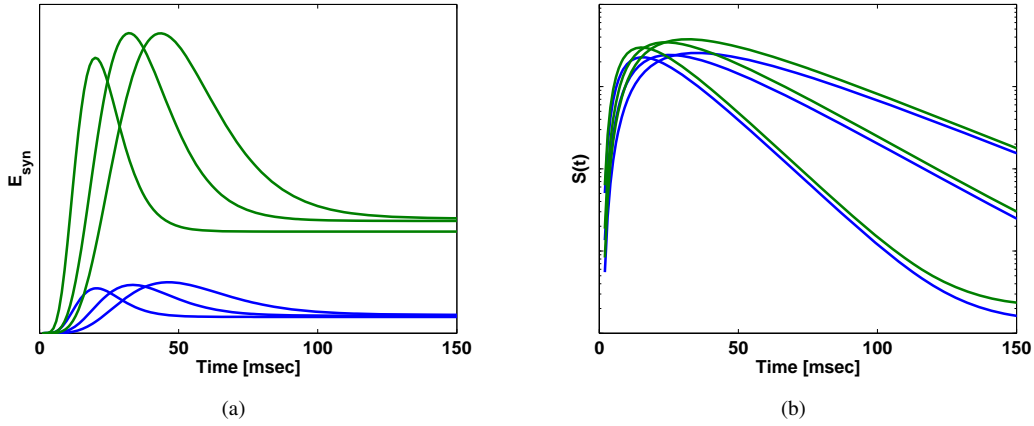


**FIGURE 6.2:** Solutions and time evolutions of synaptic energy and corresponding synaptic strength in case of two different input frequencies  $\Delta_{\text{isi}}^{-1}$ : the blue lines correspond to 200 Hz (the same from Fig. 6.1) while the green lines are for the 50 Hz. Model parameters and initial conditions are the same from Tab. 6.1 used to generate the solutions in Fig. 6.1. (a) The time evolutions of the synaptic energy in case of both input frequencies. The relative positioning of energy states is function of the used initial resources and timing constants. (b) Semilog scale for the  $y$ -axis to show the final synaptic strength values corresponding to the different energy states from (a).

**TABLE 6.1:** The values of both the controlling parameters and initial conditions involved in the solution of the dynamical system of MSSM. These values are chosen to be biologically plausible following (Fuchs, 1998; Shon and Rao, 2003)

Parameter	Comment	$\sigma_1$	$\sigma_2$	$\sigma_2$
$\tau_C$		3 msec	5 msec	7 msec
$\tau_V$		8.4 msec	14 msec	19.6 msec
$\tau_{N_t}$		13.5 msec	22.5 msec	31 msec
$\alpha$		0.0905	0.0905	0.0905
$\tau_{\text{epsp}}$		9 msec	15 msec	21 msec
$C_o$		0.05	0.05	0.05
$V_o$		3.45	3.45	3.45
$k_{\text{epsp}}$		10	10	10
$k_{N_t}$		1	1	1
$k_{N_t, V}$		1	1	1
$C(0)$	Initial condition for ODE solver	0.0150	0.0090	0.0064
$V(0)$	"	0.1233	0.0740	0.0529
$N_t(0)$	"	0	0	0
$E_{\text{psp}}(0)$	"	0	0	0
$S(0)$	"	0	0	0
$E_{\text{syn}}(0)$	"	0	0	0

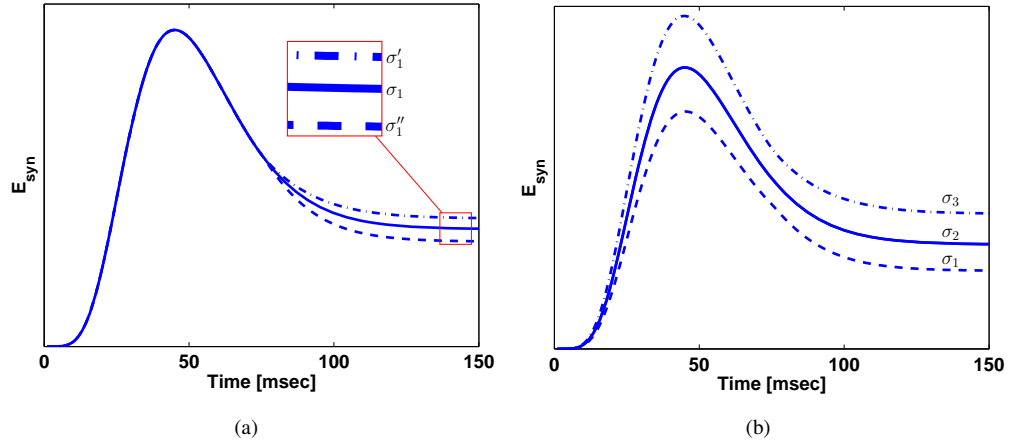


**FIGURE 6.3:** Solution of the dynamical system with the same settings for model parameters from Fig. 6.1 while the input frequency is altered. Model parameters and initial conditions are the same from Tab. 6.1 used to generate the solutions in Fig. 6.1. (a) Solution in case of feeding standard input with 200 Hz for the first half of the simulation epoch followed by  $\pm 10\%$  change in input frequency for the second half of the simulation epoch. The final three states are considered a main states with two variations (as deviations from the main central one) (b) Opposite to the case in (a), solution in case of feeding input of 200 Hz with  $\pm 10\%$  change in input frequency for the first half of the simulation epoch followed by standard input with unchanged frequency for the second half of the simulation epoch. Three unique states are observed in this case.

beginning lead to three distinguishable energy profiles with final three different states. At a glance, this analysis suggests that the synaptic model keeps a kind of memory to the stimuli interrupting its normal flow of energy over time. Although this might not be new, it supports the main goal of studying the synaptic dynamics from an energy-related point of view. That is, considering this energy profile of the MSSM and its relation to synaptic responses gives novel and more insights into the potential roles of this model in regulating and may be controlling the network behaviour.

There is an important and relatively significant difference between the analysis presented here in this work and other studies that discuss the stability and the persistent activity of synaptic dynamics, see e.g. (Barak and Tsodyks, 2007). In these studies, the long-term potentiation in relation to steady-state responses is the core subject of investigations. On contrary, here the analysis is limited to find stable operating points within the energy regime over time intervals which range between 50–300 msec (von der Malsburg, 1999) in order to cop with the time scales over which mental and cognitive functions are relevant (Singer, 2007). The approach of analysing the synaptic models based on their steady-state responses is already evaluated in Sec. 5.1. It is explained why such an approach does not deliver relevant information about the actual behaviour or the dynamics of a synaptic model as it suppresses its core feature which being dynamic.

The results of the analysis with the MSSM presented here so far agrees with a great significance with the experimental findings from (Barrett et al., 2009; Montgomery and Madison, 2004; Sarasola et al., 2005; Torrealdea et al., 2006). These experimental studies have only pointed out implicitly that synapses seem to feature a set of discrete operating points. However, there was no

indication about why and how these states may emerge or on which basis these states are developed. The energy-based analysis presented in the previous sections based on the MSSM dynamics answers these questions. Moreover, these analyses shed some light on the role of synaptic dynamics attributed to the MSSM in achieving synchronized behaviour within a network, this is the core of the next sections.

The role of the incorporated biophysical details in the MSSM model is highlighted as well when these analysis are applied e.g. to the Markram-Tsodyks model. The results from the Markram-Tsodyks model report that it is not capable of experiencing different energy levels in response to different initial conditions at the same input frequency. The model is not sensitive (actually it is immune) as well to noisy inputs. The energy-related analysis and approach presented here can not be applied to those complex biophysical models that don't feature any postsynaptic actions in their dynamics, e.g. the Destexhe-Mainen-Sejnowski model (see App. A).

### 6.6 Stable Spiking Patterns Emerge from Stable Synaptic Energy?

The introduction and analysis of the synaptic energy concept with the demonstration of the stable behaviour is important because this concept carries and delivers new information about the extended role of the MSSM in the collective network dynamics. It encapsulates a novel conceptual paradigm that helps in understanding some of the already existing observations and to emphasize on the crucial role of synaptic dynamics especially in the information processing in neural systems. As an example of what to be comprehended from using such concept in understanding certain network behaviours, the relation between the synaptic energy and synchronous activity within a neural ensemble is considered. The issue of synchrony is briefly explained in Sec. 6.3, it describes the observed synchronous discharge (firing) from a number of neurons within a neural ensemble. Synchrony is the ability of the neural system, in terms of inherited flexibilities, to represent higher level symbols (complex pieces of information) by combining more elementary symbols (Singer and Gray, 1995; von der Malsburg, 1999). This is implemented on the level of neurons within a single population or across several ones. The causal relation between the synaptic energy with the MSSM and this synchronous firing is formulated in the following theoretical formulation.

Basically, experimental studies report that energy during synchronized firing between two coupled neurons can not be zero (and it is of course not negative): *"When the two neurons are coupled they are forced to oscillate in regions of the state space where the long run average of their energy derivative is no longer zero. That means that an extra flow of energy is required to maintain the synchronized regime"* (Torrealdea et al., 2006). Differently stated from a biological point of view, there is an energy release at postsynaptic sites which is responsible for holding a synchronized firing regime (Sarasola et al., 2005, 2004).

Using the proposed concept of FSE and based on the involved dynamics of the MSSM, a novel analytical and theoretical explanation for the above experimentally supported statements is



presented that agrees with their biological basis. In order to introduce the idea of relating the stable synaptic energy states of the MSSM to network dynamics, the following premises are considered for a *fully recurrent network* consisting of  $n$  neurons interconnected with  $m$  MSSM synapses (an example is given in Fig. 6.4): a) An input with stationery randomly distributed (e.g. Poisson distributed with mean  $\lambda$ ) inter-spike intervals (ISI) and a suitable background noise intensity are maintained, b) A number of the synapses  $s$ , where  $s \subset m$ , are allowed to reach for a stable minimum of energy transfer provided that there are  $l$  neurons, where  $l \subset n$ , are directly connected to the  $s$  synapses, and c) These  $l$  neurons have enough excitatory synaptic connections with the rest of neurons  $(n - l)$  in the network. Then, the following proposition is true provided that the synapses are represented with the MSSM:

**Proposition 6.2.** *For a given network with  $n$  neurons, if  $s$  synapses operate at any of the local energy minima and sustain stable synaptic energy  $E_{\text{Syn}}$  to  $l$  neurons, then the rest of the network  $((n - l)$  neurons) is forced to follow gradually the stable activity of the  $l$  neurons, provided that the temporal features of input signal are maintained. If the coherent activity of these neurons is observed over a time window  $\mathcal{W}$ , after a suitable time  $T$ , where  $T \gg \mathcal{W}$ , a general new state of synchronous discharge from all  $n$  neurons should be observed. This defines a network synchrony state.*

*Proof.* According to this proposition, an energy state (or actually a set of synaptic energy states) is(are) encoded within the neural network into a state of synchrony. The proof follows a Gedankenexperiment. Fig. 6.4 gives an illustrative example of the process described in Prop. 6.2. For the network schematic in this figure, it is a recurrent network with three spiking neurons and the interconnections are synapses modelled with the MSSM. Only the forward synapses  $S_1$  and  $S_2$  are assumed to be able to change the values of their model parameters in response to the input spike train. The goal of the assumed self-tuning process is to find the lowest stable level of the synaptic energy. After certain time duration, the synapses shall be able to operate at an operating point that corresponds to this low stable energy level, the operating point is indicated with the big red point in Fig. 6.4. This operating point corresponds to stable level of synaptic energy that reflects a stable transfer of postsynaptic potential. Since the temporal and statistical input features are stationery, the synapses remain operating at this level. When the synapses start operating at the stable synaptic strength level, a certain firing pattern from neurons  $N_2$  and  $N_3$  is expected. As long as other synapses are not experiencing a change in their values,  $N_1$  renders a firing pattern that integrates both the latter firing pattern from other neurons via backward synapses and the input one. Again,  $S_1$  and  $S_2$  will try to adopt the new changes in the input pattern from  $N_1$ . At this point there is two possible cases: a) The new  $N_1$  firing pattern still carries the same information content as the original one from the input alone. Or, b) The  $N_1$  firing pattern carries new information content that encodes the network response through the synergetic contributions from  $S_1$ ,  $S_2$ ,  $N_2$  and  $N_3$ . In the first case, the synapses shall keep their energy level, i.e. they will not search for another stable level of energy. Consequently, the over all network firing pattern shall continue over

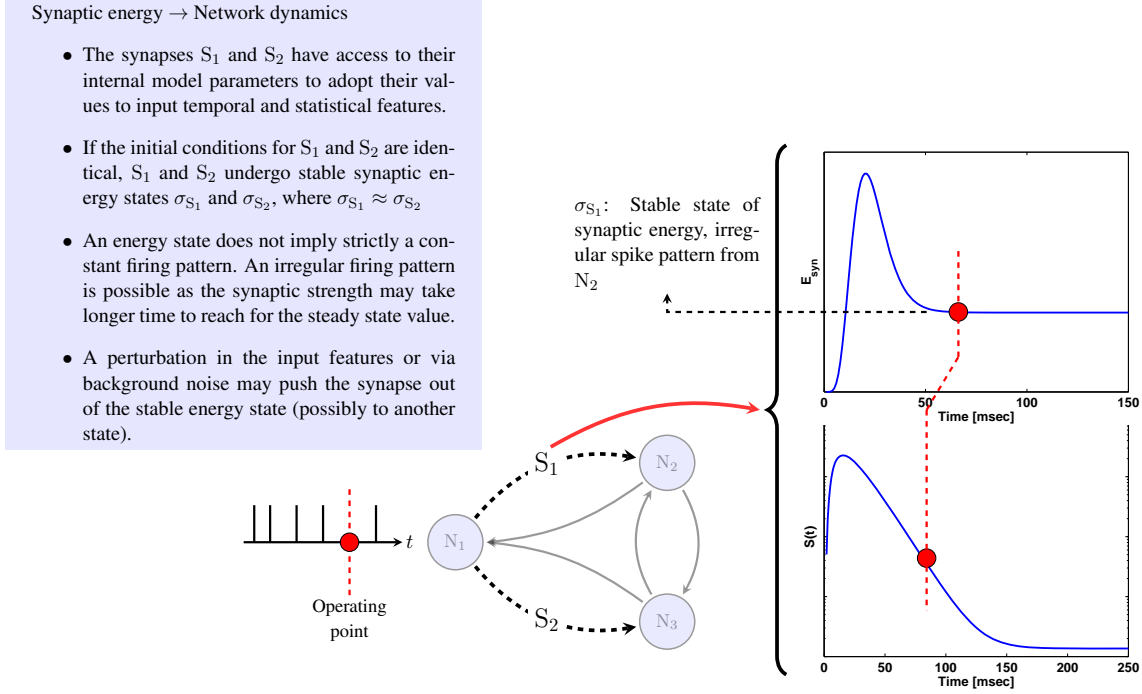


**FIGURE 6.4:** A hypothetical simulation to indicate the relevance of defining the synaptic energy and its relation to network dynamics. The example given in this illustration is generalized in Prop. 6.2. When a synapse operated at a stable energy level which corresponds to an operating point that features a stable synaptic energy, the synaptic dynamics drive the network to a regime of synchronized firing. The firing pattern can be a regular or an irregular pattern. For details see the text in the proof of Prop. 6.2.

time till either new information content is presented or when the synaptic background noise adds this new information content. In the second case, the synapses will seek for another new level of energy that corresponds to the new information content. This search shall be sustained till the network stabilizes again or it stays in search till some new information is fed in.  $\square$

**Remark** This scenario seems very difficult to be analytically analysed and traced in a bit larger network, say with five neurons and four tunable synapses. This difficulty recalls for the feature attributed to the information processing in CNS as being *emergent* as discussed in Ch. 1.

From the above proposition and its proof scenario, the most important message to keep in mind is that: it is possible using the MSSM to show that the synaptic energy levels and their corresponding network synchrony states are the representation of the input information. Differently stated, synaptic energy levels and their corresponding network states based on the MSSM dynamics encode the input information as states of synchronous discharge or as certain firing pattern across the neural ensemble. This agrees with the analysis made by van der Malsburg on the information flow in the visual cortex (von der Malsburg, 1999). Moreover, it agrees as well with the results reported from studies that investigate the behaviour of the Boltzmann machines with regard to visual

attention. Similar to the Hopfield network, the Boltzmann machines implement the energy minimization approach but with stochastic neurons (Ackley et al., 1985). It has been shown that such a network feature sets of activity states which persist after the removal of the stimuli in fashion similar to hallucination in the visual attention (Reichert et al., 2011). This support the postulates made here about the storage of input representations over the synchrony states. Changing this network state means, thus, either the reception of new information content or that the current input information requires a different level of representation.

The results in Fig. 6.1 show that the MSSM has indeed stable operating points in terms of its synaptic energy ( $E_{\text{Syn}}$ ) as a function of its own internal states. The MSSM exhibits a minimum of dichotomous capacity of operating points when the system is perturbed with a fluctuation in perceived input frequency through background noise. Following the postulates in Sec. 6.4.1, a network that uses this synaptic model, on one hand, and when it features a learning update rule for its model parameters (see e.g. (El-Laithy and Bogdan, 2011b)), should be able to exhibit *at least* two levels of internal synchrony: any current (starting) state and a new one to which the network evolves after the application of an input. A small condition should be added at this point, these internal synchrony states can be observed if the window  $\mathcal{W}$  of observing this synchrony satisfies  $\mathcal{W} > 100$  msec. Otherwise, such states according to Prop. 6.2 are not observable. The time window constraint copes with the statements from von der Malsburg (Singer, 1999; von der Malsburg, 1999) regarding the minimum accepted window of synchrony for binding-by-synchrony and those recent argumentations by W. Singer (Singer, 2007). Thus, the theoretically developed concept about the synaptic energy proposed here provides a novel analytical explanation for the experimentally deduced time constraints. The network behaviour as described in this paragraph is investigated in more details in Ch. 9 when the synchrony states on the network level is considered.

## 6.7 Discussion about Energy/Synaptic States

The introduced hypothetical free synaptic energy function and the shown stable operating points are in general novel analytical explanations to the experimentally and theoretically observed aspects of the relation between synaptic action and states of synchrony. These stable operating points represent energy-based explanations for the experimentally observed synaptic states (Barrett et al., 2009; Montgomery and Madison, 2004). This energy-based perspective might be viewed as of special importance due to the biological plausibility. The energy related aspects are fundamental principles that underpin almost all the biophysical processes on the cellular/subcellular level, e.g. protein folding and lipid cell membrane formation. Illustrating this energy-based underlying mechanism with the MSSM analytically in this work calls for more experimental research to validate the introduced hypothetical synaptic energy function.

### 6.7.1 State Transition or Phase Transition?

By recalling the general conceptual regime of the Hopfield network, a network goes from one state of energy to another under certain conditions applied on it from its ambient. The transition between energy levels in this physical model is a phase-transition. The system undergoes a phase transition that corresponds to a singularity in the normal system response.

Biologically, a synchronous activity within a neural ensemble is believed to represent a mental state (Singer, 2007; von der Malsburg, 1999). The transition from one mental state to another (i.e. from one level of synchrony to another) is observed experimentally while investigating some cognitive tasks (Singer, 1999). Following the argumentation in (Chumbley et al., 2008), such transition is more plausible to be considered only as change in the energy regime without experiencing a singularity in the system response, i.e. it is a state-transition.

Experimental evidences show that the level of noise has a great influence on the coherence and thus the synchrony within the neural ensemble (Fellous et al., 2003; Levina et al., 2009). If the noise intensity is changed, the system either reaches for another state corresponding to the new noise conditions or remain in search for it (Fellous et al., 2003). Consequently and according to the theoretical proposition introduced in Prop. 6.2, the basic hypothesis that neural systems experience a sequence of *state-transitions* is supported. This state transition originates from a state transitions on the synaptic levels that builds up internally into a state transition on the network level. The state transition corresponds to the collective effect of the input and the existing noise intensities instead. One more experimental support for this plausibility is that there is no evidence that any neural ensemble exhibit either chaotic or violent non-controlled behaviour (that is normally featured at singularities) during the transition from one synchrony state to another (Fellous et al., 2003).

## Discussion Part I

*"Die Kunst ist es, ein komplexes Problem innerhalb eines kurzen Vortrages allgemein verständlich darzustellen."*

**Martin Bogdan, Attributed**

### 7.1 Overview of the Used Approach

The biological computational abilities attributed to the CNS , e.g. the visual perception and working memory, are emergent features cannot be simply traced back to a set of simple rules as introduced in Sec. 1.5 and 1.6. These abilities are the result of the interaction and synergy between the involved processes performed via neuronal and synaptic dynamics in response to sensory information (input stimuli). Emulating these cognitive functions are seen feasible when a certain basic level of information processing is captured and simulated. The conscious selection of which details to be regarded (for simulation and emulation) and which to be ignored is part of the contribution introduced in this thesis. This conscious selection presumes that certain details are features of the biological construction and not relevant to the computational capabilities of the CNS. That is, certain details are not to be modelled because they do not contribute to the computational functionalities attributed to the biological neural systems. This conceptual selection of the details applies to the functions (abilities) required to be imported in the artificial neural system as well. It is important to note that by taking any level of details as basic and by simulating this *basic* level of information processing, another assumption is implicitly made. It is assumed, therefore, that the simulated basic level does not need to be emulated. The inner workings of the simulated level are therefore ignored. This assumption is made either to simplify the general problem or because those latter inner workings are believed to be irrelevant to the problem of interest. The thesis at hands adopts a general approach that assumes that importing the computational abilities from the CNS into the world of implementable systems require (as sufficient and necessary) a balanced combinations between biophysical details and low computational complexity. This implies that very low

level biophysical details could be regarded as irrelevant for explicit incorporation, e.g. the involved protein dynamics and detailed kinetics of ion channels within synaptic dynamics.

As a novel conceptual framework to study the CNS, some argumentations might be presented over the above described approach of handling the abstraction levels of the CNS's organizational ones. While the used approach in general here assumes that a middle level of abstraction that represents a balanced combination and integration of biophysical details as well as computation complexity is adequate, already running research projects adopt another different approach. These research projects such as the Blue-Brain project (Markram, 2006) and the Brain Emulation project (Sandberg and Bostrom, 2008) assume that the finest biophysical details are a crucial part of the target system. Till the moment of writing these lines and up to the knowledge of the author, these research projects did not deliver significant findings about the information processing mechanisms within the brain yet. Obvious reasons for this might involve that the complexity of the modelled mechanisms are far beyond the available computation power. Besides, certain technological limitations may stand against acquiring a real understanding of certain internal mechanisms. For instance, the most sophisticated patch-clamp setup<sup>1</sup> can record precisely the membrane potential of only 12 neurons simultaneously (Markram, 2006) while a mini-cortical column may have up to 1000 neurons.

On the contrary, the approach presented in this thesis and the reported results in the previous part (as illustrated in Ch. 5 and 6) and the following one contribute already to a novel understanding paradigm to the information processing in the brain. The main reason behind being able to introduce this understanding is keeping the needed balanced combination and integration of biophysical details as well as computation complexity on two abstraction levels. These levels are the synaptic dynamics (part I) and the required basic information processing functions on a network level (which will be shown and discussed in the second part of the thesis). In the following, the results about the synaptic dynamics part is discussed.

## 7.2 Modelling Synaptic Dynamics

The quest for building a brain-inspired information processing system starts with simulating the relevant neuronal and synaptic dynamics. The focus of this work is synaptic dynamics. Hence, it has been assumed that some low-level details underlying the synaptic actions can be suppressed. These low level details may involve:

- The detailed kinetics of ion channels.
- The synaptic intrinsic latencies: travel delays of vesicles to presynaptic membrane and of neurotransmitter within synaptic cleft to postsynaptic membrane.

---

<sup>1</sup>The patch clamp technique is a laboratory technique in electrophysiology that allows to study of the excitable cells such as neurons.

- The diversified profiles of neurotransmitter release and binding at postsynaptic sites.

As for the synaptic dynamics, the need for a balanced synaptic parametrization has become more obvious in the last decade (Markram and Tsodyks, 1996). As pointed out before, the first neuronal model is the biophysical model of an action potential from Hodgkin and Huxley in 1952 (Hodgkin and Huxley, 1952). The first real synaptic model might be the Markram-Tsodyks model proposed in 1998 by Markram et al. (Markram et al., 1998). Afterwards, the trials to present synaptic models continue with variations in the amount of considered details and the generality of the model. The first part of this thesis is the introduced contribution to these trials. Based on the formerly available synaptic models, it was assumed that representing a biologically plausible synaptic model is only achievable at increased complexity. The introduced MSSM defies this assumption. As explained in Ch. 4, this biophysical model is developed without any compromise on biological plausibility.

The MSSM describes the basic relevant internal synaptic processes from the three involved synaptic regions: the presynaptic preparation of the synaptic action, the transfer to the synaptic cleft, and the integration of the synaptic action on the postsynaptic site. The simplicity of this model is obvious when it is compared to other recently developed models, e.g. the Lee-Anton-Poon model explained in Ch. 3. The MSSM captures the required synaptic dynamics and models the essence of synaptic variability through 12 model parameters while the Lee-Anton-Poon model features 33 parameters. The latter model after simplification is reduced to the Markram-Tsodyks model (Lee et al., 2009). According to certain settings the MSSM is still fully functional with nine parameters only; by setting  $N_{to}=0$ ,  $k_{N_t}=1$  and  $k_{N_t,V}=1$ .

The biological plausibility of the MSSM is validated in Ch. 5 against a biological counterpart. With the MSSM it is achievable to reliably predict the firing activity of a thalamic postsynaptic neuron with a goodness greater than 92%. This performance outperforms those achieved with the classical approaches of modelling the synaptic dynamics such as the  $\alpha$ -functions and the Markram-Tsodyks model. Furthermore, the goodness of prediction is still better than the performance achieved by Lee-Anton-Poon model, although the latter is much more complex than the MSSM, the results are summarized in Tab. 5.2. The data set from (Carandini et al., 2007) has made it possible to validate the biological plausibility of the MSSM. This check of plausibility using biological recordings is of a special importance because it represents a rigorous evidence that the MSSM fulfils the required performance. According to this prediction benchmark task, the MSSM is biologically plausible and computationally optimum when compared to the available models of synaptic dynamics. Since such data sets are not available from all research groups, it remains to be seen if the MSSM would perform always with similar reliability.

The results and analyses reported in Ch. 6 are the first theoretical energy-based proposition about the underlying mechanism of the experimentally observed occurrence of synaptic states. It is proposed that the synapse modelled with the MSSM operates at certain settings of its model parameters that ensure sustaining the lowest possible energy profile. This energy minimization

concept introduced for the MSSM agrees with the general concept of free energy minimization known in thermodynamics. Such agreement with one of the basic rules of physics in general is a novel theoretical evidence from this thesis that the synaptic dynamics play a crucial role in the information processing among the neurons within the neural circuitries (and consequently in spiking neural networks (SNN)) apart from its role in memory. In order to comprehend this, it is important to recall that the synaptic transmission (release) is evidently a stochastic process (Abbott et al., 1997; Zucker, 1989; Zucker and Regehr, 2002) and this stochastic nature is also considered to be the reason behind generating novel reactions on the cognitive level in response to previously registered sensory inputs (Singer and Gray, 1995). However, the reactions on the network level and the network behaviour are not chaotic (van der Velde and de Kamps, 2006). Unstable reactions and network behaviours are attributed to pathological regions and malfunctioning cortical regions. Hence, stable network behaviour in general is indeed a requirement from neurobiology. The trade-off between being stochastic in nature and still delivering a stable operating point is resolved using the MSSM and through the concept of the free-synaptic energy presented in this work.

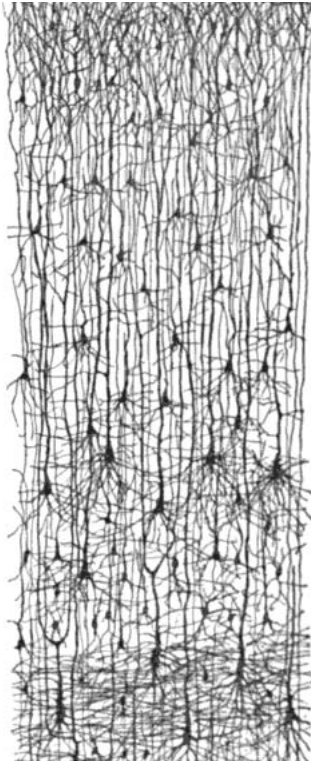
This suggests that the MSSM represents the required balance between being biophysically adequate in details and being computationally simple. Since synaptic models are developed in order to be used in simulations, the need for simplicity is obvious especially when large scale simulations are considered. Simulating the basic information processing functions observed in the cortical regions or in the CNS in general requires detailed simulation and analysis of network dynamics. With complex synaptic representation such simulations and analyses are either not practicable or extremely difficult. Adoption of the MSSM in simulations with spiking neuronal models overcomes these problems and opens new avenues in understanding novel aspects about the emergent information processing capabilities of neural circuitries in the CNS. Moreover, it enables SNN to adopt (and to emulate) similar processing capabilities. The second part of this thesis investigates the latter statements.

The first part of this thesis fulfills sufficiently the aims described at the beginning of this thesis regarding the first considered level of abstraction which is the level of neuronal and synaptic dynamics. The MSSM reliably captures the required essence of synaptic dynamics and its dynamics are in agreement with various biological and biophysical perspectives. Following the discussion about emulating the behaviour of the biological neural circuitries mentioned in Sec. 1.6, the inner workings of these networks are then successfully captured through the MSSM. Importantly, this is accomplished at an optimized computational cost. The following part of the thesis continues based on the reported results to investigate the behaviour of the SNN when the MSSM is incorporated for the synaptic representations.



# Part II

## **SIMULATION OF BASIC INFORMATION PROCESSING IN CNS USING MSSM**



After investigating the detailed dynamics of synapses, Part II is concerned with importing these dynamics into the mechanisms of information processing regarded as basis for the computational power of the CNS. It starts with Ch. 8 in which a reinforcement learning framework for dynamic synapses is introduced. It enables the Hebbian-based modulation of synaptic dynamics. Afterwards in Ch. 9, the energy-based analysis of synaptic dynamics and the involved role of synchronous behaviour in spiking neural networks is explored and investigated in details on a network level. Finally, the whole conceptual framework is wrapped up into a novel theoretical and analytical basis of a brain-inspired finite-state machine, this is reported in Ch. 10. This novel class of state-machines represent a propositional investigation to a possible practical and implementable computation model that is able to be a brain-inspired information processing system. As a future work, the latter computation model can make it possible to develop systems that can co-exist and bidirectionally communicate within the CNS. These implications, limitations and theoretical considerations along with the take-home messages from part I are fully discussed in Ch. 11.



# Learning with Dynamic Synapses

*"Much learning does not teach understanding."*

**Heraclitus**

## 8.1 Introduction

In this part of the thesis, the focus is to import the capabilities of the MSSM into the networks level aiming at achieving more biologically plausible behaviour from the information processing point of view. The first aspect of information processing considered in this part of the thesis is learning. Being able to learn is an important basic required information processing capability of the neural circuitries within the CNS. As mentioned in Ch. 1, learning here denotes the very basic ability of learning on a network level rather than learning at the level of cognitive functions, for instance learning a language is a learning ability on the cognitive level. The very basic meaning of learning regarded in this context is the ability to extract the relevant information contents from the input stimuli and transfer this knowledge to the neural ensemble on the small networks level. This embraces the ability to generate certain spiking patterns corresponding to predefined input ones (El-Laithy and Bogdan, 2011b). The required output spiking patterns integrate at higher processing levels from which animal/human behaviour originates.

Evidences have accumulated emphasizing that synapses present the major contribution in learning capabilities within neural systems (Purves, 2008). Hence, this chapter investigates whether a spiking network that uses the MSSM for its synaptic representations is able to capture a specific computational task to deliver a predefined output from a given input. The importance of introducing this learning framework goes beyond its relevance to the MSSM in this thesis. Applying the proposed learning framework to the MSSM makes it relevant to almost the entire class of synaptic models which plausibly *model* the biological synaptic action. This relevance can be realized by recalling what actually changes in the real synapses when it is mentioned that synapses are plastic dynamical systems that keep memory of its past experience. In the classical simulations of ANN

learning changes those weights which represent the strengths of the synaptic connections. But within the CNS, the synapses are not weighting factors. It is obvious that the involved electro-chemical mechanisms are being altered and modulated through the inherited learning mechanism and consequently the collective synaptic response in the transmission of the input is modified. Similarly, the MSSM does not feature any synaptic weight, the synaptic response from the MSSM is the resultant from the synergy among the synaptic state parameters in response to the stimulus. Thus, in the context of the approach adopted in this thesis it is obvious and practical to start this part of the thesis by discussing the issue of learning considering the MSSM within spiking artificial neural networks (SNN). The class of models that can benefit from the presented learning framework include the biophysical ones and those phenomenological ones as well, e.g. the Markram-Tsodyks model. In general, learning with the aforementioned meaning is a basic information processing tool that is involved in all higher required processing in the CNS.

In fact this framework has been already developed to be used in the prediction task discussed in Ch. 5. In order to maintain the conceptual order, explaining the learning framework is shifted to this point in the thesis. Thus, the reader might feel that the concepts presented here have already been used in Ch. 5, there the context does not allow to go into the details and to explain the background of the learning process.

### 8.2 Reinforcement Learning for Dynamic Synaptic Models

Learning in neural networks in general can be achieved by two main strategies, namely either by supervised or unsupervised learning. Unsupervised learning is guided by correlations in the input information to the network. D. Hebb postulated in 1949 (Hebb, 1949) that the modifications in the synaptic transmission efficacy are driven by the correlations in the firing activity of the pre- and postsynaptic neurons. The Hebbian learning rules implement the dependence of synaptic changes on the relative timing of pre- and postsynaptic action potentials. In relation to this, synaptic transmission efficacy is characterized as well by the so called spike-timing dependent plasticity (STDP), as given in Sec. 3.5.2. Formally, STDP is either the potentiation of a synapse when the postsynaptic spike follows the presynaptic spike within a time window of a few tens of milliseconds or the depression of the synapse when the order of the spikes is reversed. Since this is consistent with the postulates of D. Hebb, sometimes this type of STDP is referred to as Hebbian STDP. When the sign of the change in the synaptic strength is changed, the process is known as anti-Hebbian STDP. Synaptic changes following a learning algorithm modulate the STDP either via the Hebbian or the anti-Hebbian rule (Gerstner and Kistler, 2002). One of the attractive models in this regard is the Bienenstock-Cooper-Munro (BCM) model for the development of orientation selective cells in the visual system (Baras and Meir, 2007). The Hebbian learning rule of this model is considerably supported from experiments on long-term potentiation (LTP) and long-term depression (LTD) (Pennartz, 1997).

Many studies have investigated how the Hebbian-based learning algorithms can be applied to empower the performance of neural networks and especially of those use either spiking neuronal models and/or synaptic models that implement STDP, see e.g. (Farries and Fairhall, 2007; Urbanczik and Senn, 2009) for recent reviews. A correlation based Hebbian learning rule for spiking neurons was presented reporting that correlations between input and output discharges tend to stabilize (Kempter et al., 1999). A biologically plausible learning algorithm for multilayer neural networks was introduced in (Klemm et al., 2000). It was shown that the learning algorithm has allowed the network to solve partially the exclusive-Or (XOR) problem without back-propagation. Applying both Hebbian and anti-Hebbian rules in a recurrent network that implements STDP was investigated as well by (Carnell, 2009). It has been shown that this combination leads to approximate convergence of the synaptic weights. These studies were focused on the computational properties of STDP, thus they have illustrated its function in neural homeostasis, supervised and unsupervised learning. The used synaptic dynamics in these studies were limited to the simple phenomenological models.

Notably, a number of theoretical analyses have reported that Hebbian and anti-Hebbian modulation of STDP can either minimize or maximize the postsynaptic (neuronal) firing variability to a given specific presynaptic input (Carnell, 2009; Florian, 2007; van Rossum et al., 2000). These studies have suggested that combining Hebbian rules and reinforcement learning (RL) (Sutton and Barto, 1998) facilitate the simulation of the learning abilities of biological neural systems. A number of studies have investigated the tenability of integration between both concepts. For example, the ability to reduce the required learning steps for certain tasks in comparison to applying RL alone was investigated (Bosman et al., 2004). Unfortunately, the tasks were poorly defined to be used for general machine learning regimes. Applying the RL rules to the spike-response model (SRM) was performed by (de Queiroz et al., 2006). This has been done by adding a Hebbian term to the RL rule. The latter study was directed as well to investigate the influence on the number of learning steps. It has been shown that RL can occur via correlating the fluctuations in irregular spiking with a reward signal in networks composed of neurons firing Poisson spike trains (Seung, 2003; Xie and Seung, 2004). Another study has tried to teach a network of spiking neurons to output specific firing patterns on different time scales and in response to varying input combinations (Farries and Fairhall, 2007). The means of evaluating the performance of the network in former studies, e.g (Florian, 2007; Xie and Seung, 2004), are questionable because in these studies the used synaptic models realize temporal coding e.g. the Markram-Tsodyks model while the output of the network was rate coded.

Commonly through all these studies, the modulation targets solely the synaptic weights in the synaptic parametrization, i.e. only the spike-timing *independent* part of the synaptic parametrization is tuned. Little attention has been paid to the direct modulation of the synaptic hidden parameters, e.g. response and recovery time constants.

In order to get an impression about the relevance of applying a learning rule to tune directly the synaptic hidden parameters, some related topics are reviewed in the following. Adopting the spike-timing dependency in the synaptic action presumes that pre- and postsynaptic spiking activities influence the internal mechanisms result in the synaptic action itself. Shortly stated, there is a sort of closed-loop feedback mechanism regulating the synaptic action observed through changes in the synaptic plasticity (Markram et al., 1998; Zucker and Regehr, 2002). In chemical synapses, the calcium ions buffering plays in general a facilitatory role and is triggered by arriving spikes at the presynaptic terminal. This buffering enhances the transmission of the presynaptic spike by urging the release of neurotransmitter from the vesicles into the synaptic cleft. The extent of this facilitatory role is, however, bound to the contribution of other mechanisms such as the pool size of the ready to release vesicles and post-release recovery timing constants of neurotransmitter. There is a dependence between the utilization of the synaptic resources (ions and neurotransmitter) and the overall synaptic action, which is modulated by the spike timing at the presynaptic site. The synaptic action consequently affects the postsynaptic activity. Latencies between postsynaptic spikes allow for the uptake of neurotransmitter from the cleft and for the resynthesize of vesicles within the presynaptic terminal. These latencies are basically modulated by the release process that is originally presynaptically regulated (Zucker and Regehr, 2002). Thus, there is an interdependence between STDP (as the correlation between presynaptic and postsynaptic spiking) and the synaptic resources e.g. the concentration of neurotransmitter and ions. As briefed, the interdependence originates from the relation between the synaptic action and the relative timing of pre- and postsynaptic action potentials. This interdependence suggests that learning frameworks in general may specifically tune the internal synaptic dynamic mechanisms according to predefined inputs/outputs combinations.

For the general class of synaptic models that implement STDP, the overall synaptic response originates from two contributions: the synaptic weight (if exists in the model parametrization as in the Markram-Tsodyks model) and the dynamic spike-timing dependent mechanisms. The latter arises from the synergy among the hidden synaptic parameters e.g. via response time constants and scaling factors. Maass and Zador have reported that applying gradient descent tuning to hidden parameters of their stochastic synaptic model can lead in principle to learning within a neural circuit (Maass and Zador, 1999; Natschlager et al., 2001). This approach is based on the previous work by (Back et al., 1995; Back and Tsoi, 1991; Namarvar et al., 2001); it has been shown that synaptic dynamics modelled in general as finite-impulse response filters can be learned through modulating their hidden parameters. Biologically plausible synaptic models that implement temporal coding via STDP can be characterized in general as integrated (multi-layered) finite-impulse response filters (Garimella, 2008). It has been shown that applying the RL modulation directly to the model parameters of the Markram-Tsodyks model within SNN can indeed results in convergence in the parameters subject to learning and the network is able to capture the required computations (El-Laithy and Bogdan, 2011b).

Hence, the core objective in this chapter is to propose an appropriate, but yet simple, learning algorithm that implements both Hebbian- and RL rules for spiking networks with MSSM synapses via tuning the synaptic model parameters rather than the synaptic weights. The availability of such framework opens new avenues in adopting the class of complex biophysical synaptic models in processing of neural signals and computations. As explained before, these synaptic models do not feature any scalar weight factors as synaptic weights, which is why they are not utilized widely in signal processing tasks that require the tuning of model parameters to achieve certain regime of dynamics characterized by predefined mapping between input and output spike patterns.

### 8.3 Reinforcement Learning Framework

RL is a proven tool for developing an intelligent agent without an explicit supervisor and without a teaching set (Sutton and Barto, 1998), in which a reward signal is generated from the interaction with the environment and it represents the source of supervision. In order to explain the proposed learning framework, let us first consider the simulation setup. A network similar in structure to the one used in (Florian, 2007; Xie and Seung, 2004) is considered, see Fig. 8.1(a). The network has two input neurons  $N_1$  and  $N_2$  feeding their outputs via one hidden layer ( $N_3, N_4, \dots$ ) to one output neuron  $N_{out}$ . All synaptic connections are represented using the MSSM of synaptic dynamics. The network output is a spike train  $f$ . Inputs are spike trains with Poisson-distributed inter-spike intervals and are fed to input neurons. In parallel, the input spike trains are fed to an XOR gate<sup>1</sup>. The latter XOR gate provides the correct output (target output) as a reference spike train  $g$ . The following sections answer the basic question of how this setup (Fig. 8.1(a)) can be mapped to the RL configuration (Fig. 8.1(b)).

#### 8.3.1 Reward Signal

It has been described that a reward signal (or a feedback parameter),  $\mathcal{R}wd$ , can be derived to represent the progress in capturing certain temporal dynamics (El-Laithy and Bogdan, 2011c; Farries and Fairhall, 2007). This reward is based on the distance between the target spike trains and the network's actual output. As for the distance, van Rossum introduced an algorithm, which is used here to calculate the distance between two spikes trains (van Rossum, 2001). It is a dimensionless distance that calculates the dissimilarity between two spike trains. It is calculated by filtering both trains with an exponential filter, and calculating the integrated squared difference of the two trains. Each spike at time instant  $t_j$  in  $f$  is convolved with an exponential function  $\exp(t - t_j/\tau_s)$  with  $t > t_j$ , leading to the time series  $f(t)$ . Likewise each spike in  $g$  is convolved with this exponential function, resulting in the time series  $g(t)$ . From the resulting time series  $f(t)$  and  $g(t)$ , the van

<sup>1</sup>Details of simulation are given in section 8.4

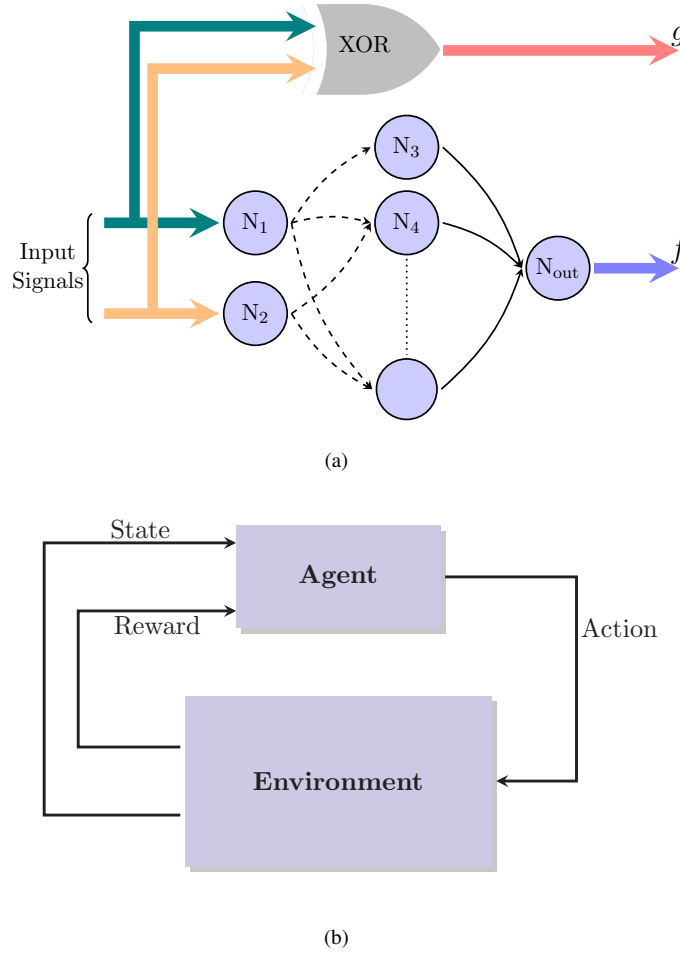


**FIGURE 8.1:** (a) Schematic of network setup and simulation. Different-colored input lines indicate nonidentical inputs spike trains. Dashed arrows represent those synaptic connections allowed for learning (details are explained in section 8.3.5). (b) Basic reinforcement learning: agent-environment interaction.

Rossum distance measure reads:

$$\mathcal{D}(f, g) = \frac{1}{\tau_s} \int_0^\infty [f(t) - g(t)]^2 dt, \quad (8.1)$$

where  $\tau_s$  is the time constant of the exponential filter. It controls the extent of the effect from each spike on the following spikes, i.e. it determines the time scale of this distance measure. Here  $\tau_s$  is set arbitrarily to 15 msec.

In order to reduce the effect of the input variability on the observed performance, the reference spike train and network's output are temporally coded (or binned) with a non-overlapping temporal window (Farries and Fairhall, 2007) with width  $\mathcal{W}$  taken first to be five msec. During each time window, having one or more spikes is interpreted as having a digital one (High) otherwise as zero (Low). Thus, for any spike train of length  $L$  that is binned with  $\mathcal{W}$  msec window, the spike trains are mapped to shorter versions with length  $L/\mathcal{W}$ . In other words, output spike train  $f$  with a 200 msec epoch is mapped to a binned version  $F$  that is 40 steps long. Similarly,  $g$  is mapped to  $G$ .



Hence, the reward signal is defined as

$$\mathcal{R}wd = e^{-\alpha \mathcal{D}(F, G)} \quad (8.2)$$

where  $\alpha = 0.01$ . This definition of  $\mathcal{R}wd$  maps the distance  $\mathcal{D} \in [0, \infty)$  to the range  $[1, 0)$ , with a maximum reward value of unity when the distance vanishes, i.e. at identical outputs.  $\mathcal{R}wd$  is dimensionless; this is a key property in the introduced framework. Because of the required consistency of physical units (will be clear in Eq. 8.3) as the value of the reward signal is used to modulate synaptic parameters that represent certain biophysical quantities with physical units.

### 8.3.2 Mapping the Simulation Setup to a RL Scheme

In a standard RL problem (See Fig. 8.1(b)), an agent represents the learner and the decision maker. Everything outside the agent is its environment. The environment tells its agent about its current state (activity) and it also gives rise to rewards. The agent tries to maximize these rewards over time (Sutton and Barto, 1998). As for the temporal difference (TD) RL scheme used here, the environment state is the input patterns represented during each episode (trial). The policy is formulated by both the synaptic model and the update rules, it sets the dynamic synaptic strength that is used in each trial dynamically. The action is the output spike train from the network respectively from its output neuron. The XOR gate and the calculation of  $\mathcal{D}$  are viewed as an advisor for the learning agent. Differently stated, the network itself is the agent. This agent has two policies, the synaptic parametrization and the update rule. Attached to this agent there is an advisor. The latter calculates the distance from the reference spike train, apply binning and feed the reward value to the update rule (the agent's second policy)<sup>2</sup>

The enhancement in the synaptic model (the agent's first policy) aiming to improve the quality of the action is better derived by a temporal difference error rather than the reward values (Farries and Fairhall, 2007). In other words, instead of modulating the changes in the tuned parameters with the reward values, the temporal error between the desired reward and current reward values is used to modulate the changes in the tuned parameters. The TD approach was basically introduced without neurobiological evidences as it was not developed for neural networks at first place (Sutton and Barto, 1998). Biologically, it has been shown that the firing activity of dopamine neurons in many cortical regions appear to resemble the error function in the TD algorithm (Chorley and Seth, 2011; Schultz et al., 1997) which supports the biological plausibility of the RL framework in general.

<sup>2</sup>Two rules support this description of the RL setup (Sutton and Barto, 1998). First, a policy represents a sensory-output rule. It is the agent's way of behaving to the input information. Second, any thing that cannot be changed arbitrarily by the agent is considered to be outside of it and thus part of its environment.

### 8.3.3 Hebbian Update Rule

The dynamics of any synaptic action are governed through the contribution of electro-chemical mechanisms represented via its model parameters. Denote by  $m$  each of these parameters within any synaptic model, according to the pairing between pre- and postsynaptic activity, the value of  $m$  is either increased or decreased following the Hebbian rule  $\Delta m = \eta \cdot m$ , where  $|\eta| < 1$  is the learning rate (Farries and Fairhall, 2007; Namarvar et al., 2001). The realization of this basic Hebbian rule reads as follows (see Fig. 8.2): the values of parameters contributing to the facilitatory mechanisms are increased and the contribution of the depressive mechanisms are decreased when a spike at the presynaptic neuron induces a desired spike at the postsynaptic neuron. The term "desired" refers here to a correct hit. If the presynaptic spike does not induce a postsynaptic spike, and no spike is expected, the process is flipped. Whether the spike is desired or not is judged by comparing to the reference spike train. So far, it is supervised learning in full sense. For RL, a reward-based error signal  $\delta_{Rwd}$  is applied to the eligible synapses to update their parameters:

$$\Delta m = \eta \cdot m \cdot \delta_{Rwd} \quad (8.3)$$

where  $\eta$  is set to 0.01.  $\delta_{Rwd}$  is the temporal difference error that is usually calculated as a prediction error. It is normally calculated as the difference between the ideal (or expected) reward and a scaled value of the current one (Sutton and Barto, 1998). Scaling the current reward is made via trace decay parameter  $\lambda$ . In this study  $\delta_{Rwd}$  is the temporal difference error between the unscaled values ( $\lambda = 1$ ) of the current reward and the previous one from the previous trial. It reads

$$\delta_{Rwd} = \mu(\mathcal{R}wd_{\text{previous}} - \mathcal{R}wd_{\text{current}}), \quad (8.4)$$

where  $\mu$  is a scaling factor to match the order value of  $\delta_{Rwd}$  to the order of the parameters under training. It is set to 7 throughout the simulation.

On episodic basis (after each trial), the sign of the error value is used to alter the direction of the change in the parameter value, either to increase or to decrease the value of the tuned parameter. Having a signed value, this learning rule allows anti-Hebbian synaptic plasticity (Farries and Fairhall, 2007; Namarvar et al., 2001). Recalling that the direct modulation of the synaptic model parameters implement a gradient descent (Back et al., 1995; Back and Tsoi, 1991), the proposed rule here optimizes the error function  $\delta_{Rwd}$  in a heuristic way. The implicit objective of achieving a stable maximum reward is preserved via minimizing the error value  $\delta_{Rwd}$  (Farries and Fairhall, 2007). Calculating the reward values from the distance between the spike trains without binning reinforces the input variability. This deteriorates the results significantly as the fluctuations in the temporal error will be too high. Thus, the binning is used to suppress this variability and to isolate, to a certain extent, the performance of the learning from its effect.

For the task under investigation, the hidden model parameters subject to training are arbitrarily chosen as:  $C_o$ ,  $V_o$ ,  $\tau_C$  and  $\tau_V$ . By modulating these model parameters, both core facilitation and

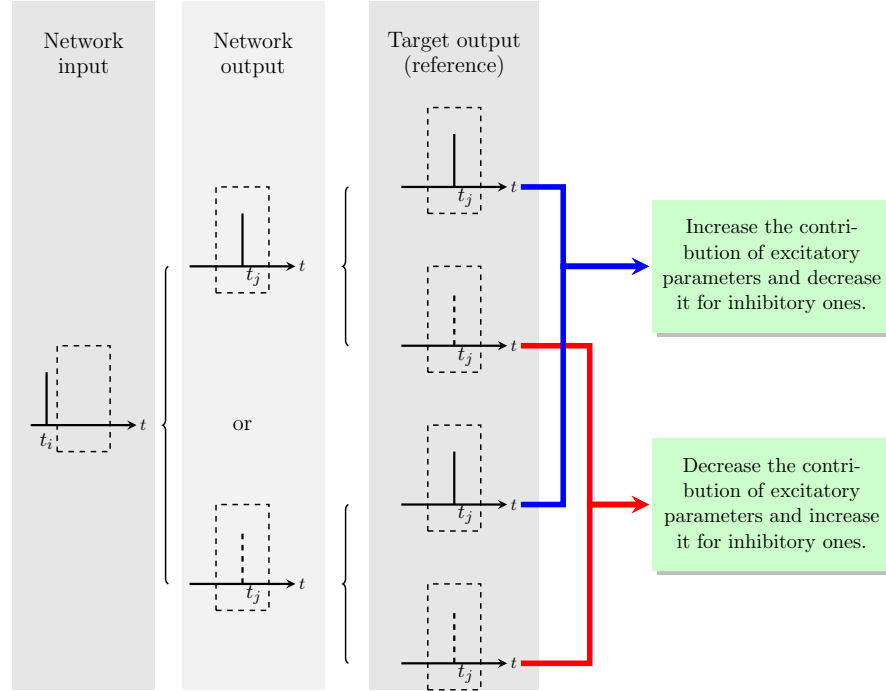


**FIGURE 8.2:** Schematic illustration of the applied Hebbian learning scheme in case of input spike arriving the input neuron at  $t_i$ . This illustration is similar to the one given in Ch. 5 (Fig. 5.4), there it highlights only how to apply the Hebbian update rule to the synaptic model parameters on the level of one synapse to one postsynaptic neuron. Here, the illustration is the generalized case on a network level. Changes are still applied directly to the synaptic model parameters but according to the network input/output behaviour. Dashed vertical segments indicate a missing spike at the shown time instant. Dashed boxes illustrate the span of coincidence time window over which correct spike timing is regarded. Having the same existing/missing spike between the second and the third column indicates a correct event. In case that there is no input spike at  $t_i$ , the same logic is applied.

depression mechanisms are influenced. Recalling the note mentioned above after Eq. 8.2 about  $\mathcal{R}wd$  being dimensionless, if the reward values have units of e.g. bits and  $m$  denotes  $\tau_C$  or  $C_o$  Eq. 8.3 will not be longer correct.

**Remark about learning in Ch. 5** By comparing the Hebbian learning rule used in Ch. 5 (Eq. 5.6) to the one defined here (Eq. 8.3), it implies that Eq. 5.6 is a reduced version of the one used here when  $\delta_{\mathcal{R}wd}$  is taken to be a fixed value set to unity.

### 8.3.4 The Reference Spike Train

In the proposed framework, the availability of and need for the reference spike train represents a major issue. It may be argued that, on contrary to supervised learning, the actual desired output (reference) should not be used in RL to correct the behaviour of the agent. Instead, an agent extracts the required information about the next action from the history of both the environment behaviour and rewards. This is done implicitly in the proposed framework. The distance between the output and reference spike train is applied only on episodic basis. Thus, the history of the

networks behaviour is used as it is compared to the reference one and the distance gives rise to the reward signal. Therefore, the proposed framework models correctly a RL problem with a plausible realization to synaptic STDP. As mentioned, the value-function here is the distance between the reference and output spike trains. From a macroscopic (cognitive) point of view, the need for the reference spike train calls for the need of memory to accomplish learning in general. This in turn raises a fundamental question of whether memory is a prerequisite for learning or not. Here it is accepted that memory is needed for learning, at least for the condition when the input information has never presented to the network before. In the simulations presented here, this condition is fulfilled.

### 8.3.5 Eligibility Traces

Eligibility denotes synapses that has contributed to either a correct or false output spike. These eligible synapses can be determined either analytically as in (Farries and Fairhall, 2007; Florian, 2007; Xie and Seung, 2004) or phenomenologically as in (Fiete and Seung, 2006; Kimura and Hayakawa, 2008; Lee and Kwon, 2008). In order to keep complexity at a minimum, the latter approach is the one adopted in the presented study. In general, this approach depends on the understanding of the flow of spiking activities within the network. In other words, for a series of neuronal activities, synapses of the neural network do not influence the timing of the output spike with identical contributions. Here, it is chosen to allow only forward synaptic connections between the input neurons and the hidden neurons to be learned (shown as dashed lines in Fig. 8.1(a)).

## 8.4 Simulation and Results

A network with a hidden layer of five neurons is implemented. The network has one output neuron, i.e. the network size is eight neurons<sup>3</sup>. The neurons are modelled as LIAF units and the synapses are implemented with the MSSM. The values of the LIAF model parameters are:  $\tau_h = 20$  msec,  $h_{rest} = -70$  mV and  $h_{th} = -60$  mV. In this network setup three synapses are set to be inhibitory: two synapses between input neurons and the hidden layer, and only one synapse is inhibitory between the hidden layer and the output neuron. The hidden model parameters subject to training are:  $C_o$ ,  $V_o$ ,  $\tau_C$  and  $\tau_V$ ; their initial values are arbitrarily set at 0.05, 4.5, 2.34 msec and 9.18 msec respectively. Other parameters, which are fixed and not subject to training, are arbitrarily set at  $\alpha = 0.095$ ,  $k_{epsp} = 2.5$ ,  $\tau_{N_t} = 12$  msec,  $\tau_{epsp} = 9$  msec,  $k_{N_t} = k_{N_t, V} = 1$  and  $N_{t_o} = 0$ .

To get a real impression about the involvement of the training process and the effect on the parameters subject to training, five different spike train pairs are presented to the input neurons independently. Fig. 8.3(a) shows a pair of the input spike trains. Note that the epoch of these spike trains is the simulation epoch of 200 msec ( $L$ ) and  $\mathcal{W}$  is set to four msec. Each pair is presented

---

<sup>3</sup>From classical neural networks, the minimum number of neurons required to solve the XOR problem is five (Nee-lakanta and DeGroff, 1994).

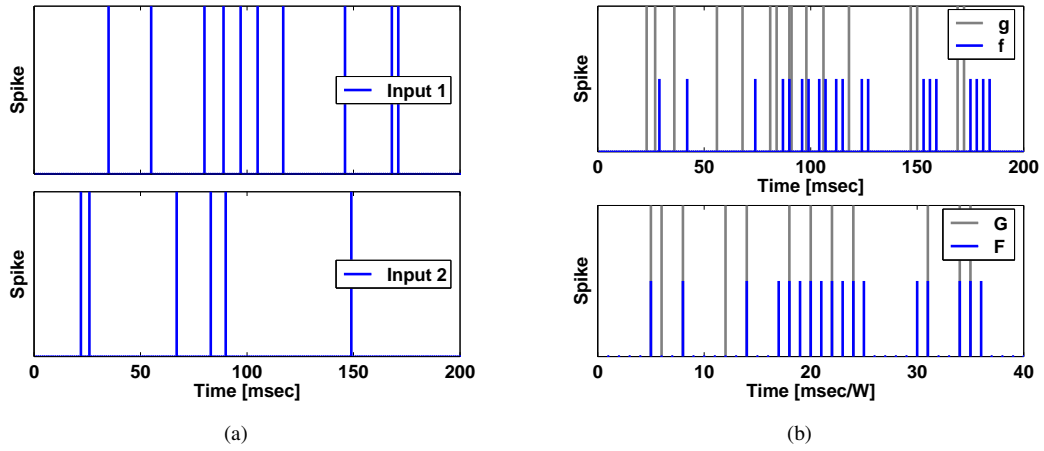


**FIGURE 8.3:** (a) Sample of input spike trains. (b) Sample of network untrained output. Light Gray lines indicate the locations of reference spikes. The blue lines are those correspond to  $f$  or  $G$  in the top and lower panels respectively. The lower panel shows the filtered versions  $F$  and  $G$  that correspond to the  $f$  and  $g$  from the upper panel. Note that in the lower panel the length of  $F$  (or  $G$ ) is  $200/\mathcal{W}$  where  $\mathcal{W} = 5$ .

for 300 episodes, additive white Gaussian noise is fed to all  $E_{psp}(t)$  of all synapses in parallel. The noise signals are generated separately and they are not identical for all synapses. The noise alters the input pair continuously within each episode. With this noise the network tries to compute the XOR of altered versions of the inputs to get a single specific output pattern. The network output before training is given in Fig. 8.3(b). Along the training episodes, the variation in the distance  $\mathcal{D}(F, G)$  and the reward signals  $\mathcal{R}wd$  are calculated. They are given as mean values across the five simulations of input/output pairs in Fig. 8.4.

As seen from Fig. 8.4, the values of the reward signal starts near 0.65 and increase gradually after the first 120 episodes. After 200 episodes of presenting the noisy input pattern the values start slowly to converges over 0.85. The reward values indicate the performance of the RL process. The ultimate objective of any RL framework is to maximize the reward to the learning agent. The average over the last 50 episodes is  $0.8518 \pm 0.0741$ . The distance between the reduced versions of the network output and the target indicates the performance of the learning process as well. The smaller the value, the closer the network output to the target output. After convergence, the average of  $\mathcal{D}$  over the last 50 episodes is  $3.331 \pm 1.81$  while the values start between nine and 10. That is, as training advances the network's output comes closer to coincide with the target spike train.

The time evolutions of the trained parameters are illustrated in Figs. 8.5(a)–8.5(d) for  $C_o$ ,  $V_o$ ,  $\tau_C$  and  $\tau_V$  respectively. These time evolutions are for a trained excitatory synapse. Sample comparisons between the time courses from excitatory and inhibitory synapses are given in Fig. 8.6. Self-organized behaviour is observed. That is, the final values of trained parameters converge to self-consistent values over the training trials when either of the initial values change. Fig. 8.7 shows this in terms of the dynamic synaptic strength ( $S(t)$ ) and according to the parameters subject to training. Fig. 8.7(a) shows the evolution of the dynamic synaptic strength from training

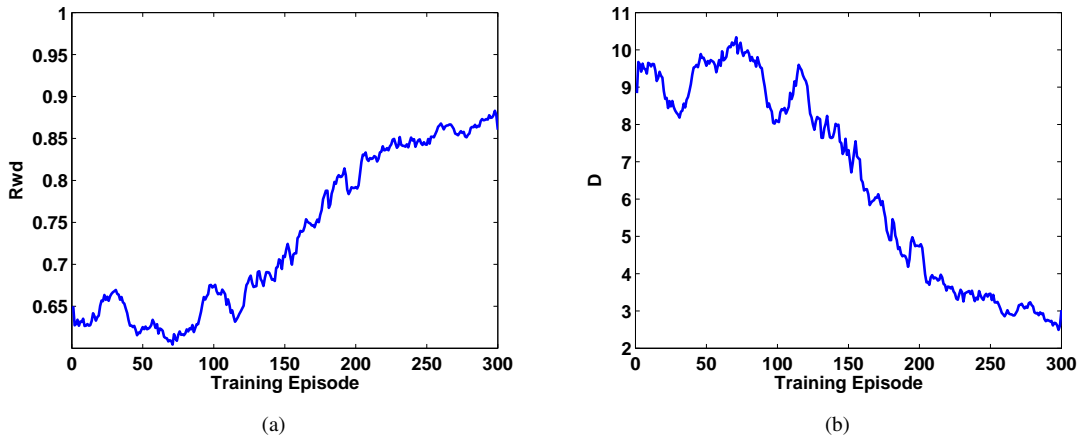


**FIGURE 8.4:** Simulation results in case of five neurons in the hidden layer, at window set to four msec. Values are mean over five different input/output signals. (a) The course of reward signal with training episodes. (b) Distances between the reference and the output signal,  $\mathcal{D}(F, G)$ .

of the five samples. Although the traces start from different values, there is a clear tendency to converge towards similar values. This is much clearer in Fig. 8.7(b) and 8.7(c), they illustrate the time courses of the changes in  $\tau_C$  and  $\tau_V$  respectively. Starting from different initial values does not affect the range within which the values converge with advance in training.

The effect of changing the binning window size  $\mathcal{W}$  is investigated as well. Beside four msec, two other values are tested;  $\mathcal{W}$  is set to five and six msec separately. As the binning window is changed, the length of the original spike trains  $f$  and  $g$  are changed as well in order to keep the length of the reduced ones similar in all cases. For example, when  $\mathcal{W}$  is four msec  $L$  is 200 msec while at  $\mathcal{W}$  is six msec  $L$  is set to 300 msec. As expected, a better performance is observed at larger window sizes. Because there is an increased suppression of the temporal details relative to the single spike scale. Fig. 8.8 illustrates the mean and standard deviation values of both measures  $\mathcal{Rwd}$  and  $\mathcal{D}$  after convergence (the last 50 episodes) at the tested values of  $\mathcal{W}$ . As seen from the figure, the enhancements are mainly observed in the standard deviations of the mean values of  $\mathcal{Rwd}$  and  $\mathcal{D}$ . This supports the motivation to use binning at first place. As mentioned in Sec. 8.3.3, binning is used to reduce the effect of the input variability on the learning process. In another sense, it compensates for the network complexity, a much larger network might be able to account for this variability and deliver the same performance over the single spike time scale.

Values of  $\mathcal{D}(\cdot)$  depend on the time scale parameter  $\tau_s$ , consequently the values of  $\mathcal{Rwd}$  depend on it as well. It can be shown that the change in distance due to spike insertion and displacement is inversely proportional to  $\tau_s$  (van Rossum, 2001). In simple words, greater values of  $\tau_s$  give rise to smaller values of distance between the spike trains. Since the distance measure plays a critical role in the introduced framework, the effect of  $\tau_s$  on the performance is investigated. The simulations are repeated with values of  $\tau_s$ : 5, 10, 15, 20 and 25 msec with five neurons in the hidden layer and at  $\mathcal{W}$  is at five msec. As long as  $\tau_s > \tau_C$  and  $\tau_s \ll L$ , no significant influence on the performance is observed. Otherwise, i.e. either at  $\tau_s < 1.5$  msec or  $\tau_s > 25$  msec in the proposed setup, the

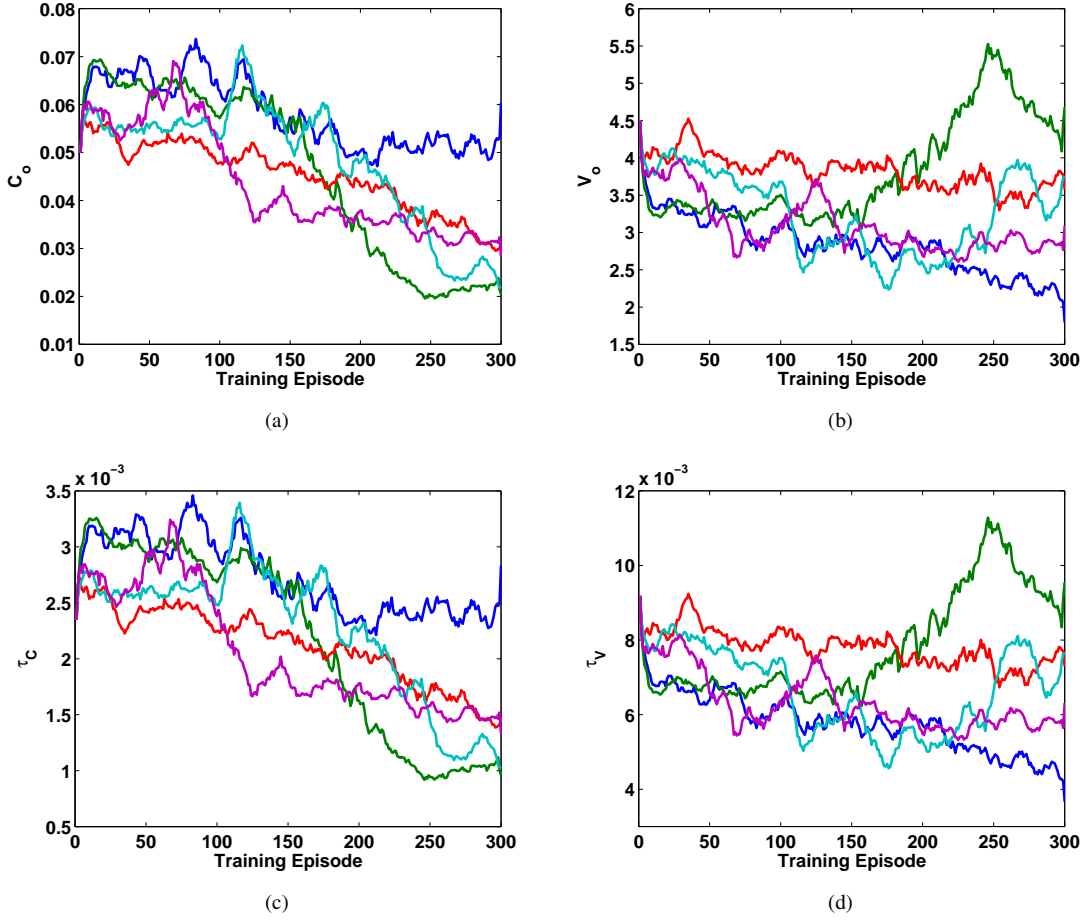


**FIGURE 8.5:** Evolution of the trained parameters:  $C_o$  in (a),  $V_o$  in (b),  $\tau_C$  in (c) and  $\tau_V$  in (d). In all subfigures the colours indicate five different excitatory synapses subject training.

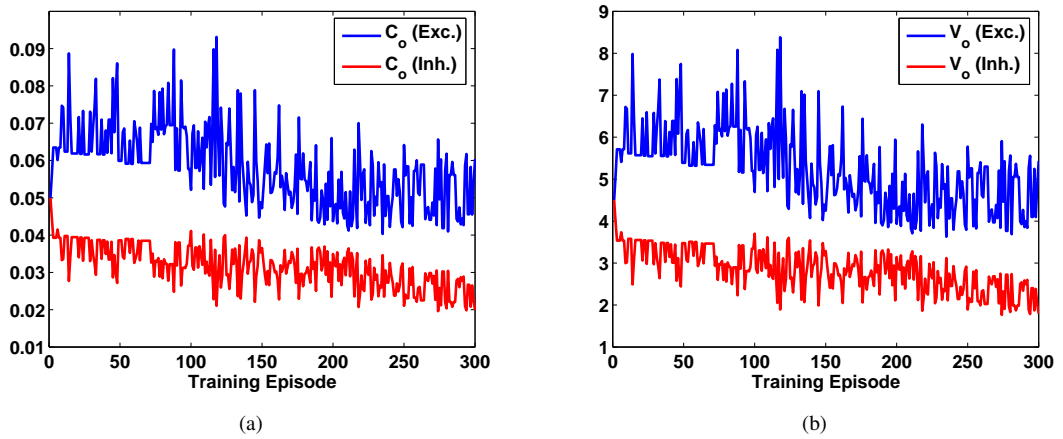


**FIGURE 8.6:** Changes in synaptic model parameters from excitatory vs. inhibitory ones. (a) Time courses of changes in the values of  $C_o$  of excitatory synapse (blue line) and inhibitory one (red line) (b) Time courses of changes in the values of  $V_o$  of excitatory synapse (blue line) and inhibitory one (red line)

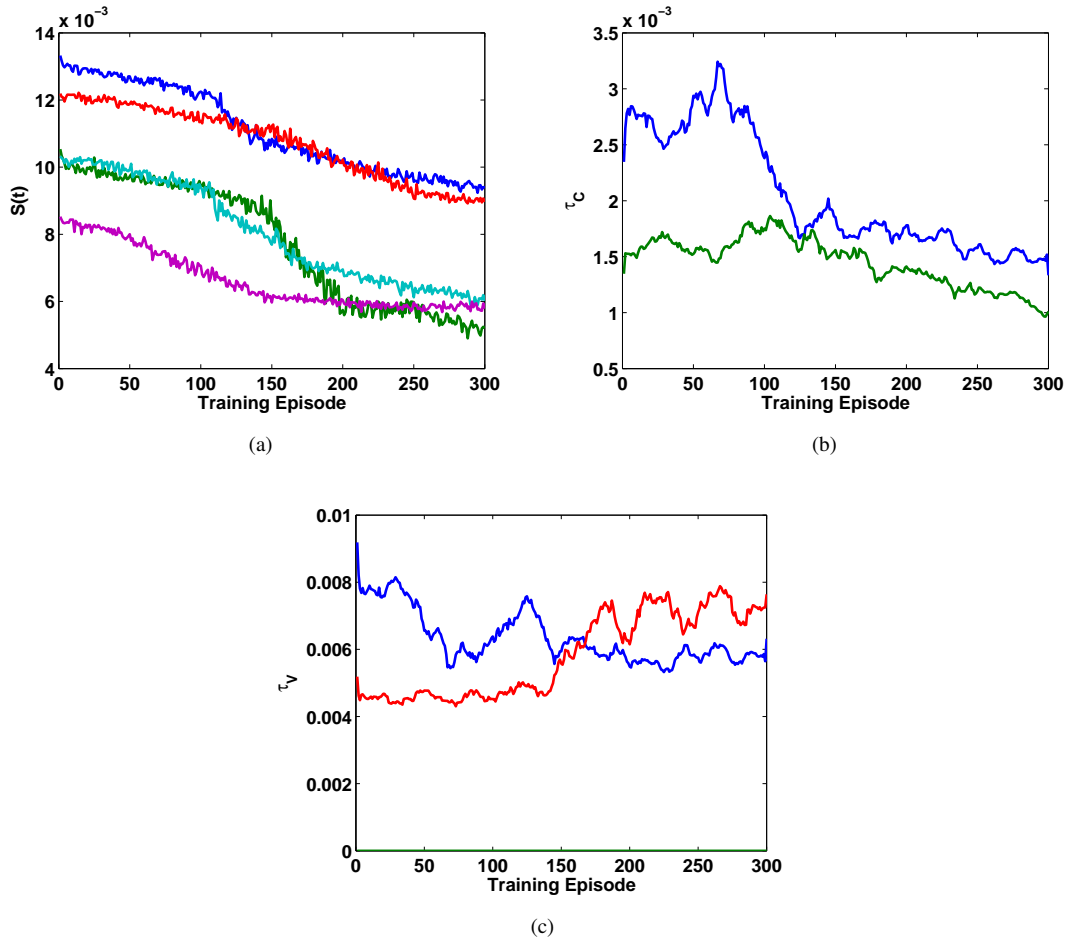


**FIGURE 8.7:** (a) The time evolutions of the dynamic synaptic strengths, the colours indicate five different excitatory synapses subject to training. (b) Starting from different initial values, the self-organized behaviour is illustrated via the end values of the trained model parameter  $\tau_C$ . (c) Similar to (b), the self-organized behaviour via the time evolution of the change in the values of  $\tau_V$ .

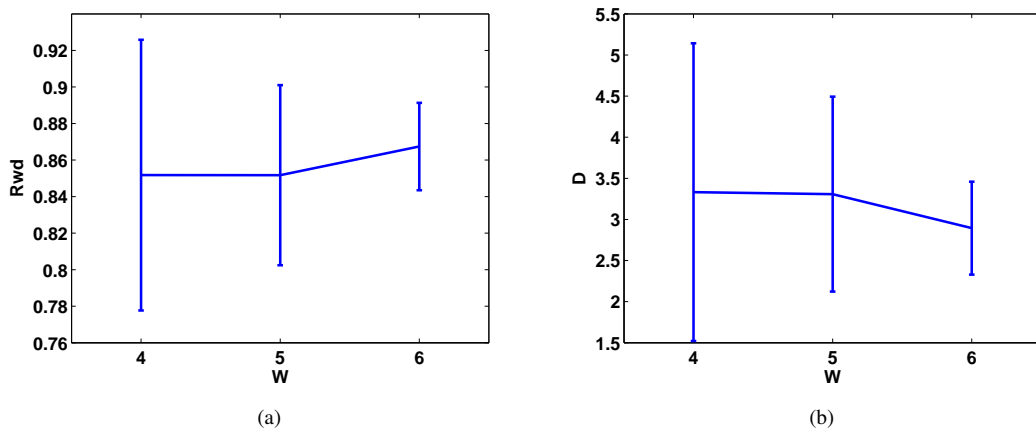


**FIGURE 8.8:** Plots showing the effect of the bin window size  $W$  on learning performance in terms of  $R_{wd}$  in (a) and  $D$  in (b). Values of reward and distance are mean values over 10 different input/output pairs and the range gives the standard deviations. For each input/output pair the final value of reward and distance are those mean values over the last 50 episodes.



reward values  $\delta_{\mathcal{R}_{wd}}$  are too large (or too small) to correct the direction and the update rate properly. Therefore, the performance turns to be critically stable. This can be compensated by changing the scaling factor  $\mu$  correspondingly. Similar limitation was reported in (Farries and Fairhall, 2007) as the Gaussian filtered version were used instead of the exponential one as smoothing filters for the spike trains. The restrictions made on  $\tau_s$  here do not limit the usage of the learning framework.

Simulation is repeated with 10(14) neurons over two hidden layers (five(seven) neurons each), that the network size is 13(17) neurons. The enhancement in the performance does not exceed 1%(1.5%). A real improvement of the performance shall be accomplished by introducing stronger depression within the network via increased number of inhibitory synapses. As mentioned above, introducing a solution for the XOR problem is not the core of this analysis. Therefore further analysis to enhance the performance was not implemented in this work.

## 8.5 Discussion

A proof-of-concept for the above used framework has been introduced in (El-Laithy and Bogdan, 2010a, 2011b) where the phenomenological model of Markram-Tsodyks was used to model the synaptic connections. In the cited two papers the base line synaptic response  $J$  of the Markram-Tsodyks model has been kept fixed and was excluded from the training for the sake of emphasizing the role of direct tuning of synaptic model parameters. Here the MSSM is used instead. It should be mentioned that a solution for XOR problem is not explicitly intended. Although the MSSM performs better than the Markram-Tsodyks in capturing the XOR computations, a better performance in solving the XOR problem is not the purpose of the given simulations in this thesis. The simulations here aim to show the applicability of the introduced framework on biophysical synaptic dynamics realizing STDP and to support the biological plausibility of the introduced learning framework.

Developing this framework is basically motivated by the need of a proper and simple learning algorithm for the spiking networks that utilize dynamic synapses. In these networks, the synapses are not represented as weighting constants. Hence, altering the synaptic response via the classical back-propagation or the  $\delta$ -rule is not appropriate (Florian, 2007). Moreover, the analytical derivation, for example in (Xie and Seung, 2004) and other similar studies are based, to a certain extent, on the assumption that the neurotransmitter release is independent of the spike generation process at any particular time. Although this is not wrong as an assumption, it limits the application of their techniques from being extended for other synaptic models, in which the probabilistic nature of the neurotransmitter release is only responsible for the spike generation (El-Laithy and Bogdan, 2010b; Lee et al., 2009).

As for the XOR computations, comparing the results reported here to the count of correct hits reported e.g. in (Florian, 2007) may be performed in a separate study. Because the goal in this attempt is to account for the temporal features in the output and this is a key issue that distinguishes

the presented framework from former ones. The spiking output of the network here is highly characterized by its temporal contents. In relation to this, a distance measure that accounts for the statistical features of the compared signals, e.g. stochastic event synchrony measure (Dauwels et al., 2009), may represent an added value to the introduced framework. Determining which distance measure to use in estimating the reward values is a research point in itself to be tackled in a separate study.

The detected self-organizing behaviour for the tuned parameters suggests that the synaptic dynamics encode the statistical features of the inter-spike intervals implicitly. In other words, the temporal information embedded within input spike trains are encoded in the dynamics of the synaptic connections. This demonstrates the central role of the implemented learning framework not only in realizing the required computation, but to capture the input temporal information and to store it within the synaptic dynamics. This in turn agrees with very basic postulates from D. Hebb (Hebb, 1949), see Sec. 8.1.

The availability of the reference spike train along with holding the reward value from previous trial require a memory in the simulated neural system. This does not represent a problem in simulation environments, since computers are equipped with enough computational resources to accomplish this. However, this raises an important issue when the biological counterparts are under investigation: Are biological neural systems able to provide such reference outputs and keep some kind of traces to indicate the previous success (or failure) in generating their recent outputs? There is no means to check whether there is an ability to generate a reference output, however there are evidences that neural systems keep traces about the correctness of the recent neural actions; the detection of the so called P300 signal in brain-computer interface experiments is a direct example of such indication, see e.g. (Teixeira et al., 2010) for a recent review. This signal is a specific form of electroencephalogram (EEG) waves and is used as a measure of cognitive function in decision making processes. The mechanism underlying the generation of such signal is not clear, its existence suggests however that neural systems compare their planned response to the required (correct) response. This sheds more light on the plausibility of the proposed framework.

Intuitively, the introduced framework is not confined either to the Markram-Tsodyks synaptic model or to the MSSM. The estimation of the reward signal does not presume certain characteristics of the synaptic model. Based on this sense of generality, the approach presented here is useful in cases where stochastic, biologically plausible or complex representations are required for implementation with SNN (El-Laithy and Bogdan, 2010b, 2011b). Considering the simple mathematical implementation of the update rule and calculation of the reward values, this framework can be used as an online adaptive scheme for controlling and tuning networks performance via the modulation of the involved synaptic dynamics.

## 8.6 summary

The introduced results and network behaviour indicate that the learning framework proposed here is able to regulate the dynamic part of the synaptic response in the MSSM and to capture the required input-output relation. Such success in modulating the mechanisms within the MSSM based on and in order to control the behaviour of the network, complements the development of the MSSM. This is a new evidence that the dynamics of the MSSM are adequately and efficiently represented which consequently allows the learning framework to register the input information onto the synaptic dynamics. Furthermore, having both the MSSM and being able to tune its performance to affect the behaviour of a network prepares the way in front of obtaining benefits from the capabilities of the MSSM on a network level. The first aspects of these benefits is thus the ability to learn a predefined input/output computational task presented in this chapter. The next chapter investigates a more complex information processing aspect on the network level based on the properties of the MSSM, it is the issue of "Binding by Synchrony".



# Synchrony States: Binding by Synchrony

*"Insanity: doing the same thing over and over again and expecting different results."*

**Albert Einstein**

## 9.1 Introduction

So far, a number of milestones are introduced. First, it is the novel synaptic dynamic model (MSSM) that is able to capture the required essence of synaptic variability at an optimum and balanced complexity along with low computational requirements in comparison to the other available models (e.g. the Leen-Anton-poon), as presented in Ch. 4 and 5. Second, this synaptic model along with the related energy based analysis presume that the synaptic dynamics in a network drive the network behaviour into stable internal representation of the input information, see Ch. 6. During the search for this stable representation, synaptic parametrization requires certain means of modulating its state parameters via altering the values of its model parameters, i.e. a learning framework. This learning framework is presented in Ch. 8 as the third milestone in this thesis. The remaining question is then how the network activities with the MSSM will evolve over time? Is the network through its synapses able to find a stable operating point with internal level of synchronous firing? It is important to understand the relevance of achieving such synchronization of neural firing within a network before investigating this aspect. Achieving temporal firing synchronization within spiking neural networks (SNN) with certain criteria represents a very important step on revealing one of the most challenging questions about signal processing in the brain. It is, how the brain solves the binding problem? The binding problem is one of the major questions in neuroscience, it wonders how can the brain integrate distinct information from different neuronal working groups into a unified knowledge and experience (Revonsuo and Newman, 1999). *"The solutions of the binding problem proposed in literature until now are controversial and hotly debated in neuroscience. Years of research have shown that the binding problem cannot be solved*

easily" (Velik, 2008). Implementing a solution to this problem using SNN opens new avenues towards the development of brain-inspired artificial information processing systems. In this chapter a mechanism (or a solution) which is very plausible and well supported by the experimental studies (explained below) is revised (actually reborn) by showing that it does work and it can be implemented within SNN using the MSSM. This mechanism is the "binding by synchrony" (von der Malsburg, 1999). Up to the author's knowledge, this is a very first trial to import this paradigm from being only observed into implementation in SNN using dynamic synapses (the MSSM); this aim at copying the emergent computational capabilities of the biological neural systems.

In the following section more light is shed over the details of the binding issue and why it is viewed as a "problem" at first place. Next sections discuss in more details the issue of binding by synchrony as a possible solution for the problem and how this is tackled in this work using SNN that use the MSSM for the synaptic representations.

### 9.2 The Binding Problem

From the literature of neuroscience the term "binding" is defined in general as *"the ability of the biological neural system, in terms of inherited flexibilities, to construct higher level symbols by combining more elementary symbols"* (Singer and Gray, 1995; von der Malsburg, 1981). A first original example illustrating the problem with binding has been discussed by Frank Rosenblatt in 1961 in his book "Principles of Neurodynamics: Perceptrons and the Theory of Brain Mechanisms" (von der Malsburg, 1999). The example presented by Rosenblatt assumes a perceptual system consists of four neurons, see Fig. 9.1. Two neurons respond to the presence of geometrical objects. The first is active in response to the presence of a triangle. The second responds to the presence of a rectangle. Both generalize over position. The third and fourth neuron respond to the position of the object, i.e. for the upper and lower positions respectively. The latter neurons generalize over the type of the object. When only one object is presented to the network, it responds reliably. If two objects are presented simultaneously to the network, e.g. a triangle in the upper half and rectangle in the lower half, all the four neurons are activated as shown in the lower case in Fig. 9.1. This example shows that the presence or absence of features alone is not sufficient to represent multiple objects simultaneously. Because it is not clear whether the triangle or the rectangle is in the upper position. The neural data structure has no means of *binding* the object triangle to the feature top or the feature bottom to the object rectangle. This is the binding problem. Such a "conjunction error" can be induced in humans if they are given insufficient viewing time (which is usually not the case). The cases of misperceptions are also coined as "illusory conjunctions" (Treisman and Gelade, 1980).

The central nervous system does not experience this problem in general (Gray, 1999). It is only a problem for neuroscientists while trying to reveal how cognition is performed in the brain. However, the misperceptions or the illusory conjunctions may occur in normal brains when the

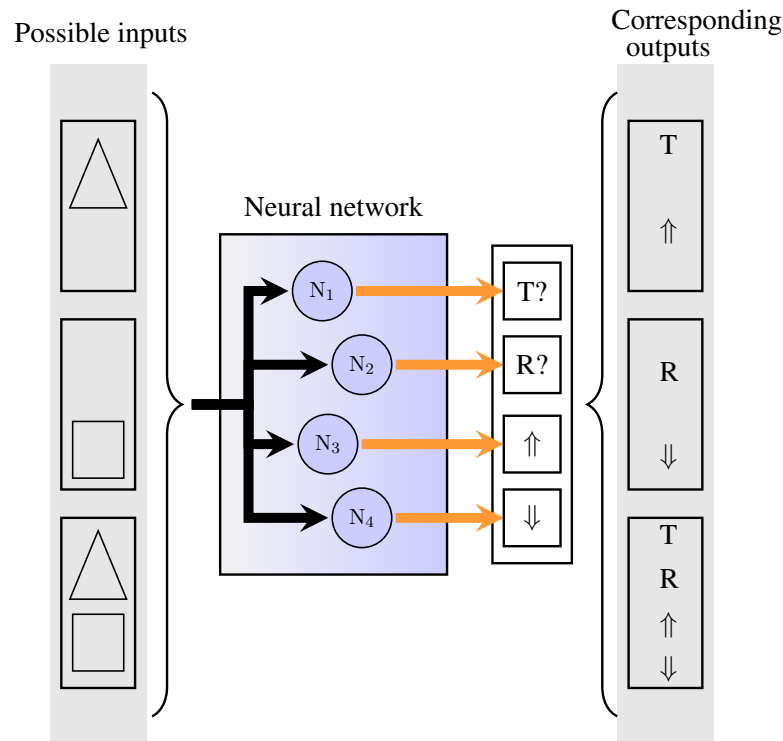


**FIGURE 9.1:** The Rosenblatt's illustration of the binding problem. In the middle there is a hypothetical perceptual system (Neural network) with four neurons. The network structure is neither feedforward nor any certain classical one, however it is assumed that the network is able to perform the described recognition task (see text for details). Each neuron respond to either an object (T: Triangle or R: Rectangle) or a feature (Up arrow: Top or Down arrow: Down). In the lower case when both objects are presented to the network, all four neurons are active. Therefore, the responses for objects and features are bound. Figure is made after the illustrations from (Velik, 2010; von der Malsburg, 1999)

brain experiences temporal or capacity limitations; for example, when attention is distracted, when objects are briefly visual or are visual with a deteriorated resolution (Treisman and Gelade, 1980). Besides, an increasing number of objects in a large receptive field increases the erroneous cases of feature binding. In pathological cases and because of brain malfunctioning regions the binding problem may be observed as well. The Balint's syndrome is a condition when the person is able to perceive only one object at a time. This syndrome is characterized by the damage of both parietal lobes (Perez et al., 1996).

### 9.2.1 Classes of The Binding Problem

Although the term binding itself may be defined as the ability to integrate basic symbols to construct more complex ones, the term binding problem does not refer to a single concept. It refers rather to a class of problems. That is, how the brain is able to resolve between e.g. two objects with two different features simultaneously. The illustrated example in Fig. 9.1 shows a spatial binding problem since the objects are figures and the features are the spatial positioning; it can be on a temporal scale as well when the objects are for instance two tones and the features are the

frequency ranges. The binding problem may be also classified as being a cognitive binding problem or a perceptual binding problem. The latter involves unifying resolvable aspects of percepts. Cognitive binding problem refers to relating a concept to a percept. These classes may be further subclassified according to a neural modality, a sensory or motor reconstruction.

It is important to notice that the binding is a problem as long as it suppresses the bound information rather than integrating these information into new pieces of information. The brain requires the concept of binding itself from a theoretical point of view in order to be able to handle the required cognitive and perceptual tasks. It is obvious that the brain needs binding almost everywhere and across all processing levels. However, binding is investigated in only very few regions of the brain (Velik, 2008). The most studied region is the visual cortex and consequently the visual binding. Visual binding is the process of building relations and linkages between optical features of visual perceptual objects. Features are color, boundaries, motion, foreground, background and size. The act of seeing seems an easy and seamless process, person perceive objects, motions and scenes without any awareness of the mechanisms underlying the process of perception these objects and related features. The brain, however, process a continuous stream of a huge amount of information. The details and the involvement of binding in the process of visual perception are relatively the only well studied binding process, see (von der Malsburg, 1981) for an excellent review and (Velik, 2008, 2010) for recent overviews.

Other sorts of binding are barely found in the literature. Cross-modal binding, action control binding and perception-action binding are briefly mentioned in a number of discrete studies, see e.g. (Hommel and Milliken, 2007; Robertson, 2003). Shortly stated, these arts of binding discuss the relevance of integrating information from different sensory receptors. These pieces of information are stored in diverse areas of the brain (localized and decentralized) that require binding in order to exhibit a unified recognition of the environment and a unified action.

### 9.2.2 Potential and Possible Solutions (Mechanisms)

After exploring the basics of the binding problem, here the plausible and potential solutions are discussed. The solutions are seen potential and possible as being concluded from cognitive, neuropsychological, neurophysiological and theoretical studies. In fact, the literature of neuroscience often highlights that the binding problem shall continue to be a research and investigation point for much longer time. All the available mechanisms are hypothetical solutions which are logically accepted. They are not a priori the underlying mechanisms of handling binding in the brain. They have been hypothesized to explain how a coherent representation can be made from pieces of information distributed throughout the brain (Hommel and Milliken, 2007). The following list briefs these plausible and potential solutions to the binding problem (Singer, 2007; Velik, 2010):

- **Combination coding:** The model of combination coding started with the early stages of studying the visual cortex, the concept is inspired by the convergent hierarchical nature of



the visual processing pathway. This model of binding assumes that sensory information is integrated, encoded and condensed over and over as the information pathway gets higher (Revonsuo and Newman, 1999). The combination coding emerges here with each level along this hierarchy. Specialized cells respond only to combinations of features, they are so called combination coding cells. This hierarchical processing path results in an increase in the complexity of the neuronal representations because increasingly complex features are represented by higher levels in the visual hierarchy. That way, a small group of neurons or a single neuron (the grandmother cell or the cardinal cell theory) receives and react to convergent inputs from populations of neurons at preceding lower levels in the hierarchy.

Although the model may seem plausible at first glance (some implementations for visual recognition systems are inspired and developed from this model), many open question are still there (Bauer, 2005). The model assumes cells with high specificities, how are these cells trained to gain such specificity? How could these neurons be pre-wired for all possible distinguishable shapes, objects, colours, ... etc.? These questions are argumentations against the "cardinal cells" or "grandmother cells" theory<sup>1</sup>. A cardinal cell would have to be idle until its pattern appeared again, eventually for decades (von der Malsburg, 1981). Only the core concept of this type is still plausible (Bauer, 2005; Singer, 2007).

- **Population coding:** This is the generalization of the combination coding approach. Instead of representing the integration of features by single or a small group of neurons at a specific cortical region, features could be represented by the activity of a population of neurons localized in certain cortical area or distributed across levels of cortical hierarchy (von der Malsburg, 1999). The information content of any stimulus is its firing pattern. This stimulus pattern can be represented by a distinct (or even a unique) pattern of firing in a distributed population of neurons. The concept of this mechanism agree with the representational capacity of the cortical networks. That is, the distinct patterns to be represented surpasses the number of neurons involved in representing the stimuli. Hence, an infinite cognitive state space is no more a problem to be mapped into the limited physically existing state space of the brain.

Although it may be attractive, the problem with this theory is the so-called superposition problem. How can one or more distinct patterns be identified from the many others that are present in the same network at the same time? The essence of this problem is the question how members of a representation are identified as belonging to one representation and how interferences among simultaneous representations are avoided.

- **Binding by feature:** The main difference between this mechanism and the population coding is which type of sensory information is represented and bound. In population coding there is no specified description hypothesized of the information to be encoded via the distributed neural activity. Binding by feature assumes that the neural circuitry is able to extract

---

<sup>1</sup>Shortly stated: One object, one neuron

the features relevant to an object and react to these features (Schrobsdorff et al., 2007). Distinct features are extracted and are bound to represent a certain object within the cortical circuitry, e.g. by spatial association in visual perception (Bauer, 2005). Binding by feature extends the cognitive capacity of neural system. Instead of representing the objects themselves, only their features indicate their existence and the varying combinations of features distinguish the different objects from each other.

Binding by feature has the same drawback as population coding, i.e. the superposition problem. Furthermore, there are argumentations that without attention the features can barely be bundled but not bound (Engel et al., 1999; Engel and Singer, 2001). The major strength point in considering binding by feature is that it does not contradict with any other potential binding mechanism.

N.B. Apart from being in general plausible or not, all the three mechanisms (combination, population and by feature binding) are *conceptual* solutions that do not involve any description of how these mechanisms can be explained in terms of the spiking activity of cortical circuitries. Recalling Fig. 1.4 from Ch. 1, these binding mechanism are supposed to be accomplished on a network level or even higher. The link to the second lower level of organization (abstraction) that of cellular (neuronal) and synaptic activities is missing, there is no detailed insights about how can the spiking behaviour of a neural circuitry be related to e.g. binding by feature especially away from the visual cortex. As for such a relation to the spiking behaviour of the network, the next mechanism represents accounts for such a link:

- **Binding by synchrony:** This mechanism is called temporal coherence or temporal binding as well (Singer, 1999, 2007). It is one of the most famous and well established conceptual solutions for the binding problem. It is mainly based on investigations made to the visual cortex and visual perception. This concept was first well formulated and introduced by von der Malsburg in 1981 by studying the integration of visual sensory information (von der Malsburg, 1981). It might be viewed as an extension of the population coding with an important core concept of incorporating "time". Incorporating the temporal dimension as a key player in this binding mechanism distinguishes this solution from all other mechanisms. The basic idea of binding by synchrony is that the binding problem can be solved by temporal correlation or synchronization of neuronal discharge (firing). Spike trains of neurons representing features of the same object (or the objects themselves) are mutually correlated in time. Spike trains of neurons representing features of dissimilar objects are decorrelated or anti-correlated in time. Synchrony serves as a signature of relatedness which is modulated by attention from a cognitive point of view. Synchrony consolidates the interactions among the members of the same assembly. Different assemblies are distinguished from one another by the temporal independence of their spiking patterns. Therefore, multiple distributed signals can coexist in the same network of cortical area at the same time, i.e. parallel simultaneous different representations. Being flexible and dynamic are among the

main advantages and strength points of binding by synchrony (Singer, 2007). The main arguments against the plausibility of this mechanism were the few experimental evidences that binding is linked to synchronized firing indeed within cortical networks (Shadlen and Movshon, 1999).

There are still other mechanisms which are viewed as potential and possible such as: binding by attention, binding by knowledge and binding on demand (Hommel and Milliken, 2007; Treisman and Gelade, 1980). These mechanisms require by definition lower level procedures of binding. For example, binding by knowledge implies that diversified features representing certain portion of the knowledge are bound through contextual information and past experience. Thus, binding by feature is a prerequisite for the mechanism of binding by knowledge. This dependence applies for binding by attention, by knowledge and on demand without exception. Hence, these mechanisms represent a higher level of abstraction in the hierarchy of neural functions which seems implausible within the context of this work at hands. The implausibility is not meant as implausible to be found in the brain. On contrary, each of these solutions contributes (somehow) to a certain relative extent in the binding process within the brain probably at higher cognitive abilities (Singer, 2007). However, these high level binding mechanisms do not help in revealing the core required information processing methods utilized in the brain as they suppress lower details and underlying processes. Only the theoretically basic (middle level) solutions are relevant for studying and investigation in general and in this work accordingly because solutions are thought of as basic when they are directly linked to the spiking behaviour of neural ensembles. Therefore they are a priori implementable using SNN which is one of the main pivots of this thesis.

The argumentations have been reported that a true practical solution for the binding problem is a weighted mixture of all hypothesized solutions (Engel et al., 1999; Velik, 2008). The concatenation of algorithms is usually a secure way to achieve progress along any certain methodology. However, following the approach with the thesis at hands a precise selection of the mechanisms to be implemented and further investigated is as crucial as the plausibility of the mechanism itself. Differently explained, revealing the biological approach of binding and implementing it would not be doable by hit-or-miss selection of the approaches. Moreover, even by accepting the assumption that all hypothesised mechanisms are contributing to the observed mental capabilities, combining these mechanisms of binding together would be possible only if the basic binding mechanisms out of the other higher ones are realized and revealed at first place.

After having elucidated the general solutions and mechanisms of binding, binding by synchrony is of special interest. This special interest has two reason. First and more important, it represents an independent basic binding mechanism. It is independent of other mechanisms and directly related to network activity. This type of binding is anticipated as applicable and implementable within SNN. Being achievable in a simulation environment opens the way for emulating those higher neural functions that require binding by synchrony as an information processing basis,

e.g. content addressable memory. Whether binding by synchrony is achievable with SNN based on the MSSM capabilities or not, is the question tackled in this chapter.

The second reason is related to the global view of the brain as being a sort of a finite-state machine (Koch and Tononi, 2008; van der Velde and de Kamps, 2006). Briefly, experiencing a certain level of synchronized activity within a neural ensemble can be interpreted as experiencing a *transient* state in a finite-state machine. This state is part of the internal representation of the sensory information, background and past activities within this neural ensemble. Hence, the information processing within this neural ensemble can be traced and explained as transitions between different temporally defined set(s) of states. The topic of finite-state machines is explained in much details in the next chapter (Ch. 10) and the whole idea is manifested in Ch. 11. The next sections explain in more details the mechanism of binding-by-synchrony.

### 9.2.3 Binding by Synchrony: Temporal Coherence

Temporal coherence in the firing activity of groups of neurons is widely observed as a common feature throughout the neocortex (Tsodyks et al., 2000). The analysis of the responses of stimulated neurons of cat's visual cortex (König et al., 1995) confirmed that activated neurons can reliably produce synchronous discharge with the precision of a few milliseconds. Investigating the key factors in exhibiting such synchronous activity (Hansel et al., 1995) related these observations to both the pure excitatory and the intrinsic time course of synaptic interactions. According to the explanation by (Fries, 2005; Fries et al., 2001), neural communication is supported by neural coherence. Activated neural groups oscillate and thereby undergo rhythmic excitability fluctuations, which produce temporal windows for communications. It has been argued that only coherently oscillating neural groups can interact efficiently, because their communication windows for input and for output are open at the same times. By these matters, a flexible communication structure is provided, which reinforces the cognitive flexibility. This might be conceptually similar to the situation of resonance in electrical circuits. When input impedance of a loading circuit matches the output impedance of the supplying one, resonance occurs featuring a maximum power transfer from the supplying circuit to the loading one. Here, temporal correlations allow for maximum information transfer from the sensory sources to the processing neural circuitries. Thus, neuronal temporal synchrony could allow the information about stimuli to be conveyed as temporal relations between neural sites and provide the basis for integrating different features representing the same object.

The plausibility of temporal coherence as a binding mechanism is supported from different perspectives. For example, neurons and synapses are sensitive to the timing of their inputs as shown in the first part of this thesis. Moreover, psychophysical observations suggest that the temporal precision of cortical neurons is important for guiding behaviours; humans are sensitive to timing differences as small as 150  $\mu$ sec (von der Malsburg, 1999).

Despite the plausibility of the mechanism there is no theoretical framework that explains how binding by synchrony works as an information processing basis (LaRock, 2007). Tackling the latter issue along with indicating the role of optimum synaptic modelling come clear through the following sections.

### 9.3 Synchrony States

Synchrony states as a concept has emerged from studies mainly made in the visual cortex. Such states are involved when any group of neurons show a degree of synchronous firing over a time scale much longer than that attributed for unitary spikes (von der Malsburg, 1999). In order to observe this state, this temporal synchrony (or temporal correlation)<sup>2</sup> is defined over a time period  $T_{\text{sync}}$ . With this period of time (or Psychological Moment) a neural state is defined. At times greater than  $T_{\text{sync}}$  one observes only a sequence of states (state history). Below this time window a state cannot be defined. The need to maintain this state of temporal correlation for periods greater than few milliseconds was supported by the argumentation that such temporal window is required in order to confine the behavioural conditions fitting the higher brain functions and difficult tasks that require sustained level of activity (Singer and Gray, 1995). In this sense, states of synchrony are involved in the processing of sensory inputs, see e.g. (Gilbert and Sigman, 2007; Poulet and Petersen, 2008). Moreover, it has been argued that attention and awareness emerge from the interacting dynamics in terms of synchrony states among distributed neural ensembles (Tallon-Baudry, 2004). Von der Malsburg stated that plausible values for the time window to define a synchrony state could be in the range of 50 - 200 millisecond and may be also extended to involve minutes if other mental aspects are in concern (von der Malsburg, 1999). Within this time window, the actual signal fluctuations are not relevant (for a complete review please refer to (Averbeck et al., 2006; Salinas and Sejnowski, 2001; Singer and Gray, 1995)).

Recalling the Rosenblatt's example from Fig. 9.1, binding by synchrony resolves the overlap in responses by temporal differentiation. Binding by synchrony postulates that the neurons  $N_1$  and  $N_3$  fire synchronously over a time scale  $T_{\text{sync}}^{(1)}$  while the neurons  $N_2$  and  $N_4$  fire synchronously over a time scale  $T_{\text{sync}}^{(2)}$ . Experiencing two different patterns over two different time scales solves the binding problem explored in the Rosenblatt's example.

The generation of synchrony (but not states of synchrony) within SNN was addressed in many theoretical studies, e.g. (Bressloff and Coombes, 2000; Campbell et al., 1999; Hansel et al., 1995; Mikula and Niebur, 2005; Neltner and Hansel, 2001; Vreeswijk and Hansel, 2001). These studies confirmed the ability of a SNN to sustain the temporal synchrony over the time scales of few milliseconds even with sharp synchronization on the time scale of single spikes. In general, these studies simulated a population of LIAF neurons with adequate interconnectivity. Their discussions highlighted the major role of excitatory interconnections to achieve a certain degree of synchronous

<sup>2</sup>Von der Malsburg did not mean explicitly the mathematically known cross-correlation, instead the general sense of being temporally correlated

activity. Tsodyks et al. presented a notable study where they considered the non-linear (frequency dependent) synapses for the generation of synchronous firing (Tsodyks et al., 2000). Their results showed that the incorporation of nonlinear synapses in recurrent networks provide the basis for the emergence of short-time synchronous activity.

The ability of maintaining a level of synchrony (a synchrony state) within a SNN that uses MSSM would be a direct implication of the added values and benefits from using such a balanced synaptic model. Furthermore, sustaining a state of synchronous activity over time scales of tens of milliseconds represents a further validation to the energy profile proposition, see Prop. 6.2. In this proposition it is argued that the synapses while seeking for stable and low synaptic energy level, can reinforce certain synchronized firing patterns within a network. The process of seeking an operating point, that is attributed by a stable and low energy level, requires a framework that enables the synapse to tune the values of its model parameters. This framework is the learning framework introduced in Ch. 8. Maintaining synchrony states within SNN using the MSSM might be the first step on defining a novel theory about the information processing in the brain based on the concepts of finite-state machines.

Up to the author's knowledge, no implementation of SNN was able to show that such sustained synchronous behaviour is achievable. As mentioned above, synchrony over the time scale of a pair of milliseconds has been shown, e.g. (Tsodyks et al., 2000). This extreme short term synchronization has been simulated using the Markram-Tsodyks model. It was stated that sustaining a high level of synchrony for a longer time window is not achievable. The inability of the network dynamics to sustain the required synchronized firing for time windows of e.g. hundred milliseconds was the main obstacle against the utilization of the mechanism of binding by synchrony as brain-inspired information processing basis.

A basic framework for generating synchrony states with the MSSM coupled to a LIaF neurons has been proposed in (El-Laithy and Bogdan, 2009, 2011c). Preliminary results have shown that SNN with the introduced framework are able to sustain special regimes of activity with synchronous discharge over biologically tenable periods of time. Here, the detailed description and analysis of this framework along with the involved results are reported. Specifically, the ability of a network comprising LIaF neurons and MSSM synapses is investigated as whether it is able to implement the concept of synchrony (the temporal correlations) among the signals of grouped neurons as states of synchronous activity. The goals are: a) To construct a SNN that, when driven by randomly generated spike trains, is able to transform input signals combined with background synaptic activity into correlated outputs and b) To show the ability to sustain such level of synchrony over a considerable long time course.

## 9.4 Simulations

The biologically accepted network size, in which temporal correlation can be observed and effectively utilized, is not precisely specified (Tsodyks et al., 2000). There are some hypothetical suggestions discussing the tenability of the network size. For example, Singer has analysed the major factors affecting the ability of a group of neurons to exhibit synchronous activity (Singer and Gray, 1995). He has pointed out that the network size could be as small as two mutually coupled neurons and may be up to 100 neurons. Herzog and Gerstner have argued that if synchrony is an essential feature for the brain activities, it should also be feasible in small networks (Herzog et al., 2007). They called this "the small network argument", or the new benchmark for consciousness. Thus, they reported, there is a minimal model or a small network that satisfies the criteria underlying consciousness, e.g. temporal synchrony, but it is not conscious itself. They stated that groups of up to seven neurons are sufficient to experience memory, learning, or synchrony. Based on the analysis done in (Dodla and Wilson, 2008), a network of two neurons should be able to achieve spike-to-spike synchrony when enough mutual conductance is available.

Thus, two basic network setups are used. A schematic of the first network is in Fig. 9.2(a) with the input being fed only to the first neuron,  $N_1$ . The network consists of three mutually interconnected neurons. Only excitatory synapses are simulated. A bigger network is simulated as well, it consists of eight neurons as in Fig. 9.2(b). The input is also fed to  $N_1$ , and similar to the smaller network, the feed back to the input neuron is only possible from the neighbouring neurons; in this case from  $N_2$ ,  $N_3$  and  $N_4$ . In both networks, all the synaptic connections are modelled with the MSSM as described in Ch. 4. In order to represent the existence of the synaptic background activity, additive white Gaussian noise is fed directly to synaptic activity ( $E_{psp}(t)$ ) during the entire simulation epoch. The neurons are LIAF units and the model parameters are:  $\tau_h = 20$  msec,  $h_{rest} = -70$  mV and  $h_{th} = -60$  mV. All synaptic connections used for the simulations are represented with the MSSM. Some of the synaptic model parameters are subject to training as explained in next section:  $C_o$ ,  $V_o$ ,  $\tau_C$  and  $\tau_V$ . Other synaptic parameters, which are fixed and not subject to training, are arbitrarily set at  $\alpha = 0.095$ ,  $k_{epsp} = 2.5$ ,  $\tau_{N_t} = 12$  msec,  $\tau_{epsp} = 9$  msec,  $k_{N_t} = k_{N_t, V} = 1$  and  $N_{t_o} = 0$ .

The input is a set of 400 spike trains, each with a Poisson-distributed inter-spike intervals for an epoch of 150 msec. This time epoch corresponds to  $T_{sync}$  and is arbitrarily selected as a median value for the proposed temporal range over which a synchrony state is plausible. The spike generator is adjusted to generate spikes with a maximum overall firing-rate of 50, 100 or 200 Hz. Meanwhile, at each synapse a white Gaussian noise is added locally to the induced postsynaptic potential from this synapse. The level of the noise can be modulated via linear amplification.

The main hypothesis of binding by synchrony from von der Malsburg did not identify or assume any biological means of how the neural circuitry detects the synchrony. For representing synchrony within the simulations, the cross-correlation based measures are generally accepted for the detection of synchrony (Mikula and Niebur, 2005; Tsodyks et al., 2000). Correlograms are

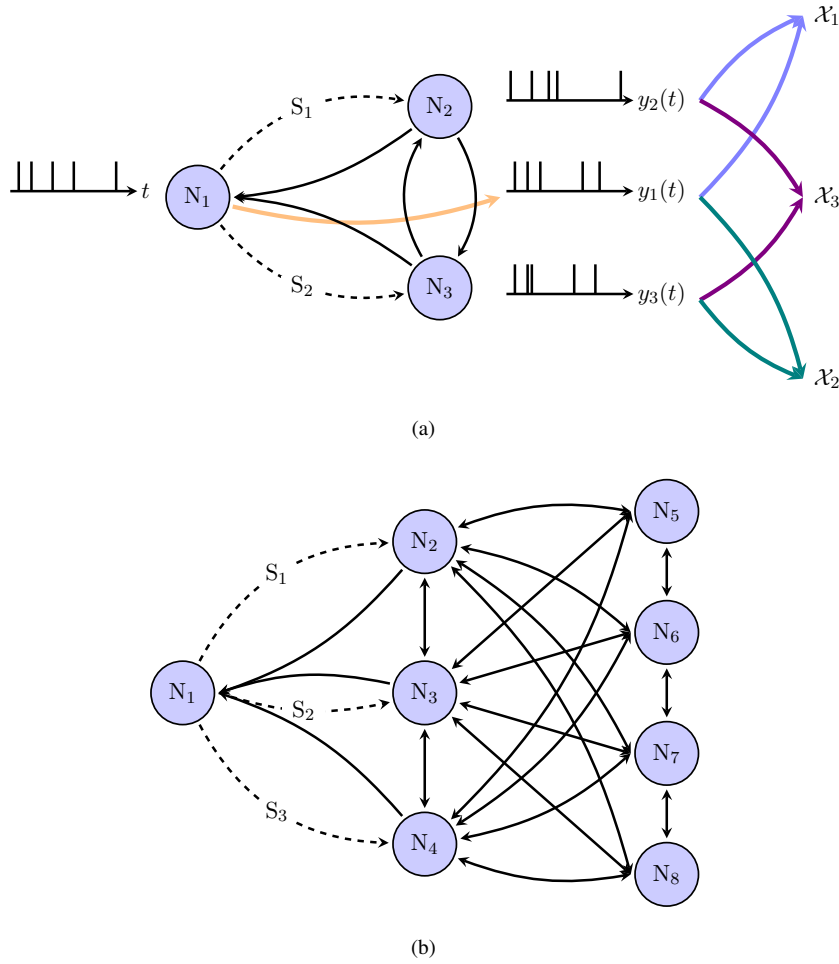


**FIGURE 9.2:** Network schematic. (a) Three neurons network. The dashed lines are those synapses permitted to be trained. Double arrowed connections represent a mutual connection. Horizontal-right oriented arrows: output signals from each neuron:  $y_1$ ,  $y_2$  and  $y_3$ . Vertical-two-headed arrows: the corresponding cross-correlation coefficient:  $\mathcal{X}_1$ ,  $\mathcal{X}_2$  and  $\mathcal{X}_3$ . The trained synapses are from  $N_1$  to  $N_2$  and  $N_3$ . (b) Eight neurons network. The dashed lines are those synapses permitted to be trained. Double arrowed connections represent a mutual connection. The details of the outputs and the calculation of cross correlation are omitted for clarity. The trained synapses are the synapses from  $N_1$  to  $N_2$ ,  $N_3$  and  $N_4$

not considered in this study based on reviews about their analytical reliability, see e.g. (Brody, 1999). A correlation-based measure calculates the cross-correlation coefficient between neural responses (spike trains) after applying a Gaussian filter on the responses (Schreiber et al., 2003). The width of the Gaussian filter is chosen to be equal to the used neuronal refractory period at 2 msec. The maximum cross-correlation coefficient between the filtered spike trains is used to indicate the degree (level) of synchrony among the responses of the neurons in the network. As given in Fig. 9.2(a), between each pair of neurons the level of synchrony is calculated resulting in  $\mathcal{X}_1$ ,  $\mathcal{X}_2$  and  $\mathcal{X}_3$ . The algebraic mean of these cross-correlation coefficients  $\bar{\mathcal{X}}(t/T_{\text{sync}})$  is the detected level of synchrony at the simulation episode number  $t/T_{\text{sync}}$ .



## 9.5 Learning Framework

The learning framework has been given in details in Ch. 8 (in Sec. 8.3.2). In this section only some remarks are given about the modifications made to the mentioned details before. These changes affect neither the general concept nor the basic structure of the learning idea. These changes are applied in order to let the framework agree with the required task, such as the definition of the reward values and the need for binning of the output spike trains.

The modulation of the learning rate is controlled by the sign and the value of the temporal difference of the reward signal  $\delta_{\mathcal{R}wd}$  similar to the discussion presented in Sec. 8.3.2. But the reward signal here is the detected synchrony level  $\bar{\mathcal{X}}(t/T_{\text{sync}})$  instead of the distance measure. The distance measure  $\mathcal{D}$  is not further required in detecting the synchrony among the spiking responses because temporal deviations are not as crucial to temporal coherence as it is to the XOR computations. A major difference between the framework presented before and the one applied here is the binning of spike trains. In this chapter no binning is required because the evaluation of the cross-correlation coefficient is less sensitive to spike timing. Thus, the equations of the learning framework are:

$$\Delta m = \eta \cdot m \cdot \delta_{\mathcal{R}wd}, \quad (9.1)$$

$$\delta_{\mathcal{R}wd} = \mu(\mathcal{R}wd_{t-1/T_{\text{sync}}} - \mathcal{R}wd_{t/T_{\text{sync}}}), \quad (9.2)$$

and

$$\mathcal{R}wd = \bar{\mathcal{X}}(t/T_{\text{sync}}) \quad (9.3)$$

Eq. 9.1 is identical to the learning rule of Eq. 8.3 which is the basic Hebbian update rule. In Eq. 9.2,  $t - 1/T_{\text{sync}}$  and  $t/T_{\text{sync}}$  replace the "previous" and "current" suffixes from Eq. 8.4 respectively. The definition of the  $\mathcal{R}wd$  signal in Eq. 9.3 replaces that from Eq. 8.2. The model parameters subject to training and which are denoted by  $m$  in Eq. 9.1 are chosen to be:  $C_o$ ,  $V_o$ ,  $\tau_C$ ,  $\tau_V$  and  $\alpha$ . By modulating these model parameters, both core facilitation and depression mechanisms are tuned. The initial values are selected from a uniformly distributed random generated values.

The changed definition of the reward values used in this chapter satisfies the general requirements of a reward signal in a reinforcement learning problem. The objective of the learning process is to sustain the maximum available value of the internal synchrony among the neurons. The combined Hebbian and anti-Hebbian approach applied through this learning framework avoids jumping out of stability as long as input features unchanged. This statement is supported with observations from Ch. 8, the convergence of the reward values and the self-organizing behaviour in the trained values are two examples of the stable performance by the learning process. This stable performance is expected to be driven by the network dynamics itself in the case under investigation. Recalling the Gedanken experiment described in the proof of Prop. 6.2, the learning mechanism

is the means of the synaptic quest for stable operating point. When the MSSM model parameters reach the set of values (an operating point) which result in the lowest stable synaptic energy, the synapses try to keep their dynamics at or close to this operating point; i.e. the network should sustain a level of internal synchrony.

## 9.6 Results

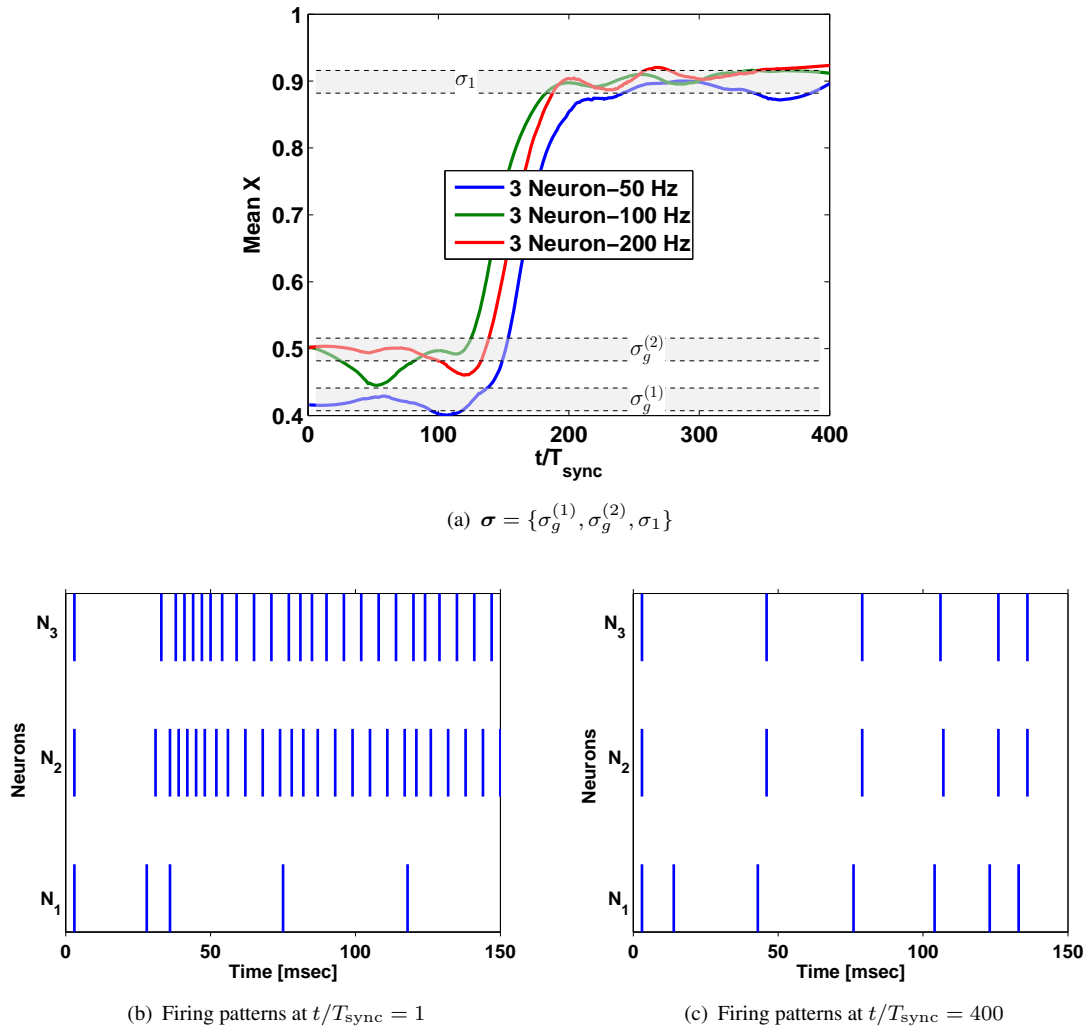
Fig. 9.3 illustrates the results of the simulation with the three neurons network. Fig. 9.3(a) shows the time evolution of the detected level of synchrony (Mean  $X \equiv \bar{\mathcal{X}}(t/T_{\text{sync}})$ ). In this figure there are three different lines corresponding to three different frequencies of the input spike trains that are fed separately. In all three input cases, after almost 100 simulation episode ( $t/T_{\text{sync}} \geq 100$ ) the network sustains a very high level of synchronous firing among its neurons. Although the input frequencies of the spike trains are different, the achieved levels of synchrony over  $T_{\text{sync}}$  are self-consistent as the values of the final detected synchrony levels are about 0.9 for the three lines. Presuming the numerical values of the detected levels of synchrony, Fig. 9.3(a) illustrates three synchrony states; this defines the states vector  $\sigma = \{\sigma_g^{(1)}, \sigma_g^{(2)}, \sigma_1\}$  of this network under this specific input/learning conditions. The states are shown in Fig. 9.3(a) as ranges of the detected synchrony levels highlighted with shaded stripes between dashed lines and annotated with the state symbol. These ranges are arbitrarily defined based on the detected synchrony levels. In the set of states a  $\sigma_g^{(\cdot)}$  refers to a ground synchrony state, i.e. a starting state. Using different input frequencies induces two starting (ground) states. The states capacity of this network is the cardinality of the state vector  $|\sigma|$ . This states capacity ( $\sigma_{\text{tot}} = |\sigma|$ ) depends mainly on the network topology, input information, learning rule, the resolving power of the used measure of detecting the synchrony level, and before all the synaptic dynamics. The implications of the detection resolution of the measure are further discussed in Sec. 9.7.4. Figs. 9.3(b) and 9.3(c) show the over all firing patterns from the three neurons at the first simulation episode ( $t/T_{\text{sync}} = 1$ ) and at the final simulation episode ( $t/T_{\text{sync}} = 400$ ).

Obviously, the firing pattern shown in Fig. 9.3(c) illustrates a high degree of synchronization among the neurons in the network, while at the beginning the firing activities from the neurons are decorrelated. Therefore, it is accepted to consider that the final activity is a *synchrony state* but the activities at the beginning do not represent a state. This actually is partially correct, the firing patterns at the beginning are out of synchrony but the basic postulates of binding by synchrony have confirmed that only *sustaining a degree of synchrony* indicates the existence of a synchrony state (von der Malsburg, 1999), and that the firing pattern itself during  $T_{\text{sync}}$  is irrelevant as it corresponds to the representation of input information. Hence, since the degree of synchrony is sustained from one episode to the next over almost 100 episode a synchrony state is definitely defined.

Another indicator of considering whether a synchrony level represents a synchrony state or not is the energy level maintained at this synchrony level. According to Fig. 9.3(a) and following Prop. 6.2, one should expect a transition from a high energy level to a lower energy level that coincides with the transition from both  $\sigma_g^{(1)}$  and  $\sigma_g^{(2)}$  to  $\sigma_1$ . Fig. 9.4(a) illustrates the time evolution of the average synaptic energy of all the synapses. Comparing this figure to Fig. 9.3(a), the transition in energy level coincides indeed with it from the synchrony level. This is not only a support for the hypothesized theoretical scenario given in the proof of Prop. 6.2, it represents a further validation for the proposed concept and analysis in Ch. 6 as well. It should be noticed that since the first level of energy represent a synchrony state it may represent the lowest one under other simulation conditions. Fig. 9.4(b) shows the average time evolution of the dynamic synaptic strengths of the synapses subject to training.

As for the eight neurons network, Fig. 9.5 shows the time evolution of the network behaviour and the network's internal dynamics. Similar to the network with three neurons, the bigger network with eight neurons has shown the ability to sustain a new level of synchrony among its neurons after a starting phase. The state vector in this case involves three ground states and one new state; the vector state is  $\sigma = \{\sigma_g^{(1)}, \sigma_g^{(2)}, \sigma_g^{(3)}, \sigma_1\}$ . States are illustrated as well in Fig. 9.5(a). Furthermore, similar to the case with three neurons network the final synaptic energy levels during synchrony are lower stable ones after an increase in the synaptic energy levels during the search for the stable operating points. Two differences are observed in comparison to the three neurons network behaviour. First, the transition from the starting levels of synchrony to the new one for two input settings takes about 200 simulation episodes. This means that under the conditions of the proposed framework, a bigger network might need a longer time to maintain the first synchrony state before undergoing the transition, that in comparison to the time needed with the three neurons network. However, this observation is not restrictive. The third line corresponding to the 200 Hz input case undergoes the switch to the new level of synchrony after almost the same number of simulation repetitions alike to the number required in the three neurons network. The delay in detecting the new level of synchrony in some of the input cases is due to competition between the synapses to stabilize their operating points. This may be obviously seen by investigating Fig. 9.5(b) where the time evolutions of the dynamic synaptic strengths are shown. The lines correspond to 50 and 100 Hz inputs experience some ups and downs before reaching the final level of synaptic strength. This is reflected in the evolution of the synaptic energy as well, see Fig. 9.5(c).

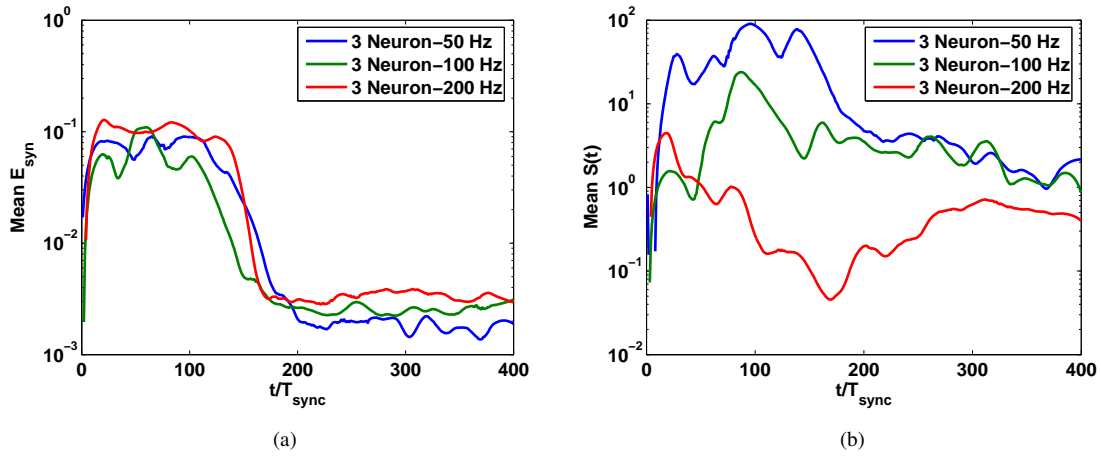
The second observation can be seen by studying Fig. 9.5(b), the dynamic synaptic strengths here experience an increase in their values, they become stronger along the excitatory profile. This is not seen in the three neurons network because in this network the input reaches the rest of the network almost unchanged via one input neuron, the synapses need just to adjust their model parameters to match the input temporal features allowing for synchrony to emerge. However, in the bigger network the synapses need to amplify their effect on the succeeding neurons (a strong excitatory regime) in order to be able to transfer the input temporal features into the entire network. The need of strong excitatory connections agrees with the already observed and reported properties



**FIGURE 9.3:** Three neurons network behaviour during the search for synchrony states. (a) Mean  $X \equiv \bar{\mathcal{X}}$  is the detected level of internal synchrony. According to this measure, the network maintains a new level of synchronous firing among the neurons of the three neurons network. The areas between the dashed lines indicate a margin that define the detected synchrony states that form the state vector  $\sigma$  (see text for details). (b) Raster plot of the firing activity of the three neurons network over the first simulation epoch. The three spike trains are obviously out of coherence. (c) The firing activity of the three neurons at the last simulation epoch. The firing pattern are almost identical across the three neurons. In (b) and (c) most lower trace is for  $N_1$  and the most upper one is for  $N_3$ .  $T_{\text{sync}} = 150$  msec.

of biological synapses in many studies, see e.g. (Tsodyks et al., 2000). This adds to the evidences that the MSSM indeed captures the essence of the synaptic action.

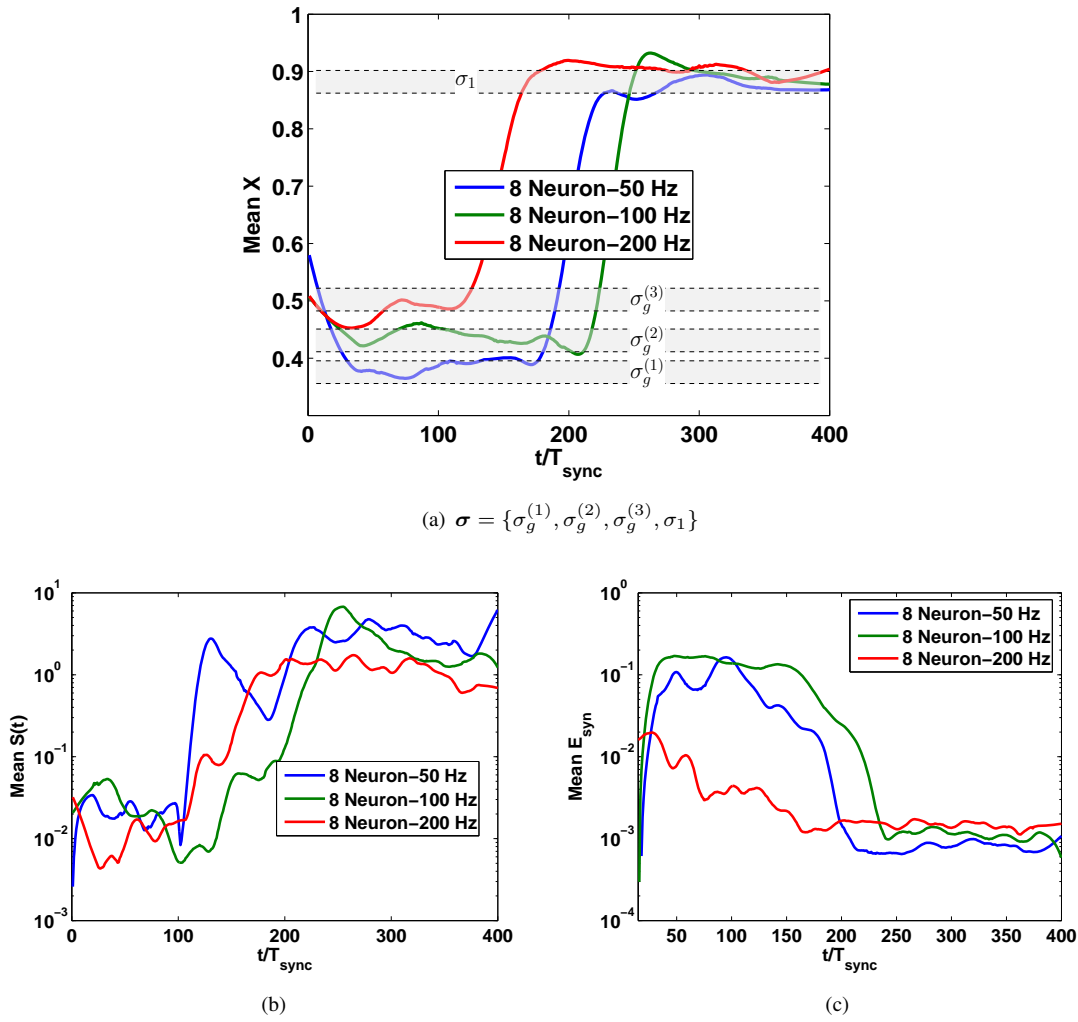
As mentioned before, additive white Gaussian noise is added to the synaptic activity during simulations. The effect of changing the intensity of the noise on the network behaviour is investigated. Taking the already used level of noise as a standard one, other two noise levels are used independently instead of the standard one with the eight neurons network. These intensities are selected to be either much higher or lower than the standard one. The results are shown in Fig. 9.6 for both lower and higher noise intensities. The detected synchrony levels in both cases



**FIGURE 9.4:** (a) Mean  $E_{\text{syn}} \equiv \bar{E}_{\text{syn}}$  is the mean synaptic energy across all the synapses in the network. The synaptic energy is calculated according to Eq. 6.1. (b) Similar to (a), Mean  $S(t) \equiv \bar{S}(t)$  is the average dynamic synaptic strength across the trained synapses (i.e. the feedforward synapses between the input neurons and the second layer). Mean  $S(t)$  is shown for the three different input spike train frequencies. Subfigures (a) and (b) are semi-log plots on the  $y$ -axis.

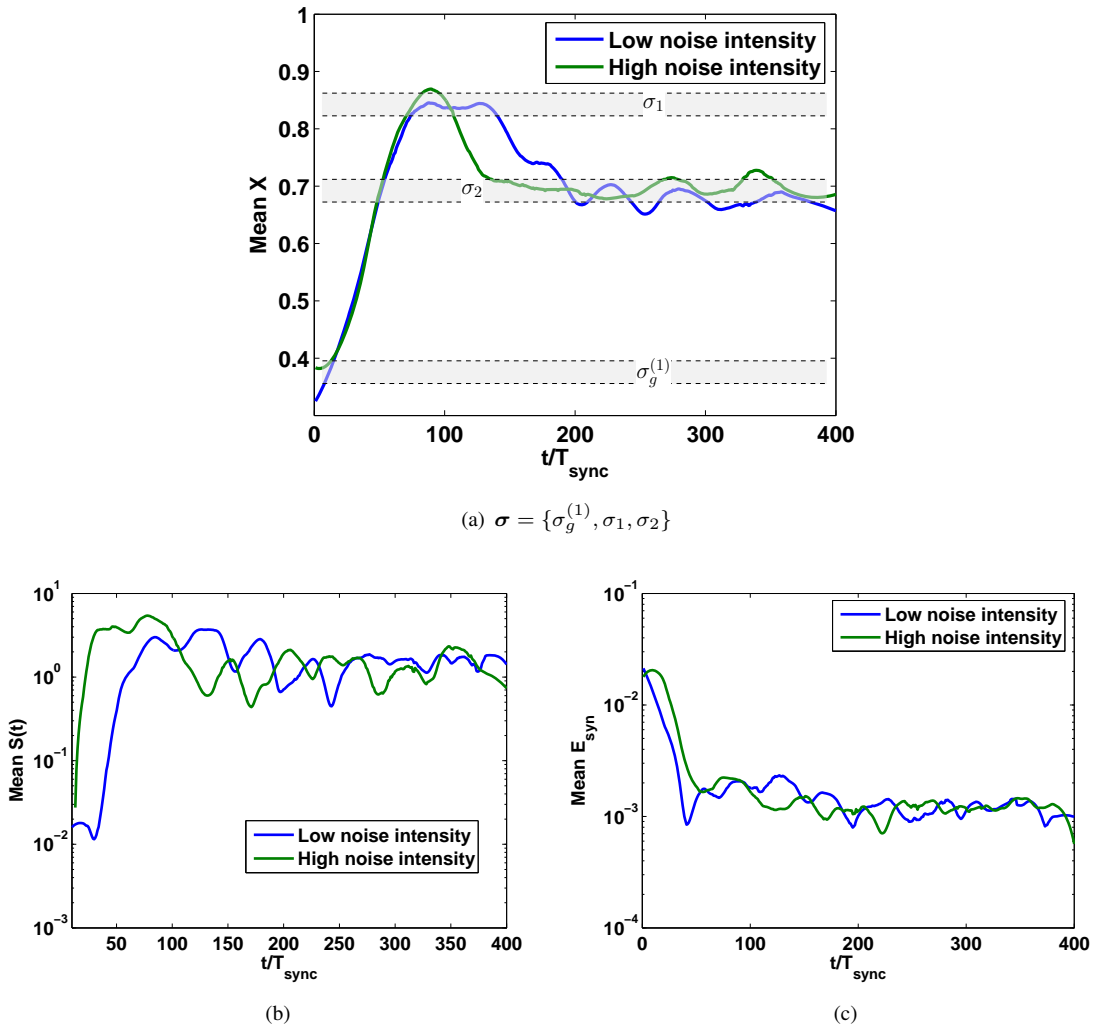
are shown in Fig. 9.6(a), the lines after the starting state reach for a level of synchrony similar to those demonstrated with the standard noise level (see Fig. 9.5(a)) and then drop to a lower level of synchrony. With the higher noise level it is expected to experience lower synchrony levels because the higher noise intensity decorrelates the firing patterns. However, the same synchrony levels are achieved with both the higher and the lower noise intensities. This suggest that a synchrony level (a synchrony state) represents the network's response to the information content as well as to the temporal features embedded within the inputs. With both noise intensities the internal dynamics  $\bar{S}(t)$  and  $\bar{E}_{\text{syn}}$  of the network are shown in Figs. 9.6(b) and 9.6(c) respectively. The time evolutions of the synaptic strengths using the different noise intensities show the establishments of strong excitatory synaptic dynamics similar to the case of using the standard noise level. Furthermore, the time evolutions of the synaptic energy alike the previous case with standard noise intensity drops to lower levels of synaptic energy as the network sustains a new level of synchrony.

Another case is investigated to elucidate the influence of noise intensity on the network behaviour. The simulation epoch is split into two parts: The first part spans over the first 200 simulation episodes and the second is the rest of the simulation episodes. The low and high noise intensities are applied in an interlaced manner along the simulation. By this sequence, during the first part of the simulation the low noise level is fed to the network while the high noise level is fed during the second part of the simulation. The simulation is repeated with the before sequence of inputs is reversed. The results of these simulations are illustrated in Fig. 9.7. First to be observed from Fig. 9.7(a) is that the time evolutions of the detected synchrony levels are different from all previous shown levels. The line correspond to the Low-High sequence reports a synchrony level that is below the synchrony level reported in Fig. 9.5(a). Although this level is similar to the levels in Fig. 9.6(a) but on a different course, the detected level in Fig. 9.7(a) does not experience the



**FIGURE 9.5:** Internal network dynamics (eight neurons) along the search for synchrony states. (a) Mean  $X \equiv \bar{X}$  is the detected level of internal synchrony. According to this measure, the network maintains a new level of synchronous firing among the neurons. The areas between the dashed lines indicate a margin that define the detected synchrony states that form the state vector  $\sigma$  (see text for details). (b) Mean  $S(t) \equiv \bar{S}(t)$  is the average dynamic synaptic strength across the trained synapses, i.e. the feedforward synapses between the input neurons and the second layer. This mean dynamic synaptic strength is shown for the three different input spike train frequencies. (c) Similar to (b), mean  $E_{\text{syn}} \equiv \bar{E}_{\text{syn}}$  is the mean synaptic energy across all the synapses in the network. The synaptic energy is calculated according to Eq. 6.1. Subfigures (b) and (c) are semi-log plots on the  $y$ -axis.

transient increase before the final stable level. The second line corresponding to the High-Low sequence is below the synchrony level reported in Fig. 9.5(a) as well. Before the end of the second part of the simulation, the detected level of synchrony drops to a lower level of synchrony that coincides with the synchrony level of the Low-High sequence. The seek for a low level of synaptic energy is sustained as obviously seen from Fig. 9.7(b). The areas between the dashed lines in Figs. 9.6(a) and 9.7(a) indicate a margin that define and represent the synchrony states vector  $\sigma = \{\sigma_g^{(1)}, \sigma_1, \sigma_2, \}$ . The state vector in both figures coincides in terms of the corresponding levels of synchrony.

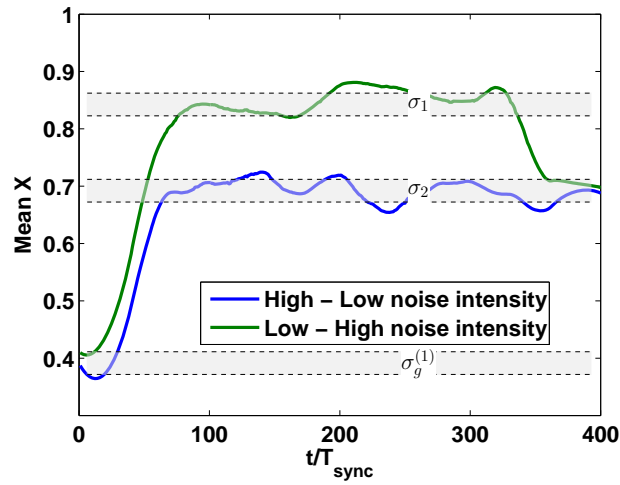
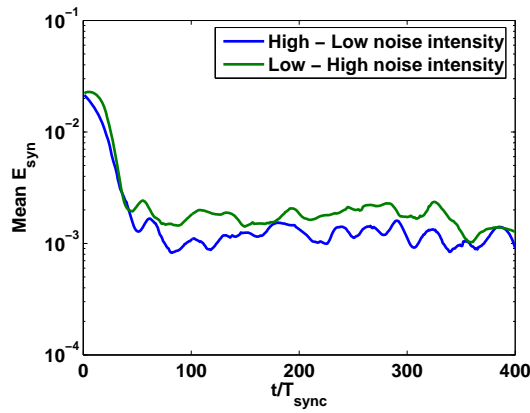


**FIGURE 9.6:** The influence of different noise levels on the eight neurons network behaviour and internal dynamics during the search for synchrony states. Two noise intensities are used instead of the standard one. These intensities are selected to be either much higher or lower than the standard one. Input frequency of spike trains is 50 Hz. (a) Mean  $X \equiv \bar{X}$  is the detected level of internal synchrony. According to this measure, the network maintains new levels of synchronous firing among the neurons. The areas between the dashed lines indicate a margin that define the detected synchrony states that form the state vector  $\sigma$  (see text for details). (b) Mean  $S(t) \equiv \bar{S}(t)$  is the average dynamic synaptic strength across the trained synapses, i.e. the feedforward synapses between the input neurons and the second layer. (c) Similar to (b), mean  $E_{\text{syn}} \equiv \bar{E}_{\text{syn}}$  is the mean synaptic energy across all the synapses in the network. Subfigures (b) and (c) are semi-log plots on the  $y$ -axis.

## 9.7 Discussion

### 9.7.1 Synchrony States and Energy Levels

The basic results about synchrony levels and corresponding synaptic energy reported for Figs. 9.3(a), 9.4(a), 9.5(a) and 9.5(c) report major findings from the thesis at hands. These illustrations are obvious evidences that synchrony states are achievable and that the synaptic dynamics


 (a)  $\sigma = \{\sigma_g^{(1)}, \sigma_1, \sigma_2\}$ 


(b)

**FIGURE 9.7:** The influence of successive different noise levels on the eight neurons network behaviour and internal dynamics during the search for synchrony states. Two noise intensities are used in sequence. These intensities are selected to be either much higher or lower than the standard one. Input frequency of spike trains is 50 Hz. (a) Mean  $X \equiv \bar{\mathcal{X}}$  is the detected level of internal synchrony. According to this measure, the network maintains new levels of synchronous firing among the neurons. The areas between the dashed lines indicate a margin that define the detected synchrony states that form the state vector  $\sigma$  (see text for details). (b) Mean  $E_{\text{syn}} \equiv \bar{E}_{\text{syn}}$  is the mean synaptic energy across all the synapses in the network. Subfigure (b) is a semi-log plots on the  $y$ -axis.

from the MSSM follow the energy profile proposed before in Ch. 6. The network behaviour elucidates a definite discrete set of states  $\sigma$ . These results are the first implementation of synchrony states within SNN which is achieved here due to the computational capabilities inherited through the dynamics of the MSSM.

Studying Fig. 9.6, the influence of the noise on the detected synchrony and the network dynamics has revealed important observations. Although the detected synchrony levels are different from those reported with the standard noise level in Fig. 9.5(a), the internal dynamics with the low and high noise intensities have shown similar tendencies and behaviour to those tendencies and



behaviour with the standard noise intensity. Changing the information contents (via noise intensity) is reflected via maintaining different synchrony states and different courses for finding them. Meanwhile, the network follows the same path of establishing strong excitatory synaptic dynamics and finding a minimum synaptic energy operating point in both cases. This points out again that the synchrony level represents the network response to the information contents.

The first ground states  $\sigma_g^{(1)}$  is almost the same throughout all the figures of the detected synchrony.  $\sigma_g^{(3)}$  in Fig. 9.5(a) coincides with  $\sigma_g^{(2)}$  on Fig. 9.3(a). This suggest that the set of states  $\sigma$  found from all these figures characterizes this network setup (is a network property) in response to the input features embedded within the used input spike trains. Figs. 9.6(a) and 9.7(a) illustrate further important observations about binding by synchrony. In fig. 9.6(a) as the low or high noise is fed into the network, both levels of synchrony are experiencing a sort of transient increase that reaches between 0.8 and 0.9 ( $\sigma_1$ ). Then both drop to a level of 0.7 ( $\sigma_2$ ). When the noise levels are fed in sequence, one level of synchrony stays at the 0.7 ( $\sigma_2$ ) while the second one is sustained between 0.8 and 0.9 ( $\sigma_1$ ) and then drops to  $\sigma_2$ . Although it might be not clear what a certain level of synchrony implies exactly about the input information, these two illustrations suggest that the low and high noise levels represent new information contents that are differently processed within the network resulting in four different behaviours over two well defined states  $\sigma_1$  and  $\sigma_2$ .

Exhibiting these four different behaviours supports the core concept introduced in this part of the thesis: *Maintaining a synchronized firing pattern (a synchrony state) within a neural circuit or across several ones signalises both the completion of internal processing and internal representation of the information contents streamed from the input data. Such network behaviour is achievable since the MSSM equips the network with an adequate dynamic repertoire that makes such network behaviour available.* This statement is the revision introduced here to the concept of binding by synchrony. As mentioned before, the former studies that has tackled the issue of synchrony states have shown that synchronous firing is only achievable over the scale of a pair of milliseconds, see e.g. Tsodyks et al. (2000).

The complement of this concept is the answer to the open question of where is the information stored in the neural circuitry. It is widely accepted that memory formation is done within the synaptic dynamics through LTP/D (Grimwood and Morris, 2000; Whitlock et al., 2006). Furthermore, it has been shown that the representation of the information is probably done at the level of synapses rather than cells (Gilbert and Sigman, 2007). This role of synaptic dynamics is not a new concept, it is a widely accepted concept throughout the literature of the neural science starting with the revolutionary work of D. Hebb (Hebb, 1949).

Moreover, Fig. 9.4(a) and 9.5(c) are a simulation based validation and a further proof of the theoretical analysis of the synaptic energy function proposed in Prop. 6.1. In the derivation of the synaptic energy function of Eq. 6.1 a set of assumptions are made to simplify the analysis. The results from the simulations coincide surprisingly with the estimated shape of the synaptic energy time evolution while searching for a stable low energy level operating point, see Fig. 6.1(a). In

relation to this, building strong excitatory synaptic connections using the MSSM dynamics in parallel to sustaining a network synchrony state adds to the analytical evidences supporting that the MSSM is capable of inheriting the core features of the biological synapses needed for achieving this network behaviour.

### 9.7.2 Roles of Binding by Synchrony in Information Flow

A basic question emerges from the results reported in this chapter, how long is it required to sustain a synchrony level apart from the span of  $T_{\text{sync}}$  itself? For example, in Fig. 9.3(a) is it required to keep and maintain the synchrony state after exhibiting it after 150 repetitions? This question wonders actually about the role of binding by synchrony in the information processing beside being a mechanism for the binding functionality within the CNS. It discusses the next step in the flow of information and the following procedure in information processing sequence after sustaining a synchrony states. Tackling this question requires first considering the measure of detecting the synchrony state itself.

The means of detecting the level of synchrony is a major issue in the context of binding by synchrony. As mentioned before, when von der Malsburg postulated this concept at the very beginning he did not specify a measure or a methodology by which synchrony or coherence is detected and indicated. Missing a clear definition for this measure has been a major argument against binding by synchrony. The measure used in the simulations in this chapter, i.e. the mean value of maximum correlation coefficients between pairs of neuron outputs, is an analytical tool which has no biological or experimental basis. A way out from this problem has been introduced by assuming that some neural circuitries in the cortical regions might be responsible for sensing the coherence of involved neural ensembles and assemblies (El-Laithy and Bogdan, 2011c). From a pure biological point of view such way out might be even not need at all. Regardless of the hierarchical structure of the cortical areas and away from the circadian master clock (Antle et al., 2005), the brain has not a master internal clock or a macroscopic maestro that coordinates the flow of information processing and the data streaming to and from different regions (Supp et al., 2007). The control of information flow is however a logical prerequisite of multitasking to allow for data and symbol integration by the end of every information processing act. Hence, the control over information flow in the CNS ought to be performed automatically (without a bus-controller as the case in the PC's motherboard).

Back to binding by synchrony, accepting the proposition of the energy minimization as an underlying mechanism for coherent and synchronous firing is indeed a biological plausible solution for the question about the data flow control. As mentioned above in Sec. 9.2.3, sustaining synchrony replicates the situation of resonance in electrical circuits. At resonance a maximum power transfer takes place, at synchrony new information is being processed and represented based on the formerly processed pieces of information as they are stored in the current synaptic states of activity. Meanwhile, the output of the neural ensemble at synchrony carries the representation of

the processed pieces of information, i.e. these pieces of information are forwarded to the succeeding stages of processing. This description of the information processing flow is supported by the theoretical argumentation posted by Singer (Singer, 2007) that *"the cerebral cortex continuously moves from one point to the next in an inconceivable multidimensional space"*.

The information processing flow described above is then a progression through a multidimensional state space (of the network). During this progression the system continuously changes its functional structure as it is changed by the experience, from processing and representing the information content from the input, it gains over time. Thus, the system can not return to a previous experience, but it can recall it. A big difference should be observed between returning to a previous experience and recalling it. For example, the second time a certain object is visually seen it recalls a different dynamic state (or sequence of states) to the one(s) initiated at first time. The difference between two dynamic representations, according to the realization presented in this work, can be over the span of  $T_{\text{sync}}$ . Over this  $T_{\text{sync}}$ , the same firing pattern(s) or slightly altered is(are) expected.

### 9.7.3 In Comparison to the Hopfield Approach

The behaviour of Hopfield networks is based on an energy minimization concept similar to the one proposed here. The approach presented here adopts that a network tries to find energy minima in their state space, please review the introduction of Ch. 6. The Hopfield network minimizes its total energy, this has implied some limitations on this approach. These limitations are those biologically non-plausible concepts: e.g. the symmetrical nature of neural circuitry, non-graded response of synaptic representations and the fixed set of internal states (Neelakanta and DeGross, 1994). The generalized Hopfield network (GHN) proposes theoretical but yet limited analytical solutions to the first two limitations, i.e. the symmetrical nature of network and the non-grade representation of synaptic dynamics (Ma, 1999). Some other approaches are presented via the Willshaw models (Golomb et al., 1990) which are basically an extension of the Hopfield network to adopt more biologically tenable issues, e.g. stochastic asynchronous interconnectivity update of network activity. However, these approaches force restrict constraints on network connectivity (Neelakanta and DeGross, 1994). Hence, in this work a potential solution for the randomness of the internal states is presented. This is performed through the influence of noise, initial conditions and the update rule. All these factors help to relocate those expected stable point(s), as illustrated in section 6.5, and consequently the network behaviour at it (them). The inherited adaptivity of the networks originates solely from the MSSM dynamic behaviour.

One major difference between any of the aforesaid approaches and the proposed one is: Here *synaptic dynamics of the MSSM* are *solely* considered to be capable of driving the network into a synchrony state through their energy profile. This does not eliminate the role of the neuronal dynamics as explained in other studies, but rather indicates the significance of the role that can

be manifested with these synaptic dynamics as well. The margins of transition between stable synchronization and chaotic behaviour remain to be investigated.

#### 9.7.4 The State Capacity

The state(s) capacity is the expected total number of states a network can impose in general. Identifying this capacity is important to understand the real capabilities of the proposed network with the introduced synaptic model in information processing. This is not a straightforward task, selecting a certain measure of synchrony different from the one implemented in this study may reveal different levels of synchrony. For example, the resolving power of the used measure may be not able to differentiate between two levels of synchrony which are observed currently as a single level. Therefore, it is in general difficult to determine an exact estimate of the possible number of states to be expected in a certain simulation setup. Some bounds on the minimum capacity can be estimated. Following Prop.6.2, it can be shown that the minimum number of states in a network is  $\sigma_{\text{tot}} \geq 2$ .  $\sigma_{\text{tot}}$  is a function of the network structure, update rule and input variability. That means, a network has at least a dichotomous capacity of synchronous states.

The difficulty in deriving a general rule to estimate the state capacity originates basically from the fact that the available capacity of states is a varying emergent attribute for every network. According to the analysis made in this chapter, the network *experiences* these states as its own response to the input information, its structure, synaptic background noise and the inherited ability to change (via learning) its internal dynamics (synaptic dynamics). That indicates, the network does not feature a fixed set of states independent from its environment. The complexity of the network (which is described through its structure and density of interconnectivity) plays a very crucial role in setting the states capacity of the network and consequently it describes the network's computational abilities. Shortly stated, the complexity promotes computational capabilities. Although this might be viewed as a naive and logical rather than an important conclusion remark, this concept needs more attention in the light of the reported analyses and discussions so far. In order to illustrate this concept some perspectives are revised in the following chapter.

The networks used in this chapter belong to the class of dynamic networks (*DN*). These networks are those combining both biologically realistic neuronal and synaptic dynamics (dynamic synaptic models and spiking neurons) (Maass and Sontag, 2000). Such networks (independent of which level of details is incorporated in the used functional units) feature a wide range of capabilities for processing temporal and spatio-temporal patterns in a very efficient manner which is linked to the superior synaptic capabilities of the MSSM for *real-time* processing of sensory inputs. In order to illustrate these capabilities along with the issue of complexity, larger networks are seen more relevant for such investigations. This is seen doable with the MSSM that can deliver the expected biological plausibility to the network behaviour at a balanced level of complexity. These investigations are illustrated in the next chapter when the concept of binding by synchrony is investigated within the context of finite-state machines.

## 9.8 Summary

Binding by synchrony is a hypothetical mechanism that explains how the brain is able to resolve between simultaneously presented sensory information and to process them "in parallel". Although the framework of binding by synchrony is hypothetical, there is a long list of experimental and theoretical evidences that it is plausible and support adopting it as a main basic information processing procedure. Consequently this motivates importing such biological capability of information processing into dynamic neural networks (SNN with dynamic synapses). Implementing the framework of binding by synchrony within dynamic networks requires maintaining certain behaviour within the network that is characterized by synchrony states.

The ability of maintaining and exhibiting this network behaviour with synchrony states is attributed to the dynamic features of the MSSM. Former studies that have tackled the issue of temporal synchrony, stated that states of synchronous discharge among neurons within a spiking network was only sustainable for few milliseconds, for instance using the Markram-Tsodyks model as by (Tsodyks et al., 2000). Using the MSSM and regarding the results reported in this chapter based on the energy based concept from Ch. 6, the entire framework of binding by synchrony is seen not only as working but as "well and alive". Dynamic networks using the MSSM are able to sustain the synchronous behaviour and to implement the concepts of synchrony states. The discussions of the role contributed by synchrony states in the information flow among neural circuitries seems plausible and practical. It suggests that binding by synchrony performs a sort of control over the information flow beside being the means of distinction between overlapped internal representations within a neural ensemble. All the reported results and suggested concepts are in agreement with the accumulated theoretical and experimental evidences supporting the plausibility of the binding by synchrony mechanism.



# Chapter 10

## Temporal Finite-State Machines

*"Brain: an apparatus with which we think we think"*

Ambrose Bierce

### 10.1 Introduction

The presented topics so far indicate that a proper modelling of synaptic dynamics allows for reliable emulation of the experimentally observed mechanisms that underpin the behaviour of biological neural circuitries. This is shown on the level of a single connection as a single synapse to a single neuron in Ch. 5. The optimized MSSM allows a reliable simulation of the postsynaptic activity of a thalamic neuron in the visual cortex. The extent of added values from such a proper synaptic modelling is then explored on a network level in Ch. 9 using the learning framework from Ch. 8. In Ch. 9 and following the theoretical analyses reported in Ch. 6, it is shown that a dynamic network that uses the MSSM is able to represent the input sensory information internally as a definite set of discrete synchrony states. Furthermore, an important ensuing remark emerges from the previous chapter: A group of neurons experiences a synchrony state in response to the input information. This group of neurons switches to another state of synchrony upon receiving new input information. This switching mechanism among states suggests that the information processing within this group of neurons is a biological implementation of the classical automata or the famous finite-state machines (FSM).

One of the notable theoretical discussions that analyses the differences between the general Turing machines (TM) and FSM when considering the brain was presented by van der Velde in (van der Velde, 1993). It has been shown that neural systems that are arranged in networks are definitely a class of FSM but not a TM. It was discussed that TM represent an idealization of this class of state machines, because the TM by definition should incorporate infinite memory capacity and more important an infinite state space (Koch and Tononi, 2008). This infinite capabilities are not logically accepted to be describing a biological cognitive system; in spite of the essence of

extreme variability and productivity recognized in the cognitive behaviour. Thus, a question can be formulated: How can a neural system, either biological or artificial, with a real finite physical state space be related to the infinite cognitive state space? The simplest answer is that each existing physical representation in the network should be able of the perception and the delivery of more than one behavioural or cognitive action, i.e. real-time multitasking (van der Velde, 1993; van der Velde and de Kamps, 2006). This implies that the same physical system (here to be an artificial neural network) carries out implicitly multiple computational tasks within the same activity period that corresponds to a certain input. That is, different outputs can be simultaneously processed out from the same system status.

Multitasking can be redefined in the context of binding by synchrony with the existence of more than one subset of neurons that can independently represent the input information as definite sets of discrete synchrony states. Having this diversified parallel processing of information within the same neural network, multiple readout functions can be processed to produce different target outputs from the same input information and in real-time. Parallel to the framework of binding by synchrony, some preliminary work has been made to investigate the concept of multitasking by introducing the computational model of liquid-state machines (LSM) (Maass et al., 2002; Natschläger and Maass, 2002). The cited studies have shown that a dynamic network is able to process input information and to generate multiple outputs via a set of readout maps (relatively smaller and less complex networks). These maps reprocess the internal activity of the network.

The following sections review the work of the LSM and discuss its aspects of computational power. Afterwards, the basis of the proposed novel class of FSM is introduced using the MSSM-based framework of binding by synchrony, the novel proposed class is referred to as the temporal FSM (tFSM).

### 10.2 Liquid State Machines

Taking the feature of "multitasking" as a key property, liquid-state-machines (LSM) proposed by W. Maass (Maass et al., 2002) present an abstraction of the possible techniques used in the biological organism to *compute*<sup>1</sup>. This class of state-machines accounts for time as a major factor in representing inputs and obtaining responses. The term *liquid* in this context refers to two main issues: First, the relation to biology, and second that the collective (overall) physical state changes during the continuous presentation of the input (Maass and Markram, 2004). The general framework and implementation of the LSM have shown that multitasking is achievable within LSM (Maass et al., 2002). Fig. 10.1 shows a simplified illustration of a single recurrent network arranged in a column was used as a core engine that processes certain input spike trains. The activity

---

<sup>1</sup>The framework of the LSM is the other pioneering reservoir computing method, developed independently from and simultaneously with the Echo-state networks (ESN) that utilize the same concepts and setup (Lukoševičius and Jaeger, 2009). ESN were developed to promote the training algorithms for recurrent neural networks and were not targeting the biological tenability with the computations in the brain.



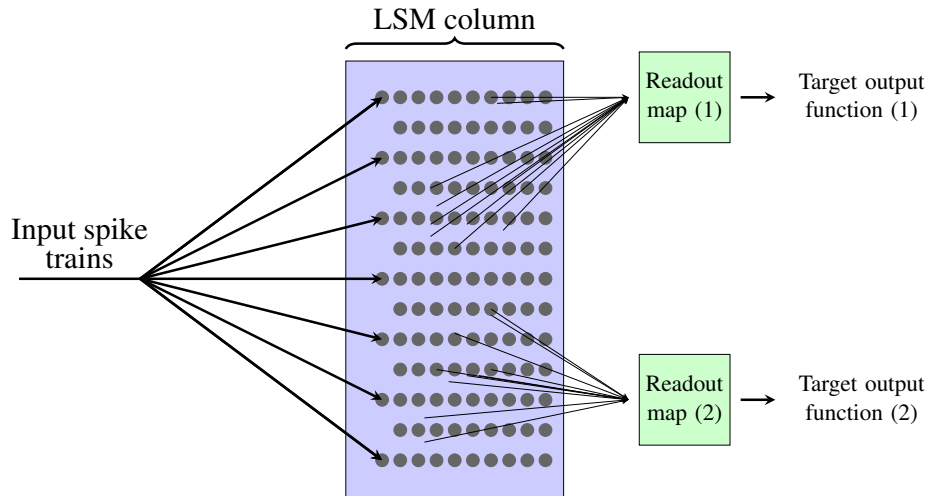


**FIGURE 10.1:** Overview of the LSM concept. The gray dots represent neurons (nodes) and the nodes are randomly located in the figure for the sake of illustration (it is supposed to be a column structure), their relative positioning and number is irrelevant. For clarity, synaptic connections are omitted and only two readout maps are shown. This illustration applies for all variations of reservoir computing. Input spike trains are fed to certain input neurons. The rest of the network (all nodes) process these inputs. The readout maps read the activities from certain groups of neurons and process it further to generate the required target functions.

of this column is then read from a number of side networks (readout maps). Each readout map is trained for a specific task. All the readout maps get their inputs from the same pool of computations which is the LSM column (but not strictly from the same neurons) and transfer this activity to different responses (Maass, 2007; Maass et al., 2002). This implementation reveals many issues, mainly that mapping from an infinite state space to the finite physical state space is achievable provided that enough transformation side systems (readout maps) are available.

Although there are some limitations and setbacks with the approach of the LSM that are discussed below, LSM materialize many issues into concrete implementable forms and methodologies (Maass and Markram, 2004; Maass et al., 2002). LSM allow to benefit from the wide range of already available models of dynamic synapses and spiking neuronal models. It has been shown mathematically (Maass and Markram, 2004) that the implementation of LSM with various computational representation does not alter the main properties of the LSM (e.g. multiprocessing and multitasking abilities), but may affect the computational power of the system. The computational performance of the LSM-based systems in general was analysed mathematically in (Maass and Markram, 2004) based on the work of (Maass and Sontag, 2000; Natschläger and Maass, 2002).

### 10.2.1 Computational Performance of LSM

The idea behind LSM is to construct a dynamic network that process the input information and in parallel there are certain readout maps (other networks) that take the internal network activities as input in order to generate predefined targeted outputs. The readout maps read their inputs from the computing reservoir found within the basic network. As for reservoir computing, the framework

of LSM is similar in terms of the approach to the simultaneously and independently developed concepts of Echo-state networks (Jaeger, 2001; Lukoševičius and Jaeger, 2009; Schrauwen et al., 2007). The main difference between them is that LSM use more sophisticated and biologically realistic models of spiking neurons and dynamic synaptic models in the reservoir. It has been shown that this difference from other reservoir computing approaches enables LSM to be superior to other approaches when the input information (i.e. the input signals) have complex temporal and statistical features, e.g. speech data (Verstraeten et al., 2007).

It was argued that the computational performance of LSM is characterized (as necessary and sufficient) through two macroscopic properties: the separation property (SP) and the approximation property (AP) (Maass and Markram, 2004; Maass et al., 2002). SP, on one hand, reflects the ability of the system to process two different inputs in two different ways that brings two different outputs. The difference between the outputs represents the ability of the system to separate between the inputs, this corresponds to the resolving power of the LSM. In other words, if the system perceives the differences between two different inputs, the response of the system to these inputs shall be dissimilar. The elastic description of being different is not restricted by definition to certain signal property, however, it is taken by convention to be related to the timing and statistical properties of the signal either to be input or output one. AP, on the other hand, addresses the ability of the system via the readout maps to transform its internal activities into predefined outputs. Thus, AP is more related to the required multiple tasks that are to be defined for each read-out map, while SP describes an *intrinsic* property in the LSM since it is solely dependent on its internal *perception* of the input.

The computational performance of LSM specifically and all reservoir computing approaches in general is a widely debated issue (Lukoševičius and Jaeger, 2009; Schrauwen et al., 2007). Some basic analyses have argued that dynamical systems achieve optimal computational capabilities if their dynamics operate on the "edge of chaos". Edge of chaos as a term refers to the transition boundary between order and chaos. However, it has been shown that the region of best computational performance should depend on the task to which the network performs (Legenstein and Maass, 2007). And that in the specific case of LSM (and consequently for the LSM-based approaches) the separation property is a more suitable quantitative measure for evaluating the computational performance of a neural microcircuit. Thus, only SP and the involved computational power of the network are considered in the presented work, AP and readout maps-related computational aspects are briefly discussed in the next chapter and left for future work.

In the next sections the basic mathematical foundation of LSM is presented. Namely, it is the computational model of the dynamic networks (*DN*). In relation to this, the class of networks with the MSSM proposed in investigating binding by synchrony belongs to the class of dynamic networks as well. Therefore, the MSSM-based framework of binding by synchrony is attached to the mathematical foundation of *DN* in order to formulate a novel and more powerful understanding about their computational power.

### 10.3 Dynamic Networks

The LSM as well the novel computational model (to be proposed below) belong to the class of  $DN$ . This class of networks features a set of different and more enhanced properties than those attributed to the classical ANN or even to the SNN. It is important however to review some basic mathematical notation before discussing either these features or discussing the advantages and the limitations of the LSM. The definitions and mathematical formulations here are based on the cited papers from (Maass et al., 2002; Maass and Sontag, 2000) but are not adopted from these papers. Unless the formulations are referred to certain references, the formulations are developed for the sake of this thesis.

**Definition 10.1.** The class of dynamic networks  $DN$  is the networks that combine biologically realistic synaptic and neuronal dynamics. For a dynamic network  $\mathcal{N} \in DN$ , the input is an input function  $u(\cdot)$  and the value of this input function at any time  $t$  is  $u(t)$ . This dynamic network implements an operator  $\mathcal{F}$  applied to the input function and performs the mapping to a set of output functions  $\mathbf{y}(\cdot)$ , the size of the output functions set is the number of neurons in the core network excluding the input ones. A subset  $k$  of the output functions can be mapped to another output function  $z(\cdot)$ .

Mathematically, Def. 10.1 can be formulated for a dynamic network  $\mathcal{N}$ :

$$\begin{aligned} \mathcal{F} : u(\cdot) &\mapsto \mathbf{y}_{\mathcal{N}}(\cdot); \text{ where } (\mathcal{F}u)(t) \rightarrow \mathbf{y}_{\mathcal{N}}(t), \\ \text{and there is } \mathbf{y}_k(\cdot) &= \{y_1(\cdot), \dots, y_k(\cdot)\} \\ \text{where } \mathbf{y}_k(\cdot) &\in \mathbf{y}_{\mathcal{N}}(\cdot), \text{ and } \mathbf{y}_k(\cdot) \mapsto z(\cdot), \end{aligned}$$

where  $\{y_1(\cdot), \dots, y_k(\cdot)\}$  are the time varying outputs of a *subset of neurons*  $k$  in the network  $\mathcal{N}$ .

It is important to notice that in the computational model of  $DN$ , there is no output layer in the network. All the neurons in the main column (except those input ones) can be involved in transferring the network activities to the readout maps. This is different from the classical definition of ANN as mentioned in Sec. 3.3. The merit and importance of such model are clarified in the following sections.

Based on the mathematical analyses in (Boyd and Chua, 1985) it has been proved that such a network can approximate any arbitrary given time-invariant operator with fading memory (See App. C)  $\mathcal{F}$  (Maass and Sontag, 2000; Natschlager et al., 2001). Mathematically, this implies that  $\mathcal{F}$  can be approximated by a dynamic network  $\mathcal{N} \in DN$ , i.e. for any  $\epsilon > 0$  there exists some  $\mathcal{N} \in DN$  such that  $|(\mathcal{F}u)(t) - \mathcal{N}u(t)| < \epsilon$  for all  $t \in \mathbb{R}$ . Differently stated, the dynamic network  $\mathcal{N}$  can approximate any nonlinear function  $\mathcal{F} : \mathbb{R} \rightarrow \mathbb{R}$  that can be parametrized as a sequence of (finite or infinite) Volterra series (Boyd and Chua, 1985). Accepting that cortical circuitries perform, in an abstract way, a set of dynamic nonlinear computations, the mathematically proven computational ability of  $DN$  suggests that a dynamic network that is complex enough is able

to emulate the computational power of a cortical circuit; specifically provided that the synaptic and neuronal models can reliably mimic the essence of the required information processing power. Besides, the computational power of the  $DN$  is related to the cortical columns due to the similarity of structure, both feature a central column of computational nodes and lateral connections to side readout maps (networks).

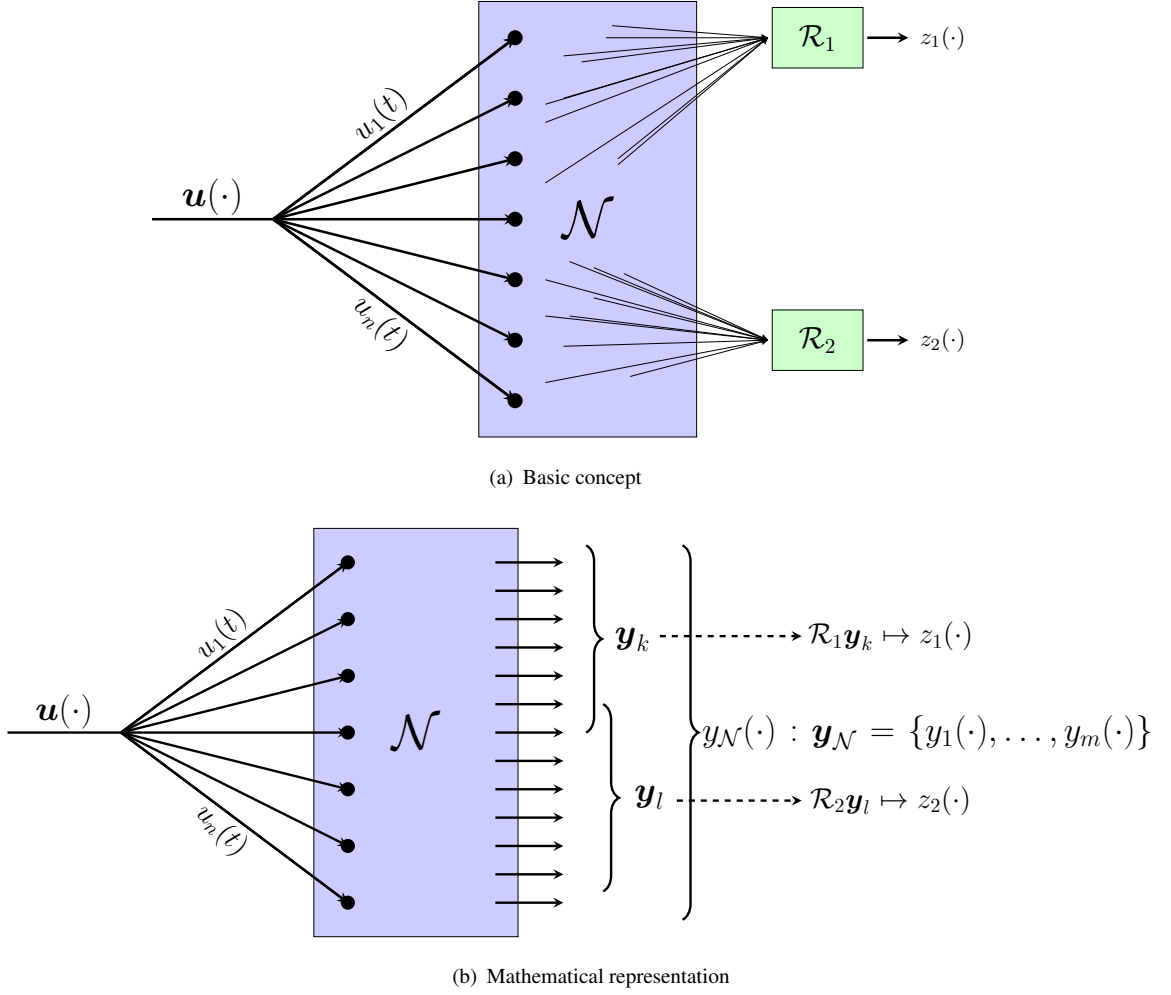
Till this point the network takes a single temporal pattern (a spike train) as an input. For a multi-input temporal patterns, the input functions are then a set of continuous functions  $\mathbf{u}(\cdot) = \{u_1(\cdot), \dots, u_n(\cdot)\}$  and  $\mathbf{u} \in U^n$  where  $U$  is a class of uniformly bounded input functions. Hence the operator  $\mathcal{F}$  performs the mapping  $\mathcal{F} : U^n \rightarrow \mathbb{R}^{\mathbb{R}}$  (where  $\mathbb{R}^{\mathbb{R}}$  is the class of all functions from  $\mathbb{R}$  into  $\mathbb{R}$ ). It still holds that  $\mathcal{F}$  can be approximated by a dynamic network  $\mathcal{N} \in DN$ , i.e. for any  $\epsilon > 0$  there exists some  $\mathcal{N} \in DN$  such that  $|\mathcal{F}\mathbf{u} - \mathcal{N}\mathbf{u}| < \epsilon$  for all  $\mathbf{u} \in U^n$ , see (Maass and Sontag, 2000) for more details. Having multiple inputs to the network empowers the network with more internal representations about the input which should enhance the network's capability of having more readout maps representing more target functions.

Fig. 10.2(a) gives a simplified schematic of the setup of a network that implements the LSM approach as a dynamic network. The readout maps are other side networks. These networks receive their inputs from groups of neuron within  $\mathcal{N}$  and implement simpler operators on these inputs. By definition, overlap between the neuron groups is allowed. A more detailed mathematical illustration of the computational model is given in Fig. 10.2(b).

## 10.4 Binding by Synchrony within Dynamic Networks

From the above a dynamic network can perform a very wide class of computations that are required to generate a certain set of intermediate representations of the input which is the network activity ( $\mathbf{y}_{\mathcal{N}}(\cdot)$ ). This network activity is so rich with information about the inputs that any other related output function ( $z(\cdot)$ ) can be generated from it. This perspective does not force the network itself to approximate the target output function  $z(\cdot)$ . Instead, the network explores all the information contents from the input and hold these internally represented contents onto the network activity. The target function then needs a simpler system than the network to read a subset from the network activity and to transfer it to the target output. This framework is inspired from the cortical columns (Maass and Sontag, 2000).

Two important remarks follow the above description of the dynamic networks and their computational abilities. First, according to the computational model described for the  $DN$ , a dynamic network stores its own representation about the input using its synaptic dynamics and this internal representation can be extracted using the activities of neurons within this network and transferred to external systems. In view of that, the computational ability of the  $DN$  which is based on a rigorous mathematical foundation supports the independently and theoretically developed statement



**FIGURE 10.2:** Schematic illustration of the basic concept of all reservoir computing approaches including LSM in (a) and with more mathematical details in (b). In these illustrations  $\mathcal{N}$  is the dynamic network or the computational reservoir (sometimes referred to it as neuronal bank or LSM engine). The whole network activity is stored in the vector  $\mathbf{y}_{\mathcal{N}}$  with  $m$  output functions where  $m$  is the number of neurons in the dynamic network. And at any time  $t$ , the network activity is  $\mathbf{y}_{\mathcal{N}}(t)$ . Only two readout maps are shown here for clarity. These maps are illustrated as boxes in (a) and as dashed arrows originate from the subset of neurons from which the map takes its inputs in (b). For two subsets of neural activities  $\mathbf{y}_k$  and  $\mathbf{y}_l$  there are two readout maps (networks)  $\mathcal{R}_1$  and  $\mathcal{R}_2$  that produce two target functions  $z_1(\cdot)$  and  $z_2(\cdot)$ . In (a) and (b) the neurons (nodes), except the input ones, are omitted for clarity.

from Ch. 9: the network activity is the network's internal representation of the input information, this internal representation defines the synchrony states.

Second, from the above features about dynamic networks the network output can lead to a function  $z(\cdot)$  for each specific subset  $k$  of neurons in  $\mathcal{N}$ . This agrees in principle with the main postulate from binding by synchrony (Ch. 9): *a group of neurons* experience a certain level of synchrony when *certain input information is processed* and when this group of neurons has a reliable internal representation of the input information on the synaptic dynamics among this group.

Therefore, in this thesis the paradigms of binding by synchrony and the analyses of dynamic networks are merged to construct, first, a novel understanding about the computational capacity

in the light of both frameworks (explained in this section). Second, this merge between the two frameworks is the basis of introducing the novel computational model of finite-state machines (explained afterwards).

As for the understanding of the computational capacity, the capacity of states (the cardinality of the states vector) within a group of neurons within a dynamic network reflects, thus, the computational power of this specific group in exploring the information contents of the input stream. The readout map connected to this groups benefits from this inherited computational power. This computational power indicates the ability to fully represent the input information internally within this group of neurons on the involved synaptic dynamics. The computational power of the dynamic network  $\mathcal{N}$ , however, is related to the ability to hold simultaneously other target functions which requires a parallel formation of other neuronal assemblies (groups). Thus, the following corollary is presented in this work to complement the mathematical derivations reported in (Maass et al., 2002; Maass and Sontag, 2000) about the computational power of  $DN$

**Corollary 10.2.** *The computational power of a dynamic network  $\mathcal{N} \in DN$  is determined through its capacity of real-time multitasking: the number of the possible simultaneous neuronal assemblies that bound by synchrony. The states capacity of any subset group of neurons  $k$  in the dynamic network  $\mathcal{N}$  is only an indication of the computational power of this specific neural assembly. The capacity of states of the subset  $k$  reflects the capability of this neural assembly to compute a certain target function from the available input information within the dynamic network  $\mathcal{N}$ .*

**Remark** Hence, the computational power of a dynamic network  $\mathcal{N}$  is a two dimensional quantity or a spatio-temporal property. The spatial dimension represents the possible number of independent neural assemblies, i.e. the spatial resolution of processing within the network. The temporal dimension is its temporal resolution that gives the possible number of states sustainable within each assembly in the dynamic network in response to specific input information. See Fig. 10.3 for a better visualization of this concept. Therefore, it is logically to accept that the computational power is task specific, as the temporal resolution depends on the input information. Although this remark is theoretically developed in this thesis, it agrees with the conclusions from (Legenstein and Maass, 2007) where it has been shown that the computational power of a class of dynamic networks is related to the task in terms of the inputs and the required outputs. To put this concept in a nutshell, the computational power can be quantitatively indicated by the capacity of possible neuronal assemblies and the state capacity of each assembly.

A synchrony state signals the formation of a neuronal assembly that implements a certain implicit function. According to Cor. 10.2, the role of synaptic dynamics imported with the MSSM in the implementation of dynamic networks gets more important. The formation of neuronal assemblies is achievable only when the synaptic dynamics are up to the required variability and flexibility as performed with the MSSM. The variability and flexibility within the synaptic model

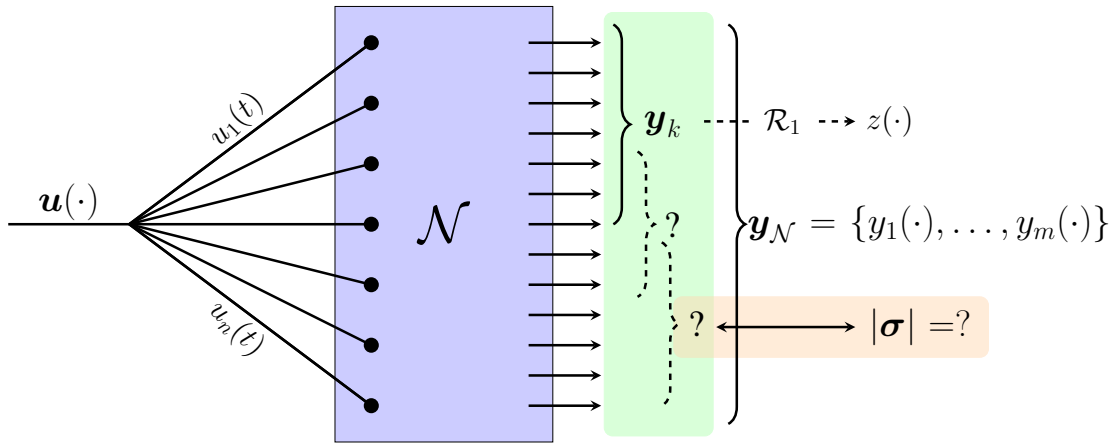


**FIGURE 10.3:** Schematic illustration of the novel computational power concept of the dynamic network  $\mathcal{N}$ . The whole network activity is stored in the vector  $\mathbf{y}$  with  $m$  output functions. And at any time  $t$ , the network activity is  $\mathbf{y}(t)$ . The dashed arrow indicates the mapping from a subset of neurons (a neuron assembly) into a target function  $z(\cdot)$ . The dashed braces indicate the question of how many neural assemblies can be formed within  $\mathcal{N}$ . The existing assembly  $k$  and the unknown ones represent the first (spatial) dimension in the computational power of the network. The size of the states vector within any assembly (the states capacity of this specific neural assembly) represents the second (temporal) dimension involved to describe the computational power of the dynamic network.

are needed to allow for the overlap (sharing) between different groups of neurons within the same dynamic neural network.

Cor. 10.2 supports the biological relevance and plausibility of both the usage of MSSM into the framework of dynamic networks specifically and the significance of the framework of dynamic networks in general. The theoretical need for multitasking to explain the biological computational capabilities from the work of van der Velde (van der Velde and de Kamps, 2006) agrees with the postulates presented in Cor. 10.2 based on the synchrony states framework of computations; this framework is achievable via implementing the MSSM. Implementing the concept of multitasking through the formation of simultaneous groups of neurons within a network has a biological basis following the analysis made to the brain circuitry in a behavioural context, see e.g. (Gilbert and Sigman, 2007) for a review. These analysis emphasised that a cortical area performing one function (computation) does not eliminate the ability for performing simultaneously entirely different function(s), or at least to carry some information that is related to other function that this area can perform. This implies that the representation of sensory information is made on "as needed-basis" that is reflected through the switching between appearing/disappearing cell assemblies throughout the same cortical area. And the representation of sensory information is done "at level of synapses rather than cells" (Gilbert and Sigman, 2007) which highlights the contribution of the MSSM in implementing such internal representation of the input information.

### 10.4.1 The Separation Property

For the SP, it measures the distances between the network activities in response to two inputs that are slightly different from each other. For two sets of input spike trains  $u(\cdot)$  and  $v(\cdot)$ , the corresponding network activity at any time  $t$  from Fig. 10.2(b) is  $\mathbf{y}_{\mathcal{N}}^u(t)$  and  $\mathbf{y}_{\mathcal{N}}^v(t)$  respectively. According to the notation used in (Maass and Markram, 2004; Maass et al., 2002), these network activities at a single time instant were referred to as network states. In order to avoid ambiguity with the formal definition of state used in this thesis and the one used by (Maass et al., 2002),  $\mathbf{y}_{\mathcal{N}}^u(\cdot)$  and  $\mathbf{y}_{\mathcal{N}}^v(\cdot)$  are referred to as the network activities and not as states. The average distance  $\|\mathbf{y}_{\mathcal{N}}^u(t) - \mathbf{y}_{\mathcal{N}}^v(t)\|$  between these activities is recorded then as time series (function of the time  $t$ ) after the onset of the input, where  $\|\cdot\|$  denotes the Euclidean norm.

In the following section there is a comparison between the performance of the basic LSM approach presented in (Maass et al., 2002) and the implementation using the MSSM in terms of the SP. According to the merged paradigm between binding by synchrony and LSM introduced in Sec. 10.4 implementing the MSSM for the LSM should reveal much more computational capabilities. The implementation of the LSM approach using the MSSM introduces the novel LSM-based computational model of the temporal FSM (tFSM). From Sec. 10.4, the tFSM framework should promote the computational capabilities of the LSM and overcome the limitations of the computational model of the LSM (explained in Sec. 10.5.1 after reporting the LSM results). The following section illustrate the simulations of the tFSM framework. The focus of the work at this point is to explore the basic computational power of the dynamic network regardless of which application is in mind.

## 10.5 Simulations

### 10.5.1 Results and Limitations of LSM

Similar to the setup reported in (Maass et al., 2002) the network setup is a column of 135 neurons. They are randomly connected in a single column. Neurons (20% of which are randomly chosen to be inhibitory) are located on the grid points of a 3D grid of dimensions  $3 \times 3 \times 15$  with edges of unit length, see Fig. 10.4(a). Regarding the connectivity structure (not shown in the figure for clarity), the probability of a synaptic connection from neuron  $a$  to neuron  $b$  (as well as that of a synaptic connection from neuron  $b$  to neuron  $a$ ) is defined as  $A \cdot e^{-(D(a,b)/\lambda)^2}$ , where  $\lambda$  is a parameter that controls both the average number of connections and the average distance between neurons that are synaptically connected.  $D(a, b)$  is the Euclidean distance between neurons  $a$  and  $b$ . Depending on whether  $a$  and  $b$  are excitatory ( $E$ ) or inhibitory ( $I$ ), the value of  $A$  is 0.3 ( $EE$ ), 0.2 ( $EI$ ), 0.4 ( $IE$ ) and 0.1 ( $II$ ) (Maass et al., 2002).

In (Maass et al., 2002) the neurons were modelled as LIAF units and the synapses were implemented using the Markram-Tsodyks model. Fig. 10.4(b) illustrates the distances between network



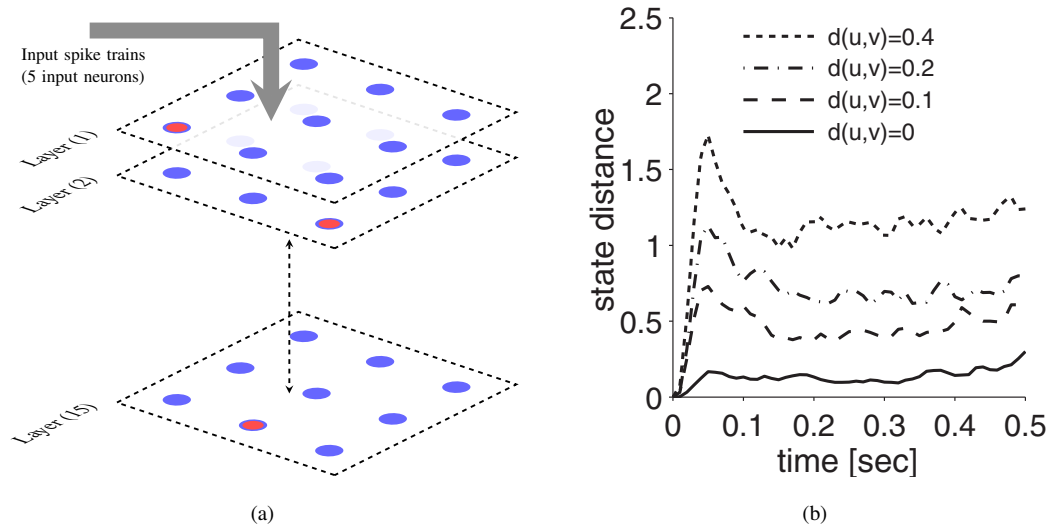


**FIGURE 10.4:** (a) Schematic of network setup. The neurons are arranged in 15 layers, each layer has nine neurons (as a  $3 \times 3$  grid). Blue circles represent excitatory neurons while those with red cores indicate inhibitory neurons (20% of excitatory ones). The synaptic connections among neurons are omitted for clarity. This column is the implementation of the dynamic network  $\mathcal{N}$  represented with the light blue rectangles in Figs. 10.1–10.3. (b) Average distance of liquid states for two different input spike trains  $u$  and  $v$ . The state distance increases with the distance  $d(u, v)$  between the two input spike trains  $u$  and  $v$ . Plotted on the  $y$ -axis is the average value of  $\|\mathbf{y}_{\mathcal{N}}^u(t) - \mathbf{y}_{\mathcal{N}}^v(t)\|$ . This subfigure is copied from (Maass et al., 2002) with permission from MIT Press.

activities corresponding to two input functions  $u(\cdot)$  and  $v(\cdot)$ . The plotted results for the values 0.1, 0.2, 0.4 of the input difference  $d'$  represent the average over 200 randomly generated pairs  $u$  and  $v$  of spike trains such that  $|d' - d(u, v)| < 0.01$ . In this implementation  $\lambda = 2$ . In order to define the distance  $d(u, v)$  between two spike trains  $u$  and  $v$ , each spike is replaced by a Gaussian function. To be precise,  $u$  and  $v$  are convolved with the Gaussian kernel<sup>2</sup>  $\exp(-(t/\tau)^2)$  where  $\tau = 5$  msec and  $d(u, v)$  is defined as the distance of the resulting two continuous functions in the  $L_2$ -norm (divided by the maximal lengths 0.5 sec of the spike trains  $u$  and  $v$ ).

By studying Fig. 10.4(b), these curves show that after the first 30 msec the difference in network activities (termed liquid states in (Maass et al., 2002)) is roughly proportional to the distance between the corresponding input spike trains. These curves report the separation performance of the LSM.

The setbacks and limitations of LSM are considered at this point. Surprisingly, it has been shown that increasing the density variable  $\lambda$  of the network's interconnectivity more than a certain value decreases the separation power of the network (Legenstein and Maass, 2007; Maass et al., 2002). Moreover, adding more columns in parallel that receive the same input functions results in the deterioration of the separation power of the network. In the case of multiple columns, the readout maps have reported better results (better AP) for the same target functions in comparison

<sup>2</sup>This is similar in nature to van Rossum distance explained in Ch. 8 with the difference of the filtration kernel. It is an exponential kernel in the case of van Rossum distance while it is a Gaussian function in this implementation. The approach from (Maass et al., 2002) is used in this thesis again to maintain the comparison basis.

to those reported in case of single column. The enhancement in the performance of the readout maps is a consequence of the increased diversity of internal activities of the same input information across multiple columns of neurons. Besides, the readout maps are networks which are trained to deliver the target outputs, the enhancement in performance is evidently related to the involved learning applied to the readout maps. However, the deterioration of the separation power leaves an open question about the computational power of the core engine of the LSM. The possible reasons for the limitations of the LSM are explained in the light of the performance of the tFSM in Sec. 10.6 after reporting the results from the tFSM in the next section.

### 10.5.2 Temporal Finite-State Machines

As for the novel implementation of LSM with the MSSM, this combination is termed the temporal FSM (tFSM). In the case of tFSM, an identical network structure to the one used in (Maass et al., 2002) as described above is used and the neurons are LIaF units (the neuron model parameters are:  $\tau_h = 20$  msec,  $h_{\text{rest}} = -70$  mV and  $h_{\text{th}} = -60$  mV). The differences are the synaptic implementation and the input data set since the input used in (Maass et al., 2002) is not available. The synaptic connections in the tFSM are represented with the MSSM by definition. The values of the MSSM parameters used for this simulation are arbitrarily selected as similar to the values from the first column in Tab. 6.1 (without the initial conditions for the ODE solver). The input spike trains are generated with Poisson distributed inter-spike intervals such that they have a certain overall firing frequency. The epoch of the input spike trains is 500 msec and the firing frequencies are 50–100 Hz with 10 Hz steps.

The generated input spike trains with different firing rates are injected in separate trials as input to the described network. The resulting neural activity is recorded for each of these inputs. An output, e.g.  $\mathbf{y}_{50}$  represents the time-varying network activity corresponds to the input  $\mathbf{u}_{50}$  which is the input with firing rate of 50 Hz.  $\mathbf{y}_{50}$  is equivalent to  $\mathbf{y}_{\mathcal{N}_{50}}$ ; the part  $\mathcal{N}$  of the suffix is omitted for clarity. The average distances between the inputs over 200 randomly generated pairs  $\|\mathbf{u}_i(t) - \mathbf{u}_j(t)\|$  are plotted in Fig. 10.5, where  $i, j = 60\text{--}100$  Hz with 10 Hz steps and  $i \neq j$ .  $\|\cdot\|$  denotes the Euclidean norm. The average of activity differences caused by the same spike train applied with two different randomly chosen initial conditions of the circuit is lower than 0.001 and is omitted from the plots for clarity.

Within the tFSM computational model, a *state* is defined as a stable representation of certain input information for a certain time interval longer than a pair of milliseconds in order to match the postulates of binding by synchrony, see Ch. 9 for the details. The transient stable difference between one response to a reference one indicates a kind of internal synchrony level in this response. This implies that transient stable distances represent transient internal states of synchrony. Within a state, single spikes and the absolute degree of coherence are irrelevant (von der Malsburg, 1999), only the existence of different levels informs about the information processing within the dynamic

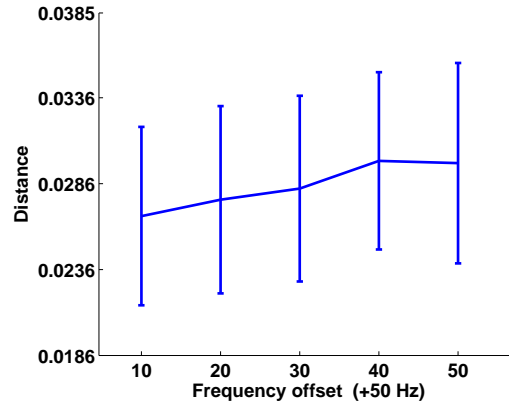


**FIGURE 10.5:** The average distances between the inputs used for the simulation of the tFSM, it is  $\|x_i(t) - x_j(t)\|$ , where  $i, j = 60\text{--}100$  Hz with 10 Hz steps and  $i \neq j$ .

network as described before in Ch. 9. Based on this concept, a specific definition of a state for the tFSM reads:

**Definition 10.3.** For the dynamic network  $\mathcal{N} \in DN$  that is characterized to belong to the class of the tFSM, for all output values  $\mathbf{y}_{\mathcal{N}}(t)$  where  $t > 0$  corresponding to the input functions  $\mathbf{u}(\cdot)$  and during the interval  $t_1 < t < t_2$ , a state  $\sigma$  is defined if  $a - \delta < \|\mathbf{y}_{\mathcal{N}}^u(t) - \mathbf{y}_{\mathcal{N}}^{\text{ref}}(t)\| < a + \delta$  where  $a$  is a constant and  $\delta$  is small.  $\mathbf{y}_{\mathcal{N}}^{\text{ref}}(\cdot)$  is a fixed reference set of output functions where  $|\mathbf{y}_{\mathcal{N}}^u| = |\mathbf{y}_{\mathcal{N}}^{\text{ref}}|$ .

Following Def. 10.3 and in order to illustrate the generation of internal states within the tFSM, the response  $\mathbf{y}_{50}$  is taken as a reference one. The activity distances of the outputs  $\|\mathbf{y}_i(t) - \mathbf{y}_{50}(t)\|$  are calculated as  $i = 60\text{--}100$  Hz with 10 Hz steps. The traces are given in Fig. 10.6(a) as a function of the time at  $\lambda = 2$ . The distances are calculated over all network activities. Basically, the network processes the different inputs in different manners. This can be clearly seen from the distances exhibited between the responses corresponding to different inputs. The distances reported for the responses vary between 0 and 0.6 (see Fig. 10.6(a)) while the distances between the input signals are found below 0.03, as shown in Fig. 10.5. The states are shown as ranges of the detected distance highlighted with shaded stripes between dashed lines and annotated with the state symbol.

Different from the results reported by Maass et al. (Maass et al., 2002) which are shown in Fig. 10.4(b), the traces of distances in Fig. 10.6(a) demonstrate that the differences in activities after the first 30 msec are not proportional to the distance between the corresponding input spike trains; see the zoomed-in captures of the first 150 msec from this plot given in Fig. 10.6(b). The activity differences form transiently stable levels are distributed in a non-uniform fashion. Recalling the randomness of both the network connectivity and the input signals, only the relative location of these transient levels to each other is relevant rather than the absolute value of the distance to  $\mathbf{y}_{50}$ . The main observation from this simulation is the set of stable levels achieved by the tFSM when the MSSM is used. By studying Fig. 10.6(b), five levels (stable parts of the lines with tiny rapid fluctuations) of activity can be counted. These levels of activities represent certain neural states

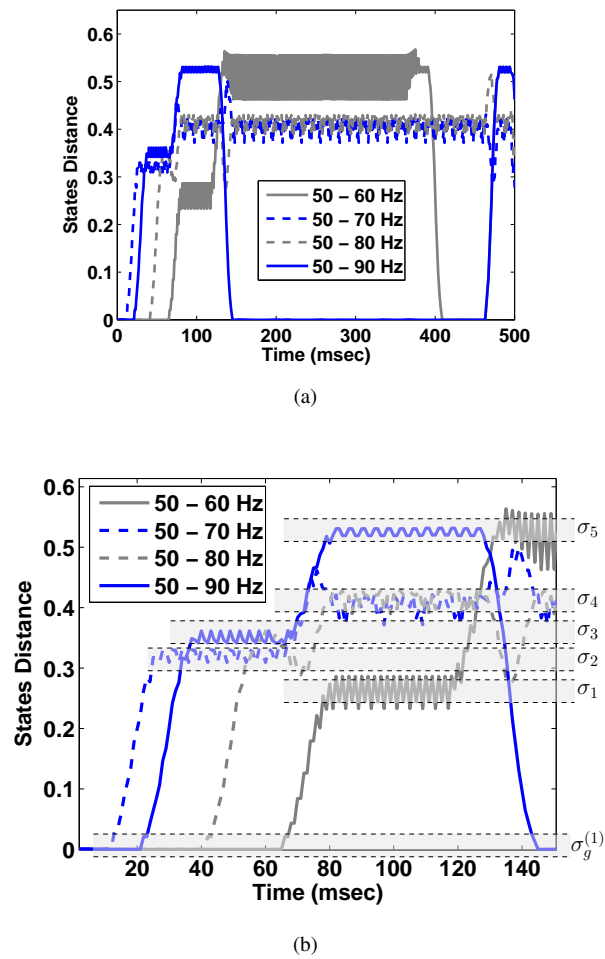


**FIGURE 10.6:** Simulation results of tFSM at  $\lambda = 2$ . (a) The time evolution of state distances  $\|y_i(t) - y_{50}(t)\|$ , where  $i = 60-90$  Hz at 10 Hz steps. (b) Zoom in of (a) for the first 150 msec. Highlighted levels indicate states, state number corresponds to the temporal sequence of appearance.

that encode input features. Moreover, each line visits different levels of distances and certain levels are commonly visited more than once over time; e.g. the distance between 0.3 and 0.4 is common between three lines, see Fig. 10.6(b).

The effect of changing the network structure (interconnectivity) on the internal representation of the information within the network is investigated as well. The whole simulation is repeated with the interconnectivity factor  $\lambda = 3$ . The results for the latter case are shown in Fig. 10.7(a) and 10.7(b). In this case, the variation and the span of the transient states change significantly. In Fig. 10.7(b), seven different levels can be clearly counted. The implications of having these states are considered in the next section.

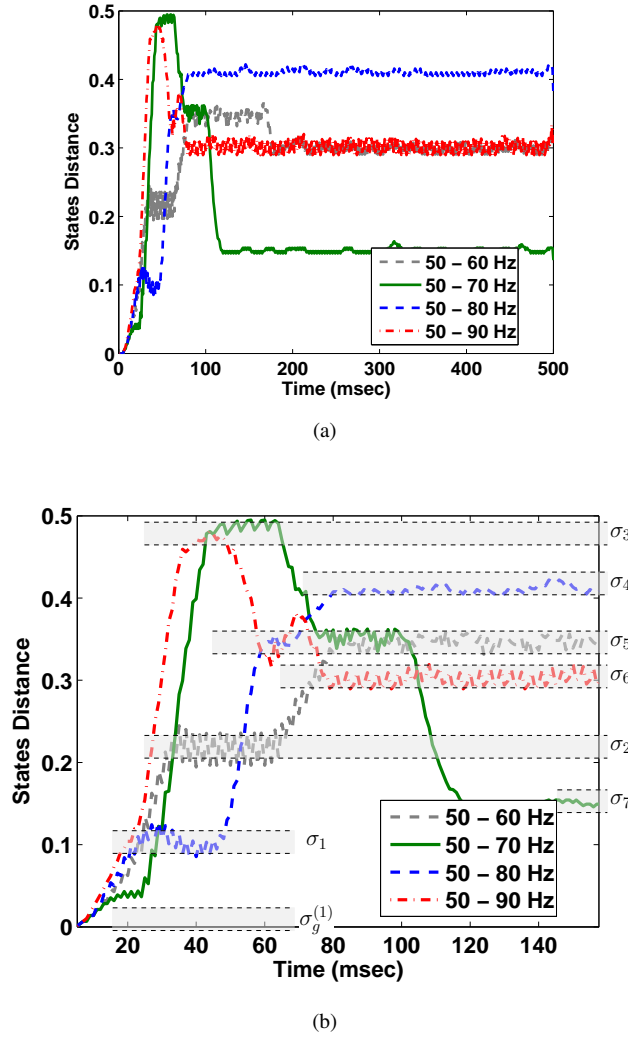


**FIGURE 10.7:** Simulation results of the tFSM at  $\lambda = 3$ . (a) The time evolution of state distances  $\|y_i(t) - y_{50}(t)\|$ , where  $i = 60-90$  Hz at 10 Hz steps. (b) Zoom in of (a) for the first 150 msec. Highlighted levels indicate states, state number corresponds to the temporal sequence of appearance.

## 10.6 Temporal Finite-State Machines vs. Liquid-State Machines

The limitations listed above in Sec. 10.5.1 about the performance of the LSM were not tackled in the literature up to the author's knowledge except in the work at hands. In order to investigate the possible reasons behind these limitations, one should consider Fig. 10.4(b) again. In this illustration the distances between the activities increase proportionally as the time of the simulation advances. This suggests that as the network performs the internal processes responsible for generating these distances, new internal representations are continuously produced. These new representations are better defined than the previous ones which results in stronger separation over time. Although this might sound attractive at first glance, this is biologically implausible. Long representation of the stimuli via sensory input channels to the CNS (visual, speech, touch, etc.)

results in the suppression of the input information due to strong depression at the preliminary input neural circuitries (Kandel et al., 1995). Cognitively, one stays aware that the stimuli are still there but their representations are never reinforced or amplified unless the inputs change. An explanation for the described behaviour of basic LSM is that it over-processes the input information. Normally, over-processing originates from the limited dynamic space of the dynamical system itself that is inherited from the functional constituents of this system (Pecora et al., 1997). This points out the influence of the limited capabilities of the Markram-Tsodyks synaptic model. Thus, the networks's internal representations are reprocessed recursively over and over resulting in this increasing distances. This might be an explanation as well for the deteriorated performance of the multiple columns arrangement.

Whereas the proposed computational model with the tFSM inherits the fundamental computational aspect from the basic LSM, it overcomes all the above mentioned limitations and setbacks. Basically the "t" in tFSM indicates the inevitable involvement of the temporal dimension as basis of defining states. Thus the tFSM is a FSM that implements the LSM using the MSSM synapses and the states are temporally coded levels of internally synchronized firing patterns. Following this definition and the from the annotated states in Figs. 10.6(b) and 10.7(b), these states along with the state transitions are the performance of the proposed novel computational model of the tFSM. These aforementioned states and state transitions reflect, in an abstract way, the overall available algorithms for computations within the network. The duration of the temporal state belongs to the states capacity as well. Long lasting states signalise more final processing situations than those shortly sustained. This can be seen from Figs. 10.6(a) and 10.7(a). Following the first 100–150 msec in the simulation, some states disappear, they are not longer visited by any activity. Other states are however sustained till the end of the simulation, some of which are first to exit e.g.  $\sigma_7$  in Fig. 10.7(b).

More important are those final set of states. For both cases with  $\lambda = 2$  and 3, the network explores the possible information contents. This corresponds to the states during the first 100–150 msec. Afterwards, the network carries only the stored information which is the internally represented information. The states capacity during this time is smaller than the one during the exploring phase, the network performs a sort of compression. The final states in case of  $\lambda = 2$  are  $\sigma_{t>150 \text{ msec}} = \{\sigma_g^{(1)}, \sigma_4, \sigma_5\}$  after the five states observed for  $t < 150$  msec. While in case of  $\lambda = 3$  the final states are  $\sigma_{t>150 \text{ msec}} = \{\sigma_4, \sigma_6, \sigma_7\}$  after the seven states for  $t < 150$  msec. This reduction in states represents a major difference between the proposed tFSM and the basic LSM approach. The reduction in the representation states suggests that the pieces of information are associated with probably more complex internal symbols following the concept of combination coding, as discussed in Sec. 9.2.2. This then agrees strongly with the basic definition of binding from van der Malsburg (von der Malsburg, 1999) and the general concepts discussed in Ch. 9: the biological neural circuitry integrates on temporal basis the simple symbols which represent pieces of information into more complex ones. This integration requires reduction in the final number of symbols after exploring the available ones in response to the input information. Moreover, by

featuring this intrinsic compression of internal representations the tFSM framework avoids the problem of over-processing.

It should be noted that only  $y_N$  is considered in the above discussion. This implies that the observed states capacity describes only this capacity when the entire network is handled as a single neural assembly. Recalling Cor. 10.2 this means that only the temporal dimension of the computational power from one group of neurons is analysed so far. It remains to be seen how many neuronal assemblies can be formed and which firing templates are constructed within these assemblies, this is the spatial dimension of the computational power of the tFSM. This can be performed by searching for repeated firing templates throughout the simulation across all neuronal combinations. Some methods were developed for this task, see e.g. (Iglesias and Villa, 2010; Tetko and Villa, 1997). This is not implemented in the work at hands and is left for future work. Besides, learning is not implemented for the used synaptic dynamics in the tFSM. When implemented, it adds more flexibility to the network in exploring all the possible needed states and to pick more properly the final ones. This is left for the future work as well.

## 10.7 Temporal Finite-State Machines vs. Cortical columns

The novel temporal stable states reflect an emergent ability to process and to represent input features at internally well defined states of activities. To understand the relevance of achieving these transient stable states, the following observed features by the analysis made to the brain circuitry in a behavioural context (Gilbert and Sigman, 2007) are considered:

- The representation of sensory information is made on "as-needed basis" that is reflected through the switching between appearing/disappearing of cell assemblies (binding-by-synchrony) throughout the same cortical area.
- Sensory information is represented "at level of synapses rather than cells". Thus, the expressive power of a neural circuitry in terms of its capacity of internal transient states reveals, for a certain extent, its computational power. This capacity may not be probed merely as "how many" but with "how long" as well.

The results reported here achieve both features within the tFSM. In particular the switching between states and the variability of their time span is accomplished for the simulated dynamic network. Adopting these features permits the tFSM to inherit novel and powerful computational aspects similar to the abilities of cortical mini-columns; this is achievable only when the synaptic dynamics are complex enough to implicitly encode the required input information. Apart from knowing the exact mechanism of content-addressable memory in cortical columns, these conceptual analyses may be adequate to entertain the assumption that the tFSM are able to emulate the content-addressable memory features observed in cortical circuitry when the complexity of the network is up-scaled to the size of a cortical mini-column.

The main computational feature, the separation property, is preserved and additional aspects are accomplished. They are the ability to sustain certain levels of synchronous activity and switch between these levels in response to input sensory information. Such capabilities permit the tFSM to capture more complex functions and features from cortical mini/hyper columns. Further investigations to probe the realization of content-addressable memory in the tFSM are left for a future study. The implemented simulations and analysis here can be regarded as only a scratch on the surface of the possible findings from this framework.



# Discussion & Conclusions

*"If the facts don't fit the theory, change the facts."*

**Albert Einstein**

## 11.1 Discussion

### 11.1.1 Recapitulation of the Ansatz and Key Results

Acquiring more insights into the actual mechanisms of information processing and the computational capabilities within the biological neural systems (BNS) is a core objective of neural science, modern computer science and computational sciences. These insights should enhance the understanding of how can the BNS accomplish such computational power provided that only limited size and energy consumption are available. It is required then to import this understanding into implementable and practical frameworks in order to benefit from it in developing the related applications for medicine and computer engineering. These frameworks are mainly the class of the novel dynamic neural networks simulated in the second part of this thesis based on the novel modified stochastic synaptic model (MSSM) presented in the first part.

As mentioned before, there are two main motivations for understanding and implementing the biological information processing capabilities: First, to help in improving the quality of the life of people suffering from post-accidental loss (either partial or complete) of functions in the brain or spinal cord and similar problems through Brain-computer-interfaces (BCI), neural prostheses and other similar approaches. Without a better understanding of the fundamental operations or sequences leading to cognitive abilities, applications like BCI or neural prostheses will keep struggling to find a proper way to help patients in this regard. Second, the field of computational science, in general, is in a real need for novel solutions for already existing and new computational problems. Although there are significant enhancements in the tools of processing, the algorithms and methodologies are still incapable of delivering the needed solutions. The main problems facing

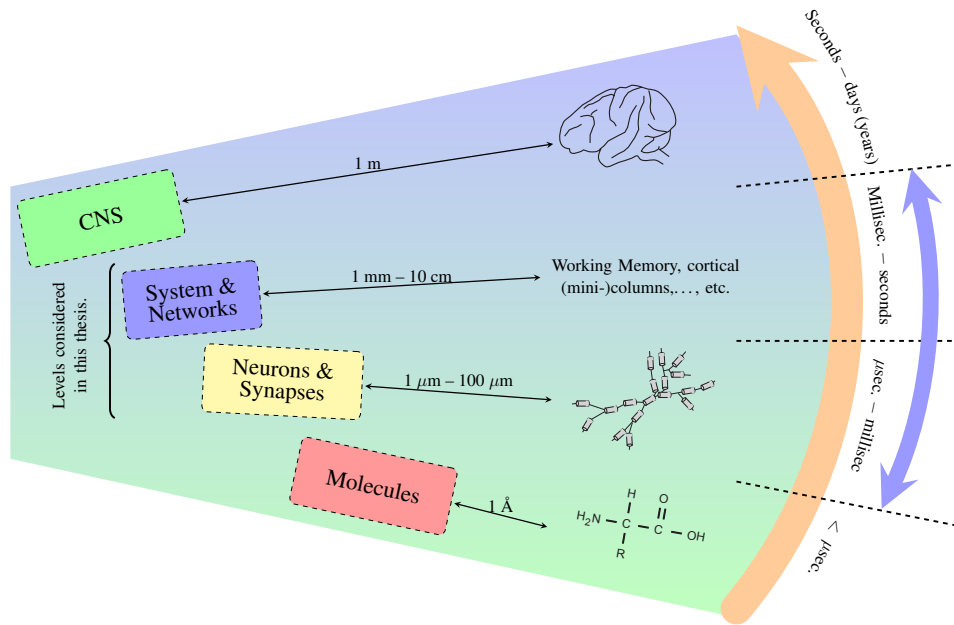


**FIGURE 11.1:** Fig. 1.4 is revised: CNS is a temporal-spatial multi-scale computational system. Temporal considerations are crucial issues of perceiving the different levels of abstractions and organization in biological neural systems. Indicated spatial and temporal levels are those considered in the thesis at hands.

computational sciences are enhancing the methods of nonlinear system identifications, prediction (e.g. predicting chaotic dynamics) and classification. These methods have a wide range of application, see e.g. (Verstraeten et al., 2007) for a comprehensive review. Transferring the knowledge about the techniques utilized in the BNS (e.g. in classification and feature association) into the world of computational sciences will significantly support and empower the available tools.

This thesis represents the contribution of the author along the track of importing a possible basic biological information processing framework into spiking neural networks (SNN). This framework involves two abstraction levels from the central nervous system (CNS): it starts from the novel modelling of the synapses as computational units (cellular level) up to emulating network behaviours in information processing tasks (network level). Differently stated, this work illustrates how certain biological basic information processing procedures on a network level can be emulated based on an optimum modelling of the inner workings on the neuronal/synaptic level. The inner workings are the synaptic dynamics and the integration of firing activities into states. This is achieved through the proper modelling of the synaptic dynamic with the MSSM (Ch. 4). The plausibility of this model is checked and validated then in Ch. 5 by comparing the dynamic performance of the MSSM to a biologically recorded data set. Furthermore, the inner workings include the implementation of the plausible conceptual framework of synchrony states based on the energy profile underlying the synaptic operation of the dynamic system described with the MSSM, see Ch. 6.

The MSSM describes the basic relevant internal synaptic processes from the three involved synaptic regions: the presynaptic preparation of the synaptic action, the transfer to the synaptic

cleft, and the integration of the synaptic action on the postsynaptic site. The simplicity of this model is obvious when it is compared to other recently developed models, e.g. the Lee-Anton-Poon model explained in Ch. 3. The MSSM captures the required synaptic dynamics and models the essence of synaptic variability through only 12 model parameters (compared to e.g. 33 model parameters in the Lee-Anton-Poon model). The biological plausibility of the MSSM is validated in Ch. 5 against a biological counterpart. With the MSSM it is achievable to reliably predict the firing activity of a thalamic postsynaptic neuron with a goodness greater than 92%. This performance outperforms those achieved with other synaptic models. The results and analyses reported in Ch. 6 are the first theoretical energy-based proposition about the underlying mechanism of the experimentally observed occurrence of synaptic states. It is proposed that the synapse modelled with the MSSM operates at certain settings of its model parameters that ensure sustaining the lowest possible energy profile. This energy minimization concept introduced for the MSSM agrees with the general concept of free energy minimization known in thermodynamics. Such agreement with one of the basic rules of physics in general is a novel theoretical evidence from this thesis that by using the MSSM the information processing from the neural circuitries can be adopted and imported to the SNN.

Based on the learning framework presented in Ch. 8, the reported results from Ch. 9 show that the proper synaptic dynamics of the MSSM allow to sustain states of activity among groups of neurons. These states represent the internal representation of the input sensory information. After exploring all the input features over the possible states the network converges to a reduced yet more complex representation of the input information. The final representation is stored implicitly and collectively in the synaptic dynamics and is ready for further processing in succeeding networks.

Following the findings from Ch. 9 and recalling the results and discussion from Ch. 10, it is shown that the proposed computational model of the temporal finite state machine (tFSM) is able to perform a sequence of information processing phases that are intuitively similar to those observed in cortical mini-columns. This emulation of the emergent capability of performing such processing is based on the simulation of the modelled inner workings of this emergent capability.

The approach that adopts the computational model of tFSM presented in this thesis makes a formal distinction between the essence of being intelligent (e.g. the brain) and the classical class of artificial intelligence, e.g. expert systems (like the IBM's Watson). This approach investigates the underlying mechanisms allowing the CNS to be intelligent, i.e. being able to learn, adapt and to invent. A main aspect in this approach is to regard the BNS (or specifically the CNS) as a multi-scale computational systems, see Fig. 11.1. Being a multi-scale computational system is a main challenge against capturing the computational capabilities of the CNS because the computations in the CNS are accomplished on a highly dynamic temporal-spatial scale. This recalls that in order to import the biological computational capabilities, the key computational properties of the dynamic networks from Ch. 10 should be essentially working on a multi-scale fashion as well. This in turn is a step on the way of developing modern computational systems that are expected to be able to

mimic the abilities of the biological counterparts and to get benefit from the revolution in modern hardware. The advances in building such systems are bounded by the understanding level of the computational properties of the CNS, and strictly by how much of this understanding is transferred to a usable technology.

One of the main advantages from the presented work is the novel treatment and handling of some already existing frameworks, such as the binding by synchrony and liquid-state machines (LSM). Such novel handling is made possible only due to the features inherited with the MSSM. This thesis performs a careful process of connecting-the-point among the related theoretical as well as experimental findings and integrates them into one usable computational model. Such an integration permits to benefit from the existing frameworks and to fit smoothly into the existing literature of computational neuroscience. Moreover, it avoids the discrepancies made before to ignore a concept as the binding by synchrony from the focus of experimental studies and to drop it out from further investigations. The proposed synaptic energy concept and the relation to synchrony states highlight many issues that need to be validated and deeply investigated from both a biophysical and experimental point of views. For example, the energy minimization principle in the brain has never been investigated from a biophysical point of view in spite of the general acceptance of considering the brain as a dynamical system.

Moreover, it emerges from the results and discussions in Chs. 6, 9 and 10 that the stochastic release of neurotransmitter does not imply that a neural circuitry should operate at the edge of chaos of its own dynamics for maximum computational power. Instead, it is more logical to have final stable states representing the input information since this leads to stable cognitive action (which is normally observed). Novel situations and unknown inputs are then handled and processed with the stochastic nature at the deep level of synaptic reactions rather than at the level of chaotic dynamics of the entire system. Thus, *new* stable reactions appear. The analysis of the dynamic behaviour of the MSSM shows analytically that this meaning is correct and confirmed. The MSSM resolves the trade-off between adopting the stochastic nature of synaptic responses and still generating smooth transitions between stable internal representations of the input information.

The new treatment applies for LSM as well. The concepts of reservoir computing were not further used in LSM-based approaches because the LSM approach was merely based on the Markram-Tsodyks model. Apart from the LSM implementation, learning was only applied to the synaptic weight of this model. This did not bring too much interest in the field of computation sciences in general and in the engineering applications specifically (Lukoševičius and Jaeger, 2009) to adopt or to develop LSM-based implementations for technical applications. Although this is not shown here, the proposed tFSM can benefit from the rich repertoire of the involved synaptic dynamics of the MSSM by allowing the synapses to change their internal model parameters according to the learning framework introduced in Ch. 8.

From a computational point of view, having a variable duration of the observed states suggests that tFSM feature a significant flexibility in sustaining different states over a variable time scale.

This adds a third dimension to the aspects of the computational power of a dynamic network: The network states capacity of having a single neural assembly may be extended to be a varying set of either fast or slow states depending on the network structure and input. This is still biologically relevant because certain computations are performed much faster than other ones even when the inputs belong to the same class.

Thus, beside the novel behaviour achieved using the MSSM in generating synchrony states within the context of binding by synchrony and tFSM, this work presents novel perspectives of dealing with the conceptual backgrounds of both foundations: binding by synchrony and finite-state machines. Such novel perspectives help in empowering the development of highly specialised SNN-based systems that represent a milestone in building devices capable of bidirectional communication with the CNS; these devices shall feature information processing cores similar to the biological neural circuitries.

### 11.1.2 Implications and Applications

The results reported and discussed in the this work open a number of avenues for applications and enhancements in the available tools and concepts within computational neuroscience. The potential applications belong to a wide multidisciplinary spectrum, the applications include (but not restricted to):

- Applications of artificial retina and related applications for the visual cortex are expected to benefit from the reliable simulations of thalamic postsynaptic activities as reported in Ch. 5.
- Large scale simulation of the tFSM framework on a true parallel computation platform. Some preliminary work has already been done in order to benefit from the processing power and data parallelism from the structure of graphic cards in nowadays computers, see e.g. the author's collaboration in (Hoffmann et al., 2010). Although the simulations were not precisely directed to the implementation of tFSM, it has been shown that using certain libraries basically developed for graphical processing units (GPUs) may boost the simulation performance in terms of the required simulation times with a factor of 1000 compared to simulations performed using Matlab (MathWorks). Long lasting simulations were usually an obstacle against the implementation of large scale simulations of basic LSM in order to compare it with e.g. cortical columns with 10,000 neurons and almost 100 times of synapses (Maass et al., 2002). These large scale simulations may also incorporate the learning framework to gain a better understanding about the real capabilities of the proposed computational model of the tFSM.
- Classification is a general task that is almost required in every computational system and throughout the computer engineering applications. In relation to the preceding point, building a biologically-inspired classification systems using the tFSM is worth developing. The inherited separation property of the tFSM performs an implicit classification by delivering

different responses for slightly different inputs. This suggests that a tFSM-based classifier is expected to deliver a superior performance to the available biologically-inspired classifiers.

### 11.2 Conclusions

This thesis has involved a multidisciplinary research of modelling and simulation of both biophysical and theoretical topics. Main issues are the synaptic modelling and simulation of basic information processing operations from the CNS using dynamic neural networks.

The presented work comprised two main pivots: synaptic dynamics and computing with synchrony states. First, it is concerned with synaptic dynamics and their role in information processing. This part introduces an optimum synaptic representation that allows for realizing the synaptic computational power with a simple biophysical model. Hence, the modified stochastic synaptic model (MSSM) is introduced. With this model the author has won an international contest organized by the INCF<sup>1</sup>. The challenge was to predict the exact spike-timing of a thalamic neuron. The MSSM has defined the current benchmark of this prediction task at 90% correct hit rate. This performance is accomplished at a balanced and optimized computational complexity. The MSSM features 12 model parameters that are compiled into 4 state parameters describing the synaptic dynamics. This model space is almost half the complexity of e.g. the Lee-Anton-Poon model which features similar amount of biophysical aspects. Besides, the mathematical formulations used in the MSSM are strictly first order differential equations that can be directly simulated as a software modules or even transferred to hardware solutions avoiding the sophisticated mathematical continuous time forms used in other models.

In the light of the achieved enhancement in computational aspects with the MSSM, the second main focus has addressed the mechanisms hypothetically used within the brain to handle basic information processing tasks, i.e. basic information representation and processing of neural information through transient states of neural activities. It is namely the synthesis of neural states via temporal correlations (synchrony). This thesis introduces a novel theoretical explanation that ascribes the status of experiencing a level of synchronous activity within a network to the intrinsic energy profile of the synaptic dynamics. In order to have a suitable learning framework for the proposed synaptic model and aiming to fit it to any required network dynamics, a Hebbian-based reinforcement learning framework is introduced. This learning framework can be used with a wide class of dynamic synaptic models. Consequently, it has been shown that the adoption of the standard methods from finite-state machines to explain computations and information processing within neural systems is possible. In relation to that, a novel computational model based on the concept of finite-state machines is introduced. It is the temporal finite-state machine (tFSM). The simulations of the tFSM framework show that some of the relevant information processing features of cortical columns can be imported and simulated. Important among these features is

---

<sup>1</sup><http://www.incf.org/community/competitions/spike-time-prediction/2009/challenge-d>

the ability to process the input information using sequences of and transitions among stable neural states. Achieving this behaviour is attributed to the proper and adequate modelling of dynamics at the synaptic level using the MSSM.

Thus, in relation to the above concluding remarks, this thesis addresses the first required properties of developing a biologically-inspired (neural) computational and information processing system. The required properties are the optimized modelling of the synaptic dynamics, representation of neural states and computation with temporal states. This work covers two levels of abstraction of the CNS: the cellular/synaptic level and the network level. Furthermore it shows a roadmap on how to adopt the biological computational capabilities in computation science in general and in biologically-inspired dynamic neural networks in specific. Direct applications of the introduced work are neural prostheses and bionic automation systems.





# Chapter 12

## Outlook

*"When one admits that nothing is certain one must, I think, also admit that some things are much more nearly certain than others."*

**Bertrand Russell**

As stated in Sec. 11.1.2, there is a set of direct applications of this work. These applications are aimed to extend the theoretical framework presented in Ch. 9 and 10 based on the core of the MSSM to implement large scale simulations. Such simulations will be then the basis for investigating more complex computational tasks as the general application of classification or the content-addressable memory.

Future work will primarily focus on developing both the conceptual and the theoretical paradigms required to introduce a novel applicable brain theory. The core objective of this theory goes further beyond understanding how the brain works. The research will aim at proposing a brain-inspired computational system. The expected system features and inherits the essence of brain's intelligence. Among the main challenges in achieving such brain-inspired computational system is the gap between the multidisciplinary scientific groups working on computational science in general (De Schutter, 2008). This gap makes it difficult to integrate findings from these contributing schemes close together. A parallel understanding of the fundamental questions about brain's computational capabilities should be utmost importance.

The future approach will tackle these fundamental questions by connecting the relevant points from the findings across all diversified fields, e.g. computer science, neuroscience and computational science. In other words, it shall concentrate only on the required levels of abstraction in understanding the required basic computational processes occur in BNS and transfer this knowledge into technological solutions. A starting point is to understand and emulate the approximation property which is required to represent the infinite cognitive state space and encode the input information from this state space into the limited and finite physical state space of the system. Precise modelling and large-scale simulations are among the main tasks in this research. Applications for

this novel computational paradigm may include neural prostheses, robotics and artificial intelligence (AI). By featuring the essence of biological computations neural prostheses may co-exist and bidirectionally communicate with cortical regions to replace impaired brain functions. Furthermore, AI systems and robots shall use smaller databases containing only the basic needed information with which they will be able to conclude needed responses in new (not preprogrammed) situations.

# Synaptic Models

## A.1 $\alpha$ -Function Postsynaptic Potential (PSP)

The  $\alpha$ -function postsynaptic response reads (Bertram, 2005)

$$E_{psp}(t) = V_{epsp} \cdot \frac{t}{\tau_{epsp}} \cdot e^{1 - \frac{t}{\tau_{epsp}}} \quad (\text{A.1})$$

where  $V_{epsp}$  is the constant maximal amplitude of EPSP, and  $\tau_{epsp}$  is the decay time constant. This kind of postsynaptic potential function can be seen as the most common representation in any synaptic model, regardless of being phenomenological or biophysical. The reason of this extensive use of this kind of response function is due to its mathematical simplicity as well as its conceptual plausibility.

## A.2 Dittmann Facilitation and Depression Model

This model approximates the experimentally determined excitatory postsynaptic current  $E_{psc}$  size as the product of the number of physical release sites  $N_T$  and the fraction of sites that undergo release on arrival of an action potential. This fraction was divided into two parts: a facilitation component  $F$  and a depression component  $D$ , both of which could range between 0 and 1:

$$E_{psc} = \alpha \cdot N_T \cdot F \cdot D. \quad (\text{A.2})$$

where the release is scaled by the average  $mE_{psc}$  amplitude  $\alpha$  to produce the final  $E_{psp}$  amplitude. The depression variable was set to unity at rest, reflecting the assumption that all potential release sites are available for release when no release activity has occurred for some time. Therefore, the resting probability of release is equivalent to the initial value of  $F$ , it is denoted with  $F_1$ .

**Facilitation** Enhancement of release is assumed to be directly related to the equilibrium occupancy of the release site by a calcium-bound molecule  $CaX_F$  with dissociation constant,  $K_F$  (see Dittman et al. (2000) for more details):

$$F(t) = \frac{1}{1 + K_F/CaX_F(t)}, \quad (\text{A.3})$$

where  $CaX_F(t)$  decays exponentially with time constant  $\tau_F$  after a jump of size  $\Delta_F$  after an action potential at time  $t_o$ :

$$\frac{dCaX_F}{dt} = -CaX_F(t)/\tau_F + \Delta_F \cdot \delta(t - t_o), \quad (\text{A.4})$$

where  $\delta(t)$  is the Dirac-delta function. For the sake of simplicity and to create an analytical expression for Eqs. A.3 and A.4 where  $CaX_F$  is allowed to decay to 0, Eq. A.3 is modified with the addition of a baseline release probability  $F_1$  in the absence of  $CaX_F$ :

$$F(t) = F_1 + \frac{1 - F_1}{1 + K_F/CaX_F(t)}, \quad (\text{A.5})$$

With this change,  $F(t)$  ranges from  $F_1$  to 1 as  $CaX_F$  increases from 0. Given a quiescent presynaptic terminal with  $CaX_F = 0$  and  $F = F_1$ , then immediately after stimulation with a single action potential,  $CaX_F$  increases to  $\Delta_F$  and  $F$  increases to:

$$F_2 = F_1 + \frac{1 - F_1}{1 + K_F/\Delta_F} \quad (\text{A.6})$$

$N_T \cdot D_1 \cdot F_1$  sites undergo a release and entered a refractory state while  $N_T(1 - D_1 \cdot F_1)$  sites remain available. If a second stimulus occurs just after the first stimulus such that no recovery from the refractory state has occurred, then the second  $E_{psc}$  will be determined by the increased release probability  $F_2$  and the remaining number of release sites as follows:

$$E_{psc,2} = \alpha \cdot N_T \cdot (1 - D_1 \cdot F_1) \cdot F_2 \quad (\text{A.7})$$

It can be shown then that the facilitation ratio is the ratio between  $E_{psc,2}$  and  $E_{psc,1} = \alpha \cdot N_T \cdot D_1 \cdot F_1$ , it is  $((1 - F_1) \cdot F_2)/F_1$ .

**Depression and Recovery** There are  $N_T$  total release sites so that

$$N_T = R + N + T, \quad (\text{A.8})$$

where  $R$  is the number of release sites in refractory,  $T$  are those in transitional state, and  $N$  are the release-ready. Let  $CaX_D$  be the calcium-bound site and  $\tau_D$  be the decay time constant. The calcium dependence of the recovery rate ( $R \rightarrow N$ ) is captured by the equilibrium binding occupancy of a calcium bound site  $CaX_D$ , which instantaneously rises by  $\Delta_D$  after an action potential

at time  $t_o$  and drifts to zero exponentially:

$$\frac{dCaX_D(t)}{dt} = -CaX_D(t)/\tau_D + \Delta_D \cdot \delta(t - t_o) \quad (\text{A.9})$$

The probability that a release site is release-competent is then given by the depression variable  $D(t)$ , governed by the equation:

$$\frac{dD(t)}{dt} = (1 - D(t)) \cdot k_{recov}(CaX_D(t)) - D(t) \cdot F(t) \cdot \delta(t - t_o), \quad (\text{A.10})$$

where

$$k_{recov}(CaX_D(t)) = \frac{k_{\max} - k_o}{1 + K_D/CaX_D(t)} + k_o. \quad (\text{A.11})$$

At first glance, the model may seem not complicated as the equations might be viewed as not mathematically complex. However, the problem with this model is that there is no clear approach to implement it in a simulation. The model was proposed to fit some experimental measurements and was not discussed for further usage. A very simplified version of the Dittmann model takes it back to the Markram-Tsodyks synaptic model.

As for the mathematical complexity, the model is not straight forward implementable with spiking neural networks because of the multiple folds of interdependence between the various parameters (Lehn-Schiøler and Olesen, 2002). Moreover, the usage of the linear multiplication in order to define the final synaptic action of the  $E_{psc}$  in Eq. A.2 does not match the extreme detailed modeling of release sites with three different classes in Eq. A.8.

### A.3 Liaw-Berger Dynamic Synapse

The Liaw-Berger synaptic model assumes that a sum of exponentially decaying functions can describe the probability of transmitter release, and that another sum of decaying exponentials can account for the receptor dynamics. Model parameters in the used kernels cannot be estimated directly from experiments, but they can be fitted to reproduce experimental results (Lehn-Schiøler and Olesen, 2002).

The simplest representation of the Liaw-Berger model (Liaw and Berger, 1996, 1997) assumes that at the presynaptic terminal there are four mechanisms. One very fast representing the incoming action potential (the activity level induced due to an arriving action potential)  $R$ , two facilitating mechanisms  $F_1$  and  $F_2$  and one feedback mechanism  $M$ . The latter parameters models a negative feedback from the postsynaptic neuron. Thus, for any spike arriving at  $t_i$  that is represented as

$\delta(t - t_i)$  the presynaptic dynamics read:

$$\frac{dR(t)}{dt} = \frac{-R(t) + \delta(t - t_i)}{\tau_R}, \quad (\text{A.12})$$

$$\frac{dF_1(t)}{dt} = \frac{-F_1(t) + \delta(t - t_i)}{\tau_{F_1}}, \quad (\text{A.13})$$

$$\frac{dF_2(t)}{dt} = \frac{-F_2(t) + \delta(t - t_i)}{\tau_{F_2}}, \quad (\text{A.14})$$

$$\frac{dM(t)}{dt} = \frac{-M(t) + \delta(t - t_{ps})}{\tau_M}, \quad (\text{A.15})$$

In Eq. A.15,  $t_{ps}$  is the time of the first induced spike at the postsynaptic after the presynaptic spike at  $t_i$ . The collective effect of these mechanisms is integrated to deliver a value of the probability of release  $Pr(t)$ , it is evaluated as:

$$Pr(t) = K_R \cdot R(t) + K_{F_1} \cdot F_1(t) + K_{F_2} \cdot F_2(t) + K_M \cdot M(t), \quad (\text{A.16})$$

where  $K_R, K_{F_1}, K_{F_2}$  and  $K_M$  are scaling factors. Depending on this probability the size of the pool of vesicles ready to release  $N^{total}$  is estimated:

$$\frac{dN^{total}(t)}{dt} = \frac{N^{max} - N^{total}(t)}{\tau_{rp}} - Q \cdot \mathcal{H}(Pr(t) - \theta) \cdot \delta(t - t_i), \quad (\text{A.17})$$

where  $N^{max}$  is the maximum allowed size of the pool,  $\tau_{rp}$  is the recovery time constant of the pool size,  $Q$  is the added quantum of neurotransmitter released. The function  $\mathcal{H}(\cdot)$  denotes the Heaviside function evaluated at the difference between the probability value at instant  $t$  and a probability threshold value  $\theta$ . The activity of the neurotransmitter in the cleft  $N(t)$  and at the postsynaptic terminal  $E_{psp}(t)$  are given as:

$$\frac{dN(t)}{dt} = \frac{-N}{\tau_N} + Q \cdot \mathcal{H}(Pr(t) - \theta) \cdot \delta(t - t_i), \quad (\text{A.18})$$

$$\frac{dE_{psp}(t)}{dt} = \frac{-E_{psp}(t) + k_{epsp} \cdot N(t)}{\tau_v}, \quad (\text{A.19})$$

In Eq. A.18,  $\tau_N$  is the decay time constant. In Eq. A.19  $k_{epsp}$  is a scaling factor and  $\tau_v$  is the membrane time potential.

Before highlighting the setbacks of this model, it is worth mentioning that the above listing of Eqs. A.12–A.19 is the reduced version of the model (Namarvar et al., 2001). If there is a number of release site  $j$  (also called the model's order) and if the four presynaptic mechanisms ( $R, F_1, F_2$  and  $M$ ) are denoted with  $F_m$ , then the presynaptic dynamics are rewritten as:

$$\tau_{j,m} \frac{dF_{j,m}(t)}{dt} = -F_{j,m} + \delta(t - t_i), \quad (\text{A.20})$$

$$Pr_j(t) = \sum_m K_{j,m} \cdot F_{j,m}(t). \quad (\text{A.21})$$

The model is obviously complex especially when its order  $j$  is taken to be more than two as the case in (Namarvar et al., 2001). Apart from the computational complexity, the model itself was never properly introduced in the literature. Almost all the scaling factors were just listed without any indication for their biophysical meaning or relation. After the work of Liaw and Berger, there is no more recent articles commenting on the matter of this model. The model also suffers from some conceptual conflicts, for instance taking the decay time constant of the  $E_{psp}$  to be the same as the membrane potential is not meaningful. It implies that the locally induced postsynaptic potentials build up and decay with the same rate as the total membrane potential of the entire postsynaptic terminal. The authors of the model presented a learning rule for this model, its application to the model constants was a little vague and not well introduced as well (Lehn-Schiøler and Olesen, 2002).

## A.4 Destexhe-Mainen-Sejnowski Synaptic Model

The synaptic model of Destexhe-Mainen-Sejnowski is the "Hodgkin-Huxley" (HH) version of the synaptic models, i.e. it uses the same description level of the mechanisms of calcium diffusion and ion channels while it features more complexity in comparison to the HH model. The model is actually too complex to be either listed or fully explained here, for the details please refer to the original paper (Destexhe et al., 1994). Briefly, this model accounts mainly for the kinetics of the presynaptic and postsynaptic dynamics on a detailed biophysical level.

On the presynaptic side, the flow of calcium ions, the trigger of the neurotransmitter release and the responses of the catalyzing receptors are considered. The model implements the dynamics of the binding process between the calcium and calcium-binding proteins rather than modelling the concentration of the calcium ions in the presynaptic terminal. It traces then the effect of the calcium-protein complex on activating the vesicles of the neurotransmitter. The model did not provide any way of calculating the concentration of the calcium flow from the presynaptic electrical activity (input spiking activity). Consequently, it has not been tested whether this model provides the desired facilitation and depression effects (Lehn-Schiøler and Olesen, 2002).

At the postsynaptic terminal, the model describes the kinetics of the AMPA, GABA and NMDA receptors. Each of these receptors is described using three state parameters (i.e. three equations of dynamics) for describing the closing, desensitized and open transitions. These state parameters generate the synaptic current of each specific receptor type. Moreover, the model estimates the reversal potential as well. It is the membrane potential at which a given neurotransmitter causes no net current flow of ions through that neurotransmitter receptor's ion channel. The collective postsynaptic current from all the receptors and after calculating the reversal potential was not provided in the original model (Destexhe et al., 1994).





# Derivations for Modified Stochastic Synaptic Model

## B.1 Derivation of Discrete Version of Maass-Zador's Stochastic Model

The discrete version of the original Maas-Zador's stochastic synaptic model was listed in (Natschläger, 1999) without derivation. The derivation was important to understand the theoretical basis of its usage. The derivation of the discrete version in general can be useful for fast simulations on specific digital processors or  $\mu$ controller. The derivation can be started for the continuous (general solution) or from the differential equation; here the differential equation is used.

Thus, let us consider the calcium buffering at the presynaptic terminal, its dynamics reads,

$$\frac{dC(t)}{dt} = \frac{C_o - C(t)}{\tau_C} + \alpha \sum_{t_i \in F} \delta(t - t_i)$$

The r.h.s can be rewritten in a difference equation form, i.e.

$$\frac{dC(t)}{dt} \xrightarrow{dt \rightarrow T} \frac{C(t+1) - C(t)}{T}$$

where  $T$  is the discretization step and  $t$  is then the discrete time index. The basic equation can be reformulated as

$$\begin{aligned} C(t+1) - C(t) &= \alpha \times T \times \underbrace{\left[ \sum \delta(t - t_i) \right]}_{\text{discrete of}} + \frac{T}{\tau_c} (C_o - C(t)) \\ C(t+1) &= \alpha \cdot T \cdot \left[ \sum \delta(t - t_i) \right] + k_C \cdot (C_o - C(t)) + C_o \end{aligned} \quad (\text{B.1})$$

where

$$k_C = \frac{T}{\tau_C} - 1$$

In the original literature describing the discrete version of this equation (Natschlager, 1999), the first term in Eq. B.1 was written as following without any comments on its origin:

$$\alpha \cdot T \cdot [\sum \delta(t - t_i)] \stackrel{?}{=} \alpha \cdot \theta(t) \quad (\text{B.2})$$

where  $\theta(t)$  is the instantaneous firing rate observed at  $t$ . This is an approximation of the input spike train and should be only used if

$$T \gg \langle \Delta_{\text{isi}} \rangle \quad (\text{B.3})$$

This condition implies that the discretization step allows for more than one spike to occur within its span. Otherwise the observed firing rate is miscalculated and does not represent the input features prior to the time instant  $t$ . Besides, the input spike train should feature a very slow transition between firing rates over the moving time window of width  $T$ . That is, the variance of the inter-spike intervals should be small. These conditions are completely missing in the basic literature of the model. Hence, the discrete version of the calcium buffering equation reads:

$$C(t + 1) = \alpha \cdot \theta(t) + k_C \cdot (C_o - C(t)) + C_o \quad (\text{B.4})$$

Similarly, the equation for the size of ready-to-release pool of vesicles reads:

$$V(t + 1) = -P(t) \cdot \theta(t) + k_V \cdot (V(t) - V_o) + V_o \quad (\text{B.5})$$

where  $k_V = \frac{T}{\tau_V} - 1$ . The definition of the probability function  $P(t)$  remains as the basic definition, keeping in mind that  $t$  here is the discrete time index.

The usability of this version of the model is bounded by the condition relating the discretization step and the average frequency of the input spike train. Therefore, extending the discrete equation to all the MSSM equations was seen as not required. Especially when the differential equations of MSSM are derived which was not the case for the Maass-Zador's model.

## B.2 Derivation of Steady-state Expression

Starting with Eq. 4.12, for a regular spike train with a frequency  $f$ , the time average of calcium buffering  $C_{\text{ss}}(f)$  is calculated by estimated the time average of the solution of this differential equation. Eq. 4.12 has already a closed form solution from the Maass-Zador stochastic synapse, Eq. 4.6:

$$C(t) = C_o + \sum_{t_i \in F} \alpha \cdot e^{-(t-t_i)/\tau_C},$$

The time average  $\langle C(t) \rangle$  is defined as

$$\begin{aligned}
 \langle C(t) \rangle &= \frac{1}{T} \int_0^T dt C(t) \\
 &= C_o + \frac{\alpha}{T} \int_0^T dt \sum_{t_i} \exp\left(-\frac{t-t_i}{\tau_C}\right) \\
 &= C_o + \frac{\alpha}{T} \sum_{t_i} \int_{t_i}^T dt \exp\left(-\frac{t-t_i}{\tau_C}\right) \\
 &= C_o + \frac{\alpha(-\tau_C)}{T} \sum_{t_i} \left[ \exp\left(-\frac{T-t_i}{\tau_C}\right) - 1 \right]
 \end{aligned}$$

For a constant input frequency  $f = 1/\Delta_{\text{isi}}$ ,  $t_i - t_{i-1} = \text{Const.} = \Delta_{\text{isi}}$ , the summation upper limit change to the total number of spikes,  $N_{\text{sp}}$ , in the input spike train  $F$ , and  $N_{\text{sp}} = T/\Delta_{\text{isi}}$ . At  $T \gg \tau_C$  and  $T \gg \Delta_{\text{isi}}$ , the r.h.s. reduces to

$$\begin{aligned}
 &= C_o + \frac{\alpha(-\tau_C)}{T} \sum_{n=1}^{N_{\text{sp}}} \left[ \exp\left(-\frac{T-n \times \Delta_{\text{isi}}}{\tau_C}\right) - 1 \right] \\
 &= C_o + \frac{\alpha(-\tau_C)}{T} \left[ \left( \exp\left(-\frac{T}{\tau_C}\right) \sum_{n=1}^{N_{\text{sp}}} \exp\left(\frac{n \times \Delta_{\text{isi}}}{\tau_C}\right) \right) - N_{\text{sp}} \right] \\
 &= C_o + \frac{\alpha(-\tau_C)}{T} \underbrace{\left( \exp\left(-\frac{T}{\tau_C}\right) \sum_{n=1}^{N_{\text{sp}}} \exp\left(\frac{n \times \Delta_{\text{isi}}}{\tau_C}\right) \right)}_{\text{vanishes at } T \gg \tau_C} - \frac{\alpha(-\tau_C)}{T} N_{\text{sp}} \\
 &= C_o + \frac{\alpha(-\tau_C)}{T} \times -\frac{T}{\Delta_{\text{isi}}}
 \end{aligned}$$

Thus, the closed form of  $C_{\text{ss}}$  reads

$$C_{\text{ss}}(f = \frac{1}{\Delta_{\text{isi}}}) \equiv \langle C(t) \rangle = C_o + \alpha \times \frac{\tau_C}{\Delta_{\text{isi}}} \quad (\text{B.6})$$

The time average of  $V(t)$  is calculated in similar fashion. The continuous time solution of Eq. 4.13 is different than the version used in the Maass-Zador's formulation. It is derived by integrating Eq. 4.13 with the initial condition that  $V(0) = V_o$ . The continuous time solution is expressed as

$$V(t) = V_o - \sum_{t_i \in F} P(V(t_i)) \cdot e^{-(t-t_i)/\tau_V} \quad (\text{B.7})$$

Applying the same approach from deriving Eq. B.6 on Eq. B.7, it follows

$$\begin{aligned}
 V_{ss} &= \langle V(t) \rangle \\
 &= \frac{1}{T} \int_0^T dt V(t) \\
 &= V_o + \frac{1}{T} \int_0^T dt \sum_{t_i} P(V(t_i)) \cdot \exp\left(-\frac{t-t_i}{\tau_V}\right)
 \end{aligned} \tag{B.8}$$

Recalling that  $P(V(t_i)) = P(t_i) = 1 - \exp(-C(t_i) \cdot V(t_i))$  and at  $T \gg \tau_V$  and  $T \gg \Delta_{isi}$ ,  $P(t_i)$  can be substituted with  $P_{ss}$ , where

$$P_{ss} \approx 1 - \exp(-C_{ss} \cdot V_{ss}) \tag{B.9}$$

Inserting Eq. B.9 in the r.h.s. of Eq. B.8, as the self-consistency equations

$$\begin{aligned}
 V_{ss} &= V_o - P_{ss} \times \frac{\tau_V}{\Delta_{isi}} \\
 0 &= \frac{\tau_V}{\Delta_{isi}} \cdot \exp(-C_{ss} \cdot V_{ss}) - V_{ss} + \left(V_o - \frac{\tau_V}{\Delta_{isi}}\right)
 \end{aligned} \tag{B.10}$$

Let  $x = \tau_V / \Delta_{isi}$  and  $y = V_o - x$ , and solving Eq. B.10 for  $V_{ss}$  it turns that

$$V_{ss} \left( \frac{1}{\Delta_{isi}} \right) \equiv \langle V(t) \rangle = \frac{1}{C_{ss}} \left[ \mathcal{Lam}\{x \cdot C_{ss} \cdot e^{(-C_{ss} \cdot y)}\} + x \cdot y \right] \tag{B.11}$$

here  $\mathcal{Lam}\{\cdot\}$  is the "lambertw" and the solution is performed using Matlab Symbolic Toolbox.

---

The case for  $N(t)$  is not straight forward as for the previous two cases. First, the differential equation of  $N(t)$  can be rewritten as

$$\frac{dN_t(t)}{dt} = k_{N_t, V} \left( -\frac{dV(t)}{dt} \right) \cdot \sum_{t_i} \delta(t - t_i) + \frac{N_{to} - N_t(t)}{\tau_{N_t}} \tag{B.12}$$

where  $k_{N_t}$  is set to one. The multiplication with the input spike train cancels the need for  $max\{\cdot\}$  operator. The continuous time solution reads,

$$N(t) = N_o + 2 \sum_{t_i} \left[ \exp\left(-\frac{t-t_i}{\tau_{N_t}}\right) \cdot \left(\frac{dV(t)}{dt}\right)_{\text{at } t_i} \right] \tag{B.13}$$

The calculation of the time average of  $N(t)$  is performed as following:

$$\begin{aligned}
 \langle N(t) \rangle &= \frac{1}{T} \int_0^T dt N(t) \\
 &= N_o + \frac{2}{T} \int_0^T dt \sum_{t_i} \exp\left(-\frac{t-t_i}{\tau_{N_t}}\right) \cdot \left(\frac{dV(t)}{dt}\right)_{\text{at } t_i} \\
 &= N_o + \frac{2}{T} \sum_{t_i} \left(\frac{dV(t)}{dt}\right)_{\text{at } t_i} \int_{t_i}^T dt \exp\left(-\frac{t-t_i}{\tau_{N_t}}\right) \\
 &= N_o + \frac{2}{T} \sum_{n=1}^{N_{sp}} \left(\frac{dV(t)}{dt}\right)_{\text{at } n\Delta_{\text{isi}}} \int_{n\Delta_{\text{isi}}}^T dt \exp\left(-\frac{t-n\Delta_{\text{isi}}}{\tau_{N_t}}\right)
 \end{aligned}$$

for  $T \gg \tau_{N_t}$  and considering a steady-state oscillation, it can be assumed that  $dV(t)/dt$  is constant from spike to spike. By evaluating the integral and rearranging, the r.h.s. reads

$$\begin{aligned}
 &= N_o + \frac{2}{T} \left(\frac{dV(t)}{dt}\right)_{ss} (-\tau_{N_t}) \sum_{n=1}^{N_{sp}} (0-1) \\
 &= N_o + \frac{2}{T} \left(\frac{dV(t)}{dt}\right)_{ss} (-\tau_{N_t}) \left(\frac{-T}{\Delta_{\text{isi}}}\right)
 \end{aligned}$$

Hence,

$$N_{ss} \left(\frac{1}{\Delta_{\text{isi}}}\right) \equiv \langle N(t) \rangle = N_o + 2 \frac{\tau_{N_t}}{\Delta_{\text{isi}}} \cdot \left(\frac{dV(t)}{dt}\right)_{ss} \quad (\text{B.14})$$

In Eq. B.14, the factor  $\left(\frac{dV(t)}{dt}\right)_{ss}$  still needs to be calculated. A possible approach is to calculate the second moment of Eq. B.13. A simpler approach can be applied starting with the following inequality:

$$V(t) \leq V_o,$$

and it holds as well that

$$V_{ss} + \frac{1}{2} \left(\frac{dV(t)}{dt}\right)_{ss} < V_o.$$

Because  $\left(\frac{dV(t)}{dt}\right)_{ss} = \max\{V(t)\} - \min\{V(t)\}$ , then it follows that

$$\left(\frac{dV(t)}{dt}\right)_{ss} < 2(V_o - V_{ss}) \quad (\text{B.15})$$

Besides, it can be shown that  $\left(\frac{dV(t)}{dt}\right)_{ss} \propto \exp(-\tau_V/\Delta_{\text{isi}})$ . Hence, it is assumed that

$$\left(\frac{dV(t)}{dt}\right)_{ss} \approx 2(V_o - V_{ss}) \cdot \exp(-\tau_V/\Delta_{\text{isi}}) \quad (\text{B.16})$$

The steady-state formula for the postsynaptic potential from Eq. 4.16 can be directly derived from this differential equation. Setting the differential part to zero, i.e. at  $dE_{epsp}(t)/dt \rightarrow 0$ , the steady-state value reads

$$EPSP_{ss} = E_o + k_{epsp} \cdot N_{ss} \quad (B.17)$$

In order to check the exactness of the steady-state calculations, the MSSM is simulated for 10 sec epoch with arbitrarily chosen parameter values in response to a regular input spike train with a varying input frequency. The input frequencies vary from 10 Hz to 200 Hz. For each input frequency, the time average of the state parameters, i.e.  $C_{ss}$ ,  $V_{ss}$ ,  $N_{ss}$  and  $E_{ss}$ , are estimated using the formulas given here and by calculating the actual mean of the last 500 msec. Fig. B.1 illustrate the time evolutions of the state parameters in steady-state as estimated overlapped with the simulated values. As seen from the boxes with zoom-in within the figures, the calculations derived here perform almost an exact estimation to the required values. The values of the synaptic parameters are given in Tab. B.1.

**TABLE B.1:** List of values used in the simulation to check the exactness of estimating steady-state values.

Parameter	Value
$\tau_C$	26 msec
$\tau_V$	35 msec
$\tau_N$	24 msec
$\tau_{epsp}$	13 msec
$N_{to}$	0
$E_o$	0
$\alpha$	0.09
$C_o$	0.5
$V_o$	3.70
$k_{epsp}$	100
$k_{N_t}$	1
$k_{N_t,V}$	10

### B.3 Dynamic Threshold & Spike-Rate Adaptation

In order to account for the dynamic SRA-refractoriness, Eq. 3.3 can be detailed as followed:

$$\tau_h \frac{dh}{dt} = (h_{rest} - h) + \sum_i E_{psp,i} - E_{ref}, \quad (B.18)$$

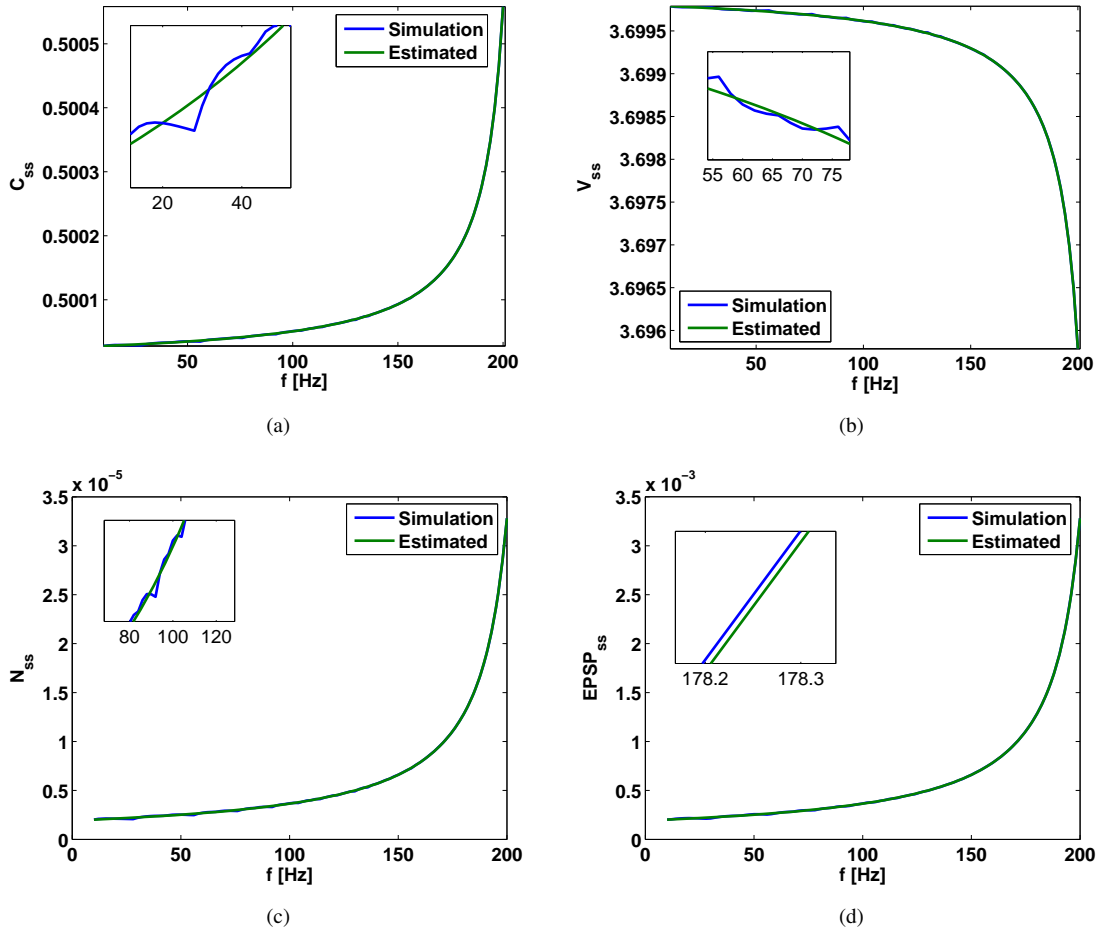


**FIGURE B.1:** Check on steady-state calculations. Both lines for simulated and estimated overlap due to the reliable estimation. Boxes within each subfigure are zoomed portions clarifying the overlap in the illustrated time courses.

$E_{\text{ref}}$  represents the reversal potential for SRA and a refractory current (Miller, 2006); it reads

$$E_{\text{ref}} = r_m \cdot (g_{\text{sra}} + g_{\text{ref}}) \cdot (h - h_{\text{rest}}), \quad (\text{B.19})$$

where  $g_{\text{sra}}$  and  $g_{\text{ref}}$  are the SRA and refractory conductances respectively (Miller, 2006):

$$\frac{dg_{\text{sra}}}{dt} = -g_{\text{sra}}/\tau_{\text{sra}}, \quad (\text{B.20})$$

$$\frac{dg_{\text{ref}}}{dt} = -g_{\text{ref}}/\tau_{\text{ref}} \quad (\text{B.21})$$

$\tau_{\text{sra}}$  and  $\tau_{\text{ref}}$  are set to 200 msec and 2 msec respectively.  $r_m$  is the neuronal resistance set arbitrarily at 90 M $\Omega$ . In the Euler-method solution of the latter two ODEs the increase in both spike-rate and refractory conductances per spike are  $\Delta_{g_{\text{sra}}} = 5 \cdot 10^{-9}$  and  $\Delta_{g_{\text{ref}}} = 200 \cdot 10^{-9}$  respectively.

Regarding the dynamic firing threshold, the value  $h_{\text{th}}$  follows a dynamic rule reported in (Wilson et al., 2001) to ensure adaptation to the incoming activity. The threshold accommodation

variables are related through

$$\frac{dh_{th}}{dt} = -(h_{th} - \sigma) + \frac{(\rho * h)}{\tau_{th}}, \quad (B.22)$$

where  $\sigma$ ,  $\rho$  and  $\tau_{th}$  are arbitrarily set at -40 mV, 0.005 and 20 msec respectively. This allows  $h_{th}$  to vary roughly between -56 mV and -50 mV.  $u$  is the membrane potential.

## B.4 Synaptic Energy

### B.4.1 Proof of Proposition 6.1

It starts with the energy function of a Hopfield network. In such a network, the total energy of the network with  $n$  neurons  $E_{tot,net}$  is defined as (Neelakanta and DeGroff, 1994)

$$E_{tot,net} = \underbrace{-\frac{1}{2} \sum_i^n \sum_j^n w_{ij} x_i x_j}_{\text{Synaptic term}} - \underbrace{\sum_i^n I_i x_i}_{\text{Input}} + \underbrace{\sum_i^n \frac{1}{\tau} \int_{x_o}^x g^{-1}(x) dx}_{\text{Neuronal term}} \quad (B.23)$$

In Eq. B.23,  $x_{i(j)}$  are the graded (rate coded) activity value of neuron  $i(j)$ .  $w_{ij}$  is the static synaptic weight between neurons  $i$  and  $j$ . Only the first term (the synaptic term) is important in the case considered here. Since a single synapse is investigated, the summations can be ignored. Hence, the synaptic energy directly from the Hopfield definition reads

$$E_{syn} = w_{ij} \times x_i \times x_j, \quad (B.24)$$

This implies that the synaptic energy is the product of the synaptic weight between the pre- and postsynaptic activity levels and these activity levels. In case of the MSSM, the neuron activity is bounded with the threshold mechanism and this mechanism is directly a function of the postsynaptic potential. Since  $E_{psp}$  is a continuous time-varying function, it maybe viewed as an indication that determines the postsynaptic activity. That is

$$x_i \leftarrow E_{psp} \quad (B.25)$$

Estimating presynaptic activity is, however, not a straight forward task. The input to the MSSM as well as any other dynamic synaptic model is a spike train. In case of a regular spike train, the presynaptic activity scales with input frequency. The presynaptic activity can be estimated to be rate coded value

$$x_j \leftarrow e^{\frac{-\Delta_{isi}}{\tau}}, \quad (B.26)$$

where  $\tau$  is a scaling constant. With this definition, the presynaptic activity satisfies  $x_j \in ]0, 1[$  as the input frequency spans from infinity to zero. The synaptic weights can be replaced with the



dynamic synaptic strength, i.e.

$$w_{ij} \leftarrow S(t). \quad (\text{B.27})$$

Substituting Eqs. B.25–B.27 in Eq. B.24, the FSE reads

$$E_{\text{syn}}(t) \approx S(t) \times E_{\text{psp}}(t) \times e^{\frac{-\Delta_{\text{isi}}}{\tau}}$$

The approximation sign is used to emphasize that this is only an *estimation* of the synaptic energy quantity. As for the units, according to the basic definition  $E_{\text{syn}}$  has units of energy per unit resistance, i.e. Volts<sup>2</sup>. This is accomplished by considering that  $S(t)$  is dimensionless from Def. 4.1 and that the quantity  $x_j$  has the same units as  $E_{\text{psp}}$  since it indicates the presynaptic activity in response to electrical input stimulation.

#### B.4.2 MSSM as Rate-coded Dynamical System

In order to analyse the MSSM as a dynamical system, the spiking nature has been suppressed. The aim of this part of the analysis is to have an insight into the underlying energy profile of a dynamical system described with the MSSM equations. It should be pointed out here that the steady-state analysis is not suitable to study the energy profile. The steady-state analysis locates the time average of the state parameters when simulation time is too long ( $T \rightarrow \text{inf}$ ). However, as for the search for stable energy states in the synaptic dynamics, the relevant time window for the analysis ranges between 50–300 msec (El-Laithy and Bogdan, 2011c; von der Malsburg, 1999).

The model equations of the MSSM are rewritten and the spiking input is replaced with the input frequency,  $f = \Delta_{\text{isi}}^{-1}$ . Note that in case of irregular input spike, it is assumed that this irregular input has a randomly distributed inter-spike intervals that follow the Poisson distribution with mean value  $\lambda$ . In case of stationariness and low overall firing rate, it can be assumed that within the time interval of the simulation epoch the input to the synaptic model can be approximated to a regular spike train<sup>1</sup> with an overall frequency of  $\lambda^{-1}$ , i.e.  $\Delta_{\text{isi}} \leftarrow \lambda$ . Thus, the MSSM for energy analysis in response to an input frequency  $\Delta_{\text{isi}}^{-1}$  reads

$$\frac{dC(t)}{dt} = \frac{(C_o - C(t))}{\tau_C} + \frac{\alpha}{\Delta_{\text{isi}}}, \quad (\text{B.28})$$

$$\frac{dV(t)}{dt} = \frac{(V_o - V(t))}{\tau_V} - \frac{P(t)}{\Delta_{\text{isi}}}, \quad (\text{B.29})$$

$$\frac{dN_t(t)}{dt} = k_{N_t, V} \cdot (\max\{0, -\frac{dV(t)}{dt}\}) + \left( \frac{N_{to} - k_{N_t} \cdot N_t(t)}{\tau_{N_t}} \right) \quad (\text{B.30})$$

$$\frac{dE_{\text{psp}}(t)}{dt} = \frac{1}{\tau_{\text{epsp}}} (E_o - E_{\text{psp}}(t) + k_{\text{epsp}} \cdot N_t(t)) \quad (\text{B.31})$$

$$\frac{dS(t)}{dt} = \frac{dC(t)}{dt} \cdot V(t) \cdot N_t(t) + C(t) \cdot \frac{dV(t)}{dt} \cdot N_t(t) + C(t) \cdot V(t) \cdot \frac{dN_t(t)}{dt} \quad (\text{B.32})$$

<sup>1</sup>Let the discretization step  $T_{\text{disc}}$  be big enough for the occurrence of more than one spike

$$\frac{dE_{\text{syn}}(t)}{dt} = e^{\frac{-\Delta_{\text{isi}}}{\tau}} \left[ E_{\text{psp}}(t) \cdot \frac{S(t)}{dt} + S(t) \cdot \frac{dE_{\text{psp}}(t)}{dt} \right] \quad (\text{B.33})$$

The analysis is based on a rate coded version of the model, this is a typical approach used throughout the literature in general, see e.g. Maass and Sontag (2000), for the sake of simplifying the problem. This system of equations is solved in Matlab with the solver (ode45). In order to check the validity of the estimated behaviour of the energy function against the situation with spiking inputs/outputs, compare Figs. 6.1(a) and 9.4(a). Of course the two time course are not identical. However, the general flow of the curve is similar which supports the introduced derivation and the used approach.

# Mathematical Definitions for Dynamic Networks

These definitions are adopted from the derivations given by (Maass and Markram, 2004; Maass et al., 2002; Maass and Sontag, 2000):

- For an input function  $u(\cdot)$ , the mapping operation  $\mathcal{F} : u(\cdot) \rightarrow \mathbb{R}$  is time *invariant* if a shift of the input functions by a constant  $t_0$  just causes a shift of the output function by the same constant  $t_0$ . That is, if  $\mathcal{G}$  is a shifting filter with  $\mathcal{G}_{t_0}u(t) = u(t - t_0)$ , then the operator  $\mathcal{F}$  at any  $t_0 \in \mathbb{R}$  applied on any input function  $u(\cdot)$  satisfies  $\mathcal{F}u_{t_0}(t) = \mathcal{F}u(t - t_0)$  where  $u_{t_0} = \mathcal{G}_{t_0}u(t)$
- The term "fading memory" refers to the class of nonlinear operators  $\mathcal{F} : \mathbb{R} \rightarrow \mathbb{R}$  that can be parametrized as a sequence of (finite or infinite) Volterra series. If an operator  $\mathcal{F}$  has a fading memory then the value of  $\mathcal{F}v(0)$  can be approximated arbitrarily closely by the value of  $\mathcal{F}u(0)$  for functions  $u$  that approximate the function  $v$  for sufficiently long bounded intervals  $[-T, 0]$ . The formal definition is:

**Definition C.1.** It is accepted that an operator  $\mathcal{F} : U \mapsto \mathbb{R}$  has a fading memory if for every  $v(\cdot) \in U$  and every  $\epsilon > 0$  there exists  $\delta > 0$  and  $T > 0$  so that  $|\mathcal{F}v(0) - \mathcal{F}u(\cdot)| < \epsilon$  for all  $u(\cdot) \in U$  with the property that  $\|v(t) - u(t)\| < \delta$  for all  $t \in [-T, 0]$ .



# Abbreviations

GABA <sub>a</sub>	$\gamma$ -aminobutyric acid
<i>DN</i>	Dynamic Networks
AMPA	2-amino-3-(5-methyl-3-oxo-1,2-oxazol-4-yl) propanoic acid
ANN	Artificial Neural Network(s)
AP	Approximation Property
BCI	Brain-computer-interfaces
BNS	biological neural systems
CNS	Central Nervous System
ESN	Echo-State Networks
FSE	Free-Synaptic Energy
ISI	Inter-spike Intervals
LIF	Leaky Integrate-and-Fire
LSM	Liquid-State Machines
LTD	Long-Term Depression
LTP	Long-Term Potentiation
MSSM	Modified Stochastic Synaptic Model
NMDA	N-Methyl-D-aspartic acid or N-Methyl-D-aspartate
RL	Reinforcement Learning
RNA	Ribonucleic Acid
SNN	Spiking Artificial Neural Network(s)
SP	Separation Property
SRA	Spike-Rate Adaptation

SRM	Spike Response Model
STD	Short-Term Depression
STDP	Spike-Timing Dependent Plasticity
STP	Short-Term Potentiation
TD	Temporal Difference
tFSM	Temporal Finite-State Machine
TM	Turing Machine

# Bibliography

- Abbott, L., Varela, J., Sen, K., , and Nelson, S. B. (1997). Synaptic depression and cortical gain control. *Science*, 275:220–224.
- Abeles, M. (1991). *Corticonics: Neural Circuits of the Cerebral Cortex*. Cambridge University Press, first edition.
- Abul-Husn, N. S., Bushlin, I., Morifjn, J. A., Jenkins, S. L., Dolios, G., Wang, R., Iyengar, R., Ma’ayan, A., and Devi, L. A. (2009). Systems approach to explore components and interactions in the presynapse. *Proteomics*, 9(12):3303–3315.
- Ackley, D. H., Hinton, G. E., and Sejnowski, T. J. (1985). A learning algorithm for boltzmann machines\*. *Cognitive Science*, 9(1):147–169.
- Antle, M. C., Kriegsfeld, L. J., and Silver, R. (2005). Signaling within the master clock of the brain: Localized activation of mitogen-activated protein kinase by gastrin-releasing peptide. *The Journal of Neuroscience*, 25(10):2447–2454.
- Augustine, G. J. and Kasai, H. (2007). Bernard Katz, quantal transmitter release and the foundations of presynaptic physiology. *The Journal of Physiology*, 578(3):623–625.
- Averbeck, B. B., Latham, P. E., and Pouget, A. (2006). Neural correlations, population coding and computation. *Nature Reviews Neuroscience*, 7:358–366.
- Back, A., Wan, E. A., Lawrence, S., and Tsoi, A. C. (1995). A unifying view of some training algorithms for multilayer perceptrons with fir filter synapses. In *Neural Networks for Signal Processing 4*, pages 146–154. IEEE Press.
- Back, A. D. and Tsoi, A. C. (1991). Fir and iir synapses, a new neural network architecture for time series modeling. *Neural Comput.*, 3:375–385.
- Barak, O. and Tsodyks, M. (2007). Persistent activity in neural networks with dynamic synapses. *PLoS Comput Biol*, 3(2):e35.
- Baras, D. and Meir, R. (2007). Reinforcement learning, spike-time-dependent plasticity, and the bcm rule. *Neural Comput.*, 19:2245–2279.
- Barrett, A. B., Billings, G. O., Morris, R. G. M., and van Rossum, M. C. W. (2009). State based model of long-term potentiation and synaptic tagging and capture. *PLoS Comput Biol*, 5(1):e1000259.

- Bauer, F. (2005). *Visual attention, Binding Problem, Gamma-frequency, Synchrony Priming*. PhD thesis, Ludwig-Maximilians-University München.
- Bertram, R. (2005). Mathematical models of synaptic transmission and short-term plasticity. In Sneyd, J., editor, *Tutorials in Mathematical Biosciences II*, volume 1867 of *Lecture Notes in Mathematics*, pages 651–653. Springer Berlin / Heidelberg.
- Bosman, R. J. C., van Leeuwen, W. A., and Wemmenhove, B. (2004). Combining hebbian and reinforcement learning in a minibrain model. *Neural Networks*, 17(1):29 – 36.
- Boyd, S. and Chua, L. (1985). Fading memory and the problem of approximating nonlinear operators with volterra series. *Circuits and Systems, IEEE Transactions on*, 32(11):1150 – 1161.
- Brager, D. H., Capogna, M., and Thompson, S. M. (2002). Short-term synaptic plasticity, simulation of nerve terminal dynamics, and the effects of protein kinase c activation in rat hippocampus. *Journal of Physiology*, pages 545–559.
- Branco, T., Staras, K., Darcy, K. J., and Goda, Y. (2008). Local dendritic activity sets release probability at hippocampal synapses. *Neuron*, 59(3):475 – 485.
- Bressloff, P. C. and Coombes, P. S. (2000). Dynamics of strongly coupled spiking neurons. *Neural Comput.*, 12(1):91–129.
- Brette, R. and Gerstner, W. (2005). Adaptive Exponential Integrate-and-Fire Model as an Effective Description of Neuronal Activity. *J Neurophysiol*, 94(5):3637–3642.
- Brody, C. D. (1999). Correlations without synchrony. *Neural Comput.*, 11(7):1537–1551.
- Brunel, N. and van Rossum, M. (2007). Quantitative investigations of electrical nerve excitation treated as polarization: Louis lapicque 1907; translated. *Biological Cybernetics*, 97(5):341–349.
- Burt, A. M. (1993). *Textbook of Neuroanatomy*. Philadelphia, 1st edition.
- Campbell, S. R., Wang, D. L., and Jayaprakash, C. (1999). Synchrony and desynchrony in integrate-and-fire oscillators. *Neural Computation*, 11(7):1595–1619.
- Carandini, M., Horton, J. C., and Sincich, L. C. (2007). Thalamic filtering of retinal spike trains by postsynaptic summation. *J. Vis.*, 7(14):1–11.
- Carnell, A. (2009). An analysis of the use of hebbian and anti-hebbian spike time dependent plasticity learning functions within the context of recurrent spiking neural networks. *Neurocomput.*, 72(4-6):685–692.
- Chorley, P. and Seth, A. K. (2011). Dopamine-signaled reward predictions generated by competitive excitation and inhibition in a spiking neural network model. *Frontiers in computational neuroscience*, 5.
- Chumbley, J. R., Dolan, R. J., and Friston, K. J. (2008). Attractor models of working memory and their modulation by reward. *Biol. Cybern.*, 98(1):11–18.
- Churchland, P. S. and Sejnowski, T. J. (1988). Perspectives on cognitive neuroscience. *Science (New York, N.Y.)*, 242(4879):741–745.



- Crick, F. and Koch, C. (2003). A framework for consciousness. *Nature neuroscience*, 6(2):119 – 126.
- Dauwels, J., Vialatte, F., Weber, T., and Cichocki, A. (2009). On similarity measures for spike trains. In Köppen, M., Kasabov, N., and Coghill, G., editors, *Advances in Neuro-Information Processing*, volume 5506 of *Lecture Notes in Computer Science*, pages 177–185. Springer Berlin / Heidelberg.
- Dayan, P. and Abbott, L. F. (2005). *Theoretical Neuroscience: Computational and Mathematical Modeling of Neural Systems*. The MIT Press.
- de Queiroz, M. S., de Berriço, R. C., and de Pinho Braga, A. (2006). Reinforcement learning of a simple control task using the spike response model. *Neurocomputing*, 70(1-3):14 – 20.
- De Schutter, E. (2008). Why are computational neuroscience and systems biology so separate? *PLoS Comput Biol*, 4(5):e1000078.
- Destexhe, A., Zachary, Mainen, F., and Sejnowski, T. J. (1994). Synaptic transmission and neuro-modulation using a common kinetic formalism. *J. Comp. Neurosci*, pages 195–230.
- Dittman, J. S., Kreitzer, A. C., and Regehr, W. G. (2000). Interplay between facilitation, depression, and residual calcium at three presynaptic terminals. *The Journal of Neuroscience*, 20(4):1374–1385.
- Dobrunz, L. E. and Stevens, C. F. (1997). Heterogeneity of Release Probability, Facilitation, and Depletion at Central Synapses. *Neuron*, 18(6):995–1008.
- Dobrunz, L. E. and Stevens, C. F. (1999). Response of hippocampus synapses to natural stimulation patterns. *Neuron (Cell Press)*, 22:157–166.
- Dodla, R. and Wilson, C. (2008). Synchrony-asynchrony transitions in neuronal networks. *BMC Neuroscience*, 9(Suppl 1):P9.
- Douglas, R., Mahowald, M., Martin, K., and Stratford, K. (1996). The role of synapses in cortical computation. *Journal of Neurocytology*, 25:893–911. 10.1007/BF02284849.
- Durstewitz, D. (2003). Self-Organizing Neural Integrator Predicts Interval Times through Climbing Activity. *J. Neurosci.*, 4(12):2003.
- El-Laithy, K. (2011). Digital analysis of neuronal branching and synaptogenesis. Master’s thesis, Universität Leipzig.
- El-Laithy, K. and Bogdan, M. (2009). Synchrony state generation in artificial neural networks with stochastic synapses. In *Artificial Neural Networks – ICANN 2009*, volume 5768 of *Lecture Notes in Computer Science*, pages 181–190. Springer.
- El-Laithy, K. and Bogdan, M. (2010a). A hebbian-based reinforcement learning framework for spike-timing-dependent synapses. In *Artificial Neural Networks – ICANN 2010*, volume 6353 of *Lecture Notes in Computer Science*, pages 160–169. Springer.
- El-Laithy, K. and Bogdan, M. (2010b). Predicting spike-timing of a thalamic neuron using a stochastic synaptic model. In *ESANN Proceedings*, pages 357–362.

- El-Laithy, K. and Bogdan, M. (2011a). A hypothetical free synaptic energy function and related states of synchrony. In *Artificial Neural Networks and Machine Learning - ICANN 2011*, volume 6792 of *Lecture Notes in Computer Science*, pages 40–47. Springer.
- El-Laithy, K. and Bogdan, M. (2011b). A reinforcement learning framework for spiking networks with dynamic synapses. *Computational Intelligence and Neuroscience*. In Press.
- El-Laithy, K. and Bogdan, M. (2011c). Synchrony state generation: An approach using stochastic synapses. *J. of Artificial Intelligence and Soft Computing Research*, 1(1):17 – 26.
- Eliasmith, C. and Anderson, C. H. (2002). *Neural Engineering (Computational Neuroscience Series): Computational, Representation, and Dynamics in Neurobiological Systems*. MIT Press, Cambridge, MA, USA.
- Engel, A. K., Fries, P., Kiehnig, P., Brecht, M., and Singer, W. (1999). Temporal binding, binocular rivalry, and consciousness. *Consciousness and Cognition*, 8(2):128 – 151.
- Engel, A. K. and Singer, W. (2001). Temporal binding and the neural correlates of sensory awareness. *Trends in Cognitive Sciences*, 5(1):16 – 25.
- Farries, M. A. and Fairhall, A. L. (2007). Reinforcement Learning With Modulated Spike Timing Dependent Synaptic Plasticity. *J Neurophysiol*, 98(6):3648–3665.
- Fatt, P. and Katz, B. (1952). Spontaneous subthreshold activity at motor nerve endings. *The Journal of Physiology*, 117(1):109–128.
- Fellous, J., Rudolph, A., Destexhe, B., and T. Sejnowski (2003). Synaptic background noise controls the input/output characteristics of single cells in an in vitro model of in vivo activity. *Neuroscience*, 122:811–829.
- Fiete, I. R. and Seung, H. S. (2006). Gradient learning in spiking neural networks by dynamic perturbation of conductances. *Physical Review Letters*, 97(4):048104.
- Fine, E. J., Ionita, C. C., and Lohr, L. (2002). The history of the development of the cerebellar examination. *Seminars in neurology*, 22(4):375–384.
- Fitzhugh, R. (1961). Impulses and Physiological States in Theoretical Models of Nerve Membrane. *Biophysical Journal*, 1(6):445–466.
- Florian, R. V. (2007). Reinforcement learning through modulation of spike-timing-dependent synaptic plasticity. *Neural Computation*, 19(6):1468–1502.
- Fries, P. (2005). A mechanism for cognitive dynamics: neuronal communication through neuronal coherence. *Trends in Cognitive Sciences*, 9(10):474–80.
- Fries, P., Reynolds, J. H., Rorie, A. E., and Desimone, R. (2001). Modulation of oscillatory neuronal synchronization by selective visual attention. *Science*, 291(5508):1560–1563.
- Friston, K. (2009). The free-energy principle: a rough guide to the brain? *Trends in Cognitive Sciences*, 13(7):293 – 301.
- Friston, K. (2010). The free-energy principle: a unified brain theory? *Nature Reviews Neuroscience*, 11(2):127–138.

- Friston, K., Kilner, J., and Harrison, L. (2006). A free energy principle for the brain. *J Physiol Paris*.
- Friston, K. J. and Stephan, K. E. (2007). Free-energy and the brain. *Synthese*, 159(3):417 – 458.
- Fuchs, H. (1998). *Neural Networks with Dynamic Synapses*. PhD thesis, Institute of Theoretical Computer Science, Austria.
- Garimella, R. M. (2008). Finite impulse response (fir) filter model of synapses: Associated neural networks. In *International Conference on Natural Computation*, volume 2, pages 370–374. IEEE Computer Society.
- Gerstner, W. (1999). *Spiking neurons*, pages 3–53. MIT-Press, Cambridge.
- Gerstner, W. and Kistler, W. (2002). Mathematical Formulations of Hebbian Learning. *Biological Cybernetics*, 87(5-6):404–415.
- Gerstner, W. and Naud, R. (2009). How Good Are Neuron Models? *Science*, 326(5951):379–380.
- Gilbert, C. D. and Sigman, M. (2007). Brain states: top-down influences in sensory processing. *Neuron*, 54(5):677–696.
- Golomb, D., Rubin, N., and Sompolinsky, H. (1990). Willshaw model: Associative memory with sparse coding and low firing rates. *Phys. Rev. A*, 41(4):1843–1854.
- Gray, C. M. (1999). The temporal correlation hypothesis of visual feature integration: Still alive and well. *Neuron*, 24(1):31–47.
- Grimwood, S. J. M. P. D. and Morris, R. G. M. (2000). Synaptic Plasticity and Memory: An Evaluation of the Hypothesis. *Science*, 23:649 – 711.
- Hammond, C. (2001). *Cellular and Molecular Neurobiology*. Academic Press, second edition edition.
- Hansel, D., Mato, G., and Meunier, C. (1995). Synchrony in excitatory neural networks. *Neural Comput.*, 7(2):307–337.
- Hebb, D. O. (1949). *The Organization of Behavior*. Wiley and Son, New York.
- Herzog, M. H., Esfeld, M., and Gerstner, W. (2007). Consciousness & the small network argument. *Neural Networks*, 20(9):1054 – 1056.
- Hodgkin, A. L. and Huxley, A. F. (1952). A quantitative description of membrane current and its application to conduction and excitation in nerve. *Journal of Physiology*, 117(1):500–544.
- Hoffmann, J., El-Laithy, K., Güttler, F., and Bogdan, M. (2010). Simulating biological-inspired spiking neural networks with opencl. In *Artificial Neural Networks - ICANN 2010*, Lecture Notes in Computer Science, pages 184–187. Springer.
- Hommel, B. and Milliken, B. (2007). Taking the brain serious: introduction to the special issue on integration in and across perception and action. *Psychological Research / Psychologische Forschung*, 71(1):1–3.

- Hopfield, J. J. (1982). Neural networks and physical systems with emergent collective computational abilities. *Proceedings of the National Academy of Sciences of the United States of America*, 79(8):2554–2558.
- Hopfield, J. J. (1999). Brain, neural networks, and computation. *Rev. Mod. Phys.*, 71(2):S431–S437.
- Iglesias, J. and Villa, A. E. (2010). Recurrent spatiotemporal firing patterns in large spiking neural networks with ontogenetic and epigenetic processes. *Journal of Physiology-Paris*, 104(3-4):137 – 146. Neural Coding.
- Immordino-Yang, M. H. (2007). A tale of two cases: Lessons for education from the study of two boys living with half their brains. *Mind, Brain, and Education*, 1(2):66–83.
- Izhikevich, E. (2004). Which model to use for cortical spiking neurons? *Neural Networks, IEEE Transactions on*, 15(5):1063–1070.
- Jaeger, H. (2001). The "echo state" approach to analysing and training recurrent neural networks. GMD Report 148, GMD - German National Research Institute for Computer Science.
- Jolivet, R. and Gerstner, W. (2004). Predicting spike times of a detailed conductance- based neuron model driven by stochastic spike arrival. *J. Physiol. Paris*, 98:442–451.
- Jolivet, R., Kobayashi, R., Rauch, A., Naud, R., Shinomoto, S., and Gerstner, W. (2008a). A benchmark test for a quantitative assessment of simple neuron models. *Journal of Neuroscience Methods*, 169(2):417–424.
- Jolivet, R., Lewis, T. J., and Gerstner, W. (2003). The spike response model: A framework to predict neuronal spike trains. In *PROC. JOINT INTERNATIONAL CONFERENCE ICANN/I-CONIP 2003*, pages 846–853. Springer.
- Jolivet, R., Rauch, A., Loscher, H. R., and Gerstner, W. (2006). Predicting spike timing of neocortical pyramidal neurons by simple threshold models. *J. Computational Neuroscience*, 21:35–49.
- Jolivet, R., Schürmann, F., Berger, T., Naud, R., Gerstner, W., and Roth, A. (2008b). The quantitative single-neuron modeling competition. *Biological Cybernetics*, 99(4):417–426.
- Kandel, E. R., Schwartz, J. H., and Jessell, T. M. (1995). *Essentials of neural science and behavior*. McGraw-Hill Professional.
- Kanter, A. (2007). The impact of synaptic depression on up-down states in neural networks: A dynamical system perspective. Master's thesis, Israel Institute of Technology.
- Kempter, R., Gerstner, W., and van J. Hemmen (1999). Hebbian learning and spiking neurons. *Phys. Rev. E*, 59(4):4498–4514.
- Kimura, D. and Hayakawa, Y. (2008). Reinforcement learning of recurrent neural network for temporal coding. *Neurocomputing*, 71(16-18):3379 – 3386.
- Klemm, K., Bornholdt, S., and Schuster, H. G. (2000). Beyond hebb: Exclusive-or and biological learning. *Physical Review Letters*, 84:3013.

- Kobayashi, R., Tsubo, Y., and Shinomoto, S. (2009). Made-to-order spiking neuron model equipped with a multi-timescale adaptive threshold. *Frontiers in Computational Neuroscience*, 3(0).
- Koch, C. (1993). *Biophysics of computation: toward the mechanisms underlying information processing in single neurons*. MIT Press, Cambridge, MA, USA.
- Koch, C. and Tononi, G. (2008). Can machines be conscious? *Spectrum, IEEE*, 45(6):55–59.
- König, P., Engel, A. K., Roelfsema, P. R., and Singer, W. (1995). How precise is neuronal synchronization? *Neural Comput.*, 7(3):469–485.
- LaRock, E. (2007). Disambiguation, Binding, and the Unity of Visual Consciousness. *Theory Psychology*, 17(6):747–777.
- Lee, C.-C., Anton, M., Poon, C.-S., and McRae, G. (2009). A kinetic model unifying presynaptic short-term facilitation and depression. *Journal of Computational Neuroscience*, 26:459–473.
- Lee, K. and Kwon, D.-S. (2008). Synaptic plasticity model of a spiking neural network for reinforcement learning. *Neurocomputing*, 71(13-15):3037 – 3043.
- Legenstein, R. and Maass, W. (2007). Edge of chaos and prediction of computational performance for neural microcircuit models. *Neural Networks*, 20(3):323–334.
- Lehn-Schiøler, T. and Olesen, L. S. (2002). Synaptic activity – learning in neural systems. Master’s thesis, University of Denmark.
- Levina, A., Herrmann, J. M., and Geisel, T. (2007). Dynamical synapses causing self-organized criticality in neural networks. *Nature Physics*, 3:857 – 860.
- Levina, A., Herrmann, J. M., and Geisel, T. (2009). Phase transitions towards criticality in a neural system with adaptive interactions. *Physical Review Letters*, 102(11):875 – 860.
- Li, C., Yu, J., and Liao, X. (2001). Chaos in a three-neuron hysteresis hopfield-type neural network. *Physics Letters A*, 285(5-6):368 – 372.
- Liaw, J. and Berger, T. W. (1996). Dynamic synapse: A new concept of neural representation and computation. *Hippocampus*, 6:591–600.
- Liaw, J. S. and Berger, T. W. (1997). Computing with dynamic synapses: A case study of speech recognition. In *Proc. IEEE Int. Conf. Neural Networks*, pages 352–355.
- Lukoševičius, M. and Jaeger, H. (2009). Reservoir computing approaches to recurrent neural network training. *Computer Science Review*, 3(3):127–149.
- Ma, J. (1999). The asymptotic memory capacity of the generalized hopfield network. *Neural Networks*, 12(9):1207 – 1212.
- Maass, W. (1997). Fast sigmoidal networks via spiking neurons. *Neural Comput.*, 9:279–304.
- Maass, W. (2007). Liquid computing. In *CiE ’07: Proceedings of the 3rd conference on Computability in Europe*, pages 507–516, Berlin, Heidelberg. Springer-Verlag.

- Maass, W. and Markram, H. (2004). On the computational power of circuits of spiking neurons. *J. Comput. Syst. Sci.*, 69(4):593–616.
- Maass, W., Natschläger, T., and Markram, H. (2002). Real-time computing without stable states: a new framework for neural computation based on perturbations. *Neural Comput.*, 14(11):2531–2560.
- Maass, W. and Sontag, E. D. (2000). Neural systems as nonlinear filters. *Neural Comput.*, 12:1743–1772.
- Maass, W. and Zador, A. M. (1999). *Computing and learning with dynamic synapses*, pages 321–336. MIT Press, Cambridge, MA, USA.
- Markram, H. (2006). The Blue Brain Project. *NATURE REVIEWS NEUROSCIENCE*, 7:153 – 160.
- Markram, H., Lübke, J., Frotscher, M., Roth, A., and Sakmann, B. (1997). Physiology and anatomy of synaptic connections between thick tufted pyramidal neurones in the developing rat neocortex. *The Journal of physiology*, 500 ( Pt 2)(Pt 2):409–440.
- Markram, H. and Tsodyks, M. (1996). Redistribution of synaptic efficacy between neocortical pyramidal neurons. *Nature*, 382(6594):807–810.
- Markram, H., Wang, Y., and Tsodyks, M. (1998). Differential signaling via the same axon of neocortical pyramidal neurons. *Proc. of the Nat. Academy of Sciences of the USA*, 95(9):5323–5328.
- McCulloch, W. and Pitts, W. (1943). A logical calculus of the ideas immanent in nervous activity. *Bulletin of Mathematical Biology*, 5:115–133.
- Mikula, S. and Niebur, E. (2005). Rate and synchrony in feedforward networks of coincidence detectors: Analytical solution. *Neural Comput.*, 17(4):881–902.
- Miller, P. (2006). Analysis of spike statistics in neuronal systems with continuous attractors or multiple, discrete attractor states. *Neural Computation*, 18(6):1268–1317.
- Montgomery, J. M. and Madison, D. V. (2002). State-dependent heterogeneity in synaptic depression between pyramidal cell pairs. *Neuron*, 33(5):765 – 777.
- Montgomery, J. M. and Madison, D. V. (2004). Discrete synaptic states define a major mechanism of synapse plasticity. *Trends in Neurosciences*, 27(12):744 – 750.
- Morrison, A., Diesmann, M., and Gerstner, W. (2008). Phenomenological models of synaptic plasticity based on spike timing. *Science*, 98:459 – 478.
- Namarvar, H., Liaw, J., and Berger, T. (2001). A new dynamic synapse neural network for speech recognition. In *Proc. IEEE Int. Conf. Neural Networks*, volume 4, pages 2985–2990.
- Natschläger, T. (1999). *Efficient Computation in Networks of Spiking Neurons Simulations and Theory*. PhD thesis, Institute of Theoretical Computer Science, Austria.
- Natschläger, T. and Maass, W. (2002). Spiking neurons and the induction of finite state machines. *Theoretical Computer Science*, 287(1):251 – 265.

- Natschlager, T., Maass, W., and Zador, A. (2001). Efficient temporal processing with biologically realistic dynamic synapses. *Computation in neural system*, 12:75–78.
- Neelakanta, P. S. and DeGroff, D. (1994). *Neural Network Modeling: Statistical Mechanics and Cybernetics Perspectives*. CRC Press.
- Neltner, L. and Hansel, D. (2001). On synchrony of weakly coupled neurons at low firing rate. *Neural Comput.*, 13(4):765–774.
- Pecora, L. M., Carroll, T. L., Johnson, G. A., Mar, D. J., and Heagy, J. F. (1997). Fundamentals of synchronization in chaotic systems, concepts, and applications. *Chaos: An Interdisciplinary Journal of Nonlinear Science*, 7(4):520–543.
- Pennartz, C. (1997). Reinforcement learning by hebbian synapses with adaptive thresholds. *Neuroscience*, 81(2):303 – 319.
- Perez, F. M., Tunkel, R. S., Lachmann, E. A., and Nagler, W. (1996). Balint’s syndrome arising from bilateral posterior cortical atrophy or infarction: rehabilitation strategies and their limitation. *Disability and rehabilitation*, 18(6):300–304.
- Poulet, J. F. and Petersen, C. C. (2008). Internal brain state regulates membrane potential synchrony in barrel cortex of behaving mice. *Nature*, 454(7206):881–885.
- Purves, D. (2008). *Neuroscience, Fourth Edition*. Sinauer Associates, Inc., 4th edition.
- Reichert, D. P., Seriès, P., and Storkey, A. J. (2011). A hierarchical generative model of recurrent object-based attention in the visual cortex. In *ICANN (1)*, pages 18–25.
- Revonsuo, A. and Newman, J. (1999). Binding and consciousness. *Consciousness and Cognition*, 8(2):123 – 127.
- Robertson, L. (2003). Binding, spatial attention and perceptual awareness. *Nature Reviews Neuroscience*, 4(2):93–102.
- Rosahl, T. W., Geppert, M., Spillane, D., Herz, J., Hammer, R. E., Malenka, R. C., and Südhof, T. C. (1993). Short-term synaptic plasticity is altered in mice lacking synapsin i. *Cell*, 75:661–670.
- Salinas, E. and Sejnowski, T. J. (2001). Correlated neuronal activity and the flow of neural information. *Nature Reviews Neuroscience*, 2:539–550.
- Sandberg, A. and Bostrom, N. (2008). Whole Brain Emulation: A Roadmap. Technical report, Future of Humanity Institute.
- Sarasola, C., d’Anjou, A., Torrealdea, F. J., and Graña, M. (2005). Minimization of the energy flow in the synchronization of nonidentical chaotic systems. *Phys. Rev. E*, 72(2):026223.
- Sarasola, C., Torrealdea, F. J., d’Anjou, A., Moujahid, A., and Graña, M. (2004). Energy balance in feedback synchronization of chaotic systems. *Phys. Rev. E*, 69(1):011606.
- Schrauwen, B., Verstraeten, D., and Van Campenhout, J. (2007). An overview of reservoir computing: theory, applications and implementations. In *Proceedings of the 15th European Symposium on Artificial Neural Networks*, pages 471–482.

- Schreiber, S., Fellous, J. M., Whitmer, D., Tiesinga, P., and Sejnowski, T. J. (2003). A new correlation-based measure of spike timing reliability. *Neurocomputing*, (52-54):925–931.
- Schrobsdorff, H., Herrmann, J. M., and Geisel, T. (2007). A feature-binding model with localized excitations. *Neurocomputing*, 70(10-12):1706 – 1710.
- Schultz, W., Dayan, P., and Montague, P. R. (1997). A neural substrate of prediction and reward. *Science*, 275(5306):1593–1599.
- Sejnowski, T. J. (1989). The computer and the brain revisited. *IEEE Annals of the History of Computing*, 11(3):197–201.
- Sejnowski, T. J., Koch, C., and Churchland, P. S. (1988). Computational neuroscience. *Science*, 241(4871):1299–1306.
- Seung, H. (2003). Learning in spiking neural networks by reinforcement of stochastic synaptic transmission. *Neuron*, 40(6):1063 – 1073.
- Shadlen, M. N. and Movshon, J. A. (1999). Synchrony unbound: A critical evaluation of the temporal binding hypothesis. *Neuron*, pages 67–77.
- Shon, A. and Rao, R. (2003). Temporal sequence learning with dynamic synapses. Technical report, UW CSE.
- Sincich, L. C., Adams, D. L., Economides, J. R., and Horton, J. C. (2007). Transmission of Spike Trains at the Retinogeniculate Synapse. *J. Neurosci.*, 27(10):2683–2692.
- Singer, W. (1999). Neuronal synchrony: a versatile code for the definition of relations. *Neuron*, 24:49–65.
- Singer, W. (2007). Understanding the brain. *European Molecular Biology Org.*, 8:16 –19.
- Singer, W. and Gray, C. M. (1995). Visual feature integration and the temporal correlation hypothesis. *Annu Rev Neurosci*, 18:555–586.
- Stieglitz, T. (2010). Manufacturing, assembling and packaging of miniaturized neural implants. *Microsystem Technologies*, 16:723–734. 10.1007/s00542-009-0988-x.
- Stringer, S., Rolls, E., and Trappenberg, T. (2005). Self-organizing continuous attractor network models of hippocampal spatial view cells. *Neurobiology of Learning and Memory*, 83(1):79 – 92.
- Supp, G. G., Schläpfl, A., Trujillo-Barreto, N., Müller, M. M., and Gruber, T. (2007). Directed cortical information flow during human object recognition: Analyzing induced eeg gamma-band responses in brain’s source space. *PLoS ONE*, 2(8):e684.
- Sutton, R. S. and Barto, A. G. (1998). *Reinforcement Learning*. The MIT Press.
- Tallon-Baudry, C. (2004). Attention and awareness in synchrony. *Trends in Cognitive Sciences*, 8(12):523 – 525.
- Teixeira, M., Castelo-Branco, M., Nascimento, S., and Almeida, V. (2010). The p300 signal is monotonically modulated by target saliency level irrespective of the visual feature domain. *Acta Ophthalmologica*, 88:0–0.



- Tetko, I. V. and Villa, A. E. P. (1997). Fast combinatorial methods to estimate the probability of complex temporal patterns of spikes. *Biological Cybernetics*, 76:397–408.
- Torrealea, F. J., d’Anjou, A., na, M. G., and Sarasola, C. (2006). Energy aspects of the synchronization of model neurons. *Physical Review E (Statistical, Nonlinear, and Soft Matter Physics)*, 74(1):011905.
- Trappenberg, T. P. (2002). *Fundamentals of Computational Neuroscience*. Oxford U. Press.
- Treisman, A. M. and Gelade, G. (1980). A feature-integration theory of attention. *Cognitive Psychology*, 12:97 – 136.
- Tsodyks, M., Uziel, A., and Markram, H. (2000). Synchrony generation in recurrent networks with frequency-dependent synapses. *J. Neurosci*, 20:50.
- Tsodyks, M. V. and Markram, H. (1997). The neural code between neocortical pyramidal neurons depends on neurotransmitter release’s probability. *Proc. of the Nat. Academy of Sciences of the USA*, 94(2):719–723.
- Umar, M., Singh, R., and Shugaba, A. (2006). Cephalometric indices among nigerians. *Journal of Applied Sciences*, 6:939–942.
- Urbanczik, R. and Senn, W. (2009). Reinforcement learning in populations of spiking neurons. *Nature Neuroscience*, 12(3):250–252.
- van der Velde, F. (1993). Is the brain an effective Turing machine or a finite-state machine? *Journal Psychological Research*, 55(1):71 – 79.
- van der Velde, F. and de Kamps, M. (2006). Neural blackboard architectures of combinatorial structures in cognition. *Behavioral and Brain Sciences*, 29(01):37–70.
- van Rossum, M. C. W. (2001). A Novel Spike Distance. *Neural Comp.*, 13(4):751–763.
- van Rossum, M. C. W., Bi, G. Q., and Turrigiano, G. G. (2000). Stable hebbian learning from spike timing-dependent plasticity. *The Journal of Neuroscience*, 20(23):8812–8821.
- Varela, J. A., Sen, K., Gibson, J., Fost, J., Abbott, L. F., and Nelson, S. (1997). A quantitative description of short term-plasticity at excitatory synapses in layer 2/3 of rat primary visual cortex. *Neuroscience*, 17:7926–7940.
- Velik, R. (2008). *A Bionic Model for Human-like Machine Perception*. VDM Verlag.
- Velik, R. (2010). From single neuron-firing to consciousness—towards the true solution of the binding problem. *Neuroscience & Biobehavioral Reviews*, 34(7):993 – 1001. Binding Processes: Neurodynamics and Functional Role in Memory and Action.
- Verstraeten, D., Schrauwen, B., D’Haene, M., and Stroobandt, D. (2007). An experimental unification of reservoir computing methods. *Neural Networks*, 20(3):391 – 403. Echo State Networks and Liquid State Machines.
- von der Malsburg, C. (1981). The correlation theory of brain function.
- von der Malsburg, C. (1999). The what and why of binding: The modeler’s perspective.

- von Engelhardt, J., Mack, V., Sprengel, R., Kavenstock, N., Li, K. W., Stern-Bach, Y., Smit, A. B., Seeburg, P. H., and Monyer, H. (2010). CKAMP44: A Brain-Specific Protein Attenuating Short-Term Synaptic Plasticity in the Dentate Gyrus. *Science*, 327(5972):1518–1522.
- Vreeswijk, C. V. and Hansel, D. (2001). Patterns of synchrony in neural networks with spike adaptation. *Neural Comput.*, 13(5):959–992.
- Whalley, K. (2009). Synaptogenesis: Making the microcircuit. *Nature Reviews Neuroscience*, 10:244–245.
- Whitlock, J. R., Heynen, A. J., Shuler, M. G., and Bear, M. F. (2006). Learning induces long-term potentiation in the hippocampus. *Science*, 313(5790):1093–1097.
- Wilson, N. R., Bodnar, D. A., Skovira, J. F., and Land, B. R. (2001). Processing of auditory mid-brain interspike intervals by model neurons. *Journal of Computational Neuroscience*, 10(2):151 – 172.
- Xie, X. and Seung, H. S. (2004). Learning in neural networks by reinforcement of irregular spiking. *Phys. Rev. E*, 69(4):69 – 79.
- Yeckel, M. F. and Berger, T. W. (1998). Spatial distribution of potentiated synapses in hippocampus: Dependence on cellular mechanisms and network properties. *The Journal of Neuroscience*, 18:438–450.
- Yusim, K., Parnas, H., and Segel, L. (2001). One-vesicle hypothesis for neurotransmitter release: A possible molecular mechanism. *Bulletin of Mathematical Biology*, 63:1025–1040. 10.1006/bulm.2001.0247.
- Zador, A. M. and Dobrunz, L. E. (1997). Dynamic synapses in the cortex. *Neuron (Cell Press)*, 19:1–4.
- Zhang, W., Zhang, Y., Zheng, H., Zhang, C., Xiong, W., Olyarchuk, J. G., Walker, M., Xu, W., Zhao, M., Zhao, S., Zhou, Z., and Wei, L. (2006). Syndb: a synapse protein database based on synapse ontology. *Nucleic Acids Research*, 35(1):D737–D741.
- Zucker, R. S. (1989). Short-term synaptic plasticity. *Annu Rev Neurosci*, 12:13–31.
- Zucker, R. S. and Regehr, W. G. (2002). Short-term synaptic plasticity. *Annu Rev Neurosci*, 64:355–405.

# Scientific Career

## Personal Information

**Full Name** Karim Ahmed Youssry Mohamed El-Laithy.

**Date of Birth** 23rd of March, 1981.

**Nationality** Egyptian.

---

## Education

**Ph.D. Computer Science. Leipzig University**, April 2008 - present.

Dept. of Computer Engineering.

Major: Computational Neuroscience

Thesis: Towards a Brain-inspired Information Processing System: Modelling and Analysis of Synaptic Dynamics.

**M.Sc. Biomedical Engineering & Systems. Cairo University**, 2006.

Dept. of Biomedical & Systems Engineering

Thesis: Artificial Neural Networks with Dynamic Synapses: A Concept of Neural Representation and Signal Processing.

Grade: Very Good.

**B.Sc. Biomedical Engineering & Systems. Cairo University**, 2002.

Dept. of Biomedical & Systems Engineering

Grade: Very Good w. Honor, ranked the second (Class of 92 student)

## *Continuing Education*

**M.Sc. Biophysics Leipzig University**, May 2011

Dept. of Soft Matter Physics

Thesis: Digital analysis of neuronal branching and synaptogenesis.

Grade: Very Good.

---

## Academic Experience

**Doctoral Research.** Dept. of Computer Engineering, Leipzig University, Apr. 2008 – present

- Thesis: Towards a Brain-inspired Information Processing System: Modelling and Analysis of Synaptic Dynamics.
- Supervisor: Prof. Dr. M. Bogdan.
- The research has involved a multidisciplinary work of modelling and simulation of both biophysical and theoretical topics. Main issues were synaptic modeling and simulating generic information processing operations in biological neural systems.

**M.Sc. Thesis** Dept. of Soft Matter Physics, Leipzig University, Oct. 2009 - May 2011

- Thesis: Digital analysis of neuronal branching and synaptogenesis.
- Supervisor: Prof. Dr. J. Käs
- The main pivots of this work were cell cultures and image processing. Random networks of neuronal cells were cultures in laboratory environment and observed under optical microscope. Observed sequences of images were further analysed using morphological analysis to detect and describe the dynamics of branching and synaptogenesis.

**M.Sc. Thesis.** Dept. of Biomedical & Systems Engineering, Cairo University, 2004-2006

- Thesis: A novel representation of artificial neural networks with dynamic synapses.
- Supervisor: Prof. Dr. B. Tawfik and Dr. M Fayek.

**B.Sc. Graduation Project.** Implementation of "Real-Time Doppler Signal Analysis using Digital Signal Processor, TI C6211".

---

## Teaching

**Teacher Assistant.** American University in Cairo, Spring 2005.

Elementary and Advanced Topics in Physics

**Instructor** CASBEC, 1999-2002

Center for Advanced Software and Biomedical Engineering Consultations, Faculty of Engineering, Cairo University Cairo, Egypt. C++, Java, O.O.P concepts and Delphi

**Instructor** Compex, 2001-2002

IBM Egypt Training Center, Cairo, Egypt. C++, Oracle Developer Tools.

# Published Work

## Journal & Peer-reviewed Conference Papers

1. **El-Laithy, K.** and Bogdan, M. (2009). Synchrony state generation in artificial neural networks with stochastic synapses. In Artificial Neural Networks - ICANN 2009, volume 5768 of Lecture Notes in Computer Science, pages 181–190. Springer.
2. Hoffmann, J., **El-Laithy, K.**, Güttler, F., and Bogdan, M. (2010). Simulating biological-inspired spiking neural networks with opencl. In Artificial Neural Networks - ICANN 2010, Lecture Notes in Computer Science, pages 184–187. Springer.
3. **El-Laithy, K.** and Bogdan, M. (2010a). A hebbian-based reinforcement learning framework for spike timing-dependent synapses. In Artificial Neural Networks - ICANN 2010, volume 6353 of Lecture Notes in Computer Science, pages 160–169. Springer.
4. **El-Laithy, K.** and Bogdan, M. (2010b). Predicting spike-timing of a thalamic neuron using a stochastic synaptic model. In ESANN Proceedings, pages 357–362.
5. **El-Laithy, K.** and Bogdan, M. (2011a). A hypothetical free synaptic energy function and related states of synchrony. In Artificial Neural Networks and Machine Learning - ICANN 2011, volume 6792 of Lecture Notes in Computer Science, pages 40–47. Springer.
6. **El-Laithy, K.** and Bogdan, M. (2011b). On the capacity of transient internal states in liquid-state machines. In Artificial Neural Networks and Machine Learning - ICANN 2011, volume 6792 of Lecture Notes in Computer Science, pages 56–63. Springer.
7. **El-Laithy, K.** and Bogdan, M. (2011c). A hebbian-based reinforcement learning framework for dynamic Synapses. J. of Computational Intelligence and Neuroscience. *In press*.
8. **El-Laithy, K.** and Bogdan, M. (2011d). Synchrony state generation: An approach using stochastic synapses. J. of Artificial Intelligence and Soft Computing Research, 1(1):17–26.

## Honors and Awards

- **2011: ENNS Student Award** for the participation in ICANN 2011, Finland.
- **2009: FACETS Award & Current Benchmark** for INCF Quantitative Single Neuron modelling challenge (Part D).



# Bibliographic Details

El-Laithy, Karim: **Towards a Brain-inspired Information Processing System: Modelling and Analysis of Synaptic Dynamics**

Universität Leipzig, Fakultät für Mathematik und Informatik, Dissertation, 212 Seiten, 67 Abbildungen, 2011.

## **Declaration of Authorship**

I, Karim El-Laithy, declare that this thesis titled, "Towards a Brain-inspired Information Processing System: Modelling and Analysis of Synaptic Dynamics" and the work presented in it are my own. I confirm that this work was done wholly or mainly while in candidature for a research degree at this University. Where any part of this thesis has previously been submitted for a degree or any other qualification at this University or any other institution, this has been clearly stated. Where I have consulted the published work of others, this is always clearly attributed. Where I have quoted from the work of others, the source is always given. With the exception of such quotations, this thesis is entirely my own work. I have acknowledged all main sources of help. Where the thesis is based on work done by myself jointly with others, I have made clear exactly what was done by others and what I have contributed myself.

## **Selbständigkeitserklärung**

Hiermit erkläre ich, die vorliegende Dissertation selbständig und ohne unzulässige fremde Hilfe angefertigt zu haben. Ich habe keine anderen als die angeführten Quellen und Hilfsmittel benutzt und sämtliche Textstellen, die wörtlich oder sinngemäß aus veröffentlichten oder unveröffentlichten Schriften entnommen wurden, und alle Angaben, die auf mündlichen Auskünften beruhen, als solche kenntlich gemacht. Ebenfalls sind alle von anderen Personen bereitgestellten Materialien oder erbrachten Dienstleistungen als solche gekennzeichnet.

Leipzig, den 19.12.2011

Karim El-Laithy